UNIVERSITÀ DEGLI STUDI DI SALERNO

UNIVERSITÀ DEGLI STUDI DI SALERNO
Dipartimento di Farmacia

PhD Program
in **Drug Discovery and Development**
XXXIV Cycle — Academic Year 2021/2022

PhD Thesis in

Design and synthesis of molecules with anti-inflammatory and/or anti-cancer activity

Candidate

Ester Colarusso

Supervisor

Prof. *Giuseppe Bifulco*

PhD Program Coordinator: Prof. *Gianluca Sbardella*

A mio nonno

a mia madre

a chi lotta per i propri sogni

Preface

My three-year Ph.D. course in Drug Discovery and Development at the Department of Pharmacy of the University of Salerno started in November 2018 under the supervision of Prof. Giuseppe Bifulco. My research project mainly focused on the design and synthesis of new anti-tumor and anti-inflammatory molecules in the frame of two projects funded by AIRC (Associazione Italiana per la Ricerca sul Cancro, Italian Association for Cancer Research).

I was interested in the identification of new binders of bromodomain containing protein9 (BRD9), an epigenetic reader involved in chromatin remodeling and overexpressed in many cancers, especially acute myeloid leukemia. Also, my research activity concerned the discovery of new inhibitors of microsomal prostaglandin E_2 synthase-1 (mPGES-1) and soluble epoxide hydrolase (sEH). Both the targets are involved in the arachidonic acid cascade and they are related to the inflammation and cancer processes.

I evaluated the binding with BRD9 through Alpha Screening assays, in collaboration with Prof. Maria Chiara Monti. Biological tests on the molecules designed for mPGES-1 and sEH were performed in collaboration with Prof. Oliver Werz of Friedrich Schiller University (Germany).

During the third year of my Ph.D., in order to improve my expertise in synthetic chemistry, I moved to the Department of Chemistry of the University of California, Berkeley (February 2021- December 2021) under the supervision of Prof. F. Dean Toste. The main goal of my research stay was to characterize and develop new stereoselective synthetic approaches useful for the future design and synthesis of new potential anti-inflammatory and anticancer molecules. Indeed, the synthesis of single enantiomers, rather than a whole racemic mixture, could be crucial for shedding light on the biological activity of that specific enantiomer. For this reason, a better understanding of stereoselective synthesis along with new synthetic approaches/methods are pivotal for the design and synthesis of future binders on the targets of our interest.

Publications

- Chini, M.G.; Giordano, A.; Potenza,M.; Terracciano, Fischer, K.; S.; Vaccaro, M.C.; **Colarusso**, **E**.; Bruno, I.; Riccio, R.; Koeberle, A.; Werz, O.; Bifulco, G.; Targeting mPGES-1 by a combinatorial approach: identification of the aminobenzothiazole scaffold to suppress PGE_2, ACS Medicinal Chemistry Letters, 2020, 783-789.

- **Colarusso**, **E.**;† Potenza, M.;† Lauro, G.; Chini, M.G.; Sepe, V.; Zampella, A.; Fischer, K.; Hofstetter, R.K.; Werz, O.; Bifulco, G.; Thiazolidin-4-one-based compounds interfere with the eicosanoid biosynthesis pathways by mPGES-1/sEH/5-LO multi-target inhibition. (Accepted to European Journal of Medicinal Chemistry Reports).

- **Colarusso**, **E.**; Ceccacci, S.; Monti, M.C.; Gazzillo, E.; Giordano, A.; Chini, M.G.; Ferraro, M.G.; Piccolo, M.; Maione, F.; Irace, C.; Bifulco, G.; Lauro, G. Identification of 2,4,5-trisubstituted-2,4-dihydro-3*H*-1,2,4-triazol-3-one-based molecules as new selective BRD9 binders. (Submitted to European Journal of Medicinal Chemistry).

- Gazzillo, E.;† **Colarusso**, **E.**;† Chini, M.G.; Giordano, A.; Potenza, M.; Werz, O.; Bifulco, G.; Lauro, G. Inverse Virtual Screening for the repositioning of benzothiazole-based small molecules on soluble epoxide hydrolase (sEH). (Manuscript in preparation).

†Authors contributed equally to the work.

Conference proceedings:

- **Colarusso, E.**; Chini, M.G.; Giordano, A.; Vaccaro, M. C.; Potenza, M.; Terracciano, S.; Bruno, I.; Riccio, R.; Werz, O.; Koeberle, A.; Bifulco G. presented at XXXIX Convegno Nazionale della Divisione di Chimica Organica, Torino (TO), September 8-12, 2019.
- **Colarusso, E.**; Chini, M.G.; Terracciano, S.; Bruno, I.; Di Micco, S.; Potenza, M.; De Vita, S.; Gazzerro, P.; Giordano,A.; Riccio, R.; Bhushan, A.; Filippakopoulos, P.; Reginelli, A.; Bifulco, G.; Lauro G. presented at Chemistry Meets Industry and Society, Salerno (SA), August 28-30, 2019.
- De Vita, S.; Chini, M.G.; Lauro, G.; Potenza, M.; **Colarusso, E.**; Ruggiero, D.; Terracciano, S.; Bruno, I.; Riccio, R.; Bode, J.W.; Koeberle, A.; Werz, O.; Maione, M.; Reginelli, A.; Bifulco, G. presented at Chemistry Meets Industry and Society, Salerno (SA), August 28-30, 2019.
- **Colarusso, E.**; Giordano, A.; Riccio, R.; Lauro, G.; Bifulco, G. presented at 44th "A.Corbella" International Summer School on Organic Synthesis 2019, Gargnano (BS), June 10-16, 2019.

Table of contents

Abstract

During the last decade, the link between inflammation and cancer has been widely reported. Accordingly, the identification of new molecules able to interfere with key biological targets involved in these pathologies is urgently needed. In light of this, my work was focused on the synthesis of new small molecules, targeting three proteins involved in these pathologies: bromodomain-containing protein 9 (BRD9), microsomal prostaglandin E_2 synthase-1 (mPGES-1), and soluble epoxide hydrolase (sEH).

BRD9 protein, a subunit of the mammalian switch/sucrose non-fermentable (SWI/SNF) complex, emerged as an attractive target for future anticancer therapy due to its overexpression in different tumor types, especially leukemia.

mPGES-1 is the terminal enzyme of the arachidonic acid cascade, responsible for producing inducible prostaglandin E_2. Therefore, selective inhibition of the inducible mPGES-1 may be considered a valid therapeutic approach to interfere with inflammation-induced PGE_2 formation. Also, it is over-expressed in tumor pathologies, and for this reason, it is considered an attractive anticancer target. Furthermore, inhibition of soluble epoxide hydrolase enzyme (sEH) leads to an increase of epoxyeicosatrienoic acids (EETs) that are anti-inflammatory mediators.

A multi-disciplinary approach was employed in these studies, in which the *in silico* drug design represented the first step (Task1). The best compounds were selected and then synthesized (Task2) and screened for their binding/inhibitory activity against the target proteins (Task 3). This step was performed through AlphaScreen assay for BRD9; for what concerns mPGES-1 and sEH, specific cell-free assays were performed in collaboration with Prof. Oliver Werz's group. Finally, the best molecules were subjected to the *in vivo* assays in collaboration with Prof. Maione (Task 4). Instead molecules failing to satisfactorily bind/inhibit the target were revaluated by Inverse Virtual Screening (IVS) (Task 5) throughout the anti-inflammatory and anticancer protein panel, with the main of repositioning them on other targets.

The results obtained during my three years Ph.D. project are reported in the three main sections, with reference with the targets of interest:

Bromodomain-containing protein 9 (BRD9). My main project goal was represented by the synthesis of the selected molecules, previously evaluated through a computational approach, and the evaluation of the binding with the protein counterpart by AlphaScreen assay. In particular, the scaffolds considered for the development of these potential binders were divided into two groups, according to the *in silico* design approach used (**Chapter 1)**.

Interaction-based approach (IBA). The scaffold chemotypes were selected based on chemical portions that would mimic acetyl lysine of H4 histone, the latter acting as the natural binder of BRD9 protein. The selection of the molecules was based on the interactions with the key amino acids for the protein inhibition, following the evaluation through molecular docking experiments. Therefore, twenty-eight isoxazolo[2,3-*c*][1,3,5]thiadiazepin-2-one-based compounds, four 4-ethyl-benzo[*d*]thiazol-2-amine-based compounds and seven 1,8-naphthyridinone-based compounds were synthesized. Preliminary AlphaScreen results highlighted the inability of these compounds to inhibit BRD9. On the other hand, *in silico*-driven repurposing investigations performed on the set of synthesized compounds highlighted a promising binding of a subset of items against estrogen receptor, soluble epoxide hydrolase, and tyrosine kinase proteins, respectively.

Structure-based three-dimensional pharmacophore-based approach (SBPA). All the compounds were subjected to a screening accounting a pharmacophore model after performing docking calculations. In particular, among the twenty-one molecules with 2,4-dihydro-3*H*-1,2,4-triazol-3-one nucleus synthesized, two (**D22** and **D25**) were able to bind the target with an IC_{50} in the low micromolar range. These molecules also showed a high selectivity profile when tested against a panel of further nine bromodomains. Starting from these encouraging data, further ten derivatives were synthesized. The binding assessment revealed that seven of

these compounds (**D26**, **D28**, **D30**, **D31**, **D32**, **D34**, **D35**) were able to selectively bind BRD9 among the panel of accounted bromodomains.

The quinazoline-4(3*H*)-one-based compounds represent the second series of molecules developed after screening them against the pharmacophore model.[93] Fourteen selected chemical items were synthesized for the subsequent biological screening applying a multistep synthetic strategy. AlphaScreen assays showed the moderate ability of two molecules (**E7** and **E13**) in binding BRD9 (binding percentage: 40%). Also, in this case, we explored the structure-activity relationship, synthesizing seven new derivatives based on structural considerations of the most promising molecules. However, the evaluation of the binding of these new derivatives has yet to be performed.

Microsomal prostaglandin E_2 synthase-1 (mPGES-1) and soluble epoxide hydrolase (sEH). In the frame of my Ph.D. project, using computational chemistry techniques, 6 combinatorial libraries were obtained by decorating the selected scaffolds with chemical items available on the Merck database. The computational approach, described in **Chapter 3**, led to the identification of a set of molecules selected for the next synthetic step, currently ongoing.

In the second case, 23 thiazolidin-4-one-based compounds were synthesized using a one-pot multicomponent reaction. 5 of these molecules (**F1**, **F2**, **F4**, **F14**, **F22**) proved to be the most promising items showing affinity for mPGES-1. These molecules were also evaluated on other enzymes of the arachidonic acid cascade to improve their efficacy in the treatment of the pathology of our interest, as described in **Chapter 3**. The synthesized thiazolidin-4-one-based compounds were first evaluated *in silico* against sEH; after that, eleven molecules chosen among those synthesized were tested in a cell-free assay to corroborate the computational prediction. Compounds **F2**, **F4**, **F8** proved to be the most promising, showing a high affinity for the protein (IC_{50}=6.3±0.4μM, IC_{50}=6.1±0.3μM, IC_{50}=6.2±0.6μM, respectively). Furthermore, a cell-free assays on COXs and 5-LO with the hits **F2**, **F4**, **F8** expanded our

investigations of interference with inflammation-related lipid mediator biosynthesis, revealing compound **F4** as a promising 5-LO inhibitor.

Finally, 8 benzothiazinone-based compounds were synthesized following the selected strategy (**Chapter 3**), and the biological assays (carried out by Prof. Oliver Werz's group) are currently in progress.

On the other hand, four compounds, initially designed for BRD9, were re-evaluated on a panel of proteins involved in inflammatory and tumor processes through Inverse Virtual Screening (**Chapter 1**). As a result, the four compounds were successfully repositioned on soluble epoxide hydrolase, and **B3** was identified as a new inhibitor of the enzyme, confirming the reliability of the prediction of the IVS approach applied and its usefulness for drug repositioning.

Finally, I turned my attention to fluorinated compounds, considering their increasing importance in medicinal chemistry due to their better physicochemical properties and their higher affinity to the target protein compared to non-fluorinate compounds. In particular, during the period at the Department of Chemistry of the University of California, Berkeley, under the supervision of Prof. F. Dean Toste, I worked on the substrate improvement in the context of a new strategy for the stereoselective synthesis of fluorodienes. In addition, using these fluorodienes as substrates, I conducted experiments aimed at developing a new enantioselective Diels-Alder (*DA*) reaction. These dienes react differently from non-fluorinated dienes; for this reason, only one *DA* procedure with fluorinated dienes is nowadays reported.

Eventually, the novelty of our method consists in the possibility to apply the *DA* to fluorodienes without any activating group and, furtherly, generating enantiopure compounds with the use of a chiral catalyst (**Chapter 4)**.

INTRODUCTION

During my three years Ph.D. project, new potential anti-inflammatory and anti-cancer molecules were identified.

Three main targets, involved at different levels in inflammation and cancer development, were thoroughly investigated: bromodomain-containing protein 9 (BRD9); microsomal prostaglandin E2 synthase-1 (mPGES-1); and soluble epoxide hydrolase (sEH).

Thanks to the financial support of AIRC (Associazione Italiana per la Ricerca sul Cancro, Italian Association for Cancer Research), new binders/inhibitors of specific target proteins were identified following a multitask protocol.

In more detail, the general workflow (**Figure 1**) included:

1) the choice of a synthetic strategy, whose building blocks were used as a starting point for the *in silico* design of new large libraries of molecules, mainly following a combinatorial chemistry approach. Afterward, a multi-step computational protocol was applied to the generated libraries for the virtual docking studies on the target protein (Task 1). The study of ligand-protein interactions played a fundamental role in the design of promising compounds;
2) synthesis of the molecules applying the selected synthetic route, followed by their purification and characterization;
3) biological assays on the targets and cell line tests for the experimental evaluation and quantification of the activity of the synthesized molecules. Compounds able to interfere with the functions of the target protein were selected as starting point for an optimization step, aimed at improving their performance in the modulation of the protein activity (including the generation of analogs of the new disclosed hits). In case of poor or null inhibition activity, the synthesized compounds were subjected to a repurposing (Task5) by Inverse Virtual Screening method (IVS). This computational technique, useful for the individuation of a specific target in a panel of anti-inflammatory and/or anti-cancer

protein, was previously developed by the research group in which the whole research project was carried out;

4) the biological activity and the toxicity of the most promising compounds have to be assessed *in vivo*, in collaboration with other research groups (Task4).

In this context, the main activity of this Ph. D. work was:

- the synthesis and the evaluation of the binding for BRD9 designed molecules;
- the design and the synthesis for molecules targeting mPGES-1/sEH.

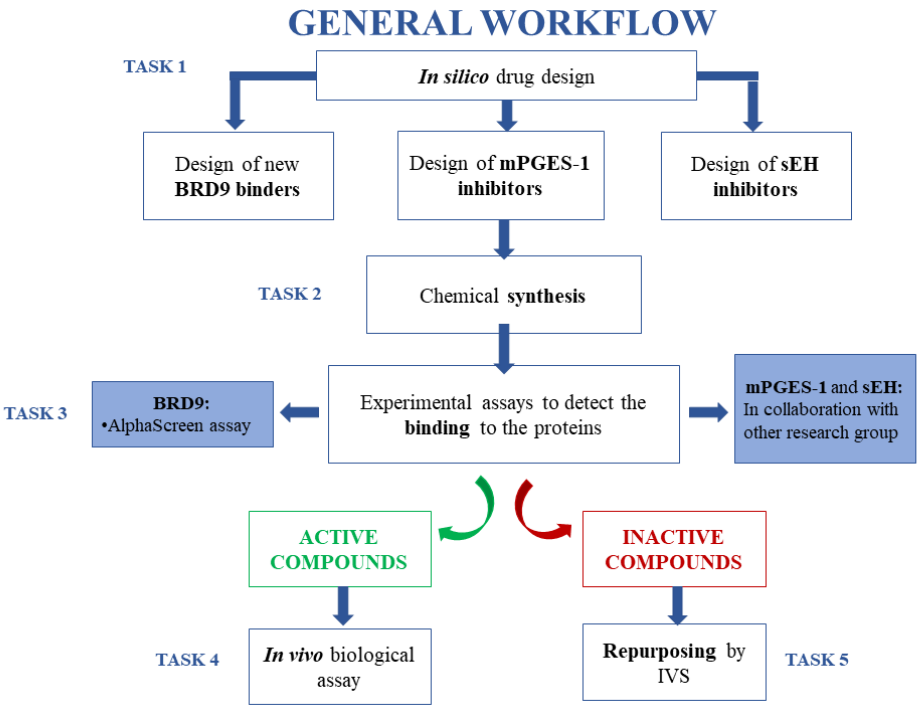

Figure 1. General workflow.

The final goal of these projects was related to the identification of molecules able to target the selected protein while also to synthesize them in large quantities in a relatively short time in order to be tested *in vivo*. In light of this, we focused our attention on fast and versatile synthetic methods. In particular, we chose:

1) *One pot procedures* (**Chapter 2**, **paragraph 2.2**; **Chapter 3**, **paragraph 3.2**). Several reaction sequences are conducted in the same reaction flask in order to reduce the

reaction and the purification time. The limited number of synthetic steps results in the reduction of reagents and solvents needed but also in the reduction of the waste formation.[1-3] Therefore, given its sustainability compared to traditional methods, one pot procedure is considered a green chemistry approach.[4]

2) *Microwave-assisted synthesis* (**Chapter 2**, **paragraph 2.5; Chapter 4**, **paragraph 4.2.2**). The main advantage of this procedure resides in the more homogenous heating by direct coupling of microwave energy with the bulk reaction mixture. This is an efficient mode of heating that results in the reduction of reaction times and improved yields. In addition, the microwave technique is particularly suitable for solvent-free reactions due to the direct absorption of the radiation by the substrates and not by the solvents; thus increasing the benefits of microwave irradiation. As one pot procedures, also microwave-based reactions are considered among the green chemistry approaches.[5]

3) *Multistep synthetic strategy* (**Chapter 2**, **paragraphs 2.3-2.6; Chapter 3**, **paragraph 3.3**.*).* After selecting a specific scaffold, in case no one-pot procedure was reported in literature, we opted for the synthetic strategy allowing the obtainment of the selected molecules in the shortest number of synthetic steps. This strategy allowed us to obtain different scaffolds featuring several functionalization to be evaluated on the target of our interest.

4) *Diels-Alder reaction (DA)* (**Chapter 4**, **paragraph 4.2.2**.). The reaction leads to a hexatomic ring closure; moreover, if the dienophile contains a heteroatom, the reaction could also allow the formation of heterocycles. In light of this, the *DA* reaction represents a powerful method to obtain cycloadduct useful in medicinal chemistry. In addition, the presence of fluorine on the final product permits to obtain promising chemical items in terms of interaction with the target and pharmacokinetic properties. For this reason, during my research stay at the University of California Berkeley, I conducted experiments aimed at describing new enantioselective Diels-Alder reactions

to be applied on fluorinated dienes, previously generated with a new approach (unpublished data) developed by Toste's group. Specifically, I focused on the development of new substrates functional to the reaction. This work gave me the opportunity of expanding my knowledge on stereoseleoselective synthesis, along with new synthetic approaches/methods that are pivotal for the design and synthesis of future binders on the targets of our interest.

CHAPTER 1

1.1 Epigenetics and epigenetic modifications

Epigenetics is a genomic branch defined as the study of the structural adaptation of chromatin to exogenous signals. Specifically, epigenetics embraces all the chromosomal modifications associated with both, DNA repair, or cell-cycle phases, and stable changes maintained across multiple cell generations. In simple words, we can say that the epigenetic mechanisms are all the inheritable changes in gene expression with no alterations in DNA sequences.[6] The term epigenetics was first introduced by Conrad Waddington, however many further definitions have been given from 1942 to date. Chemical modifications of DNA and histones are dynamically laid down and removed by chromatin-modifying enzymes in a highly regulated manner. Four different DNA modifications and 16 classes of histone modifications have been at least well elucidated. [7-9] These modifications can alter chromatin structure by modifying noncovalent interactions within and between the nucleosomes. They also serve as docking sites for specialized proteins with unique domains, called "chromatin readers," that specifically recognize these modifications and recruit additional chromatin modifiers and remodeling enzymes, which, in turn, act as the effectors of the modification. The information conveyed by the epigenetic modifications plays a critical role in the regulation of all DNA based processes, such as transcription, DNA repair, and replication. Consequently, abnormal expression patterns or genomic alterations in chromatin regulators can have profound effects and can lead to the induction and maintenance of various cancers. Hence, disruption of the epigenome is a well-recognized fundamental mechanism in cancer, and several epigenetic drugs have been proven to modulate cell survival and to be less toxic than conventional chemotherapy.[10] However, although significant advances have been done in this field, many questions still remain unsolved.

1.1.1 Regulation of chromatin by histone modifications

Chromatin or histone components are subject to a wide variety of covalent, reversible, post-translational modifications, such as acetylation, mono-, di-, and trimethylation on lysine residues, symmetric or asymmetric mono- and dimethylation on arginine residues, phosphorylation on serine and threonine residues, ubiquitination, biotinylation, and SUMOylation (Small Ubiquitin-like Modifier or SUMO) on lysine residues, and finally mono-ADP-ribosylation on arginine and glutamate residues. Although many examples of modifications within the central domains of histones have been identified, the majority of these post-translational modifications occur on the lysine amino-tails, due to their protruding position from the nucleosome core. These modifications, individually or in combination, are able to influence inheritable epigenetic programs that encode distinct nucleosome functions, such as gene transcription, X-chromosome inactivation, heterochromatin formation, mitosis, and DNA repair and replication.[11-12] Mechanistically, these functions are exerted either directly, by altering nucleosome interactions with chromatin, or indirectly, by recruiting effector proteins that, with specific modules, recognize particular histone modifications in a sequence-dependent manner. In addition to their catalytic functions, many chromatin modifying factors also possess "reader" domains, allowing them to bind to specific regions of the genome and respond to the information conveyed by upstream signaling cascades. The amino-acidic residues that line the binding pocket of the reader domains can dictate a particular preference for specific modification states, [11] whereas residues outside the binding pocket contribute to determining the histone sequence specificity. The basis underlying these epigenetic codes resides in the substrate specificity either of the enzymes that catalyze the several covalent modifications, or of the enzymes that remove these marks to reverse the modifications. Given that chromatin is the physiological template for all DNA-mediated processes, it is not surprising that histone modifications represent an essential component in controlling the structure and/or function of the chromatin, with different modifications yielding distinct functional consequences. Indeed,

site-specific histone modifications have been shown to correlate with particular biological functions such as gene transcription, chromatin remodeling and apoptosis regulation.[13]

1.1.2 Histone acetylation

Histone acetylation is an epigenetic mark, largely present at DNA promoter regions and often associated with an open chromatin structure. This makes chromatin accessible to transcription factors and can significantly increase gene expression. However, acetylation low levels are also found throughout transcriptionally active genes, and for this reason, this issue is still under debate. Histone acetyltransferases (HAT) and Histone deacetylases (HDACs) are the enzymes responsible for writing and erasing the acetylation tag on the histone tails. In particular, the histone acetyl transferase is responsible for transferring an acetyl group to the ε-amino group of side chains of lysine, using acetyl Coa as a cofactor. This type of process is mainly carried out in the promoting regions, with the preferential targets being the residues of lysine of histone H3 and H4.[14] These enzymes can make changes in several sites, destabilizing the electrostatic interaction between DNA and histone, thus facilitating the formation of a nucleosome in which transcription can take place. In contrast, HDAC have the task of restoring the positively charged lysine, which stabilizes the structure of chromatin leading to a suppression of the transcription.[15] These enzymes are able to deacetylate multiple sites within histones. In addition, some structural domains known as reader interact with tails histone acetylates, so many proteins that have this domain have acetyltransferase activity and have a specific action on histone tails. Various protein domains have been identified so far that bind specifically to acetylated histones. These include bromodomains (BRDs), double PHD finger and Yeats domains.[16]

1.1.3 Bromodomains

Bromodomains (BRDs) are protein domains able to recognize the changes introduced by the writers. The bromodomains can selectively recognize and bind ε-N-acetyl-lysine residues histone tails and play a key role in gene expression. The name bromodomains comes from the Brahma gene of Drosophila, in which the bromodomain sequence was identified for the first time. Since the first discovery, bromodomains have been found in many nuclear proteins, such as HAT, chromatin remodeling complexes ATP-dipendent, methyl-transferases and transcriptional coactivators. In more detail, the human genome encodes 61 BRDs in 46 different proteins with catalytic function involved in some pathological processes and present in most tissues: [17]

Bromodomain-containing proteins are grouped in eight main families (**Figure 2**). The most studied is the BET proteins (Bromo- and Extra-Terminal-Domain) that includes BRD2, BRD3, BRD4 and BRDT (Bromodomain testis-specific protein), such proteins encoded by paralogous genes that may have been generated by duplication of an ancestral gene.[18]

BRD7 and BRD9 proteins contain bromodomain but do not belong to the BET families. BRD7 is a subunit of a specific chromatin-remodeling complex, PBAF, the factor associated with BRG1. Several studies have highlighted its involvement in the development of multiple tumors as a gene suppressor, and is involved in both pathways p53 and BRCA1 (breast cancer).[19]

BRD9 is a component of the switch/sucrose non-fermentable (SWI/SNF) complex, important for gene expression and cell growth. BRD9 recognizes and binds acetylated or butyrate lysine residues, inducing post-translational modifications, involved in several diseases including cancer.[19]

All bromodomains share a preserved secondary structure, consisting of four α-helices (αZ, αA, αB, αC) called "BRD fold" and two loops (ZA and BC). The ZA loop connect αZ and αA helices, the BC loop connect the αB and αC helices.

The acetyl-lysine binding site (Kac region) consists of a preserved asparagine essential for the acetyl-lysine recognition of ZA and BC loops, of a hydrophobic area called "shelf", and of the first residue of the alpha helix αC called gatekeeper, the latter usually hydrophobic. In the BET family, the gatekeeper is an isoleucine-valine which limits the size of the deep part of the pocket.[20] In contrast, for BRD7 and BRD9 the gatekeeper is a tyrosine residue.

Bromodomains are classified according to the amino acid sequence at the binding site and this is important for the interaction with the ligand, for this becomes a crucial classification of the binding site in order to assess the selectivity of the inhibitors.

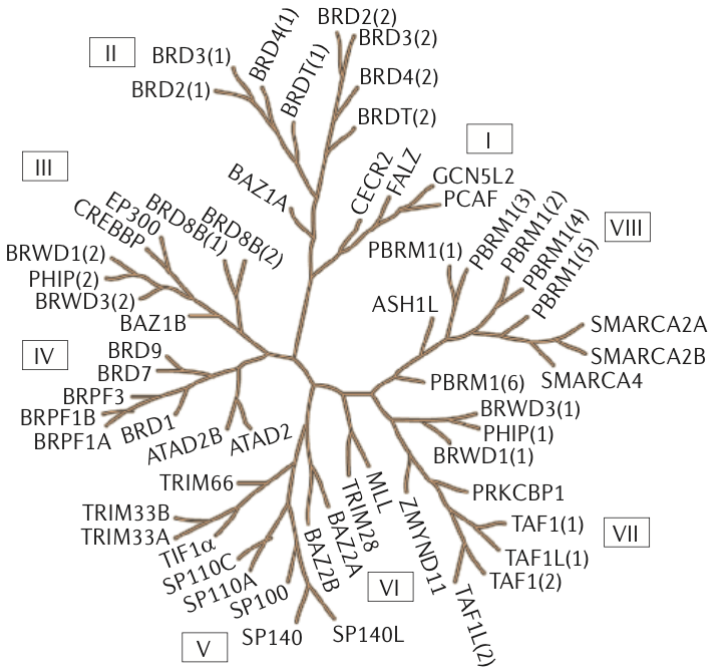

Figure 2. Phylogenetic tree of human BRDs. The different families are named by Roman numerals (I to VIII).

1.1.3.1 BRD9

BRD9, bromodomain-containing protein 9, is an epigenetic reader, subunit of the SWI/SNF chromatin remodeling complex, important for differentiation and cell proliferation. In addition, BRD9 is at the center of multiple signal transduction pathways, chromosomal activities and nuclear organization.[21]

BRD9 recognizes and binds the acetylated lysine residues on histone tails but also the butyrate histones. Structurally, BRD9 is similar to other bromodomains; therefore also in this domain the two AZ and BC loops form the binding site for the Kac, and consists of preserved asparagine.[22] In this case, Asn100 is located in a region called N-site; water molecules, adjacent to the BC loop where there is the gatekeeper, which in the case of BRD9 is Tyr106, are also present. This hydrophobic residue interacts with both the aliphatic part of acetyl-lysine and with the acetyl group, creating a wall of the bond pocket and blocking .the entrance to the lipophilic shelf.[20]

BRD9, induces post-translational modifications, which can lead to biological alterations and therefore to pathologies as severe as tumors, including acute myeloid leukemia (AML), renal carcinoma, non-small cell lung cancer, malignant rhabdidae cancer, breast cancer, cervical carcinoma and then hepatocellular carcinoma.[23]

1.1.3.1.1 BRD9 binders

Considering the structural similarity between the various bromodomains, non-selective inhibitors were first developed. LP99 is the first selective BRD9/BRD7 selective inhibitor (**Figure 3b**) which has a K_D value of 99nM versus BRD9 protein.[24] The development of such inhibitors started from a well-specified lead compound 1-methylquinolone (**Figure 3a**). This choice was made since the N-methyl amide portion is a mimetic of acetyl-lysine, forming H

bonds with an asparagine preserved and a molecule of water. A heterocycle a δ-lactam was inserted in position C7, with the idea of exploiting the hydrophobic cavity ZA for selective inhibition of the protein. Subsequently, a methyl was introduced in position 4, interacting with the hydrophobic portion at the surface, thus increasing the affinity of the compound. The valerolactam was further derivatized to increase the selectivity: a phenyl that interacts with another hydrophobic cavity was inserted at C6, while a sulfonamide group creating a further H link between the NH of the group and Gly43 carbonyl group and hydrophobic interactions with Phe47 was introduced at C5. Finally, the compound was solved in its enantiomers. In fact, co-crystallization studies showed the enantiomer targets BRD9 is the 2*R*,3*S*.

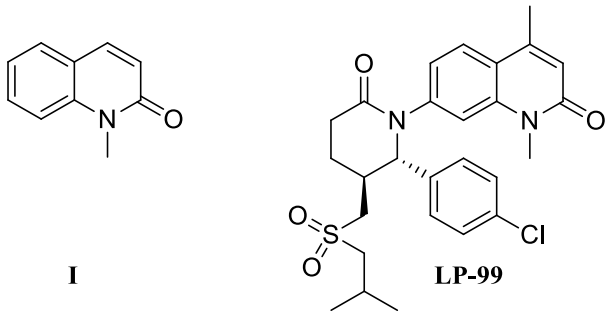

I **LP-99**

Figure 3. Structure of LP-99 and its lead compound.

The approach used to improve selectivity was to analyze the area ZA less preserved than BRD9, highlighting how carbonyl and methyl were critical for the interaction with the anchoring site. In the ZA channel, an important amino acid, i.e. Phe44, gives T-stacking (π-π) interactions with phenyl. The introduction of electron donor groups on phenyl has improved potency and selectivity by increasing the T-stacking interaction; in particular, 3,5-dimethoxyphenyl is used, which adopts a conformation allowing optimal T-stacking interaction with the Phe44.

Studying what are the changes in the area of the linker ZA, they observed an increased selectivity towards BRD9 compared to BRD7 counterpart due to reduced flexibility of BRD9 compared to BRD7. Compounds BI-7271, BI-7273, BI-9564 (**Figure 4**) were disclosed by enlarging the structure of dimethylpyridinone designing ring-fused compounds, showing good potency and selectivity against BRD9.[24]

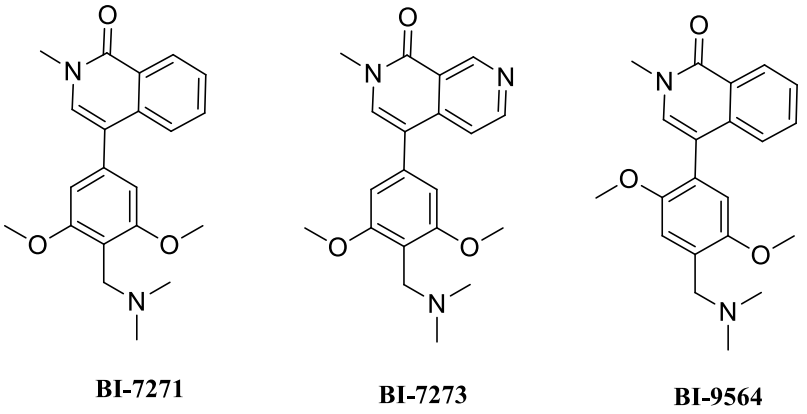

Figure 4. Chemical structure of BI-7271, BI-7273, BI-9564.

Theodoulou, N.H. et al. developed the first selective cellular chemical probe for BRD9, I-BRD9 (**Figure 5**).[25] I-BRD9 was identified through structure-based design, leading to greater than 700-fold selectivity over the BET family and greater than 70-fold against a panel of 34 bromodomains.

The carbonyl portion of the pyridonic ring forms an H bond with the NH group of the Asn100 side chain and an H bond with Tyr57 by means of a molecule of water, the N-methylpyridone group is located in a pocket consisting of Phe45 and Val49, surrounded by four water molecules mimicking the Kac residue. The rings of the thienopyridone (**Figure 5**) occupy the hydrophobic groove formed by Ala54 and Val49of the ring ZA on one side and the Tyr106 on the other. The dimethoxyphenyl in position 7 extends outwards through the ZA channel in contact with Phe44

and Ile53 on both sides, and in particular the two methoxylic groups form a network of H bond by water molecules. In fact the one in position four forms a H-bond with the carbonyl of the His42. Finally, the thienopyridone was replaced trying various substituents that could improve as much as possible power and selectivity. After I-BRD9, other inhibitors were developed and are now currently available (not showed in the present thesis) (**Figure 6**).

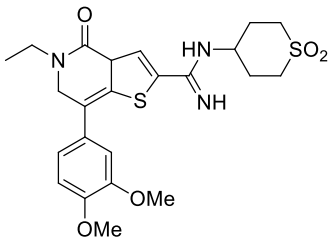

I-BRD9

Figure 5. Chemical structure of I-BRD9.

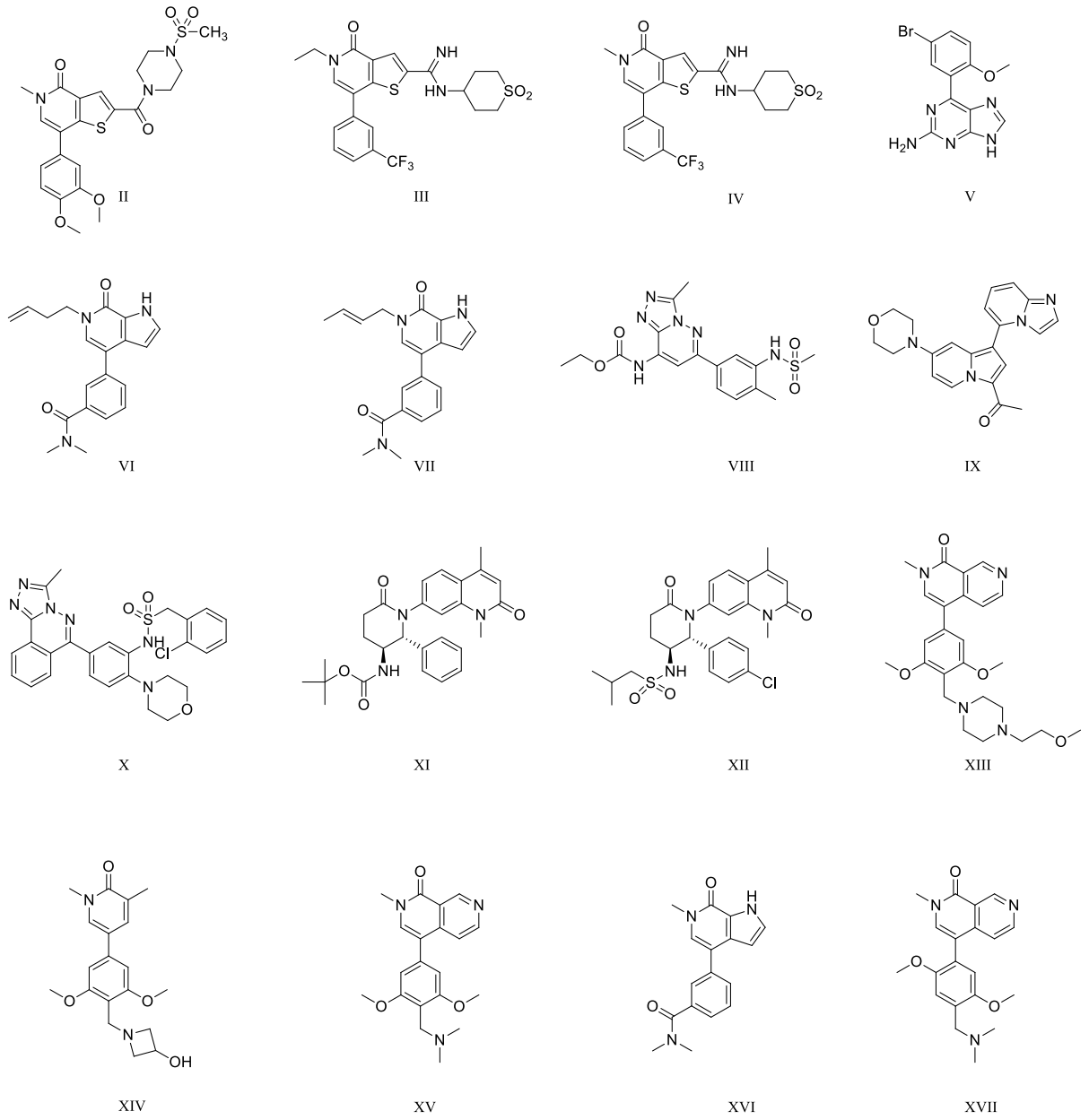

Figure 6. Structure of sixteen BRD9 binders.

1.2 Multiple pathways of the arachidonic acid cascade

Prostaglandins (PGs) represent an important class of potent biological lipid mediators that are ubiquitously found in animal tissues and are associated with physiological and pathological processes.[26-27] The most abundant PG in humans is prostaglandin E_2 (PGE_2), a key mediator of inflammation, pain, and fever, also involved in the protection of the gastrointestinal mucosa, blood pressure regulation, and ovulation. During the initial phase of the inflammatory response,

PGE_2 and related prostanoids, such as PGI_2, act as vasodilators to facilitate the tissue influx of neutrophils, macrophages, and mast cells from the bloodstream, leading to swelling and edema of the infection or the injury site.[28] PGE_2 possesses the ability to stimulate the eicosanoid class switch; indeed, it blocks the biosynthesis and the release of pro-inflammatory mediators, such as TNFα, IL-1β, IL-8 during the terminal phase of inflammation, and stimulates the formation of IL-10, lipoxins, resolving, and protections which actively antagonize inflammation.[29] Furthermore, PGE_2, stimulates the sensory nerves to increase the pain response, acts on neurons to promote pyrogenic effects, and activates a subset of T helper cells, which are characterized by the production of interleukin 17 (IL-17), important in the recruitment of monocytes and neutrophils to the site of inflammation. For this reasons, inhibiting the production of PGE_2 can be an efficient method for anti-inflammatory purposes and, considering the correlation between cancer and inflammation, also for anticancer treatment.

The PGE_2 biosynthesis starts with the release of arachidonic acid (AA) from the phospholipid membrane through the action of phospholipases A_2 (PLA_2) and phospholipase C (PLC).[30] PLA2 hydrolyzes phosphatidylcholine and phosphatidylethanolamine, the main source of AA, while PLC hydrolyzes phosphatidylinositol and phosphatidylinositol phosphate to form diacylglycerol (DAG), which, in turn, is converted by DAG lipase into 2-arachidonoyl glycerol (2-AG), an important precursor of AA.[31] The oxygenation of AA is performed by cyclooxygenases 1 and 2 (COX-1/COX-2): COX-1 is constitutively expressed in most tissues and contributes to the homeostatic PGE_2 production, while COX-2 is induced following pro-inflammatory stimuli and is essential for PGE_2 production in inflammatory processes. The COXs action produces the prostaglandin G_2 (PGG_2), which is subsequently reduced to prostaglandin H_2 (PGH_2). PGH_2 is then converted by different synthases into a variety of prostanoids ($PGF_{2\alpha}$, PGD_2, PGI_2), including PGE_2 and thromboxane A_2 (TxA_2) (**Figure 7**). In particular, the conversion of PGH_2 into PGE_2 is due to the action of PGE_2 synthases (PGES).[32]

Currently, three PGES isoenzymes have been identified: the cytosolic PGES (cPGES) and two microsomal PGESs, mPGES-1 and mPGES-2.[33] cPGES is constitutively expressed in most tissues and functionally coupled to COX-1. It is considered the main responsible for homeostatic PGE_2 production and requires GSH as an essential cofactor. [33] mPGES-1, which will be discussed in detail later, is responsible for the production of PGE_2 under proinflammatory stimuli. Its function is to downstream of cyclooxygenase (COX)-2 in the PGE2-biosynthetic pathway. Finally, mPGES-2 can convert PGH_2 derived from both COX-1 and COX-2 in PGE_2, therefore it is related to the production of PGE2 both under inflammatory stimuli and not.[34-35]

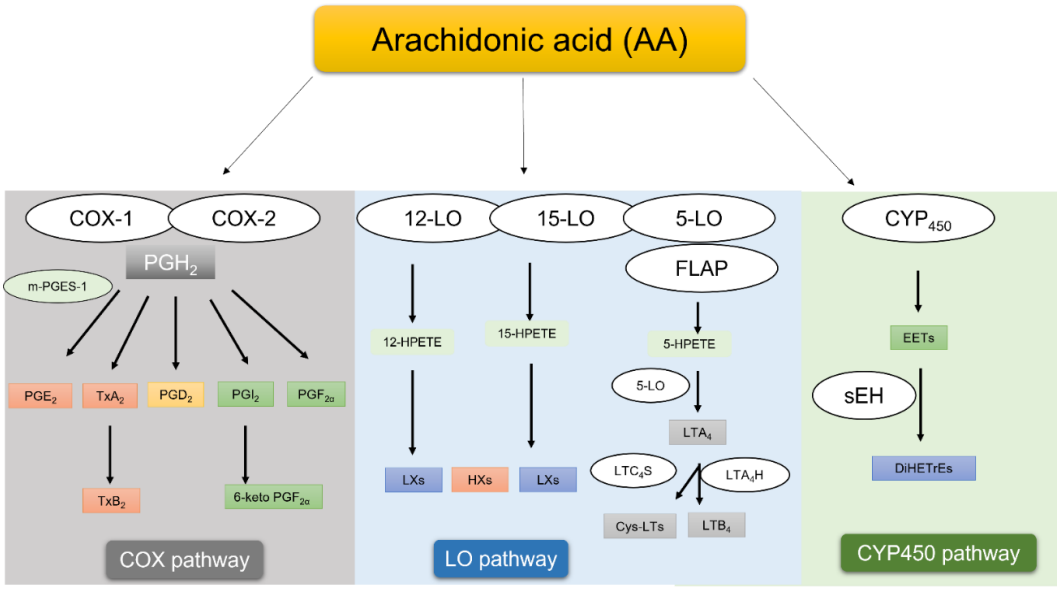

Figure 7. The three different pathways of the arachidonic acid cascade are shown, reporting each pathway's main targets and metabolites.

The classical NSAIDs, which inhibit both COX-1 and COX-2, lead to severe side effects, such as gastric irritation, kidney problems, and hypertension, caused by the massive suppression of PGE_2 which exerts pleiotropic functions included gastric protection, following the deletion of

COX-1. On the other hand, selective inhibition of COX-2 leads to cardiovascular diseases.[36] For this reason, the specific inhibition of mPGES-1, the terminal synthase in PGE_2 biosynthesis, should suppress the synthesis of prostanoids induced by inflammatory stimuli, without affecting PGE_2 constitutively expressed. This would consequently lead to fewer side effects and, thus, a better pharmacological profile for mPGES-1 inhibitors. Hence, in the last years, mPGES-1 has been the focus of extensive investigations aiming at clarifying its involvement in a range of pathological conditions like cancer genesis and progression. High levels of the enzyme and its biosynthesized product, PGE_2, have been found in several human cancers, including colon, lung, pancreas, and brain tumors. mPGES-1 overexpression appeared to be strictly correlated to a worse prognosis.[37] Often, high levels of mPGES-1 are associated with a concomitant COX-2 overexpression; however, recent studies outlined that the terminal synthase can be induced also apart from COX-2, providing evidence that these enzymes can be independently regulated. These data strongly support the possibility to target mPGES-1 activity in order to obtain the concomitant PGE_2 suppression, avoiding the toxicity associated with COX-2 inhibition.

On the other hand, the fundamental role of soluble epoxide hydrolase (sEH) and epoxyeicosatrienoic acids (EETs) in inflammation and pain has been broadly investigated in the last years. Soluble epoxide hydrolase (sEH) is another enzyme involved in the arachidonic acid cascade. When arachidonic acid is metabolized by cytochrome p450s (CYPs) produces endogenous lipid epoxides, such as the EETs and squalene oxide. sEH is responsible for EETs degradation to the corresponding diol products dihydroxyeicosatrienoic acids (DHETs), leading to the lack of their biological benefits.[38] Moreover, several studies[39-40] have shown that sEH inhibitors decrease plasma levels of pro-inflammatory cytokines and nitric oxide metabolites, thus promoting the formation of lipoxins and supporting the inflammatory resolution. These data suggest that sEH inhibitors may have valuable therapeutic effects in the treatment and management of acute inflammatory diseases. In mammalian cells, different epoxide hydrolase

isoform can be identified, each of them taking part in detoxifying mutagenic and carcinogenic xenobiotic oxiranes.[41] However, basing on the abundance of the sEH relative to the other ones in most tissues such as liver,[42] kidney[43] and intestine, this isoform majorly contributes to the metabolism of epoxy-fatty acids *in vivo*.

For these reasons, both mPGES-1 and sHE are interesting target for the treatment of inflammation and, considering their connection, of the cancer. Our group has been involved for several years in research on new hit compounds targeting mPGES-1. Moreover in the last period we turned our attention to epoxide hydrolase, to inhibit the enzyme alone or in a synergistic effect with mPGES-1.

1.2.1 mPGES-1

Prostagrandin E_2 Synthases (mPGES-1, mPGES-2, cPGES) are enzymes involved in the inflammatory response since they catalyze downstream the conversion of prostaglandin H_2 (PGH_2) in its isomer prostaglandin E_2 (PGE_2). mPGES-1 is ubiquitous, but its concentration is up-regulated after exposure to various inflammatory stimuli[44] and mediators, e.g. cytokines (LPS, IL-1β and TNF-α). Different studies reported by Jackobsson et al.[45] demonstrated the compound belongs to the superfamily of membrane-associated proteins involved in eicosanoid and glutathione metabolism (MAPEG),[46-47] together with 5-lipoxygenase-activating protein (FLAP), leukotriene C4 synthase (LTC4S) and microsomal glutathione transferases (MGST1, MGST2, MGST3).[47] The first structure was reported in 2008 by 3D-electron crystallography at low resolution,[48] and Sjögren et al. reported in 2013 the high resolution (1.16 Å) X ray crystal of mPGES-1 in the active conformation, in complex with its cofactor glutathione.[49] Structurally, it is a membrane protein of 16 kDa with a total number of 153 amino acids in mice and rats and 152 amino acids in humans because of the absence of the 11th amino acid. The tridimensional disposition of the enzyme consists of a homotrimer in the endoplasmic reticulum membrane, and each monomer is organized in four helices, named TM1, TM2, TM3 and TM4. Three

equivalent active sites are placed in the three monomers within the membrane-spanning region at each monomer interface. Each active site is oriented towards the cytoplasmic part of the protein, between the N-terminal parts of TM2 and TM4 of one monomer and the C-terminal part of TM1 and the cytoplasmic domain of the next monomer (**Figure 8**). [49]

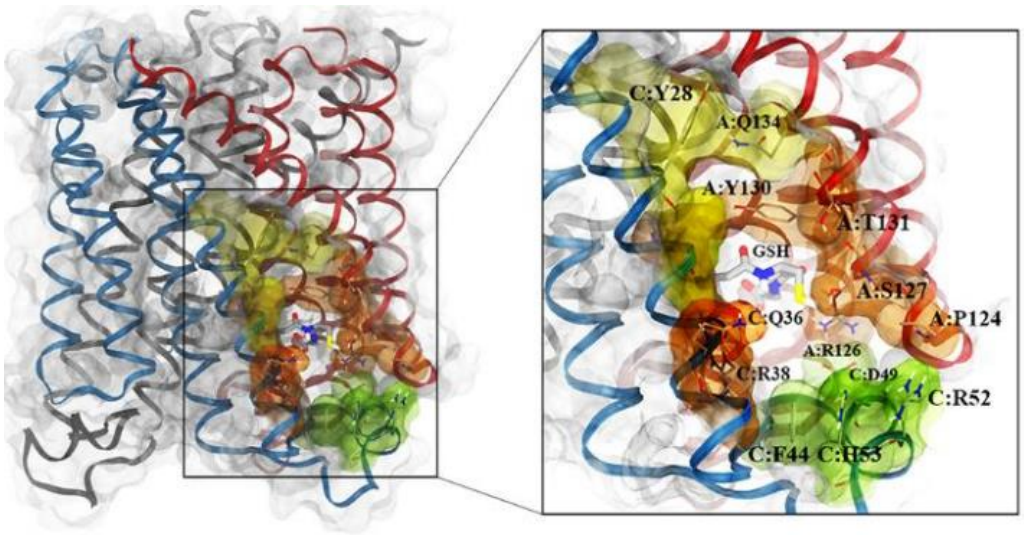

Figure 8. On the left, transparent molecular surface representation of mPGES-1, with chains A, B and C depicted in red, black, and blue ribbons, respectively; on the right, representation of the mPGES-1 binding site with the co-factor (GSH).

According to Jegerschöld et al.,[48] mPGES-1 has to perform a change from the closed to the open conformation in order to allow access of PGH_2 to the active site. In the last few years, the tridimensional X-ray structures of the enzyme have been crystallized in the open conformation. The investigation of the involvement of GSH cofactor in the catalytic mechanism by the replacement of cysteine residue by a serine residue in GSH molecule, confirmed the fundamental role of the thiol moiety in the conversion of PGH_2 in PGE_2.[50] The access of inhibitors is blocked by the so-called "gate keepers" (Thr131, Leu135 and Ala138, probably Arg52 and His53 too). Regarding Ser127 residue, it was considered able to activate the thiol moiety of the cofactor for starting the catalytic cycle, but recent studies including a combination

of site-directed mutagenesis (Ser 127 has been replaced by an Alanine) and activity assays with a structural dynamics analysis, demonstrated Ser127 is not essential for catalysis.[50] Conversely, similar investigations corroborated the crucial role of Arg126 and Asp49 in the catalysis. In detail, the interaction between the positively charged Arginine and the negatively charged Aspartate is key for the whole mechanism. In addition, analysis of the active site showed that a water molecule forms a hydrogen-bonding network between the α-carboxylate and the thiol moiety of GSH, inducing the deprotonation of the latter and the formation of the thiolate which is then stabilized by interaction with the guanidine moiety of Arg126. Two different mechanisms were proposed:

1. The thiolate attacks upon endoperoxide ring at the C-9 position, the O-O bond is cleaved, and S-O bond is formed. Simultaneously, Asp49 reduces the pKa of the C-9 proton, leading spontaneously to the yield of the PGE_2 isomer (**Figure 9a**).
2. The thiolate as a base removes the C-9 proton, inducing the cleavage of the unstable O-O bond and the formation of the product (**Figure 9b**).

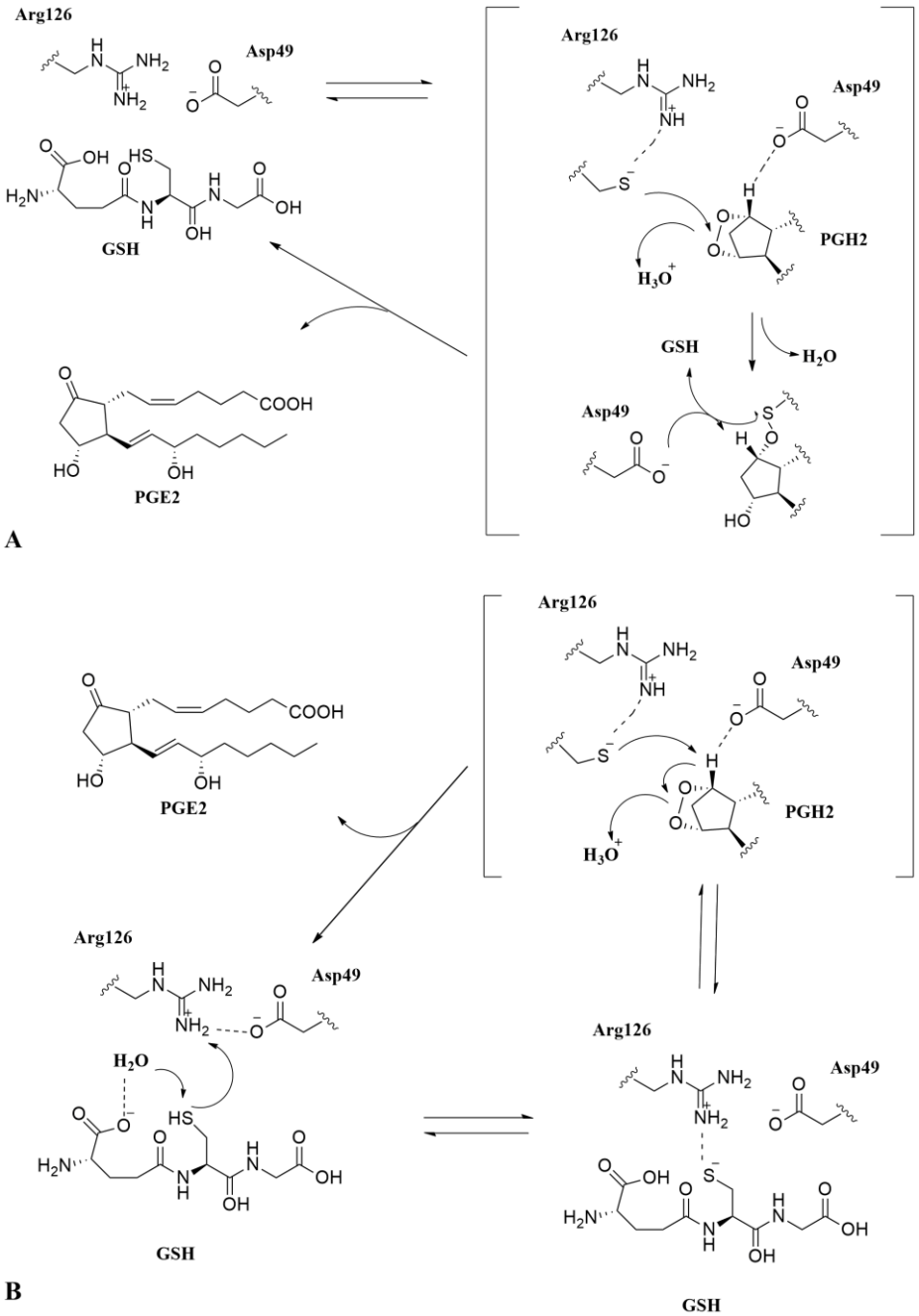

Figure 9. A) Proposed mechanism of mPGES-1; B) Alternative mechanism of mPGES-1.[50]

1.2.2 mPGES-1 inhibitors

A significant problem in mPGES-1 targeting is the sequence dissimilarity of the enzyme isoforms in the different species. For example, potent inhibitors against the human enzyme may partially or entirely lose potency against the rat isoform, mainly due to the variation of three

amino acids located in the transmembrane helix IV, which play a crucial role as gatekeepers for the active site of mPGES-1, regulating the access of a possible inhibitor. In the human enzyme, these residues are rather small (Thr131, Leu135 and Ala138), but in the rat isoform they are bulkier or aromatic (Val131, Phe135 and Phe138), and thereby prevent the access to inhibitors for steric hindrance reasons. Although a large number of potential natural[51-56] and synthetic[57-63] mPGES-1 inhibitors are reported in the literature (**Figure 10**, **11**), none of them have passed all the clinical trials yet, and consequently, no drug useful for the treatment of inflammatory and pathological states resulting from the PGE_2- synthase deregulation has been developed.

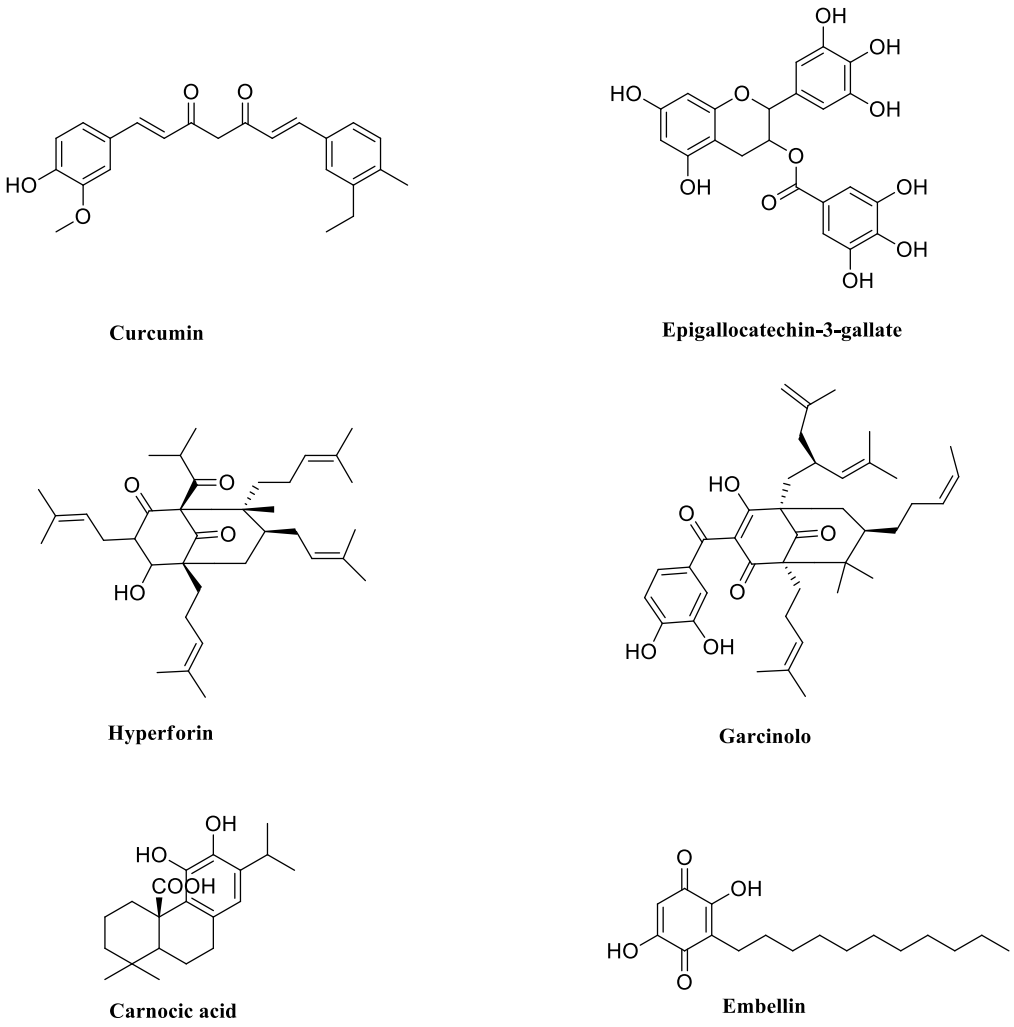

Figure 10. Structures of natural mPGES-1 inhibitors.[51-56]

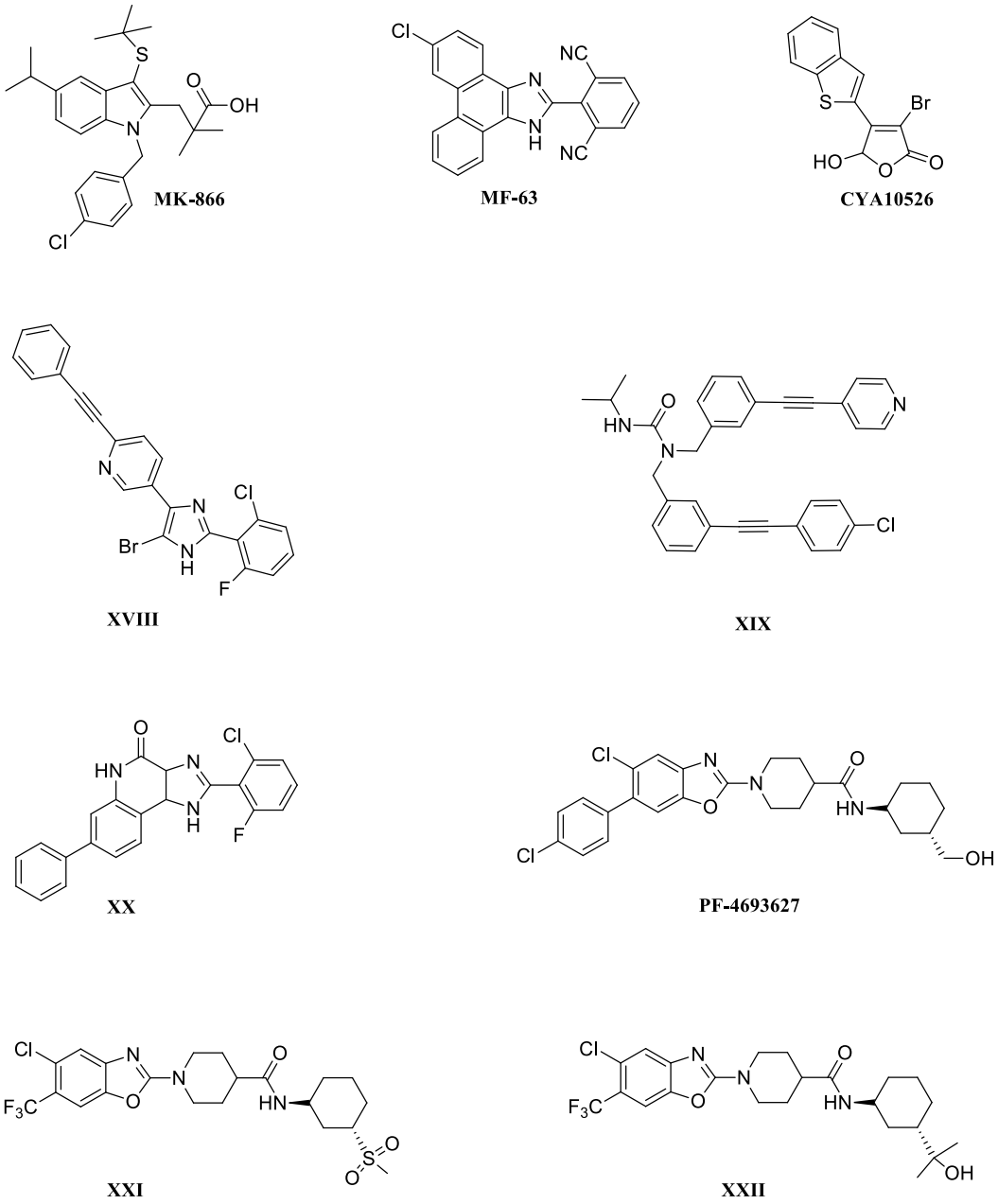

Figure 11. Structure of some of the synthetic mPGES-1 inhibitors. [57-63]

Despite the challenges associated with the exploration of this biological target, selective inhibition of mPGES-1 might represent a promising approach for the design of effective anti-inflammatory drugs lacking the severe side effects related to the use of the classic NSAIDs. Hence, the identification of potent and selective mPGES-1 inhibitors with good ADME (Absorption, distribution, metabolism, excretion) properties is a goal that must still be achieved. To date, two compounds entered the clinical trials: **GRC27864** and **LYS3023703** (**Figure 12**). [64- 65]

GRC27864[64] presents a pyrimidine scaffold (IC_{50}= 5nM); it was able to interfere with the production of PGE_2 in synovial fibroblasts and chondrocytes deriving from tissues affected by rheumatoid arthritis and osteoarthritis. Other biological assay demonstrated that it is also a potent inhibitor of recombinant guinea pig mPGES-1 enzyme (IC_{50} = 12nM) and 1000-fold selective over COX-1, COX-2, mPGES-2, cPGES, and the other enzymes of arachidonic acid cascade. It is currently in phase 2 of clinical trials (**Figure 12**). **LY3023703**, [65] the second compound that entered the clinical trials, showed a higher potency in enzyme inhibition than celecoxib. Nevertheless, the **LY3023703** clinical trial was ultimately terminated due to liver injury induced by the drug.

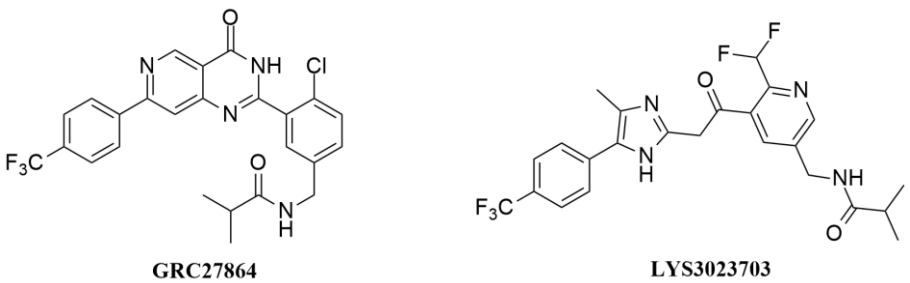

Figure 12. GRC27864 and LYS3023703 structures.

1.2.2 sEH

In mammalian cells, epoxide hydrolase exists in different isoform: epoxide hydrolase 1 (EH1 or mEH) bonding to endoplasmic reticulum, and a soluble epoxide hydrolase (sEH), the cytoplasmatic isoform. In addition, recent genome analyses have revealed two new possible epoxide hydrolases (EH3 and EH4)[66], but no data on their activity or substrate specificity have been published so far. Both mEH and sEH take part in detoxifying mutagenic and carcinogenic xenobiotic oxiranes. However, determination of kinetic constants has disclosed that the sEH hydrolyzes epoxy-fatty acids around 100-fold faster than the mEH.[67]Thus, based on the abundance of the sEH relative to the mEH in most tissues such as liver,[68] kidney[69] and intestine, and the low efficiency of mEH with these kind of substrates, the mEH certainly has a minor contribution in the metabolism of epoxy-fatty acids in vivo.[70]For this reason our attention has been focused on the soluble isoform of the hydrolase.

Soluble epoxide hydrolase has two catalytic domains, the domain for lipid epoxide hydrolase activity (sEH-H) is in the C-terminal moiety, while the phosphatase activity (sEH-P) is located in the N-terminal domain.[71]The role of sEH-H in the hydrolysis of epoxides of polyunsaturated fatty acids has been widely investigated, while the role of sEH-P is still unclear. Concerning the structure, the C-terminal domain has a molecular mass of about 35kDa (residues 235-555), and is connected to the N-terminal domain (25 kDa, residues 1-218) through a proline rich linker (residues 219-234), having thus a total mass of 65kDa.[72] The chemical mechanism of the enzyme is related to a catalytic triad (Asp333, His523, Asp495). Specifically, the epoxide group of the substrate is polarized by two tyrosine residues (381 and 465), and Asp333 performs the nucleophilic attack with its carboxylic group. However, Asp333 is firstly activated and oriented towards His523 and Asp495 (**Figure 13**),[72-73] and a recent study suggests that the protonation of His523 is essential for the right orientation of Asp333.[74]

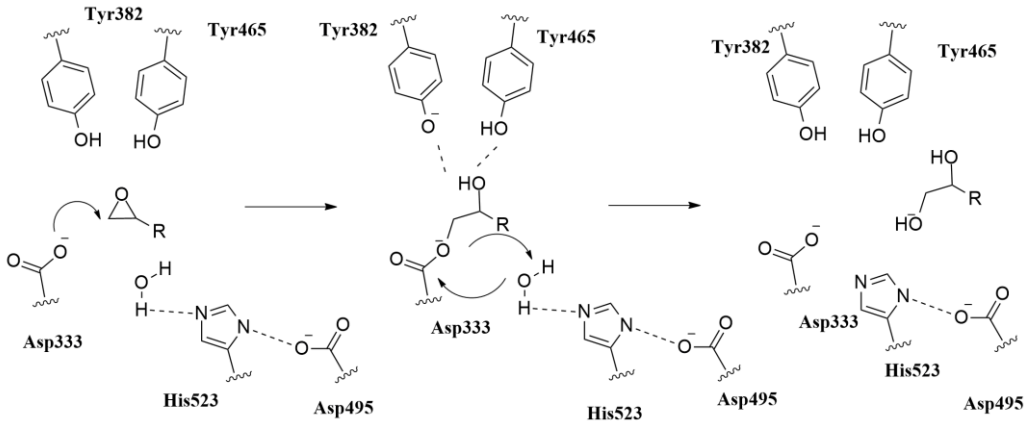

Figure 13. Chemical mechanism of soluble epoxide hydrolase enzyme.

1.2.2.1 Epoxide hydrolase inhibitors

As stated above, soluble epoxide hydrolase (sEH) inhibitors have been shown to effectively increase the levels of epoxyeicosatrienoic acids and reduce the levels of dihydroxyeicosatrienoic acids, which may be translated to therapeutic potentials for multiple disease indications. Hammock group is the pioneer in this field of research. He showed a very broad scaffold to encompass a wide range of sEH inhibitors, in which X and Y can each independently be nitrogen, oxygen or sulfur (**Figure 14a**).[75-76] In addition to ureas, amides and carbamates, numerous pharmacophore types including thioester, carbonate, ester, thiourea, thioamide, amidine, guanidine, heterocycles, aminoheterocycles or aminoheteroaryls were developed as sEH inhibitors.[77]

In 2008, Arete Therapeutics, the most active pharmaceutical company developing sEH inhibitors, described a series of derived disubstituted ureas. The nitrogen on the right is substituted with a five- or six-membered heteroaryl or heterocycle; instead, the other ones contain a phenyl or cycloalkyl group (**Figure 14b**).[78]

Then, Boehringer Ingelheim described pyrazole aniline derived amides as sEH inhibitors that, from preliminary *in vitro* and *in vivo* studies, showed activity in the treatment of T-lymphocyte mediated immunological disorders (**Figure 14c**).[78]

Also, the Merck company explored the therapeutic utility of sEH inhibitors. They discovered various 3,3-disubstituted piperidine-derived ureas with potent inhibitory activity against sEH (IC_{50}=2-5nM) (**Figure 14d**).

Finally, in the last few years, the attention has been shifted to dual inhibitors sEH/5-LO, sEH/COX-2, sEH/LTA4, with the aim to have a synergistic anti-inflammatory effects for the inhibition of multiple enzymes of the arachidonic acid cascade.[78]

In light of this consideration, we decided to apply the general workflow described before (**Abstract**) to discover novel anti-inflammatory agents targeting sEH alone or combined with different enzymes in the arachidonic acid cascade. A particular focus was given to mPGES-1, considering that, to date, there are no reported dual inhibitors mPGES-1/sEH.

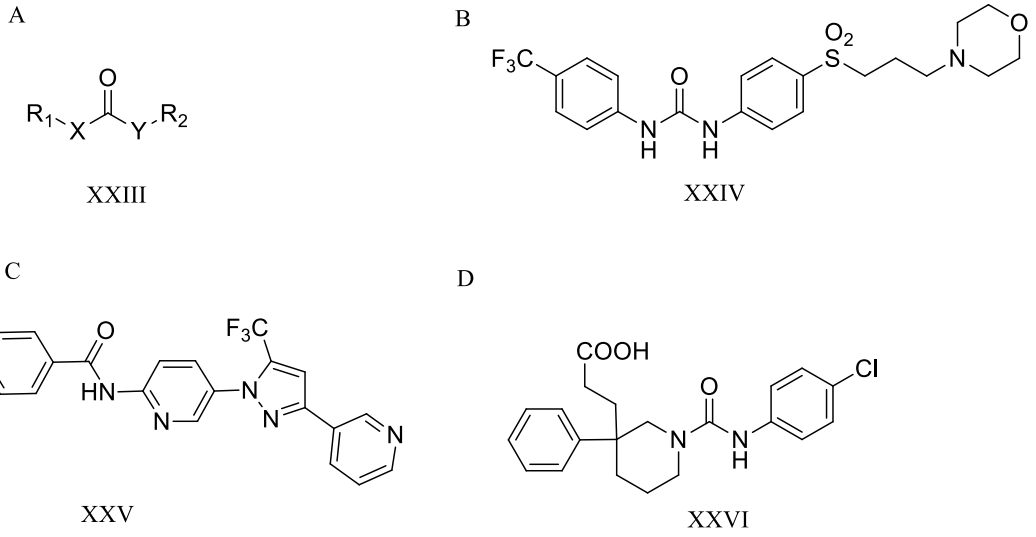

Figure 14. a) Broad scaffold of sEH inhibitors; b) structure of sEH inhibitor described by Arete Therapeutics; c) structure of sEH inhibitor described by Boehringer Ingelheim company; d) structure of sEH inhibitor described by Merck company.

1.3 Cycloaddition reactions

The cycloaddition reactions are reactions in which there is the final formation of a cyclic adduct.[79]

The addition involves the cleavage of π lengths to form new σ bonds; thus, these reactions are classified according to the number of π electron involved for each component:

- [2+2] reactions that occur between two alkenes to give a cyclobutene;
- [4+2] reactions that between a diene and an alkene to give a cyclohexene.
- [4+4] reactions that between two dienes to give polycyclic aromatic molecules.

Cycloadditions react via a pericyclic concerted mechanism, occurring with a continuous rearrangement of electrons. In light of this, some reactions occur easily, whereas others are forbidden. However, to have a better understating of this process we should refer to the orbital symmetry theory described by Woodward and Hoffman in 1970.[80]

In particular, Woodward and Hoffman described the reaction allowed and forbidden in terms of frontiers orbitals, considering only the symmetry of the Highest Occupied Molecular Orbital (HOMO) and the Lowest Unoccupied Molecular Orbital (LUMO).

When the symmetries of π orbitals in the reactants and products match, the reactions are symmetry allowed due to bond overlap in the transition state. If the symmetries of the reactants and products do not match, the reaction is symmetry forbidden. The allowed reactions occur under relatively mild reaction conditions. Instead, symmetry-forbidden reactions may actually occur, but they require much higher energies than symmetry-allowed reactions, and they occur by a different mechanism.

Cycloadditions can be also classified as thermal or photochemical cycloadditions. The cycloadditions [2+2] or [4+4] may occur when the energy source is the light, whereas the

allowed reactions [4+2] are thermal cycloadditions, in which the energy source is heat, in contrast with the forbidden ones, which are photochemical cycloadditions.

Several categories of cycloaddition were described in the literature, including:

- Diels-Alder reactions;
- 1,3-Dipolar cycloaddition reactions;
- Electrocyclic reactions;
- Sigmatropic rearrangements.

1.3.1 Diels-Alder reactions

The first description of Diels-alder reactions (*DA*) by Otto Diels and Kurt Alder in 1928 had a great impact on the world of organic chemistry. For their work on *DA* the two chemists were awarded the Nobel Prize in 1950.[81]

This reaction is a [4+2] cycloaddition between a conjugated diene and an alkene (called dienophile) to form an unsaturated six-membered ring. The reaction involves the formation of new σ-bonds, more stable than the π-bonds. As demonstrated by many reactions with several dienes and alkene as substrates, the reaction occurs due to the *syn* stereospecificity of both the alkene and the diene. In light of this, the prevailing opinions[82-84] agrees with a concerted mechanism, although the debate is still open. *DA* reactions are almost always stereospecific, which means that if an intermediate exits, it cannot have a lifetime sufficient to permit rotation or inversion.

In addition, a substituted dienophile could react in two different orientations respected to the dienes: *endo* and *exo*. In the endo mode the substituents on the dienophile are oriented toward the π orbitals of the diene, the *exo* is orientated away from the π systems. Anyway, in both cases, there is a suprafacial cycloaddition and thus are permitted. In any specific case, several

factors contribute to obtaining the *endo*/*exo* product in a different ratio. In fact, steric effects, electrostatic interactions, and London force could influence the formation of the *endo*/*exo* product.

Diels-Alder reactions are promoted by electron-donating groups on the nucleophilic diene and by electron-withdrawing groups on the electrophilic dienophile. The reason is to be sought in the theory of frontier orbitals.

The cycloaddition occurs as a result of HOMO/LUMO interactions between the electron-rich highest occupied molecular orbital (HOMO) of the diene with the electron-deficient lowest unoccupied molecular orbital (LUMO) of the dienophile. For this reason, in presence of electron-donating groups on the diene and electron-withdrawing groups on the dienophile the reaction is particularly efficient and rapid. However, the HOMO–LUMO energy gap is close enough that the roles can be reversed by switching electronic effects of the substituents on the two components, called inverse electron-demand Diels–Alder reaction. Once more, the reactivity relationship could be explained by referencing frontier orbital rules. When the diene is electron-poor and the dienophile electron-rich, the interaction occurs between the HOMO of the dienophile and the LUMO of the diene.

1.3.1.1 Catalyst of Diels Alder reactions

The best-known catalysts for Diels-alder reactions are Lewis acids[85] ($ZnCl_2$, $SnCl_4$, $AlCl_3$ and derivatives). In fact, if the dienophile is properly functionalized the Lewis acids form complexes with the carbonyl group of the dienophile, increasing the electron-withdrawing capacity of the carbonyl group, which results in lower energy of the dienophile LUMO and a consequent lower energy gap between the orbital involved.

Also, metal cations, such as copper, can catalyst several Diels -Alder reactions.[86] The reason seems to be found in the formation of a chelate with the dienophile, making also photochemical reactions possible.

Finally, the solvent also has a certain effect on *DA*. Non-polar solvents are the traditionally used ones; however, in some cases, water[87-88]or, more in general, polar solvent, could help the success of the reaction.

The positive water effect is to be sought in a double effect: the stabilization of the transition state by a hydrogen bond network or the water ability to render the solute molecules closer to have an easier interaction.

1.3.1.2 Enantioselective Diels-Alder reactions: an overview

Enantioselectivity could be achieved with a chiral catalyst. In fact, many catalysts result from chiral ligands in conjunction with a metal ion that acts as a Lewis catalyst. In this case, the cation performs the catalytic function while the bulky portion has effect on the enantioselectivity.

Another class of chiral ligands is represented by Bis(oxazoline). In 1991 Evans and Corey reported, respectively, the copper-bis(oxazoline) catalyzed asymmetric cyclopropanation of olefins with diazoacetates[89] and the enantioselective iron-bis(oxazoline) catalyzed Diels-Alder reaction of 3-acryloyl-1,3-oxazolidin-2-one and cyclopentadiene.[90]

Also, a tryptophan-derived catalyst that promotes the *DA* reaction between 5-benzyloxymethyl-1,3-cyclopentadiene and 2-bromopropenale (important in prostaglandin synthesis) is reported. The reaction is particularly advantageous, in fact occurring under the tryptophan-derived catalyst reveals an enantiomeric excess of 99%.

The results of the recent chemistry Nobel prize David W. C. MacMillan and Benjamin List fit into this context.

In Mc Millan works,[91] starting from an enantiopure amine, the formation of an iminium ion activates the diene in the Diels-Alder cycloaddition, and the starting chiral amine catalyst is reconstituted after the formation of the *DA* product. On the other hand, Benjamin List described the use of imidodiphosphorimidates (IDPi) to catalyze the *DA* reaction between 4,4-dialkyl-substituted cyclohexadienones with cyclopentadiene.[92]

However, these are just the most famous examples of an open and evolving field of research.

RESULTS AND DISCUSSION

CHAPTER 2
Identification of BRD9 binders

2.1 Introduction

BRD9, a protein module over-expressed in several cancers, including leukemia, belongs to the BRDs family and the complex SWI/SNF subunit. The protein is responsible for recognizing acetylated residues, influencing the regulation of gene transcription.

The scaffolds considered for the potential binders are divided into two groups depending on the *in silico* approach employed for the selection:

- *Interaction-based approach (IBA);*
- *Structure-based three-dimensional pharmacophore-based approach (SBPA).*

Following the *IBA* approach, the molecules were selected after assessing the presence of a set of key interactions with the receptor counterpart. In this case, the scaffolds were chosen evaluating the presence of some chemical portions that would mimic acetyl-lysine of H4 histone, ligand agonist of BRD9 protein. In this context, isoxazolo[2,3-*c*][1,3,5]thiadiazepin-2-one, 4-ethyl-benzo[*d*]thiazol-2-amine and 1,8-naphthyridone-based compounds were considered. Preliminary AlphaScreen results highlighted the inability of these compounds to bind BRD9. For this reason, Inverse Virtual Screening studies were performed on the set of synthesized compounds, with the aim of repositioning them on targets involved in anti-inflammatory and anti-cancer mechanisms other than BRD9.

Instead, the *SBPA* approach allowed us to screen all the selected scaffolds and/or small molecules with the pharmacophore models,[93] after performing docking calculations. In fact, 3D-structure-based pharmacophore models[93] related to BRD9 were recently developed in our research group, representing useful tools for quickly selecting the most promising compounds from virtual screening experiments. Specifically, using known BRD9 binders as template, the following pharmacophore models were disclosed (**Figure 15**):

- a fragment-related pharmacophore model identifying new promising small chemical probes targeting the protein region responsible for the acetyl-lysine recognition (AHRR 4-points model);
- two pharmacophore models for the selection of compounds featuring drug-like properties (AAHHRRR and AAHRRRX 7-points models).

Following this method, the 2,4-dihydro-3*H*-1,2,4-triazol-3-one and quinazolin-4(3*H*)-one-based libraries of compounds were accounted and the related outcomes are reported in the following paragraphs.

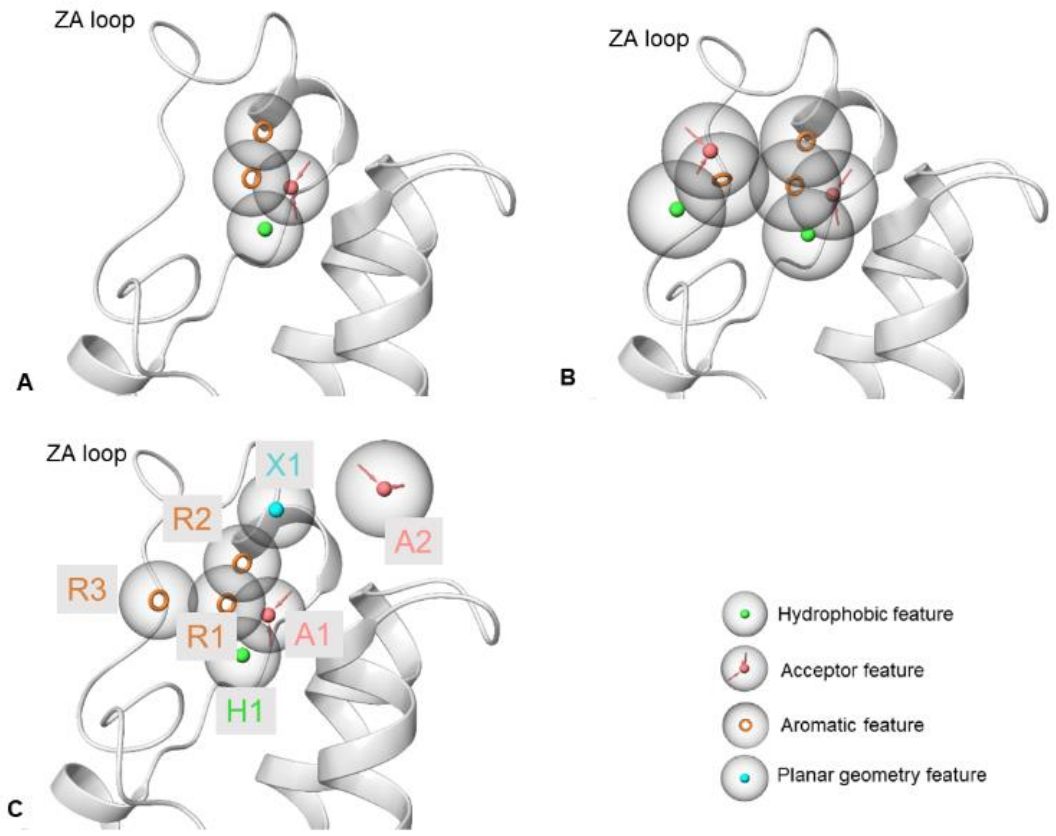

Figure 15. A) AHRR 4-point pharmacophore model ("pharm-fragment"); B) AAHHRRR 7-point pharmacophore model ("pharm-druglike1") from drug-like ligands; C) AAHRRRX 7-point pharmacophore model ("pharm-druglike2").[93]

2.2 Evaluation of isoxazole[2,3-*c*][1,3,5]thiadiazepin-2-one-based compound as potential BRD9 binders

In this study, we have investigated the isoxazole[2,3-*c*][1,3,5]thiadiazepin-2-one scaffold to identify new potential anticancer agents that interfere with BRD9 protein. The "privileged scaffold" feature of the thiadiazepinic ring has been widely analyzed in different studies, highlighting important effects in medicinal chemistry, such as antimicrobial, analgesic, anticoagulant, and antidepressant activity.[94] On the other hand, the isoxazole chemical platform exhibit a wide spectrum of targets and broad biological activities, including anticancer, antimicrobial, and anti-inflammatory.[95] Therefore, the investigation of condensed isoxazole scaffold with the thiadiazepine ring could lead to the discovery of new interesting pharmacological compounds.

In our work, the presence of a chemical structure similar to the acetyl-lysine on the isoxazole[2,3-*c*][1,3,5]thiadiazepin2-one suggested that these compounds could target the BRD9 binding site as histone H4, its natural agonist (**Scheme 1**).

Finally, molecules with this chemical structure could be quickly synthesized by a one-pot three-component reaction.[1] Specifically, using a 3-aminoisoxazole, mercaptoacetic acid and aromatic aldehydes in presence of para-toluenesulfonic acid (PTSA) as a catalyst, the derivatives could be obtained (**Scheme 3**).[1]

Also, integrating this quick-chemistry with the above-reported computational combinatorial approach could prove useful in medicinal chemistry.

2.2.1 Design

Following this synthetic scheme, an extensive library of molecules having this nucleus was built. According to the eleven commercially available amino-isoxazoles, eleven amino-

isoxazoles were considered and combined by the Combiglide software[96] with 3070 aromatic aldehydes commercial available, leading to the formation of a library of 33770 molecules. Then, through the Ligprep[97] function of Maestro software, all the possible stereoisomers and tautomers at the physiological pH of these molecules were generated, thus arriving at a library of 67540 ligands. Once the library was built, the related pharmacokinetic properties of each item were calculated using the Qikprop.[98] the application of the Lipinski filter was the following step,[99] which allows to obtain drug-like molecules.

Molecular docking calculations were then performed using the Virtual Screening[105] Workflow tool:

- High-Throughput Virtual Screening, (HTVS), saved the first 60% of the compounds ranked by docking score and used as input for the next phase;
- Standard Precision scoring and sampling phase (SP), saved first 60% of compounds ranked by docking score and used as input for the next phase;
- Extra Precision scoring and sampling phase (XP) generated 20 poses for each ligand and saved the first 80% of compounds ranked by docking score as final output.

Based on the interaction patterns (Tyr106, Asn100, Phe44)(**Figure 16**) and docking score, twenty-eight compounds (**A1**-**A28**, **Scheme 2**) were selected for the next steps of synthesis and biological evaluation.

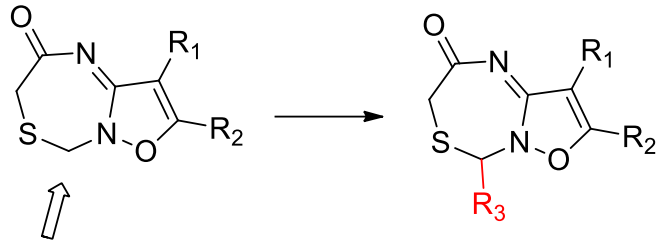

R_1= -H, -CH_3.
R_2= -H, -CH_3, -Ph.
R_3= -Ar

Scheme 1. Isoxazole[2,3-*c*][1,3,5]thiadiazepin-2-one scaffold structure and modifications.

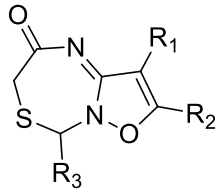

COMPOUND	R_1	R_2	R_3	COMPOUND	R_1	R_2	R_3
A1	H	H		**A15**	H	CH_3	
A2	H	H	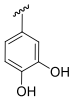	**A16**	CH_3	CH_3	
A3	H	H	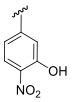	**A17**	H		
A4	H	H	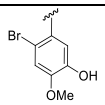	**A18**	H		
A5	H	H		**A19**	H		
A6	H	H	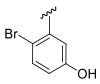	**A20**	H		
A7	H	H		**A21**	H		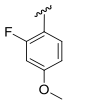
A8	H	H		**A22**	H		
A9	H	H	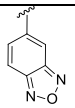	**A23**	H		
A10	H	CH_3		**A24**	H		
A11	H	CH_3		**A25**	H		
A12	H	CH_3		**A26**	H		
A13	H	CH_3	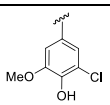	**A27**	H		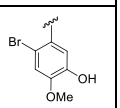
A14	H	CH_3		**A28**	H		

Scheme 2. Chemical structure of compounds **A1**–**A28.**

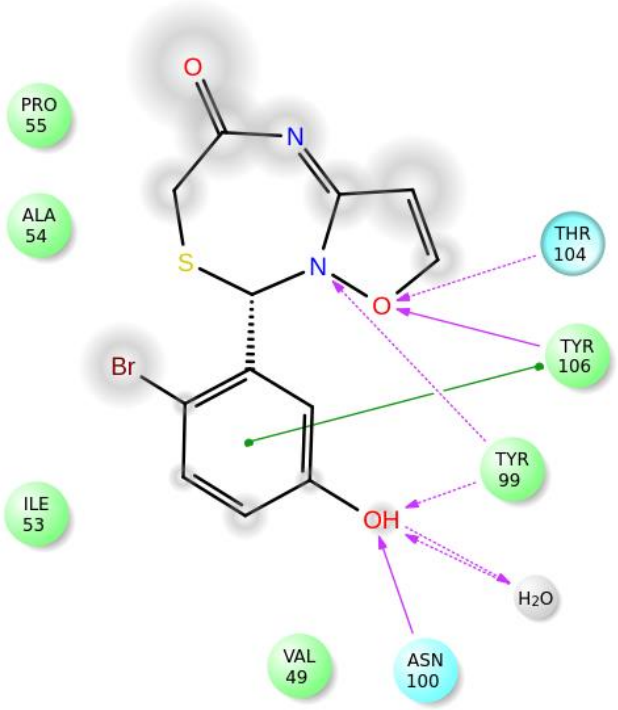

Figure 16. 2D interaction diagram of compound **A12** in the BRD9 binding site. Violet arrows representing H-bonds, green arrows representing π-π stacking.

2.2.2 Chemical synthesis

According to the procedure reported by Rajanarendar et al.[1] isoxazole[2,3-*c*][1,3,5]thiadiazepin2-one containing bisheterocycles were synthesized applying a one-pot multicomponent reaction in which 3-aminoisoxazole, the mercaptoacetic acid and an aromatic aldehyde were put to react in presence of PTSA in dry CH_3CN at reflux. Specifically, 3-aminoisoxazole and the mercaptoacetic acid were stirred at reflux for 4h in presence of acid condition generated from the catalyst to obtain the reaction intermediate. After observing the complete formation of the intermediate, a substituted benzaldehyde was added to the reaction mixture and the reaction proceeded under these conditions over-night (**Scheme 3**).

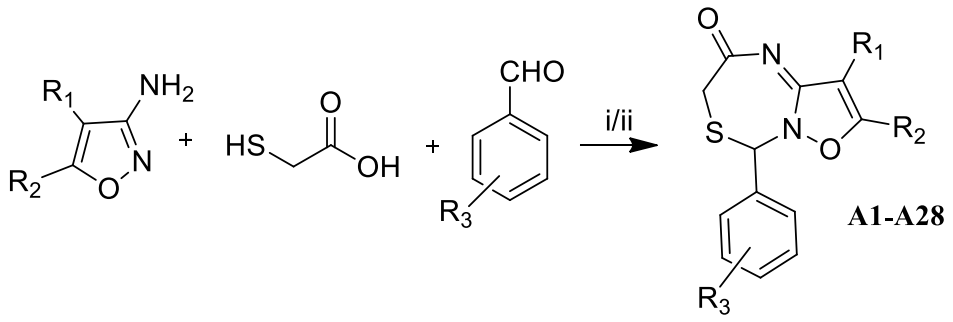

Scheme 3. Synthetic strategy adopted for the synthesis of compounds **A1-A28**. *Reagents and conditions: i) PTSA; dry CH_3CN, reflux, for compounds **A1-A12, A16-A28**; ii) PTSA; solvent-free, MW, 120°C, 200W, 15 minutes, for **A13-A15** compounds.*

Compounds **A13-A15** were synthesized via microwave procedure. In this case, electron-donor groups on the aromatic ring of the benzaldehyde decrease the partial positive charge of the carbonyl carbon resulting in less reactivity. In this context, we opted for the microwave-assisted synthesis in which the absorption and transmission of energy is completely different from conventional heating. Conventional heating is a superficial heating process and the energy is transferred from the surface to the bulk by convection and conduction. Therefore, the surface is at a temperature higher than the bulk, and the vessel must be overheated to achieve the desired temperature. In contrast, microwave irradiation produces efficient internal heating by directly coupling microwave energy with the bulk reaction mixture. This is an efficient mode of heating that result in the reduction of reaction times and improved yields. In addition, the microwave technique is particularly suitable for solvent-free reactions due to the direct absorption of the radiation by the substrates and not by the solvents; thus increasing the benefits of microwave irradiation classifying the technique among green chemistry approaches. For this reason, we opted for microwave-assisted synthesis in solvent-free conditions. The reaction to obtain the intermediate proceeded at 120°C, 200W, for 15 minutes; then the benzaldehyde was added and the reaction proceeded for 10 minutes in the same temperature and power conditions.

Both the procedures cannot avoid the use of PTSA as a catalyst. In fact, the plausible

mechanism for the formation of such compounds provides for the reaction between aminooisoxazole and mercaptoacetic acid activated by PTSA form the amide derivative, the reaction intermediate. Subsequently, the nucleophilic group (-SH) of the intermediate attacks the carbonyl of the substituted aromatic aldehyde, always activated by the PTSA. Finally, the nitrogen of the isoxazole ring, made of several nucleophilic group NH, performs a nucleophilic attack on aldehydic carbon, which is subsequently dehydrated to obtain the final compounds. For this reason, the presence of the acid condition is pivotal for the reaction, and the PTSA represents the best catalyst to use in terms of yield and efficiency, as [1]Rajanarendar et al. suggested.[1]

2.2.3 AlphaScreen assay (Amplified Luminescent Proximity Homogeneous Assay)

All the synthesized compounds have been screened with AlphaScreen technology in order to evaluate their potential inhibition toward the protein. AlphaScreen technology is routinely utilized in high throughput screening assays, to quantify analytic accumulation or depletion, biomolecular interactions, and post-translational modifications.[100] When a biological interaction brings the beads together, a cascade of chemical reactions produces a greatly amplified signal.

The use of donor beads coated with streptavidin allowed the conjugation to terminally-biotinylated histone peptide substrate. In contrast, the acceptor beads coated with a nickel chelator allowed the conjugation to GST-tagged protein (**Figure 17**).

Laser excitation (680 nm) of a photosensitizer within the donor beads converts ambient oxygen to singlet oxygen. The binding of BRD9 to the H4 histone enables an energy transfer from the donor to the acceptor beads, which emit light in the 520 to 620 nm range and results in a measurable signal.

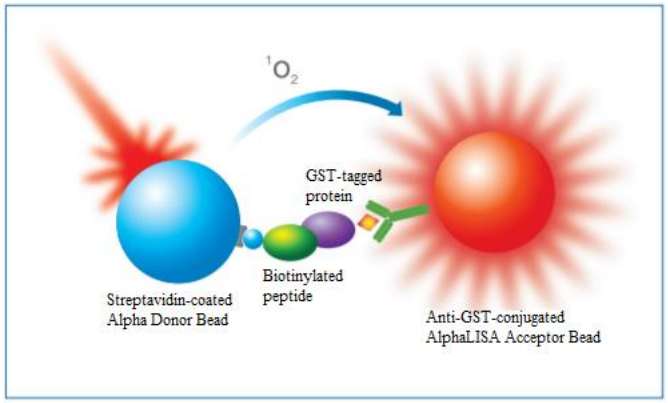

Figure 17. AlphaScreen protocol set up for bromodomain-contain protein 9.

In this set of experiments, H4 was used as positive control. In case of no interaction between the proteins and the tested compound, BRD9 targeted the H4 emitting the maximum signal. If the synthesized molecules were able to displace histone H4 from protein binding, the amplitude of the signal decreased. The decrease of the signal depended on the power of the binders: the stronger the binding, the greater the reduction in the light output.

As showed in **Table 1**, all the synthesized compounds have been evaluated against BRD9 at 10µM; however, the compounds did not show the ability to bind the protein, with a percentage of residual binding versus H4 around 90-100%. Only the molecules featuring phenyl in position 5 of the isoxazole ring yielded better results, although still not promising H4 residual binding: around 80%.

Table 1. Percentages of residual BRD9 residual binding to acetylated H4 for compounds **A1-A28**.Data are expressed as means ± SD, n = 3.

COMPOUND	RESIDUAL BINDING OF HISTONE H4Ac T0 BRD9(%)± SD	COMPOUND	RESIDUAL BINDING OF HISTONE H4Ac T0 BRD9(%)± SD
A1	97.7 ±0.4	**A15**	≥100.0
A2	93.1 ±2.2	**A16**	≥100.0
A3	92.8 ±0.9	**A17**	84.2 ±0.2
A4	94.7 ±2.1	**A18**	85.6 ±1.1
A5	97.6 ±0.9	**A19**	87.7 ±1.7
A6	93.8 ±0.8	**A20**	85.8 ±2.8
A7	92.4 ±1.8	**A21**	. 87.9 ±1.4
A8	91.1 ±1.8	**A22**	84.8 ±0.5
A9	95.8 ±0.3	**A23**	93.3 ±0.7
A10	98.9 ±2.1	**A24**	98.5 ±0.2
A11	≥100.0	**A25**	94.0 ±2.7
A12	98.6 ±0.9	**A26**	93.2 ±3.2
A13	≥100.0	**A27**	79.8 ±2.1
A14	88.6 ±0.7	**A28**	78.0 ±0.6

2.2.4 Inverse Virtual Screening for the repurposing of isoxazole[2,3-*c*][1,3,5]thiadiazepin2-one-based compounds

The poor binding of **A1**-**A28** compounds towards BRD9 (**Table 1**) prompted us to employ the Inverse Virtual Screening (IVS) approach[101-102], according to the workflow shown in **Figure 1** (**Introduction**).

IVS is a versatile methodology that can be applied for many purposes, such as predicting unknown biological targets, repurposing of approved drugs and/or repositioning already synthesized organic compounds inactive on a specific target, as in the case of **A1**-**A28** towards BRD9.

Compounds **A1-A28** were screened by means of molecular docking calculations *vs.* a panel of 1830 proteins involved in cancers, and the predicted docking energies were normalized by using 10 "blanks" compounds. Moreover, the shape similarity with co-crystallized ligands resulted in an additional parameter to lead the IVS analysis. We normalized the predicted binding energies for each small molecule, obtaining an affinity profile on the whole protein panel. As next step, we proceeded with visual inspection of the docked poses obtained, in order to identify macromolecular candidates for the experimental assays. Thus, this analysis pointed at the estrogen receptor (ESR1), androgen receptor (AR) and Beta-1,4-galactosyltransferase 1 (B4GALT1) as putative targets for the isoxazole[2,3-*c*][1,3,5]thiadiazepin-2-one-based compounds. The 87.50% of synthesized compounds of this series were detected as potentially able to bind the estrogen receptor, compared to 80% and 70% observed for the other receptors. Indeed, ESR1 was chosen for experimental assays *vs*. the compounds **A1**–**A28**.

2.2.5 Evaluation of the binding with estrogen receptor counterpart by Fluorescence resonance energy transfer (FRET)

Time-resolved FRET assay was used to quantitate the effects of binding of various small molecules to ESR LBDs. This is an extremely powerful method of identifying potential molecular interactions, suited to High Throughput Screening (HTS) since it is simple, sensitive and easily automated.

In the assay, a biotinylated nuclear receptor binding peptide (NRB) is recruited to FLAG-tagged ER LBD to bring ULight and europium (Eu) close to each other. In particular, an agonist induces the recruitment of the NRB peptide to ESR LBD, resulting in FRET. All the compounds were tested in triplicate at a concentration of 20 μM. As shown in **table 2**, compounds **A17**, **A19**, **A20** and **A28**, with antagonist activity, blocked the agonist-induced recruitment of the NRB peptide, resulting in decreased FRET. Raloxifene was used as positive control.

Table 2. The percentage of inhibition of the best compounds determined using TR-FRET. Data are expressed as means ± SD, n = 3.

COMPOUND	BINDING (%) ± SD
A17	70.1±0.9
A19	83.0±0.5
A20	74.8±0.3
A28	86.7±0.4

2.3 4-ethyl-benzothiazole scaffold as BRD9 potential binder

The 4-ethyl-benzothiazole scaffold was investigated with the purpose of selecting new promising BRD9 binders.

The idea behind the research was that molecules featuring similar shapes could likely show similar binding modes on a protein counterpart. Thus, we evaluated the shape similarity between the 4-ethyl-benzothiazole and I-BRD9 scaffold, the latter able to bind BRD9. The 4-ethyl-benzothiazole core was identified as good candidate to obtain new potential binders, featuring a 0.78 shape similarity score (value determining the alignment of two or more ligands; the closer the value is to 1, the better the alignment) (**Figure 18**). This pose overlapping is also useful for rationalizing in which position the core should be decorated and determining which groups to insert to interact with the fundamental amino acids in the binding site.

In addition, the presence of the ethyl group in position 4 of benzothiazole led us to a certain similarity with the acetyl-lysine of histone H4, useful to bind the target protein, as we already discussed.

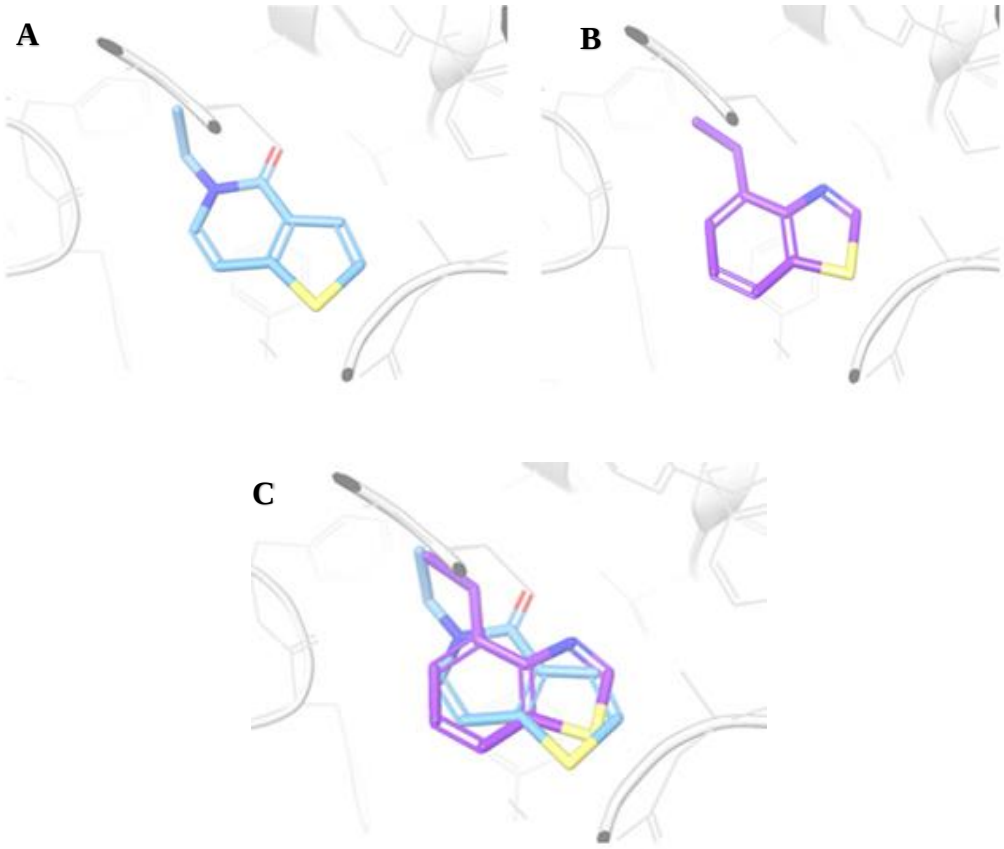

Figure 18. a) 3D structure of I-BRD9; b) 3D structure of 4-ethyl-benzothiazole; c) Superimposition docking poses of I-BRD9 and 4-ethyl-benzothiazole.

2.3.1 Design

Starting from the evaluation of shape similarity with I-BRD9 inhibitor, we decided to decorate the 4-ethyl-benzothiazole in position 2 using an acceptor/donor group able to interact with Asn100, fundamental for BRD9 inhibition, and an aromatic group in position 6 able to fit into ZA channel and interact with Phe44.

For this reason, according to the synthetic procedure, the virtual library was generated by positioning all the commercially available acid chlorides and sulfonyl chlorides in position 2, and all aromatic boronic acid in position 6, using CombiGlide software[96] (**Scheme 4**).

Using the Qikprop,[98] the related pharmacokinetic properties were calculated for all the generated compounds. Finally, the new library was filtered according to the Lipinski filter[99] to

select only drug-like compounds to be subjected to molecular docking calculations. The most promising compounds were selected for the next stage of synthesis, taking into account the docking score values and the interactions with key amino acids within the binding site, after careful visual inspection of the binding mode. In particular, the compounds interacted with the amide or sulfonamide added group by hydrogen bond with Asn100 and Tyr99, while the 4-ethyl-benzothiazole interacted with Tyr106 by two π- π bonds (**Figure 19**). In this case, only four (**Scheme 5**) out of fifteen selected molecules were synthesized. In fact, following the negative binding results against BRD9 we did not further move forward with the synthetic part while instead reevaluating by IVS the compounds already synthesized.

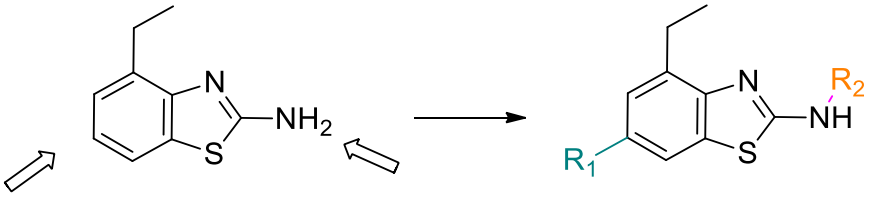

Scheme 4. 4-ethyl-benzothiazole scaffold structure and modifications.

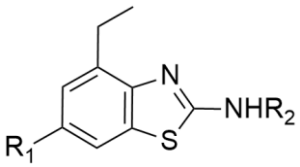

COMPOUND	R_1	R_2
B2		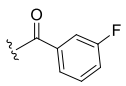
B3		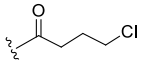
B4		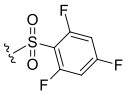
B5		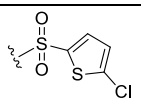

Scheme 5. Molecular structure of compounds **B2-B5**.

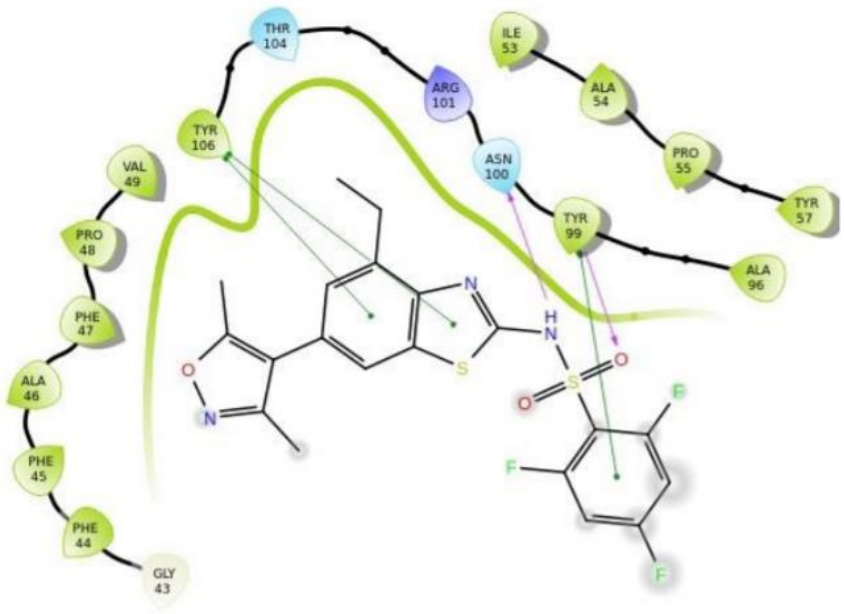

Figure 19. 2D interaction diagram of compound **B3** in the BRD9 binding site. Violet arrows representing H-bonds, green arrows representing π-π stacking.

2.3.2 Chemical synthesis

For the synthesis of the compounds **B2**-**B5**, Pd-catalyzed Suzuki-Miyaura cross-coupling followed by acylation (compounds **B2**-**B3**) or sulfonylation (compounds **B4**-**B5**) were performed. Pd-catalyzed Suzuki-Miyaura cross-coupling was achieved between the 6-bromo-4-ethylbenzo[*d*]thiazol-2-amine and the commercially available (3,5-dimethylisoxazol-4-yl) boronic acid, as shown in the **Scheme 6**. The Suzuki-Miyaura reaction was chosen for our purpose because it is an efficient and versatile method for highly functionalized biaryls synthesis, leading to good yields under mild conditions.

For the preparation of our compounds, the cross-coupling was performed under standard conditions $Pd[P(Ph)_3]_4$, carbonate as base in dioxane/H_2O (8/2) at 80°C. The reaction proceeded in high yields (78%).

Derivatives **B2**-**B3** were synthesized via condensation of intermediate **B1** with commercially available 3-fluorobenzoyl chloride and 4-chlorobutanoyl chloride, respectively. The reaction was performed using pyridine in acetonitrile at room temperature for 3 hours. Sulfonylation of the intermediate **B1** leading to compounds **B4**-**B5** proceeded overnight at reflux.

Following this procedure, the desired products were obtained in good yields (50-72%). After extraction and purification by silica gel, all compounds were purified by reversed phase HPLC and obtained with >98% purity for the following biological assays.

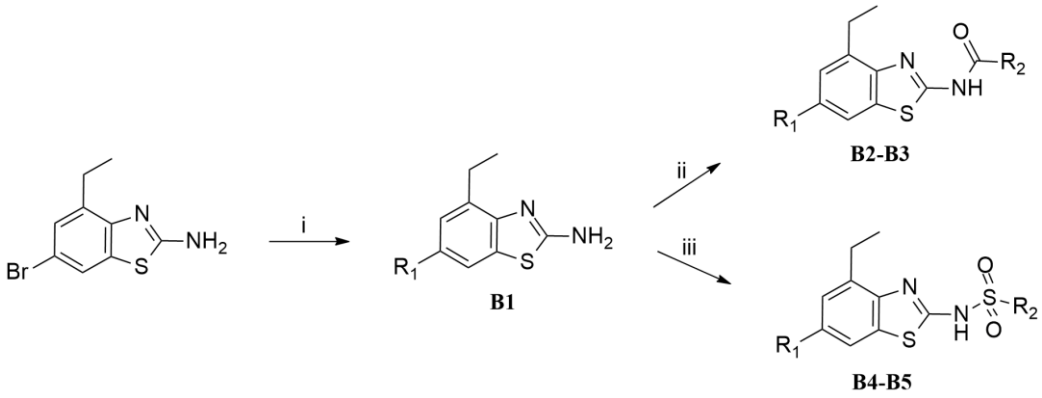

Scheme 6. Synthetic strategy adopted for the synthesis of compounds **B2**-**B5**. *Reagents and conditions: i) $R_1B(OH)_2$, K_2CO_3, $Pd[P(Ph)_3]_4$, 1,4-dioxane-H_2O, 80 °C, over-night; ii) R_2COCl, pyridine, CH_3CN, rt; iii) R_2SO_2Cl, pyridine, CH_3CN, reflux.*

2.3.3 AlphaScreen assay and revaluation of the scaffold design

The synthesized molecules were subjected to the post-processing phase to verify their ability to bind the target protein. An AlphaScreen assay was performed using a recombinant BRD9 protein. All compounds were tested in duplicate, both at a concentration of 10µM and 50µM (**Table 3**). Unfortunately, they did not show a significant binding with BRD9, even at 50 µM.

Table 3. Binding data of compounds **B2-B5** relative to BRD9. Data are expressed as means ± SD, n = 3.

COMPOUNDo	**RESIDUAL BINDING OF HISTONE H4Ac T0 BRD9(%)± SD**	
CONCENTRATION (μM)	**50**	**10**
B2	82.3±0.1	≥100
B3	80.0±4.3	99.5±1.1
B4	84.5±0.8	≥100
B5	79.0±2.4	96.4±2.4

The reasons why these compounds showed a poor binding against BRD9 were elucidated by retrospectively evaluating their fit against 3D-structure-based pharmacophore models later developed against BRD9.[93] Specifically, starting from 23 known ligands co-crystallized with BRD9, three-dimensional pharmacophore models were developed in order to improve the design of molecules targeting BRD9.[93] Briefly, in order to identify new promising small chemical probes targeting the protein region responsible for the acetyl-lysine recognition, a fragment-related pharmacophore model was introduced, and two further pharmacophore models useful for the selection of compounds featuring drug-like properties were adopted.[93] After that, the scaffold of I-BRD9, defined initially as shape query, and the new scaffold featuring the benzothiazole core were first subjected to docking calculations in a reference protein structure (PDB: code 5F1H)[103]. The benzothiazole core and, specifically, the N of the ring failed to fit into the volume where an acceptor group should be present to form an H-bond with Asn100. In contrast, I-BRD9 fits well with the three pharmacophoric features, representing the typical acetyl-lysine mimic function. These results confirmed pharmacophoric models[93] represent an excellent tool to select the best ligands, exclude the not promising ones and rationalize the absence of binding.

2.3.4 Inverse Virtual Screening and repurposing of 4-ethylbenzo[*d*]thiazol-2-amine-based compound on sEH

Considering these results, we decided to perform an Inverse Virtual Screening[102] in order to identify potential target proteins for this set of compounds for anti-inflammatory and anticancer purposes. After this screening, we focused on soluble epoxide hydrolase (sEH) enzyme, which emerged as the best target for compounds **B3**, **B4**, **B5,** and as the fourth best for **B2**.

Specifically, the amide group was very promising since it is present in many known inhibitors of this target, establishing hydrogen bonds with the side chains of Asp335, Tyr383, and Tyr466 (**Figure 20**).

In addition, the benzothiazole scaffold establishes an additional π-π interaction with Tyr381, suggesting the ability of this scaffold to interact with the hydrolase domain of sEH.

The results showed that **B3** was active on sEH, being able to reduce residual sEH activity to 30.92% (**Table 4** and **Figure 21A**) compared to control, while the others were able to bind the target moderately at μM range. For this most promising compound the IC_{50} value was determined (6.62 ±0.13μM, **Figure 21B**).

Finally, compounds **B2-B5** were tested in cytotoxicity assays. The compounds showed no significant reduction of cell viability after 24h incubation in human monocytes compared to positive control (**Figure 21C**).

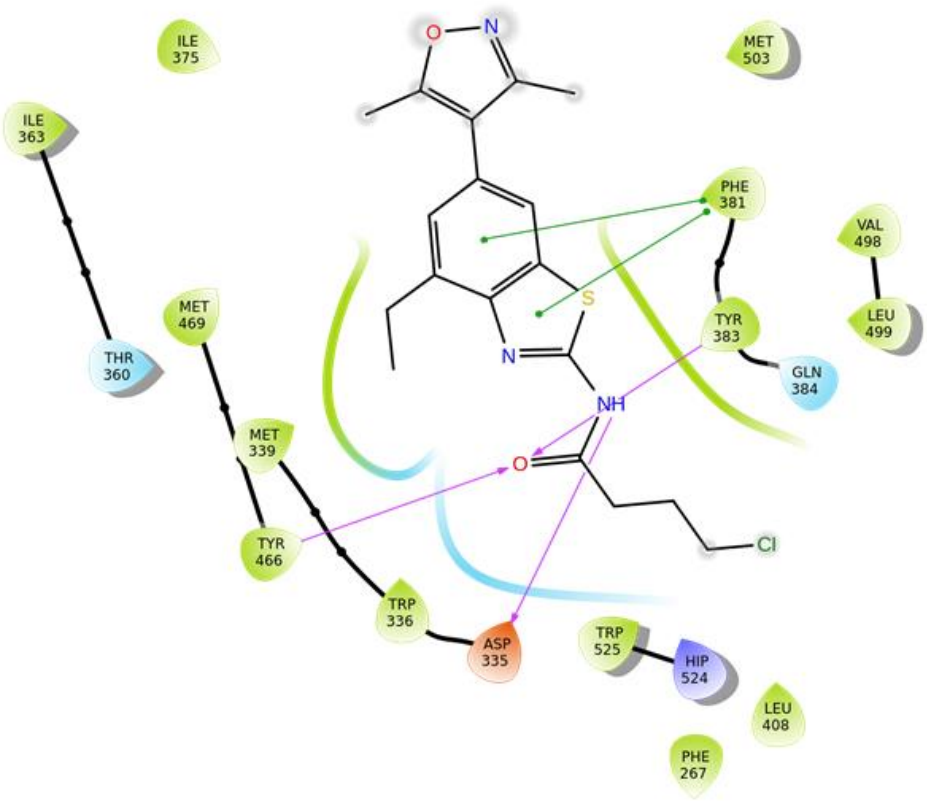

Figure 20. 2D representation of compound **B3** in sEH binding site. Violet arrows representing H-bonds, green arrows representing π-π stacking.

Table 4. Percentages of sEH residual epoxide hydrolase activity following treatment with compounds **B2**-**B5** at concentrations of 1 and 10 µM. Data are expressed as means ± SD, n = 3.

COMPOUND	**sEH RESIDUAL ACTIVITY (%)**	
CONCENTRATION (µM)	**1**	**10**
B2	83.1 ±1.0	70.7 ±1.2
B3	77.9 ±0.2	30.9 ±0.9
B4	≥100	77.5 ±0.3
B5	75.5 ±1.4	60.4 ±1.0

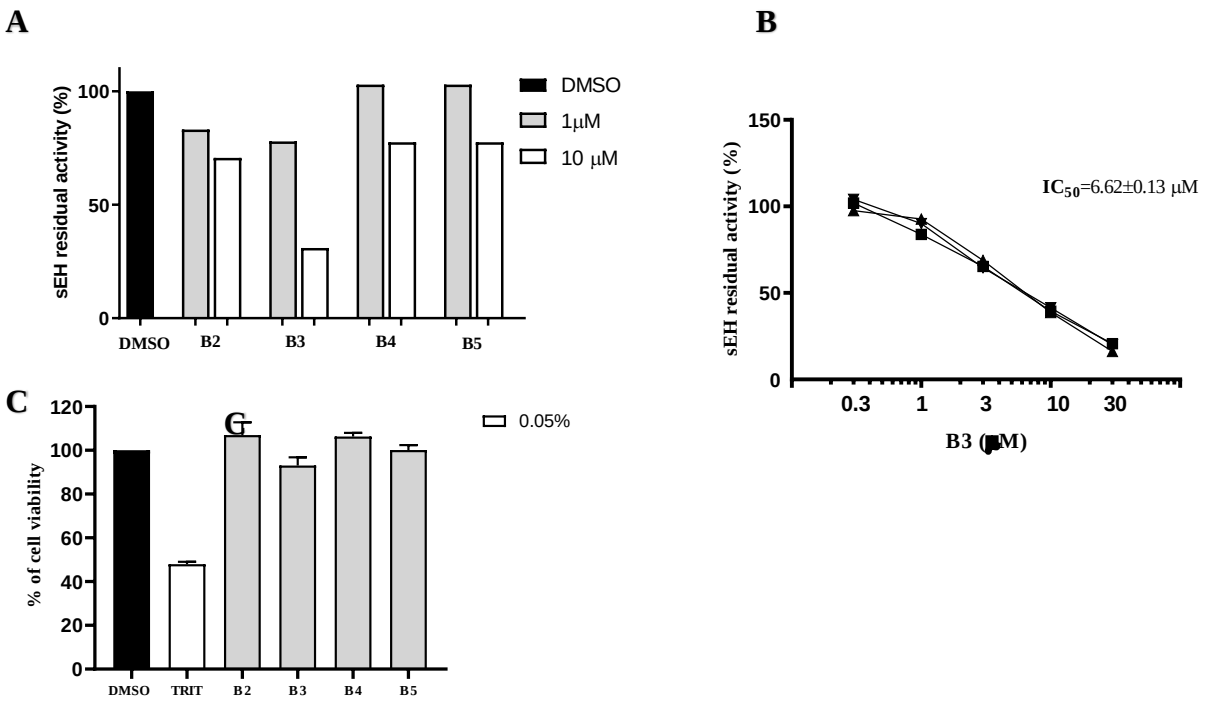

Figure 21. A) Effect of compounds **B2-B5** on sEH residual activity using DMSO as positive control; B) Concentration-response curve for inhibition of sEH. The enzyme was incubated for 15 min with compound **B3** at different concentrations (from 0.03 μM up to 30 μM) or vehicle (1% DMSO). IC_{50} 6.62 ± 0.13; C) Cell viability assays were performed with human monocytes: monocytes were treated with the test compounds **B2-B5** (10 mM), triton (1%, positive control) or vehicle (0.5% DMSO) for 24 h, and a MTT assay was performed.

2.4 Evaluation of 1,8-naphthyridone-based compounds as new potential BRD9 binders

In order to develop new small molecules as potent BRD9 binders, we focused our attention on 1,8-naphthyridone scaffold (**Scheme 7**) that was chosen as template for the rational design, for the following reasons:

- The 4-oxo-1,4-dihydropyridine-3-carboxylate structure could mimic the 1-ethylpyridin-2(1*H*)-one of I-BRD9 inhibitor and due to the presence of two nearby carbonyl groups, we hypothesized a hydrogen bond reinforced with Asn100;
- The 3-carboxylate group could also mimic the N-acetylated function of H4 histone;
- Two fused aromatic rings are widespread in many BRD9 inhibitors; they could have given interactions with Tyr106, important for selectivity;

- The aromatic substitution of nitrogen in position one could interact with Phe44 e Phe47 important for the potency;
- Finally, these fuse heterocycles are well known to represent a privileged scaffold in medicinal chemistry due to their variety of biological properties including antimicrobial, antiviral, anticancer, and anti-inflammatory activities.[104]

2.4.1 Design

We focused our attention on 1,8-naphthyridone scaffold which can be modifiable in position 1 with all commercially available ammine that represents the basic partners for the one-pot reaction reactions set up by Springfield S.A. et al.[2] According to our previous results, the presence of aromatic residues, such as Phe44 and Phe47 in the BRD9 binding site requires the use as starting molecular seed only the aromatic amine instead of the aliphatic ones. Thus, as in previous cases, we used the Combiglide software[96] to prepare the virtual library (**Scheme 7**), then through the QikProp[98] software we calculated their ADME properties and with the Ligfilter[105] option the molecules with adverse pharmacokinetic properties were discarded. The remaining molecules were tested *in silico* for their ability to bind BRD9 by means of molecular docking. Docking studies were performed by using Glide software. In particular, we docked the fragments into the catalytic cavity of BRD9 X-ray solved protein structure (PDB code: 5F1H).[103] The analysis of docking outcomes and the comparison of all tested virtual compounds revealed that they could be used to design promising BRD9 binders (**Figure 22**). In particular, as expected:

- the carbonyl group was able to interact with Asn100 via hydrogen bond;
- the fused aromatic rings interacted with Tyr106, along with van der Waals contacts;

- the residues added using Combiglide software[96] were fundamental for the filling the unoccupied binding pocket.

According to the results, we selected seven molecules that fit these requirements (**Scheme 8**).

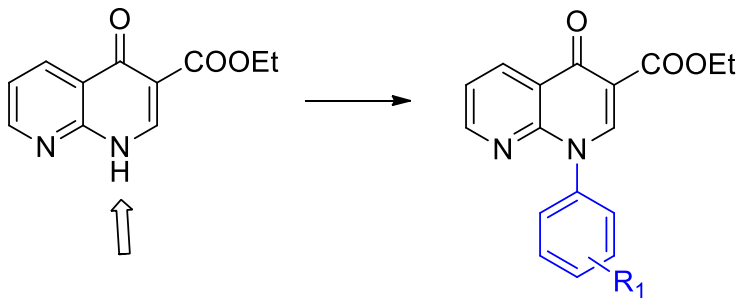

Scheme 7. 1,8-naphthyridone scaffold structure and modification.

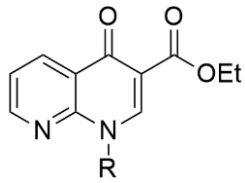

COMPOUND	R
C2	
C3	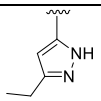
C4	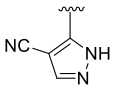
C5	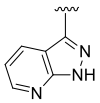
C6	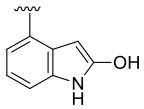
C7	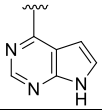
C8	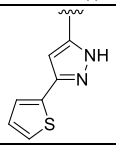
C9	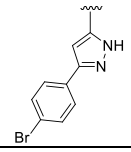

Scheme 8. Selected and synthesized 1,8-naphthyridone-based compounds.

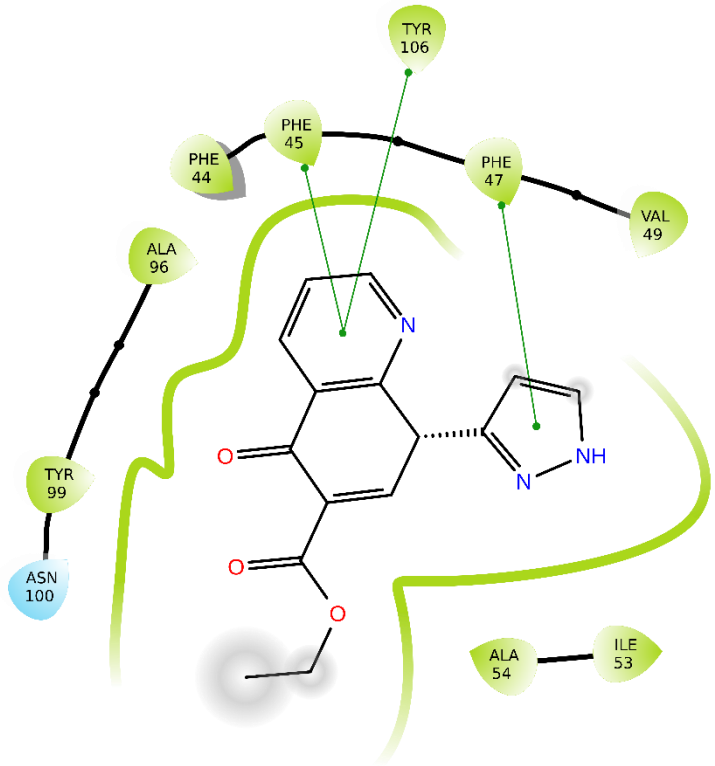

Figure 22. 2D panel representing interactions formed by compound **C5** with BRD9. Green arrows representing π-π stacking.

2.4.2 Chemical synthesis

To obtain 1,8-naphthyridone-based compound we decided to follow first the procedure reported by Springfield, S. A. et al.[2]. The authors described a new, one-pot method that involves the condensation of 2-chloronicotinoyl chloride with ethyl-3,3-dimethylaminoacrylate followed by *in situ* reaction with a variety of anilines to provide the desired 1,8-naphthyridone in a one-pot multicomponent reaction. The excess of the base and the solvent (CH_3CN) avoided the formation of a trimer of the acrylate as subproduct. In addition, they showed good yield (around 60%) for both electron-rich and electron pour aniline, decreasing only in the presence of sterically bulky groups close to $-NH_2$ group. Following this procedure, we did not find the expected product; in addition, the intermediate was isolated only in minimal amount (Yield ≤ 5%), the acrylate trimer was isolated with a percentage around 19%, and the most abundant

final product is a product resulting from the substitution of chlorine in position 2 of 2-chloronicotinoyl chloride with N,N-dimethylamine group deriving from the acrylate (**Scheme 9**).

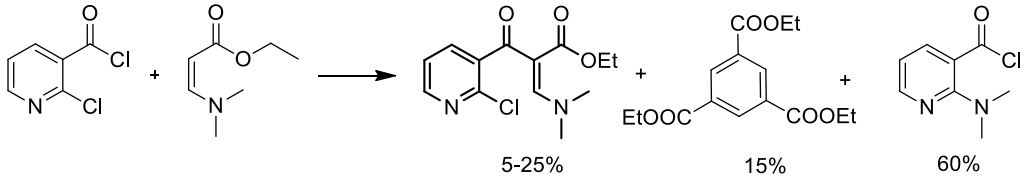

Scheme 9. Byproducts observed following the procedure reported by Springfield, S. A. et al.[2]

A second trial was carried out following the procedure illustrated by Zeng H. et al. Briefly, the intermediate was made by reaction of 2-chloronicotinoyl chloride and the N,N-dimethylamine acrylate in toluene at 50°C; then the amine was directly added, stirring for about 5–8 h at room temperature. Finally, we added the potassium carbonate, stirring for 8–10 h at 100°C. The expected product was not obtained neither following this procedure; nevertheless, we achieved the intermediate with a higher percentage compared to the first trial. We hypothesized that the failure of our second trial is associated with differences in the substrate used in our study compared to Zeng et al.: indeed, while the mentioned authors selected the 2,4,5-trifluoro-3-methoxybenzoic acid as starting materials to synthesize quinolone derivatives, our substrate was 2-chloronicotinoyl chloride. Another possible explanation for the experimental failure could be found in the amines that we used, in which the -NH_2 group was on different heterocycles. Considering that the intermediate is the only product that we obtained, we decided to split the reaction in two steps, so that it was easier to control its progress. In addition, in order to optimize the synthetic procedure and to improve the yield of the reaction, we accounted for possible effects of parameters such as temperature, the choice of solvents and reaction time on

the reaction being evaluated. The test conditions and the corresponding values of the parameters adopted for laboratory tests are given in **Table 5** below.

All the tests done with conventional heating led to poor results; only when the reaction was done in toluene at 60°C or reflux we obtained the intermediate with the 25% of the yield.

For this reason, we decided to perform the following trial through microwave-assisted synthesis. When the intermediate was synthesized with the microwave by reacting chloride, N,N-dimethylaminoacrylate and triethylamine under solvent-free conditions, using the same equivalents that gave the formation of the product by thermal route (respectively 2, 1.5 and 4), the reaction was successful with an improvement in yield from 26 to 39%. As the excess of acrylate reacted was not consumed, the reaction time was increased from 10 to 20 minutes without any yield improvement. Finally, acrylate equivalents were reduced to assess possible effects on the reaction. It was observed that with 1 equivalent of acrylate the yield became 50%, and in the presence of a slight acrylate defect the reaction improved significantly in terms of yield (84%) (**Table 5**).

The microwave reaction was conducted according to the following parameters:

- Temperature: 100°C
- Time:10 minutes
- Max power: 200W
- Max pressure: 431 PSI

The resulting solid was solubilized in DCM, washed with water and dried to give the intermediate as a yellow powder (84% yield) which was then used without any further purification. The final products 1,8-naphthyridones were obtained through a second step in which the intermediate was put to react with the amine, chosen by docking calculation on BRD9 protein, over-night in toluene at reflux (**Scheme 10**). This second reaction step proceeded easily

and with good yields (from 54 to 97%). Moreover, seven compounds were synthesized following this synthetic procedure (**Table 5**).

Table 5. Test conditions for the intermediate reaction to be optimized.

ENTRY	SOLVENT	T(°C)	STEPS	ACRYLATE (eq)	BASE (eq)	HEATING SYSTEM	YIELD
1	THF	r.t	2	1.5	4	Conventional	<5%
2	THF	60°	2	1.5	4	Conventional	<5%
3	THF	Reflux	2	1.5	4	Conventional	<5%
4	CH_3CN	r.t	2	1.5	4	Conventional	<5%
5	CH_3CN	60°	2	1.5	4	Conventional	<5%
6	CH_3CN	Reflux	2	1.5	4	Conventional	<5%
7	DMF	r.t	2	1.5	4	Conventional	<5%
8	DMF	60°	2	1.5	4	Conventional	<5%
9	DMF	Reflux	2	1.5	4	Conventional	<5%
10	Toluene	r.t	2	1.5	4	Conventional	<5%
11	Toluene	60°	2	1.5	4	Conventional	25%
12	Toluene	Reflux	2	1.5	4	Conventional	26%
13	Solvent-free	100°	2	1.5	4	MW	39%
14	Solvent-free	100°	2	1	4	MW	50%
15	Solvent-free	100°	2	0.9	4	MW	84%

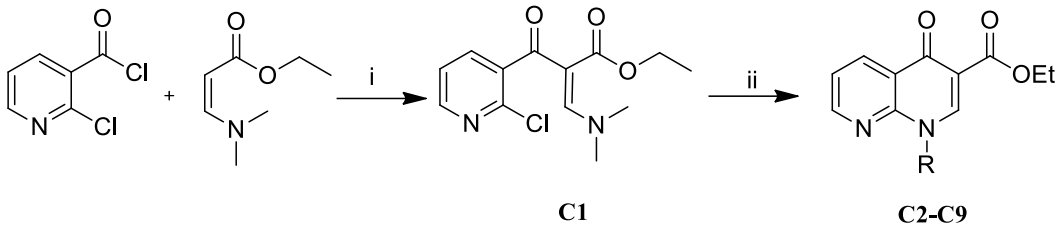

C1 **C2-C9**

Scheme 10. Synthetic strategy for compound **C2-C9**. *Reagent and conditions: i) MW, 100°C, 10 min; ii) R-NH$_2$, toluene, reflux, over-night.*

2.4.3 AlphaScreen assay and subsequent repositioning by Inverse Virtual Screening

Once synthesized, compounds **C2-C9** were evaluated for the putative binding to the recombinant BRD9 by an AlphaScreen assay. According to the results of this preliminary screening, all tested compounds were not able to bind BRD9 (**Table 6**).

Among these, two compounds (**C3** and **C4**) showed a slightly better binding towards the protein (Residual binding of Histone H4Ac to BRD9 ~87/88%). Therefore, we hypothesized that the substituted pyrazole in position 1 of 1,8-naphthyridone nucleus could be useful for the interaction. Indeed, in this case, two nitrogen of the nucleus of the pyrazole possibly bind Asn100 while the substituents in position 3 and 4, respectively of **C2** and **C4,** can be placed into the ZA channel leading to better results.

Starting from these results, we decided to reposition these molecules through Inverse Virtual Screening method. As already described (**Introduction**), IVS can rapidly search any potential targets for small sets of molecules to facilitate the drug discovery. In this case, among all the panel of anti-inflammatory and anticancer targets, CK2 alpha, Mek1 and Mek2 kinases emerged as the most promising target proteins. The binding assay will be carried out to corroborate the computational predictions.

Table 6. Binding data of compounds C**2-C9** relative to BRD9. Data are expressed as means ± SD, n = 3.

COMPOUND	RESIDUAL BINDING OF HISTONE H4Ac T0 BRD9(%)± SD
C2	98.4% ±3.1
C3	88.5% ±1.5
C4	87.6% ±1.1
C5	97.0% ±2.4
C6	97.5% ±2.3
C7	98.8% ±1.9
C8	≥100.0%
C9	94.5% ±2.0

2.5 Identification of 2,4,5-trisubstituted-2,4-dihydro-3*H*-1,2,4-triazol-3-one-based molecules as selective BRD9 binders

Here we report the investigation of 2,4,5-trisubstituted-2,4-dihydro-3*H*-1,2,4-triazol-3-one-based compounds as novel interesting BRD9 binders by applying a multidisciplinary approach including virtual screening workflow, synthesis, and biological evaluation.

Considering the *Structure-based three-dimensional pharmacophore-based approach*, our initial hypothesis was that the 2,4-dihydro-3*H*-1,2,4-triazol-3-one chemical core featured hydrogen bonds acceptor groups suitable for a putative interaction with Asn100, a conserved amino acid essential for the binding of the KAc moiety. Also, the interaction with Tyr106, fundamental for the gaining affinity in the BRD9 binding site, can be assured by the 2,4-dihydro-3*H*-1,2,4-triazol-3-one ring. Finally, this starting structure can be easily modified in order to introduce a hydrophobic group to be placed in the ZA channel, aimed at gaining

affinity for the target, and a second one responsible for the putative selectivity through interactions with specific residues (e.g., Ile 53). Importantly, the small dimension of this chemical core facilitated its interaction with the small BRD9 binding site. In addition, its "privileged scaffold" nature pushed us to investigate it; indeed, Kane M. J. et al. highlighted 5-aryl-2,4-dihydro-3*H*-l,2,4-triazol-3-ones as anticonvulsant agents while, in other studies, the antimicrobial effects of molecules based on this scaffold were reported. [106-107]

2.5.1 Design

In detail, starting from six different 2,4-dihydro-3*H*-1,2,4-triazol-3-one-based cores, we investigated the possibility of differently decorating them in the N-4 chemical position. Specifically, we evaluated the following cores (**Scheme 11**):

- 5-methyl-2,4-dihydro-3*H*-1,2,4-triazol-3-one (**1**),
- 5-ethyl-2,4-dihydro-3*H*-1,2,4-triazol-3-one (**2**),
- 2,5-dimethyl-2,4-dihydro-3*H*-1,2,4-triazol-3-one (**3**),
- 2,5-diethyl-2,4-dihydro-3*H*-1,2,4-triazol-3-one (**4**),
- 2-ethyl-5-methyl-2,4-dihydro-3*H*-1,2,4-triazol-3-one (**5**),
- 2,5-diethyl-2,4-dihydro-3*H*-1,2,4-triazol-3-one (**6**)

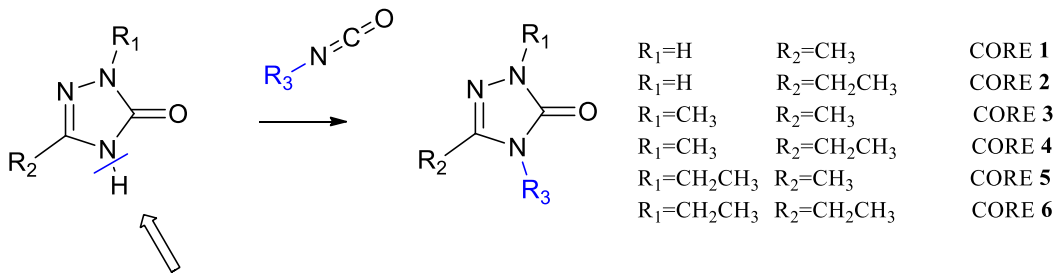

Scheme 11. 2,4-dihydro-3*H*-1,2,4-triazol-3-one-based starting **cores 1**-6

In particular, these six starting cores were selected to evaluate the influence of methyl and ethyl substituents, usually present in BRD9 binders as part of the acetyl-lysine mimic function, in gaining affinity towards the target of interest.

In more detail, both N1-C5-R_2 and O=C3-N2-R_1 moieties (**Figure 23**) could act as acetyllysine mimetics, and, moreover, the presence of methyl and ethyl groups is in accordance with the fact that BRD9, differently from other bromodomains, can accommodate alkyl groups with different length in the binding pocket, which can also improve the selectivity of small molecules on this target.[108] For these reasons, six possible combinations (**cores 1**-**6**, **Scheme 11**) were taken into account, specifically considering a hydrogen, methyl, and ethyl groups at R_1, and a methyl and ethyl groups at R_2. Molecular docking calculations were performed and the starting cores showed promising binding modes, since all the tested compounds established interactions with Asn100 (H-bond) and with Tyr106 (π-π interaction), crucial for protein activity and substrate recognition.

Starting from these computational data, the six scaffolds were combined with the 316 aryl isocyanates available at the Merck database at position 4, using CombiGlide software.[96] Specifically, the final library of compounds featured 1896 items, after accounting for the possible tautomers and protonation states and discarding all the molecules featuring not showing "drug like" properties (LigFilter software).[97]

In this virtual screening campaign, docking calculations were performed using Glide software (HTVS, SP and XP mode, according to the Glide Virtual Screening Workflow).[105] Docking experiments were performed generating a receptor grid focused on the BRD9 binding site (PDB code: 5F1H).

Specifically, the output docking poses were analysed considering docking score, analysis of the ligand-protein interactions and visual inspection (**Figure 23**).

In this way, twenty-one molecules (**D3**-**D8**, **D11**-**25**, **Scheme 12**) were selected and further screened with SwissADME web tool,[109] excluding the presence of chemical species belonging to "Pan-Assay Interference Compounds" (PAINS) chemical class.

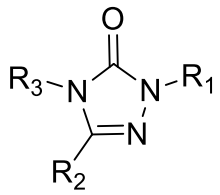

COMPOUND	R_1	R_2	R_3
D3	H	CH_3	
D4	H	CH_3	
D5	H	CH_3	
D6	H	CH_3	
D7	H	CH_3	
D8	H	CH_3	
D11	H	CH_2CH_3	
D12	H	CH_2CH_3	
D13	H	CH_2CH_3	
D14	H	CH_2CH_3	
D15	H	CH_2CH_3	
D16	H	CH_2CH_3	
D17	H	CH_2CH_3	
D18	H	CH_2CH_3	
D19	CH_3	CH_3	

D20	CH_3	CH_3	
D21	CH_3	CH_3	
D22	CH_3	CH_3	
D23	CH_3	CH_2CH_3	
D24	CH_3	CH_2CH_3	
D25	CH_3	CH_2CH_3	
D26	CH_3	CH_2CH_3	
D27	CH_2CH_3	CH_2CH_3	
D28	CH_2CH_3	CH_3	
D29	CH_2CH_3	CH_2CH_3	
D30	CH_3	CH_3	
D31	CH_2CH_3	CH_3	
D32	CH_3	CH_2CH_3	
D33	CH_2CH_3	CH_2CH_3	
D34	CH_2CH_3	CH_3	
D35	CH_2CH_3	CH_2CH_3	

Scheme 12. Synthesized compounds.

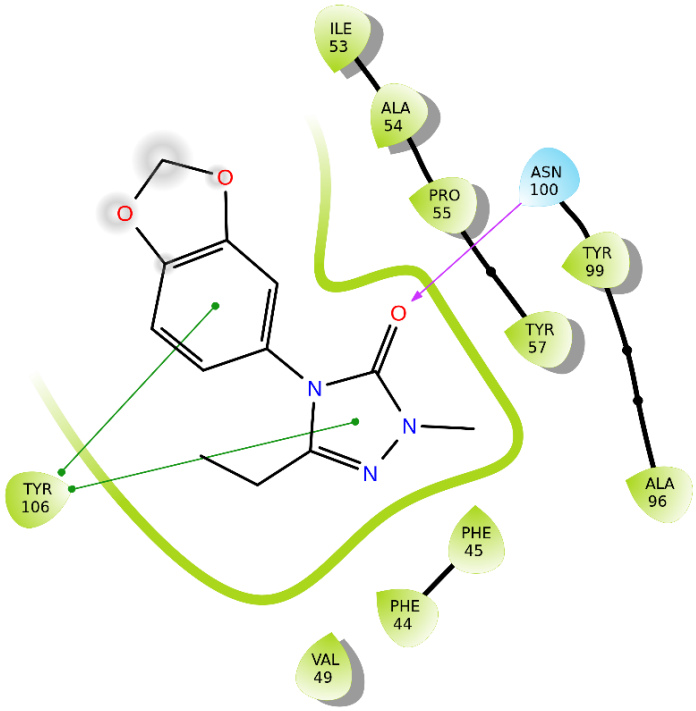

Figure 23. 2D panel representing interactions formed by compound **D25** with BRD9. Violet arrows representing H-bonds, green arrows representing π-π stacking.

2.5.2 Chemical synthesis

For the synthesis of selected compounds **D3-D8**, acetyl hydrazine was obtained by reaction between ethyl acetate and hydrazine hydrate in ethanol at reflux. Acetyl hydrazine was put to react with the specific aryl isocyanate, and the obtained urea derivatives with an excess of NaOH at reflux gave the desire products (**Scheme 13A**).

For **D11-D18**, a different synthetic approach was employed, since ethyl propionate gave lower yields if compared with ethyl acetate. The synthesis of compounds **D11-D18** was performed by a first reaction between hydrazine hydrate and different decorated isocyanates in $CHCl_3$ from 0°C to room temperature. The derivatives were put to react with propionic anhydride and the final products were obtained in the same way with an excess of NaOH (**Scheme 13B**).

N-methylation of the 2,4-dihydro-3*H*-1,2,4-triazol-3-one nucleus was then accomplished by bromomethane and NaH in dry DMF at room temperature to give compounds **D19**-**D25** (**Scheme 13C**).

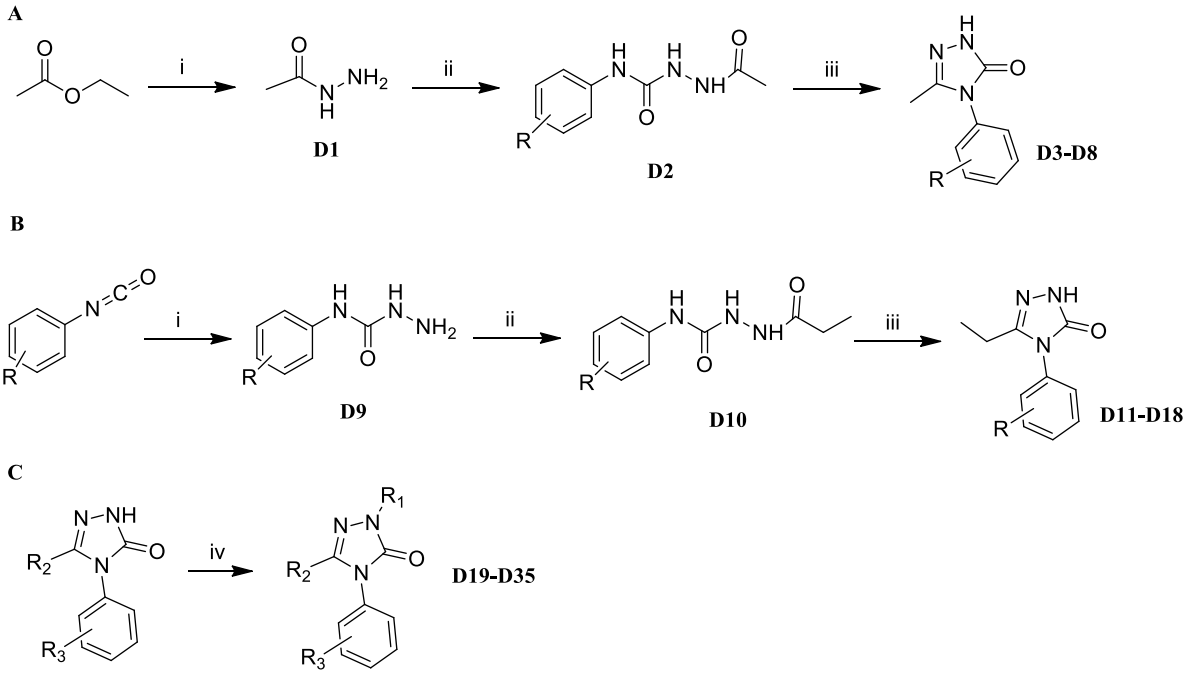

Scheme 13. A) Synthetic strategy for compounds **D3**-**D8**. *Reagents and conditions: i) NH_2NH_2, EtOH, reflux; ii)O=C=N-Ph(R), EtOH, reflux; iii) NaOH, MeOH, reflux.* B) Synthetic strategy for compounds **D11**-D**18**. *Reagents and conditions: i)NH_2NH_2, DCM, 0°C to r.t.; ii) acetic anhydride, $CHCl_3$, O°C iii) NaOH, MeOH, reflux.* C) Synthetic strategy compounds **D19**-**D35**. *Reagents and conditions: i) NaH, CH_3I or CH_3CH_2I, DMF, 0°C to r.t.*

2.5.3 AlphaScreen assay, pharmacophore screening and SAR investigations

Firstly, compounds **D3**-**D8**, **D11**-**D25** were screened against BRD9 in a cell-free AlphaScreen binding assay, using BSP-33005 as reference compound. In this experiment, glutathione S-transferase (GST)-fused BRD9 was linked to anti-GST acceptor beads through its tag, biotinylated H4Ac peptide was linked to streptavidin donor beads, favoring the interaction between the counterparts. A high AlphaScreen signal was measured due to the proximity of the mixture components allowing singlet oxygen transfer. The selected compounds were

solubilized in DMSO as vehicle and then tested at single point concentrations of 10 μM in triplicate. Among the tested compounds, **D22** and **D25** showed a promising binding to BRD9 (**Table 7**) and, accordingly, their interaction profile was further investigated by determining the IC_{50} values, confirming the promising outcomes (IC_{50}= 0.35±0.18 μM and 0.14±0.05 μM, respectively) (**Figure 24**).

Table 7. Residual binding of Histone H4Ac to BRD9 after treatment with synthesized compounds **D3-36** and related IC_{50} values for the most promising hits. Data are expressed as means ± SD, n = 3.

COMPOUND [10μM]	RESIDUAL BINDING OF HISTONE H4Ac T0 BRD9(%)± SD	IC_{50} ± SD(μM)
D3	>100	/
D4	>100	/
D5	>100	/
D6	>100	/
D7	97.8 ±0.1	/
D8	73.6 ±2.0	/
D11	97.2 ±1.8	/
D12	97.1 ±1.4	/
D13	91.8 ±1.2	/
D14	97.5 ±0.3	/
D15	94.9 ±1.1	/
D16	96.1 ±0.04	/
D17	96.99 ±1.2	/
D18	84.6 ±0.6	/
D19	86.7 ±0.2	/
D20	95.7 ±0.5	/
D21	85.3 ±2.6	/

D22	28.1 ±1.1	0.35 (±0.18)
D23	85.1 ±2.5	/
D24	76.5 ±1.6	/
D25	21.1 ±0.8	0.14 (±0.05)
D26	38.1 ±1.5	4.13 (±1.03)
D27	>100	/
D28	50.8 ±1.4	7.62(±1.88)
D29	91.2 ±0.9	/
D30	58.8 ±0.8	11.12(±0.47)
D31	35.6 ±1.2	5.44(±0.40)
D32	24.3 ±1.2	1.86 (±0.47)
D33	86.6 ±1.2	/
D34	41.2 ±1.3	4.01(±1.10)
D35	39.4 ±2.0	2.49 (±1.40)

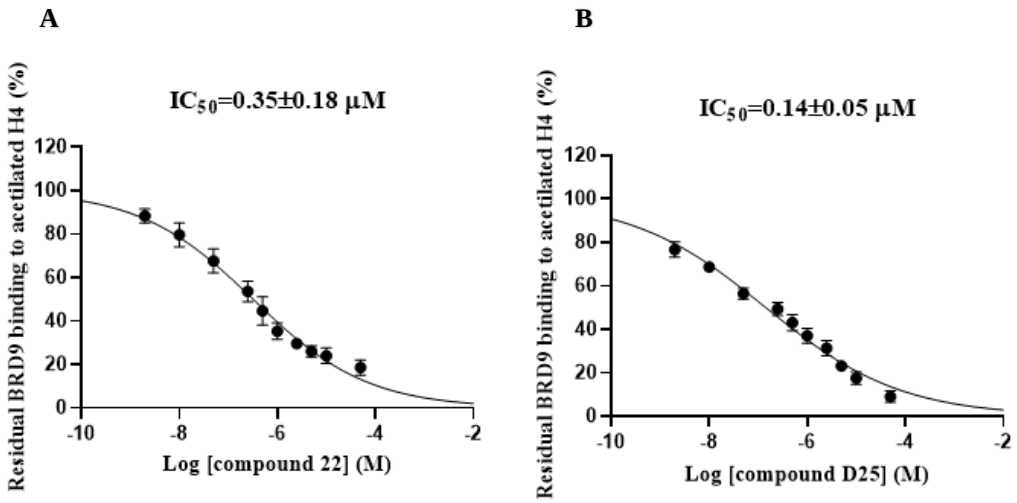

Figure 24. Concentration-response curves for the analysis of the binding on BRD9: a) **D22**, b) **D25**. Data are expressed as percentage of control (100%), means ± SD, n = 3.

Starting from these encouraging data, the selectivity over other bromodomain subfamilies was assessed for **D22** and **D25** after testing them on a panel of further nine BRDs covering most of the related human phylogenetic tree (BRD2-BD1, BRD2-BD2, BRD3-BD1, BRD3-BD2, BRD4-BD1, BRD4-BD2, BRDT-BD1, BAZ2B, CREBBP) (**Table 8**).

In general, these results highlighted the compounds featuring methyl substituent at N2 (**D19**-**D25**) as better BRD9 binders in comparison with compounds featuring the free NH (**D3**-**D18**) that instead showed a residual histone binding of about 85%. For instance, compounds **D8** and **D18**, featuring the same 4-(3,4-dimethoxyphenyl)- and 4-(benzo[*d*][1,3]dioxol-5-yl)-substituents of the lead compounds **D22** and **D25**, but lacking the N-methyl function, did not show a significant binding (73.60% and 84.59%, respectively) (**Table 7**).

During the development of further derivatives, in our group a 3D structure-based pharmacophore models was introduced for BRD9,[93] useful for accelerating the identification of new promising binders of the target from molecular docking calculations.

Thus, for rationalizing the AlphaScreen data and understanding the impact of each chemical structure on the final binding, we used this model on the synthesized compounds. In particular,

among the three models described, the "pharm-fragment" one was used, accordingly with the compounds small size. From a retrospectively analysis, we could achieve that O=C3-N2-R_1 moiety likely corresponded to acetyllysine mimetics rather than N1-C5-R_2, thus in accordance with the binding results. Moreover, compounds **D3**-**D8,** missing the alkyl group on the nitrogen in position 2, did not respect all four features as the minimum structural requirement to obtain promising BRD9 binders, which was instead respected by compounds **D11**-**D25**. Starting from this encouraging data, we evaluated a set of **D22** and **D25** derivatives. Specifically, the 4-(3,4-dimethoxyphenyl)- and 4-(benzo[*d*][1,3]dioxol-5-yl) as well as the 5-methyl- and 5-ethyl-substituents, originally present in compounds **D22** and **D25**, together with the new 2-ethyl substituent, were initially accounted to generate compounds **D26**-**D31** representing the possible six remaining molecular combinations. In particular, the ethyl substituent in position 2 was here considered to evaluate the influence of this moiety in gaining selectivity against the other bromodomains. Furthermore, further four compounds (**D32**-**D35**) were synthesized with the aim of assessing the influence of halogens on the 4-phenyl- substituent and providing useful information for the SAR investigations.

Importantly, the newly selected compounds (**D26**-**D35**) matched all the features of the "pharm-fragment". Therefore, AlphaScreen assays were then performed for compounds **D26**-**D35** to assess the binding on BRD9 (**Table 7**).

As expected, most of these derivatives (**D26**, **D28**, **D30**, **D31**, **D32**, **D34**, **D35**) were able to bind BRD9 at low micromolar range of concentrations (**Table 7**, **Figures 25** and **26**). The binding with the receptor counterpart was associated with the presence of methyl or ethyl in position 2 directing the other substituent in position 5 in ZA channel. The presence of a methyl or an ethyl in position 5 did not significantly influence the binding. On the other hand, the simultaneous presence of ethyl in positions 2 and 5 led to no binding against BRD9, as observed for the compounds **D27**, **D29** and **D33**. In fact, in these cases, the size of the molecules did not

orient the substituent in position 5 in the channel ZA. Compound **D35** (IC_{50}=2.49±1.40μM) was the only 2,5-diethyl substituted screened molecule able to bind BRD9 with the correct substituent orientation. Meta-trifluoromethyl-substituent, only present in compound **D35** among the 2,5-diethyl substituted molecules, oriented the ethyl groups 2 and 5, allowing the interaction with the ZA channel.

Lastly, the binding with BRD9 was also observed for the compounds featuring *meta* chloro and *para* fluoro substitutions of the aromatic ring, thanks to a halogen bond these substituents form with Tyr99. Therefore, among these derivatives, the N-methyl compound was the best derivative (compound **D32**, IC_{50}=1.86±0.47 μM), followed by N-ethyl derivative (compound **D34**, IC_{50}=4.01±1.10 μM), while the 2,5-diethyl derivative (**D33**) did not show activity against BRD9.

Again, the disclosed BRD9 binders **D26**, **D28**, **D30**, **D31**, **D32**, **D34**, **D35** were evaluated on the panel of nine bromodomains, confirming the selectivity against BRD9 (**Table 8**).

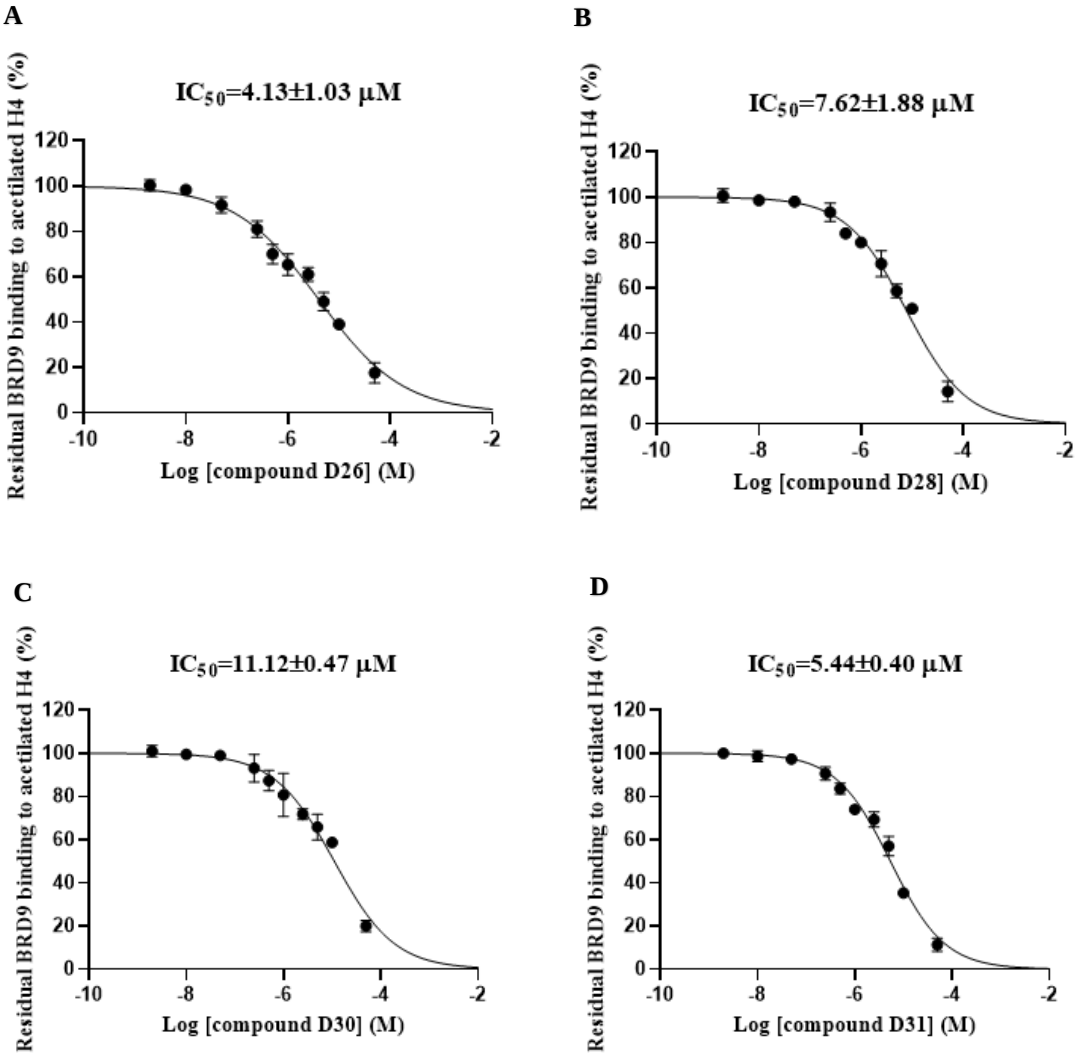

Figure 25. Concentration-response curves for the binding analysis on BRD9: a) **D26**, b) **D28**, c)**D30**, d)**D31**. Data are expressed as percentage of control (100%), means ± SD, n = 3.

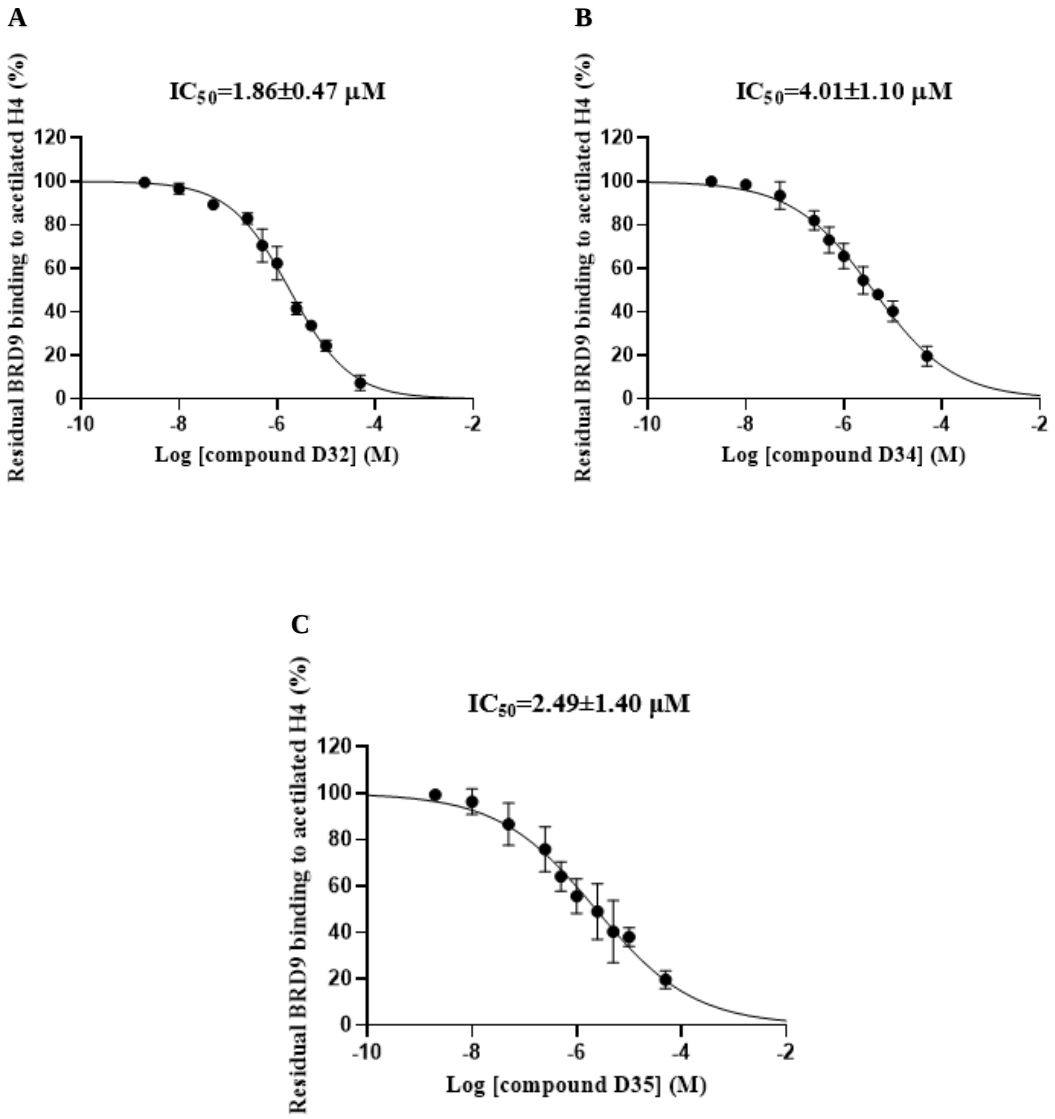

Figure 26. Concentration-response curves for the binding analysis on BRD9: a)**D32**, b)**D34**, c)**D35** on BRD9. Data are expressed as percentage of control (100%), means with ± SD, n = 3.

Table 8. Percentage of binding residue (%) ±SD of selected compounds against the reported bromodomains. Values shown as average of two separate experiments.

COMPOUND	BRD2-BD1	BRD2-BD2	BRD3-BD1	BRD3-BD2	BRD4-BD1
D22	96.5±1.3	≥100	≥100	≥100	≥100
D25	98.9±2.1	≥100	96.5±1.8	≥100	≥100
D26	≥100	96.7±2.4	97.3±1.8	97.7±0.2	≥100
D28	≥100	≥100	97.8±1.0	≥100	99.2±2.0
D30	≥100	94.4±1.5	97.3±0.8	94.9±0.5	≥100
D31	≥100	≥100	74.8±1.3	99.9±1.1	96.2±1.5
D32	≥100	≥100	≥100	98.3±1.0	99.2±1.3
D34	98.2±2.3	≥100	≥100	93.3±1.5	99.0±1.6
D35	99.0±0.6	≥100	≥100	97.4±0.5	97.7±0.1
COMPOUND	**BRD4-BD2**	**BRDT-BD1**	**BAZ2B**	**CREBBP**	**PAMPA -logPe**
D22	94.7±2.5	≥100	≥100	96.3±1.4	5.58±0.01
D25	88.6±0.7	≥100	≥100	97.7±1.2	5.23±0.04
D26	89.4±5.1	95.6±0.4	≥100	≥100	5.28±0.04
D28	≥100	97.9±0.6	≥100	≥100	5.45±0.01
D30	99.3±0.3	92.5±5.1	92.8±0.3	≥100	5.48±0.01
D31	99.2±0.3	≥100	97.5±1.2	≥100	5.23±0.01
D32	≥100	98.2±1.5	≥100	≥100	4.88±0.02
D34	≥100	98.3±1.0	≥100	≥100	4.66±0.06
D35	≥100	98.3±0.7	≥100	≥100	4.82±0.02

2.5.4 Further investigations

In collaboration with Prof. Maria Chiara Monti, these compounds were also tested in the parallel artificial membrane permeability assay (PAMPA) to measure their effective permeability (expressed as -log Pe) through an artificial lipid membrane. In this assay, compounds **D22**, **D25**, **D26**, **D28**, **D30**, **D31**, displayed a good propensity to cross the membrane in vitro (-logPe between 5.23 and 5.58) as well as compounds **D32**, **D34** and **D35** which showed a better permeation of artificial membrane (-logPe between 4.66 and 4.88) as reported in **Table 8**.

Cell assays were carried out in collaboration with Prof. Carlo Irace of the University of Naples. These best compounds were evaluated on a selected panel of human cells, composed of both healthy (keratinocytes and enterocytes) and cancer (leukaemia, breast, melanoma and colorectal) cell lines with different proliferative potential. Interestingly, all the investigated compounds shared biocompatible features. In fact, even at the highest concentrations, there was no evidence of cytotoxic responses in healthy cells. IC_{50} values higher than 500 µM corroborated the absence of detectable biological effects (**Table 9**). Concerning bioactivity on human cancer models, though based on preliminary data, a fair selectivity of action on leukemic cells was observed. Among all tested items, compounds **D22** and **D2,** already emerged as the most promising as BRD9 binders, showed IC_{50} values lower than 150 µM on Jurkat cells, revealing a weak anti-proliferative activity which deserves further consideration.

Table 9. Anticancer activity reported as IC_{50} values (μM) in Jurkat, MCF-7, A375, Caco-2, HaCaT and Enterocytes human cancer cell lines for compounds **17**, **20**, **22**, **23**, **25**, **26**, **28**, **29**, **31**. The calculation of the concentration required to inhibit the net increase in the cell number and viability by 50% (IC_{50}) is based on plots of data (n=6 for each experiment) and repeated three times (total n=18). IC_{50} values were obtained by means of a concentration-response curve by nonlinear regression using a curve fitting program, GraphPad Prism 5.0, and are expressed as mean ± SEM (total n=18) of three independent experiments.

COMPOUND	Jurkat	MCF-7	A375	Caco-2	HaCaT	ENTEROCYTES
D22	110 ± 9	> 500	450 ± 16	300 ± 14	> 500	> 500
D25	145 ± 11	500	270 ± 18	330 ± 12	> 500	> 500
D26	420 ± 19	> 500	480 ± 22	> 500	> 500	> 500
D28	315 ± 15	360 ± 14	400 ± 16	300 ± 13	> 500	> 500
D30	290 ± 13	400 ± 11	400 ± 18	370 ± 11	> 500	> 500
D31	> 500	> 500	> 500	> 500	> 500	> 500
D32	225 ± 11	> 500	500 ± 15	> 500	> 500	> 500
D34	> 500	> 500	450 ± 20	> 500	> 500	> 500
D35	270 ± 14	490 ± 18	> 500	> 500	> 500	> 500

In this scenario, the identification of novel bromodomain inhibitors was constantly pursued, in order to elucidate the biological and pathological role of these epigenetic targets in specific disease (e.g., BRD9 in acute myeloid leukaemia). Regarding BRD9 and also other non-BET bromodomains, the molecular probes already identified in previous studies and featuring high affinity for the protein modules (e.g., LP99 and I-BRD9 for BRD9) do not display a significant effect in alteration of cell proliferation in leukemic cells. The reason of such an evidence is probably due to different protein interaction domains or to the activation/inclusion of compensatory mechanisms, which entail the recognition of chromatin sites by the SWI/SNF complex. **In Table 9**, IC_{50} values in Jurkat, MCF-7, A375, Caco-2, HaCaT and Enterocytes human cancer cell lines reported for the investigated compounds highlight a partial interference

in cell proliferation, which is in line with the above reported evidences. Accordingly, to circumvent such an occurrence, the implementation of PROTAC technology [110] and the inclusion of the design of SWI/SNF multi-target compounds in developing of BRD9 inhibitors is urgently required. Regarding the design of PROTACs, one of the main limitations is related to the chemical structure of the related hit compounds, which requires an "attachment point" for the linker of the E3 ligase ligands that must not affect the original protein interaction network.[111] During the development of the here disclosed bioactive compounds, the computational studies and the implementation of 3D structure-based pharmacophore models highlighted, at first instance, the binding mode of the 2,4-dihydro-3*H*-1,2,4-triazol-3-one derivatives and, consequently, led us to identify the position on which PROTAC linkers can be attached for further optimization. Indeed, according to the detected binding modes, the substituents at N4 are oriented towards the outside of the ZA loop of the protein, which represents an optimal situation to ensure the formation of the ternary complex that a PROTAC is intended to do. Thus, modification at N4 can be considered for functionalization in order to obtain related PROTACs and to improve the biological effect in cancer cell lines.

2.6 Quinazolin-4(3*H*)-one-based compounds as new modulators of bromodomains BRD9

After choosing the 6-methylquinazolin-4(3*H*)-one and 3,6-dimethylquinazolin-4(3*H*)-one chemical cores since deemed privileged scaffolds, we observed if the requirements of the pharmacophoric model were respected.

If properly functionalized, these scaffolds could match the requirements of the AAHHRRR 7-points model (**Paragraph 2.1**).[93] In particular:

- the C=O in position 4 could represent the group able to establish the hydrogen bond with Asn100;

- the quinazolin-4(3*H*)-one chemical core could interact with Tyr106;
- aromatic groups placed in positions 2 and 8 could interact with Phe44 in ZA channel, ameliorating potency and selectivity.

Based on this consideration, position 2 and 8 of both scaffolds were modified (**Scheme 14**) taking into account an appropriate synthetic strategy for making these changes.

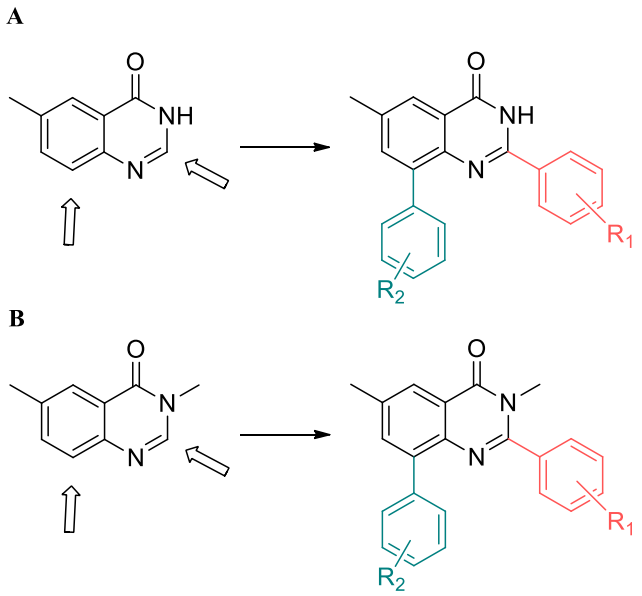

Scheme 14. a) 6-methylquinazolin-4(3*H*)-one chemical scaffold and modifications; b) 3,6-dimethylquinazolin-4(3*H*)-one chemical scaffold and modifications.

2.6.1 Design

A multi-step computational protocol was applied: starting from the chosen synthons, Combiglide[96] was used for the decoration of 6-methylquinazolin-4(3*H*)-one and 3,6-dimethylquinazolin-4(3*H*)-one with ~3000 benzaldehyde at position 2 and 570 boronic acids at position 8, respectively (**Scheme 14**). Two large libraries were obtained after combining the scaffold with the prepared reagents. Then, following the general workflow reported in the **Introduction**, the libraries were processed with the functions: LigPrep,[97] QikProp[98] and LigFilter[105] of Maestro Software.

The binding affinity for the most promising compounds was predicted through molecular docking calculations, and the best compounds were selected for the following synthesis and biological evaluation step (**Scheme 14**, **Figure 27**).

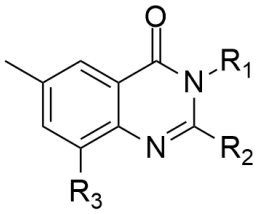

COMPOUND	R_1	R_2	R_3
E4	H		
E5	H		
E6	H		
E7	H		
E8	H	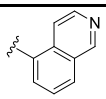	
E9	H		
E10	H		
E11	H	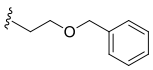	
E12	H	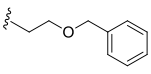	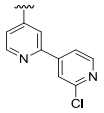
E13	H	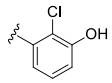	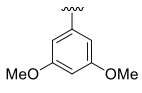
E14	H	CH_3	
E15	H	CH_3	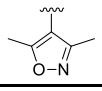
E16	CH_3	CH_3	
E17	CH_3	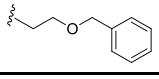	

Scheme 14. Chemical structure of compounds **E3**-**E16**, selected by docking calculations.

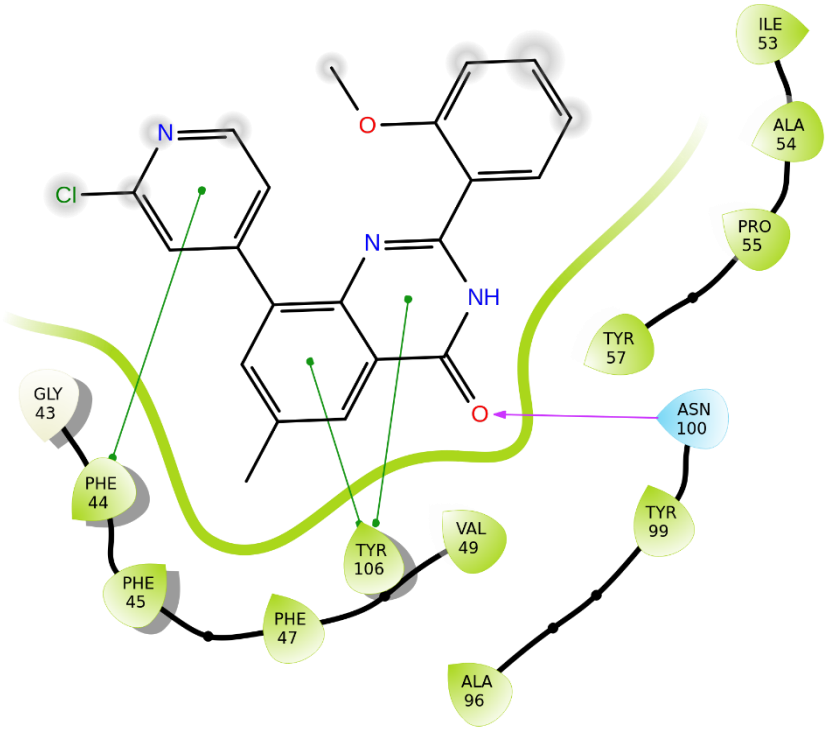

Figure 27. 2D panel representing interactions formed by compound **E4** with BRD9. Violet arrows representing H-bonds, green arrows representing π-π stacking.

2.6.2 Chemical synthesis

Compounds **E4-E16** were then prepared following a four-step synthetic route described in **Scheme 15**. First, the 2-amino-3-bromo-5-methylbenzoic acid was put to react with NH_4Cl and DIPEA, using EDC·HCl and HOBt as activator of carboxylic group, to give the 2-amino-3-bromo-5-methylbenzamide. The reaction proceeded in DCM/DMF (10/1) at room temperature for 24h.

In the second step of the reaction, the amide derivative obtained **E1** reacted with a benzaldehyde in THF, at reflux generating the formation of an imine in position 2. After 5h, molecular iodine was added to the reaction mixture that promotes intramolecular cyclisation allowing to obtain the quinazolin-4(3*H*)-one nucleus **E2**.

Instead, the intermediate **E3**, bearing a methyl in position 2, was obtained in a different reaction by oxidizing ethanol *in situ* with the TBHP to obtain the acetaldehyde needed for the scaffold synthesis. This choice was made because of the high volatility of the acetaldehyde (20.5°C), difficult to manage also at room temperature; therefore the ethanol oxidation *in situ* was preferred to acetaldehyde use.

The selected compound**s** were obtained with Suzuki- Miyaura cross coupling. The coupling was performed at 80 °C for 16h by using tetrakis(triphenylphosphine)palladium(0) as catalyst, potassium carbonate as base and a mixture dioxane/water (8:2) as the reaction solvent. All the products were obtained in high yields.

Compounds **E15-E16** were then methylated to obtained 3-methyl derivatives by using CH_3I and NaH in DMF at room temperature (**Scheme 15**).

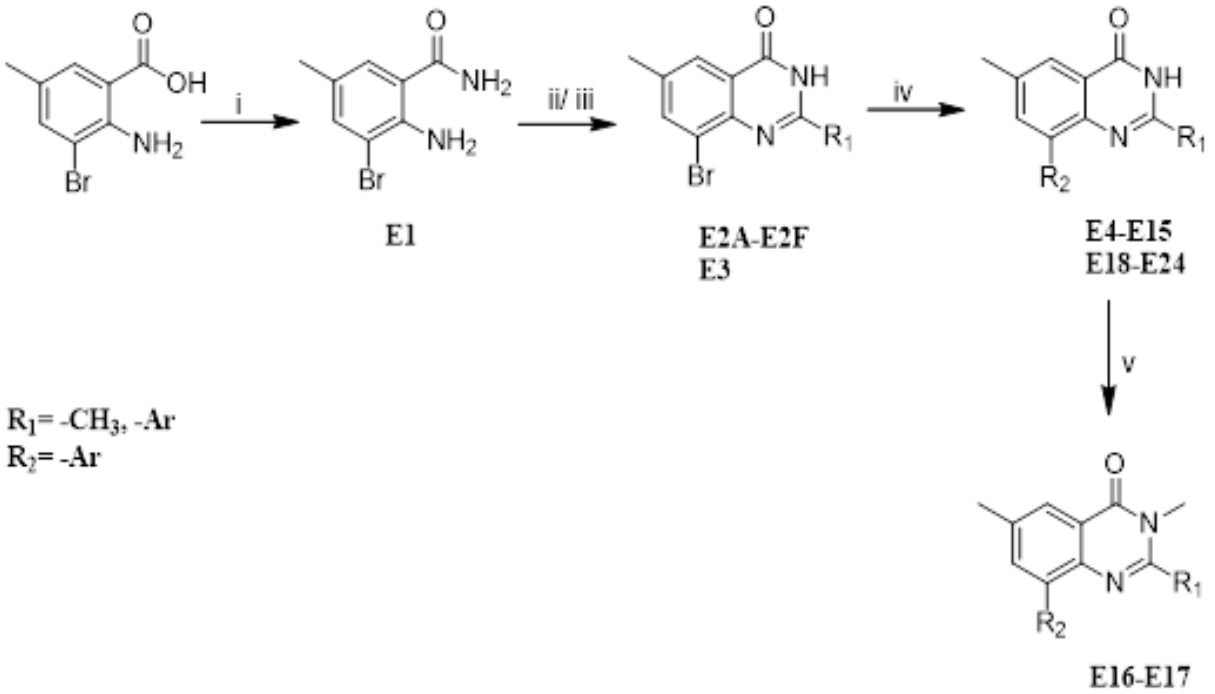

Scheme 15. A) Synthetic strategy for compounds of **E** series. *Reagents and conditions: i) EDC, HOBt, DIPEA, NH_4Cl, DMF r.t.; ii)R_1-CHO I_2, THF, reflux;*[5] *iii) EtOH, TBHP, reflux; iv) R_2-$B(OH)_2$, K_2CO_3, $Pd[P(Ph)_3]_4$, dioxane/H_2O, 80°; v)CH_3I, NaH, DMF, 0°C to r.t.*

2.6.3 AlphaScreen assay and further SAR investigations

In order to verify the binding affinity of the synthesized derivatives **E4**-**E16** all the compounds were screened by AlphaScreen assay, as previously described for the other derivatives, to assess their potential affinity against the BRD9 protein. In these new experiments, each molecule was evaluated at 10μM. For each sample, the complete binding study was performed using triplicate aliquots. The analysis of the data related to these compounds revealed that two of them, in particular compounds **E7** and **E13**, showed a promising binding affinity against the protein with a percentage of residual binding to acetylated histone of 76.7% and 65.6%, respectively (**Table 10**).

Table 10. Residual binding of Histone H4Ac to BRD9 after treatment with synthesized compounds **E4**-**E16.** Data are expressed as means ± SD, n = 3.

COMPOUND (10μM)	RESIDUAL BINDING OF HISTONE H4Ac T0 BRD9(%)± SD
E4	89.6 ±1.0
E5	86.5 ±0.9
E6	82.0 ±1.2
E7	76.7 ±1.1
E8	89.6 ±0.7
E9	93.0 ±0.9
E10	80.2 ±1.5
E11	80.4 ±2.0

E12	82.1 ±0.5
E13	65.6 ±0.4
E14	93.0 ±1.3
E15	86.8 ±1.1
E16	84.5 ±1.1
E17	83.1 ±0.8

Hence, based on this preliminary data, we hypothesized that the moderate binding was due to the presence of the methyl group in γ position compared to the carbonyl group. In fact, these groups resulted in a more spatial distance than the typical acetyllysine mimic function, present in all the BRD9 binders. Due to the lack of a starting reagent presenting the methyl in β position and to further explore the potential activity of these scaffolds, we decided to synthesize some derivatives of compounds **E7** and **E13** reversing groups in positions 2 and 8 (compounds **E18** and **E19**). Thereafter, the subsequent derivatives were synthesized (**Scheme 16**) by keeping position 8 of the compound **E7**, and modifying just groups in position 2. Group in position 8 is indeed a conserved feature among several inhibitors of the same target. Instead, position 2 was replaced with all the benzaldehydes available in our laboratory with a group -OH on the aromatic ring. This choice was based on the revaluation of the binding mode of the best derivatives. In particular, an hydrogen bond acceptor/donor group close to the carbonyl could give another bond with Asn100, strengthening the binding of the molecule with the protein (**Figure 27**).

The AlphaScreen assay to assess the binding of new synthesized compounds *versus* BRD9 is currently ongoing.

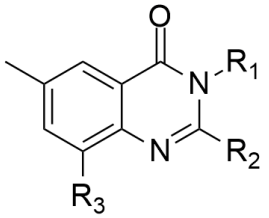

COMPOUND	R_1	R_2	R_3
E18	H	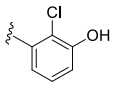	
E19	H		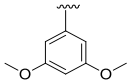
E20	H	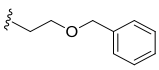	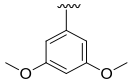
E21	H	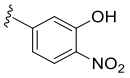	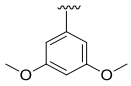
E22	H	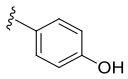	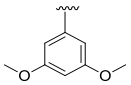
E23	H	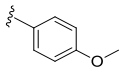	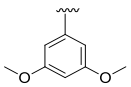
E24	H	CH_3	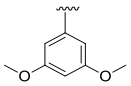

Scheme 16. Chemical structure of synthesized compounds **E17**-**E24**.

2.7 Summary

In summary, by *Interaction-based approach* we designed three sets of compounds featuring isoxazole[2,3-*c*][1,3,5]thiadiazepin-2-one, 4-ethylbenzothiazole and 1,8-naphthyridone nucleus in order to find new BRD9 binders. The Alphascreen assay highlighted the inability of the compounds to bind the target.[93]

Through Inverse Virtual Screening, the synthesized compounds were re-evaluated on a panel of proteins involved in inflammatory and tumor processes. In particular, isoxazole[2,3-*c*][1,3,5]thiadiazepin-2-one-based compounds were successfully repositioned, showing activity on the ESR receptor. On the other hand, for the benzothiazole based compounds, we identified

the soluble epoxide hydrolase (sEH) as potential target. This interesting profile was confirmed through binding assays conducted by Prof. Oliver Werz's group (University of Jena).

Finally, the evaluation of 1,8-naphthyridones on CK2 alpha, Mek1 and Mek2 kinases is currently ongoing.

On the other hand, the careful analysis of the BRD9 pharmacophore model[93] offered a direction for the more suitable decoration pattern on the 2,4-dihydro-3*H*-1,2,4-triazol-3-one and quinazolin-4(3*H*)-one-based cores. By the previously described multistep approach, we disclosed 9 new potent and selective BRD9 binders with 2,4-dihydro-3*H*-1,2,4-triazol-3-one chemical core (**D22**, **D25**, **D26**, **D28**, **D30**, **D31**, **D32**, **D34**, **D35**). Our results additionally pointed toward two weak binders (compounds **E7** and **E13**) with quinazolin-4(3*H*)-one core as promising future starting point for the development of more potent selective compounds. In this context, other seven derivatives of the same collection were synthesized and the binding assays for these new ones are now in progress.

These encouraging data corroborate the efficacy and reliability of the developed three-dimensional pharmacophore model for the design of new BRD9 binders.

CHAPTER 3
Design and synthesis of novel molecular platforms as modulators of the arachidonic acid cascade enzymes

3.1 Introduction

In recent years, mPGES-1 has attracted increasing attention as a strategic target for both inflammatory and cancer diseases, since its inhibition affects only PGE_2 levels upregulated in pathological conditions and overexpressed in several types of cancer.[112] In this context, identifying novel agents interfering with this enzyme represents a promising strategy for developing new anti-inflammatory and anticancer drugs with reduced side effects.

Moreover, targeting more enzymes involved in the arachidonic acid cascade as a dual inhibitor (mPGES-1/sEH or mPGES-1/5-lipoxygenase) is currently considered a promising strategy for the pharmacotherapy of inflammation.

For this reason, in the frame of my Ph.D., I have been involved in the discovery of new mPGES-1 and/or sEH inhibitors as candidates for drug development.

In this context, the chemical cores selected and investigated as starting templates for the development of small molecules were:

- thiazolidin-4-one (**F** series);
- benzo[*d*][1,3]thiazin-4-one (**G** series);
- 3-benzilquinossalin-2(1*H*)-one (**H** series);
- 2-(5-phenyl-2,3-dihydrobenzo[*d*]oxazol-2-yl)acetic acid (**I** series);
- furoquinoline and furoquinolinone (**J** series);
- 1,3,4-oxadiazole (**K** series);
- 4*H*-benzo[*b*]imidazo[1,5-*d*][1,4]oxazine (**L** series);
- Thiazole (**M** series);

In particular, following a structure-based drug design, with thiazolidin-4-one chemical core, the first multitarget inhibitor of mPGES-1/sEH/5-LO (**F4**) and two compounds as very promising inhibitors of mPGES-1/sEH/ (**F2**, **F8**) were disclosed.

Additionally, the benzo[*d*][1,3]thiazin-4-one-based compounds were evaluated and synthesized as mPGES-1 potential inhibitors, for which the biological assays are currently ongoing.

Regarding the remain selected scaffolds (**H**-**M** series), computational modelling techniques were used for the design of new potential inhibitors of the interested target, in order to reduce costs and time of screening. In these cases, the synthesis parts are in the early stages or have not yet started, for this reason not discussed in this Ph.D. thesis.

Finally, as already described in **Chapter 1**, 4-ethylbenzothiazole-based compounds, after disclosing a poor inhibitory activity against BRD9 were successfully repositioned on sEH by Inverse Virtual Screening method, showing the **B3** IC_{50}=6.62±0.3μM on the protein.

3.1.1 Computational modeling techniques for the design of new mPGES-1 and/or sEH potential inhibitors

The assumption that maximizing structural diversity would increase the chances of finding new hits led to the design of libraries of molecules characterized by the same scaffold with different derivatization.

Computational methods fit well into this context, allowing the generation of virtual libraries *in silico*, using a specific protocol, successively evaluated on the target protein of interest. This approach permits to predict the binding of thousands of virtual compounds with the target and to select only the most promising ones, in a time and cost effective way.

The general workflow provides (**Figure 28**):

1. The choice of a scaffold, whose building blocks are used as a starting point for the *in silico* drug design;

2. The combination of the chosen scaffold with the virtual reagents must be used according to the synthetic strategy previously selected. The virtual combination of the chosen scaffold with the reagents leads to the formation of small or large virtual libraries;
3. Application of pharmacokinetic filters and calculation of the properties of the ADME, through which all pharmacokinetically unfavorable virtual molecules of the libraries are eliminated;
4. Virtual Screening workflow, a docking analysis on the built new libraries for the selection of the best candidates. In this case, the docking path works at three different levels, which operate with a gradually increasing precision;
5. Evaluation and selection of the best molecules according to docking score, binding mode, and interactions established with the receptor counterpart, based on the reported key interactions.

The general scheme reported in **Figure 28** was used for the design of all the molecule series reported below. After that for **F** and **G** series, the synthesis steps were performed following the synthetic strategy chosen.

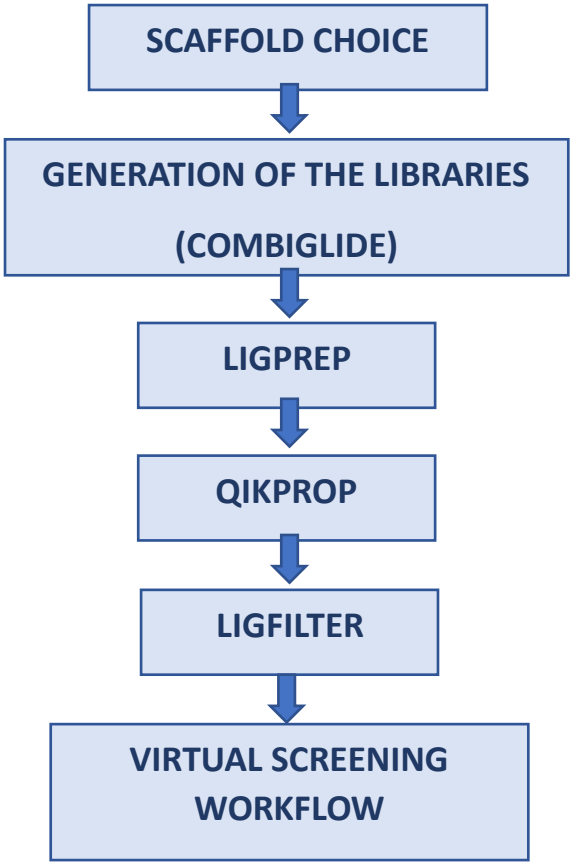

Figure 28. Multi-step computational protocol.

3.2 Thiazolidine-4-one-based compounds as mPGES-1 inhibitors

3.2.1 Design

To identify new mPGES-1 inhibitors, we firstly investigated the putative ability of thiazolidin-4-one-based compounds of inhibiting this enzyme through molecular modeling experiments and, then, we analysed them as a candidate for discovering novel anti-inflammatory agents targeting different enzymes in the arachidonic acid cascade (5-LO and sEH) by applying a well-structured workflow (**Figure 29**).

According to our previous results[113] 2,4-thiazolidinedione-based compounds are dual inhibitors of mPGES-1/5-LO, besides being involved in other biological activities;[114-115] therefore, we opted for the thiazolidin-4-one scaffold.

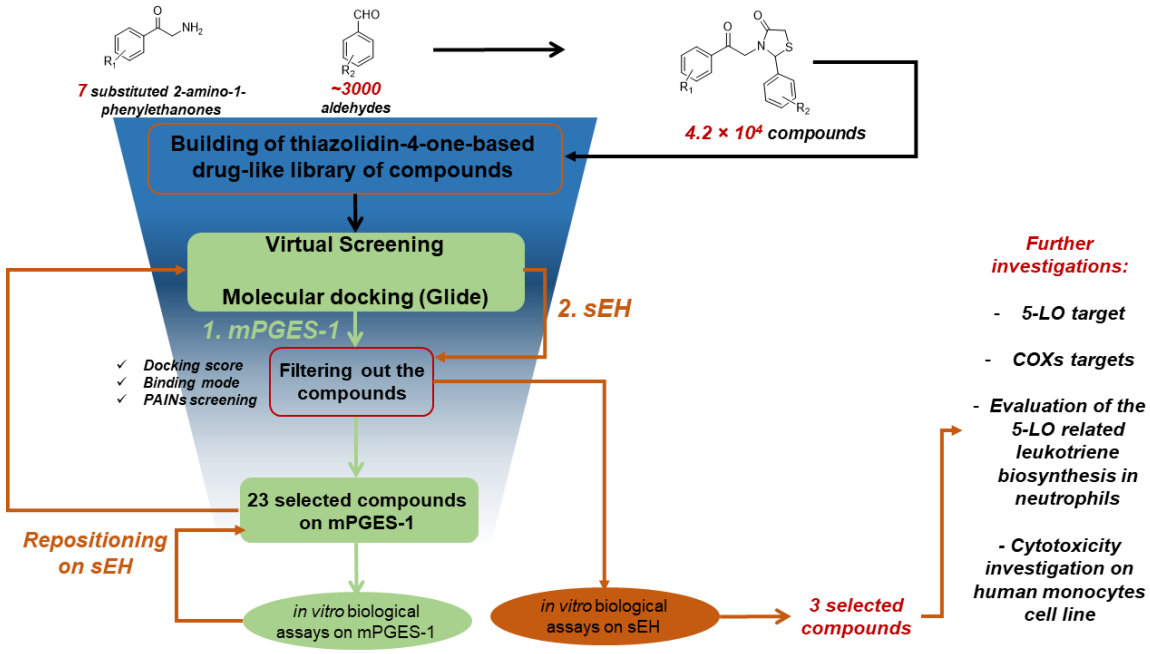

Figure 29. Workflow for the selection of the thiazolidine-4-one-based compounds.

The position 2 was modified with ~ 3000 commercially available aromatic aldehydes, and the nitrogen in position 3 with seven substituted-2-amino-1-phenylethanones, using Combiglide software.[96]

The prepared virtual library was subjected to LigPrep[97] to generate all the tautomers and protonation states to physiological pH, also accounting for the C-2 stereocenter, thus leading to the formation of both the possible stereoisomeric solutions. As in previous cases, the library has been filtered according to the pharmacokinetic parameters and then subjected to *Virtual Screening Workflow*. After visual inspection, the twenty-three most promising compounds were selected (**Scheme 17**). In particular, the molecules interacted with:

- Phe44$_{ChainB}$ and/or His53 $_{ChainB}$ *via* H–bonds and edge-to-face π-π interactions;
- Arg126$_{ChianA}$, Thr131 $_{ChianA}$, Gln36 $_{ChianB}$, Asp49 $_{ChianB}$ via polar contacts;
- GSH and with Tyr130 $_{ChianA}$, a key residue interacting with GSH as a cofactor(**Figure 30**).

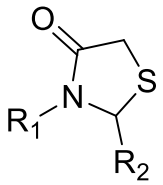

COMPOUND	R1	R2
F1	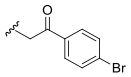	
F2	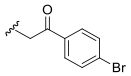	
F3	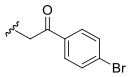	
F4	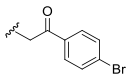	
F5	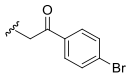	
F6	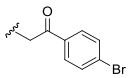	
F7	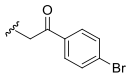	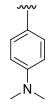
F8	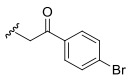	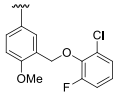
F9	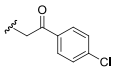	
F10	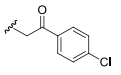	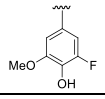
F11	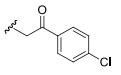	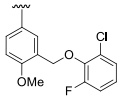
F12	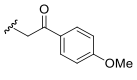	
F13	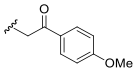	

F14	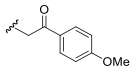	
F15	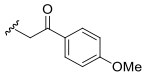	
F16	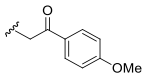	
F17	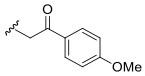	
F18	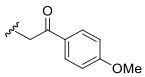	
F19	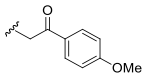	
F20	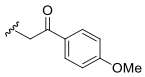	
F21	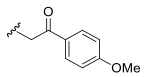	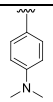
F22	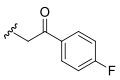	
F23	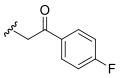	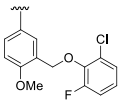

Scheme 17. Selected and synthesized thiazolidin-4-one-based molecules.

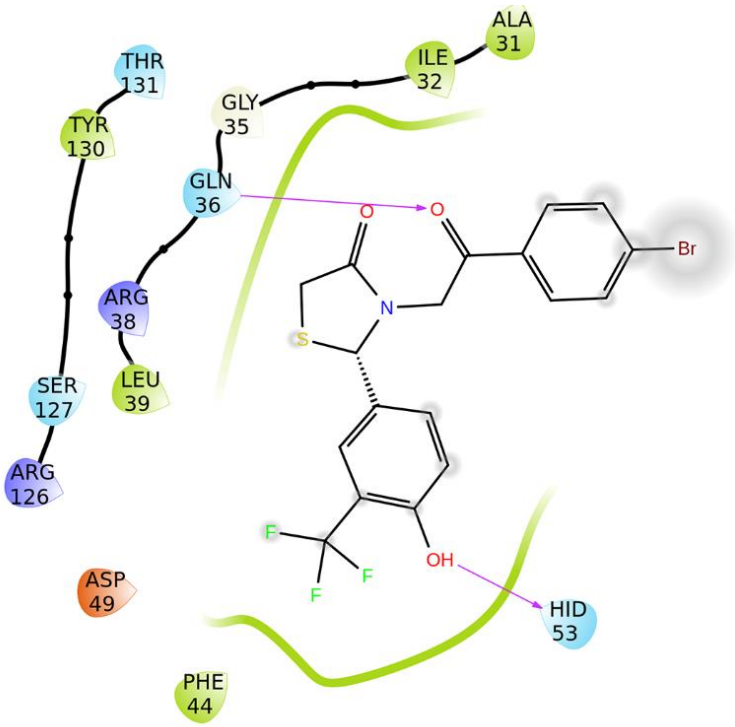

Figure 30. 2D pose of compound **F4** against mPGES-1 protein; violet arrows representing H-bonds, green arrows representing π-π stacking.

3.2.2 Chemical synthesis

The strategy for the synthesis of the identified molecules is shown in **Scheme 18**. The reaction was performed between substituted-2-amino-1-phenylethanone hydrochloride, an aromatic aldehyde, and an excess of mercaptoacetic acid in dry toluene under reflux. To prepare these molecules, we used a one-pot multicomponent reaction considering the lots of advantages of this chemical route. The first advantage offered by this approach is that a large number of molecules deriving from the virtual screening can be quickly synthesized. Moreover, it is easily integrated with the above-reported computational combinatorial approach. Secondly, one-pot chemical routes are considered "green" approaches[4] due to the less amount of reagents and solvents used according to the reduction of the number of synthetic steps and the. Nevertheless, although one-pot methods have already been described, catalysts,[116] supports[117] or microwave[118] are dramatically needed for optimizing these strategies.

In our case, the reaction proceeded with good yields in relatively short reaction times (**Table 11**) without the addition of bases or catalysts. Interestingly, the twenty-three compounds were synthesized with different yields (from 45% up to 95%, **Table 11**) depending on the specific benzaldehyde and 2-amino-1-phenylethanone adopted for the reaction. The lowest yields were observed for benzaldehydes bearing only electron donor groups on the aromatic ring (compounds **F7**, **F21**), possibly due to a lower reactivity of the carbonyl group. This hypothesis is supported by the fact that the best yields were obtained in reactions with benzaldehyde partner presenting electron-withdrawing groups (compounds **F1**, **F9**, **F20**). Comparing compounds with the same benzaldehyde, a slight improvement in the yield of the reaction was observed when 2-amino-1-phenylethanone was more basic for the presence of an electron donor group.

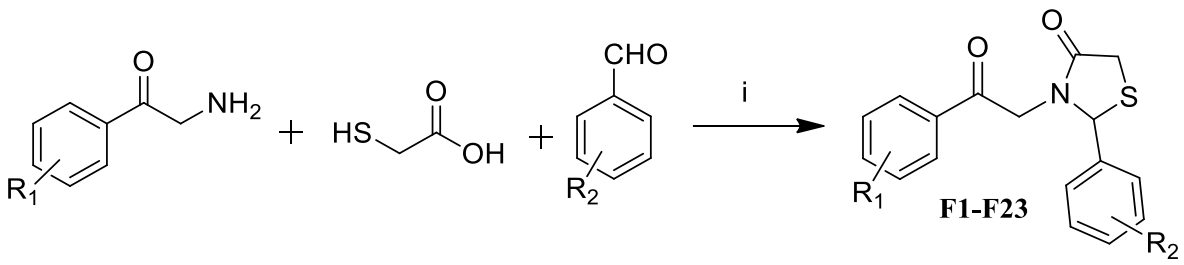

Scheme 18. Synthetic strategy adopted for the synthesis of compounds **F1-F23**. *Reagents and conditions: toluene, reflux.*

Table 11. Synthetic versatility of thiazolidin-4-one compounds.

COMPOUND	2-MERCAPTOACETIC ACID (eq.)	REACTION TIME	YIELD
F1	8	12h	92%
F2	8	24h	89%
F3	16	24h	77%
F4	16	24h	71%
F5	16	24h	87%
F6	48	120h	91%
F7	32	72h	45%
F8	8	12h	68%
F9	34	72h	95%
F10	24	72h	74%
F11	16	72h	89%
F12	8	12h	86%
F13	8	24h	90%
F14	8	24h	89%
F15	16	24h	88%
F16	24	48h	73%
F17	48	120h	78%
F18	32	48h	90%
F19	24	12h	58%
F20	32	72h	91%
F21	24	72h	49%
F22	16	12h	62%
F23	16	72h	84%

3.2.3 *In vitro* evaluation of the inhibitory activity of compounds F1-F23 on mPGES-1

A cell-free assay[119] was performed for the screening of compounds **F1-F23** against the activity of microsomal prostaglandin E_2 synthase-1 (mPGES-1) in order to investigate the presumed inhibitory activity of **F1-F23** against this enzyme. Specifically, all the compounds were tested at a concentration of 10 μM: 9 of these compounds reduced the enzyme activity, ranging from ~25 to ~50% inhibition (**F1**-**F4**, **F8**, **F14**, **F19**-**F20**, F**22**,). At the same time, a slight inhibitory potency was found for the remaining compounds (**Table 12**). Thus, the compounds **F1-F23** disclosed a partial inhibition of the activity of mPGES-1. In particular, this behavior was ascribed to the moderate ability of the non-aromatic chemical core of thiazolidin-4-one to establish all the set of interactions with the key residues in the receptor counterpart as well as to correctly orient the substituents at C-2 and N-3 in the binding pocket. In **Figure 30**, the binding mode of compound **F4**, one of the most efficient against mPGES-1 activity (reduction of mPGES-1 activity = ~50% at 10 μM).

Table 12. Values of the residual activity of microsomal prostaglandin E_2 synthase-1 (mPGES-1) after incubation with compounds **F1**-**F23** at concentration of 10 μM.

COMPOUND (10μM)	RESIDUAL ACTIVITY OF mPGES-1(%) ±SD
F1	65.2 ±2.0
F2	65.9 ±1.1
F3	72.1 ±0.5
F4	55.6 ±1.6
F5	88.9 ±0.8
F6	79.3 ±1.4
F7	87.1 ±1.5

F8	72.7 ±1.8
F9	76.5 ±1.6
F10	90.6 ±2.6
F11	84.0 ±2.3
F12	84.4 ±1.5
F13	84.9 ±1.5
F14	63.3 ±1.8
F15	85.3 ±2.2
F16	88.4 ±3.1
F17	84.9 ±0.5
F18	79.5 ±1.1
F19	72.6 ±2.0
F20	74.6 ±0.9
F21	77.8 ±0.6
F22	48.0 ±1.0
F23	88.2 ±1.3

3.2.4 Evaluation of the synthesized subset of thiazolidine-4-one-based compounds on soluble epoxide hydrolase by molecular docking calculations

Starting from the partial inhibitory activities obtained for compounds **F1-F23** against mPGES-1 and considering the importance of the soluble epoxide hydrolase as biological targets involved in formation of inflammation-related lipid mediators,[120] we decided to evaluate these

compounds also against this target protein. This choice was made precisely against the sEH since the inhibitor chemotype is typically endowed with 1,3-aromatic disubstituted urea function, [121] thus sharing a similar shape and substitution pattern with the investigated thiazolidine-4-one-based compounds. In addition, we assumed that the hydrophobic groups at positions 2 and 3 on the thiazolidin-4-one ring may be a key feature for the inhibition, considering the hydrophobic profile of the sEH active site.

In light of these considerations, we performed docking experiments on a small set of synthesized compounds (**F1-F23**). Specifically, the selection of the best compounds on sEH was performed, taking into account the chemical mechanism of the enzyme mainly based on a catalytic triad (Asp335, His524, Asp496). Specifically, the epoxide group of the substrate is firstly polarized by two tyrosine residues (383 and 466), while Asp335, which is in turn activated and oriented towards His524 and Asp496, performs the nucleophilic attack with its carboxylic group.[121]

The analysis of the docking poses of the compounds highlighted the substituents at N-3 being accommodated onto the deeper part of the binding site close to the residues involved in the catalytic mechanism. We speculated that electron-withdrawing substituents on the phenyl-2-oxoethyl moiety at N-3 could be useful for gaining interactions with the Asp335 residue (**Figure 31**). For this reason, eleven compounds (**F2-F4**, **F7-F8**, **F10-F11, F13**, **F15**, **F22-F23**) were selected to be submitted to subsequent biological evaluation to corroborate this hypothesis. Moreover, two compounds (**F13** and **F15**, featuring the 4-methoxy-phenyl-2-oxoethyl substituents at N-3) were also selected as negative controls.

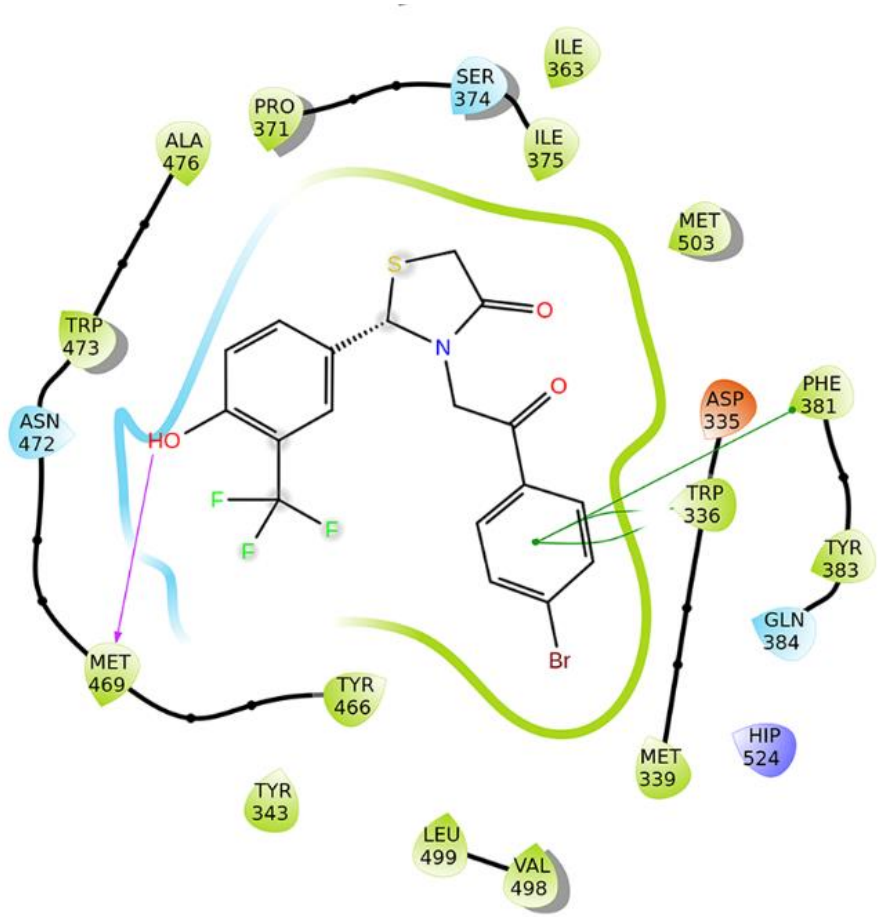

Figure 31. 2D pose of compound **F4** against sEH protein; violet arrows representing H-bonds, green arrows representing π-π stacking.

3.2.5 Biophysical assay on sEH and SAR investigations

To corroborate the computational predictions, Prof. Oliver Werz's group was involved in a cell-free assay[122] applied for screening of the selected compounds (**F2-F4**, **F7-F8**, **F10-F11, F13**, **F15**, **F22-F23**) against the catalytic activity of human soluble epoxide hydrolase (sEH). In this assay, the activity of sEH was tested evaluating the ability of sEH to enzymatically transform the 3-phenyl-cyano(6-methoxy-2-naphthalenyl)methyl ester-2-oxiraneacetic acid (PHOME), a non-fluorescent compound, into fluorescent 6-methoxy-naphtaldehyde at room temperature. The compounds were tested at a concentration of 10µM. Interestingly, among the compounds bearing a benzyloxy moiety in *meta* position on the phenyl ring at C-2 of the thiazolidinedione (**F8**, **F11,** and **F23**), only **F8** bearing a bromine atom inhibited the activity of the enzyme by

more than 50% (**Table 12**). Considering the other set of compounds (**F2**-**F4**, **F7**, **F10, F15, F13**, **F22**), inhibition of the activity by >40% in comparison to the control (100%) was observed for **F2**, **F3**, and **F4** (**Table 13**), all keeping the same 4-Br-phenyl-2-oxoethyl moiety at N-3 of compound **F8**, and variously substituted *p*-hydroxyphenyl rings at C-2. Also, reduction of the activity by 35% was observed by replacing the bromine with a fluorine atom (compound **F22**), and compound **F7**, which keeps the 4-Br-phenyl-2-oxoethyl moiety at N-3, while presenting an *N*, *N*-dimethyl substituent in *para* on the phenyl ring at C-2, inhibited the activity by 40%. Interestingly, compounds **F13** and **F8,** both bearing a donor group (a methoxy group) in *para* on the phenyl-2-oxoethyl moiety at N-3, did not show inhibitory potency against the enzyme, thus confirming our hypothesis.

The related IC_{50} values were calculated for compounds **F2**, **F4,** and **F8** considering their ability to inhibit the enzyme activity by >50% (**Figure 32**).

Table 13. Values of the residual activity of human soluble epoxide hydrolase (sEH) after incubation with the selected compounds at a concentration of 10µM.

COMPOUND (10µM)	RESIDUAL ACTIVITY OF sEH(%) ±SD
F2	37.8 ±1.1
F3	57.0 ±1.3
F4	36.9 ±1.0
F7	59.3 ±0.9
F8	40.3 ±1.2
F10	80.0 ±0.8
F11	75.0 ±1.3
F13	100.4 ±1.0
F15	94.1 ±1.5
F22	75.0 ±1.0
F23	84.1 ±1.5

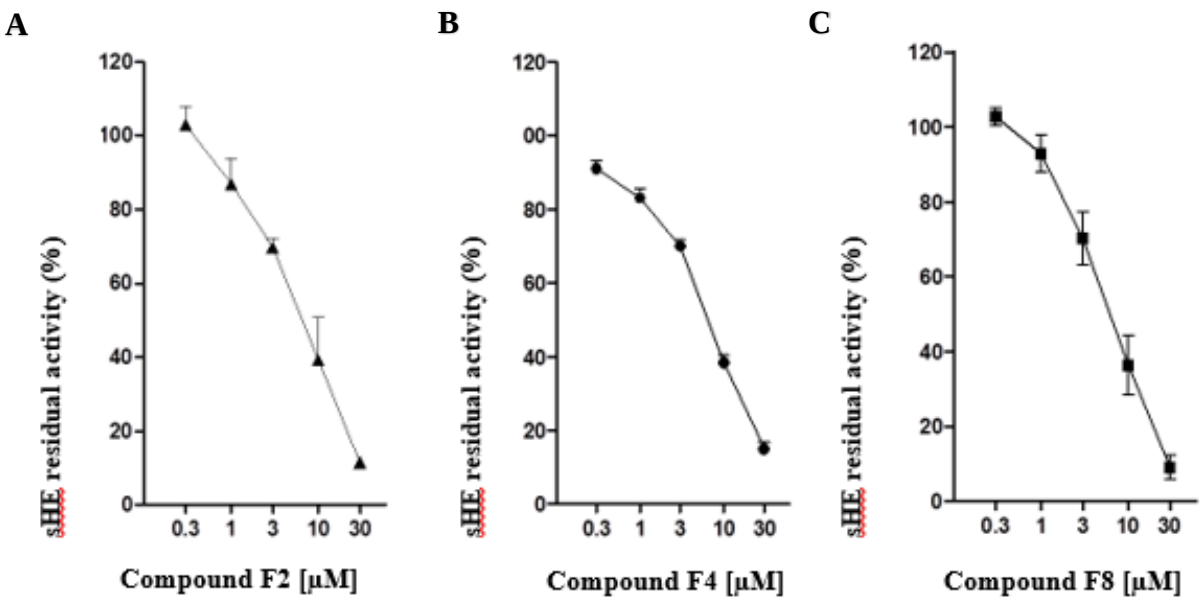

Figure 32. Concentration-response curves for the analysis of the inhibitory activity of a) **F2**, b) **F4**, c) **F8** against the human soluble epoxide hydrolase (sEH) in a cell-free assay. Data are expressed as percentage of control (100%), means ± S.E.M., n = 3.

3.2.6 Biological screening of compounds of compounds F2, F4, and F8 against COXs and 5-LO

Considering the idea that the inhibition of different enzymes of the arachidonic acid cascade can have a synergistic anti-inflammatory-anti-cancer activity, we investigated the ability of compounds **F2**, **F4**, and **F8** to inhibit the catalytic activities of COXs and 5-LO enzymes through a cell-free assay[122] using isolated COX-1 and COX-2 enzymes. Contemporary, a cell-free 5-LO activity assay[113] was performed in order to verify their ability to interfere with leukotrienes biosynthesis. Compounds **F2** and **F8** exhibited inhibitory activity against 5-LO of 39% and 30% (**Table 14**), respectively, lower than the value observed in **F4**. Concentration-response analysis of **F4** disclosed an IC_{50} value in the low micromolar range (5.0 µM, **Figure 33, Table 14**). Instead, none of the three compounds can inhibit COX enzymes (**Table 14**).

Table 14. Residual activity and IC_{50} values of compounds **F2**, **F4**, and **F8** against isolated enzymes involved in the formation of inflammation-related lipid mediators. Data of the residual enzyme activity at 10 µM test compound concentration are expressed as percentage of vehicle control (100%) and are given as means ± S.E.M. for $n = 4$.

COMPOUND	IC_{50} ± S.E.M. FOR sEH (µM)	5-LO RESIDUAL ACTIVITY (%)	IC_{50} ± S.E.M. FOR 5-LO (µM)	COX-1 RESIDUAL ACTIVITY (%)	COX-2 RESIDUAL ACTIVITY (%)
F2	6.3 ± 0.4	60.7	nt*	n.i. (> 90)	n.i. (> 90)
F4	6.1 ± 0.3	17.6	5.0 ± 0.7	n.i. (> 90)	n.i. (> 90)
F8	6.2 ± 0.6	70.1	nt*	n.i. (> 90)	n.i. (> 80)

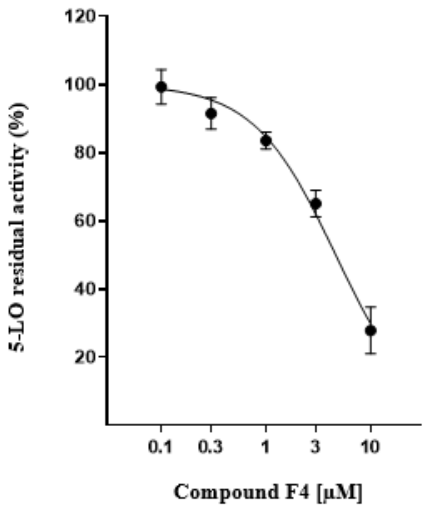

Figure 33. Concentration-response curve for the analysis of the inhibitory activity of compound **F4** against isolated 5-LO. Data are expressed as a percentage of control (100%), means ± S.E.M., n = 4.

3.2.7 Evaluation of the compounds F2, F4, and F8 for inhibition of leukotriene biosynthesis in neutrophils and for cytotoxic effects against human monocytes

Next, the capability of the test compounds **F2**, **F4** and **F8** for blocking 5-LO-mediated LT biosynthesis was investigated in intact neutrophils from human peripheral blood. The compounds were tested at 10µM in two different experimental settings, using (i) Ca^{2+}-

ionophore or (ii) Ca^{2+}-ionophore plus arachidonic acid to evoke LT formation. Interestingly, compounds **F2** and **F4** inhibited the formation of LTB_4 and its isomers as well as 5-H(p)ETE with IC_{50} values in the low micromolar range (21.8 to 4.4 µM, depending on the assay conditions; **Figure 34** and **Table 15**), whereas only a slight inhibition of 5-LO product formation was observed for compound **F8** (**Table 15**).

Finally, a cytotoxicity assay with human monocytes was performed in order to investigate possible detrimental effects of compounds **F2**, **F4** and **F8** on cell viability. Monocytes were treated with the test compounds (10 µM), triton (1%, positive control) or vehicle (0.5% DMSO) for 24 hours, and an MTT assay was performed. None of compounds **F2**, **F4** and **F8** reduced the viability of monocytes, whereas the positive control strongly reduced cell viability under the same conditions (**Figure 35)**.

Table 15. 5-LO product formation in intact neutrophils after incubation with compounds **F2, F4** and **F8**. Cells were stimulated either with A23187 or with A23187 plus AA. Data are expressed as percentage of vehicle control (100%) at test compound concentration of 10 µM (means ± S.E.M.) of $n = 6$; IC_{50} values of $n = 3$ (compound **F2**); $n = 4$ (compound **F8**).

COMPOUND	RESIDUAL 5-LO PRODUCT FORMATION (%) EVOKED WITH A23187	RESIDUAL 5-LO PRODUCT FORMATION (%) EVOKED WITH A23187 PLUS AA	IC_{50} VALUE (µM) EVOKED WITH A23187	IC_{50} VALUE (µM) EVOKED WITH A23187 PLUS AA
F2	25.5 ± 6.9	64.2 ± 6.0	21.8 ± 7.4	12.1 ± 4.4
F4	28.6 ± 7.0	19.9 ± 5.3	4.9 ± 0.6	4.4 ± 0.2
F8	70.8 ± 12.7	53.2 ± 7.1	nt*	nt*

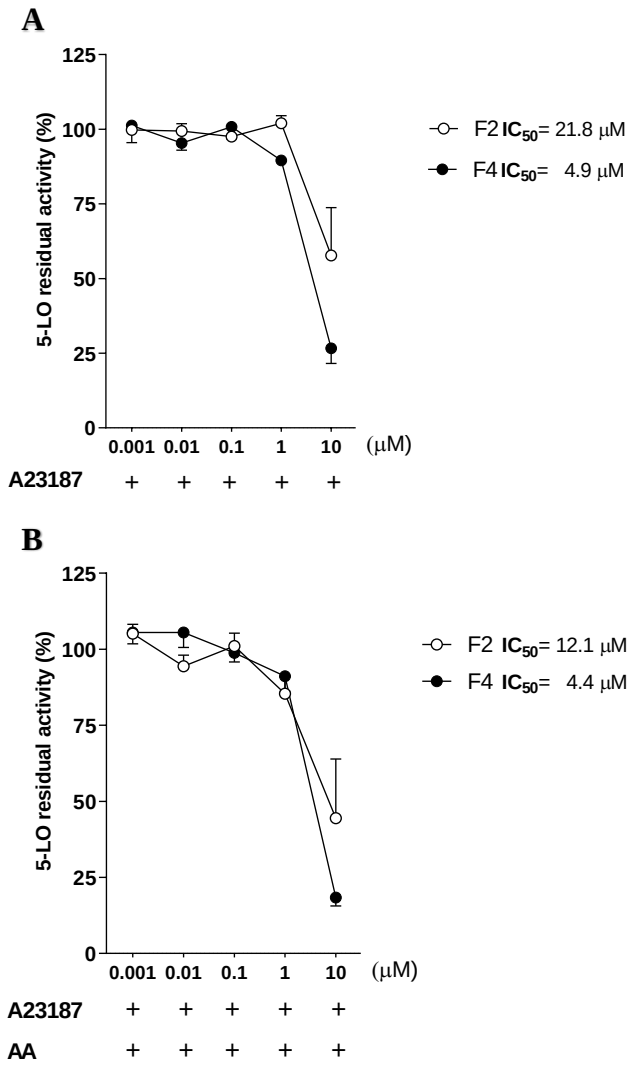

Figure 34. Concentration-response analysis for inhibition of 5-LO product formation in intact human neutrophils. Cells were pre-incubated with compound **F2**, **F4** or vehicle (0.1% DMSO) for 10 min at 37 °C, and then stimulated with 2.5 μM Ca^{2+}-ionophore A23187 for another 10 min (A) or with 2.5 μM Ca^{2+}-ionophore A23187 plus 20 μM arachidonic acid for another 10 min (B). The incubations were terminated on ice and 5-LO products were analyzed by RP-HPLC. Data are expressed as percentage of vehicle control (100%), means ± S.E.M., *n* = 3 (compound **F2**); *n* = 4 (compound **F4**).

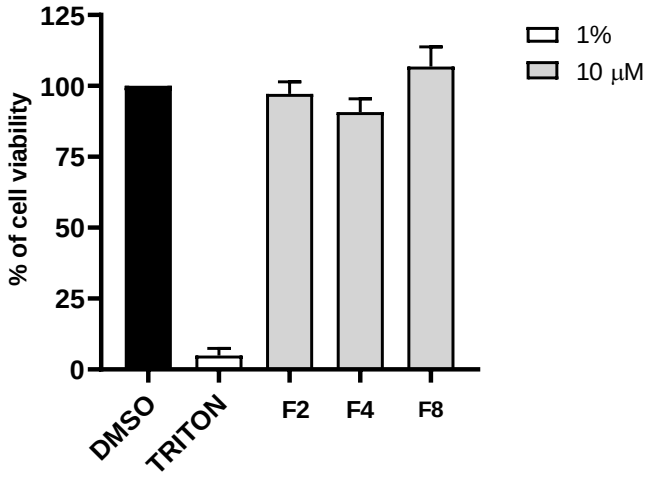

Figure 35. Cell viability assay performed on human monocytes after incubation with triton (1%), compounds **F2**, **F4** and **F8** at 10 μM or vehicle (0.5% DMSO) over 24 hours. Data are expressed as percentage of control (100%), means ± SEM, n = 3.

3.3 4*H*-3,1-benzothiazin-4-one-based compounds to target mPGES-1

In the frame of our research aimed at identifying new anti-inflammatory agents targeting mPGES-1,[113, 123-124] we also investigated the putative ability of 4*H*-3,1-benzothiazin-4-ones-based on inhibiting this enzyme through molecular modeling experiments.

Considering our previous work[124] in which benzothiazole-based compounds target mPGES-1, we focused our attention on another heterocyclic compound containing nitrogen and sulfur: 4*H*-3,1-benzothiazin-4-ones. In this structure, nitrogen and sulfur were in a six-term cycle (rather than five-term). In addition, if properly functionalized, such compounds can exert an antiproliferative, cytotoxic, and antibacterial activity, besides also showing protease inhibition.[125]

3.3.1 Design

Following the generical workflow (see **Introduction**), this project was carried out exploiting a combined approach of computational drug design, synthesis, and biological assay.

First, a virtual library of 4*H*-3,1-benzothiazin-4-ones compounds was generated following the related chemical synthesis procedure previously chosen (**Scheme 21**). Specifically, the combination of all commercially available boronic acid with the selected core allowed the generation of a library of ~900 molecules (CombiGlide software, **Scheme 19**).

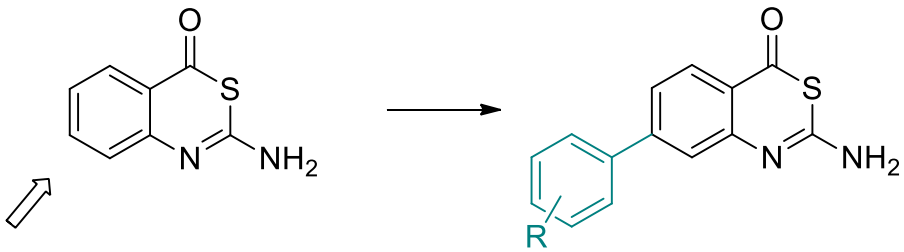

Scheme 19. Generation of the 4*H*-3,1-benzothiazin-4-ones-based library.

Afterward, the built library was filtered and tested by molecular docking experiments against mPGES-1 (PDB code: 4BPM). After carefully evaluating the docking score values and analyzing the related binding modes, the most promising compounds were selected. Interestingly, the -NH_2 group present in position 2 showed hydrogen bonding with $Tyr131_{ChainA}$, whereas $Tyr\ 130_{ChainA}$ showed Van der Waal interaction with the remaining part of the scaffold. The substituents were surrounded by $His53_{ChainB}$, $Ala123\ _{ChainA}$, $Pro124_{ChainA}$, $Ser127_{ChainA}$, exhibited two Van der Waal interactions with $His53_{ChainB}$ and $Pro124_{ChainA}$ (**Figure 36**). Taking into account this binding mode, 6 molecules were selected for the next synthesis steps (**G3**-**G8**, **Scheme 20**).

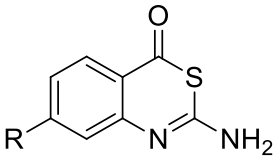

COMPOUND	R
G3	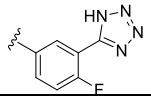
G4	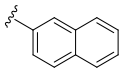
G5	
G6	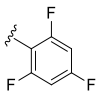
G7	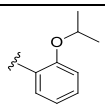
G8	

Scheme 20. Selected and synthesized compounds **G3-G8**.

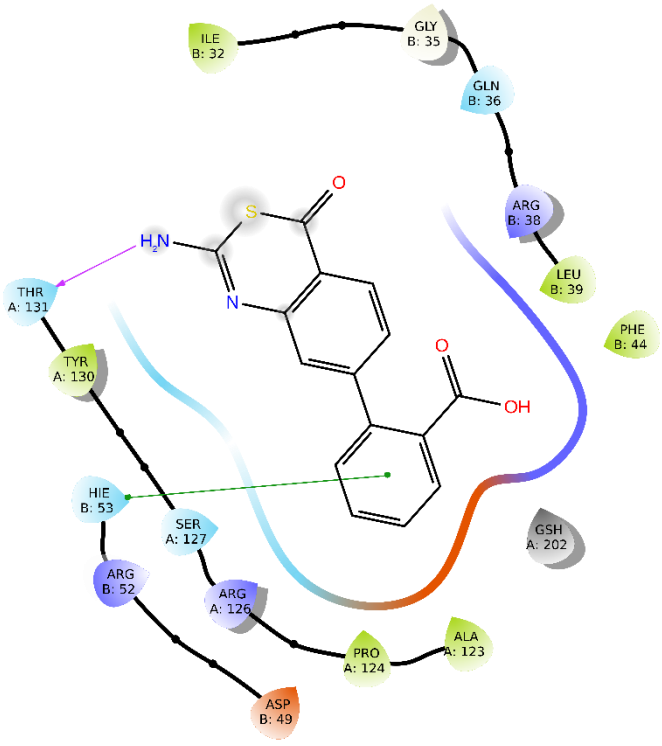

Figure 36. 2D binding pose of compound **G8**.

3.3.2 Chemical synthesis

For the synthesis of selected compounds (**G3**–**G8**, **Scheme 20**), we started with the conversion of 2-amino-4-bromobenzoic acid to obtain 2-(3-benzoyl-thioureido)-4-bromobenzoic acid (**G1**). The reaction proceeded with the use of benzoyl isothiocyanate as a reactant in acetone at room temperature for 30 minutes. Then, an intramolecular cyclization was performed on the intermediate **G1** by using H_2SO_4 (37N) for 48h at room temperature. This strategy for the scaffold synthesis was chosen since it was possible obtain the desired scaffold in two steps, with good yields (80%), and avoiding the formation of subproducts. This facilitated the purification steps resulting in purification of these intermediates only by crystallization. Last, to obtain the final products, a Suzuki cross-coupling reaction (widely used to form carbon-carbon bonds) was performed with different commercially available boronic acid, as shown in **Scheme 21**.

A small quantity of the final products for the biological tests was purified by HPLC to ensure a higher degree of purity (>95%).

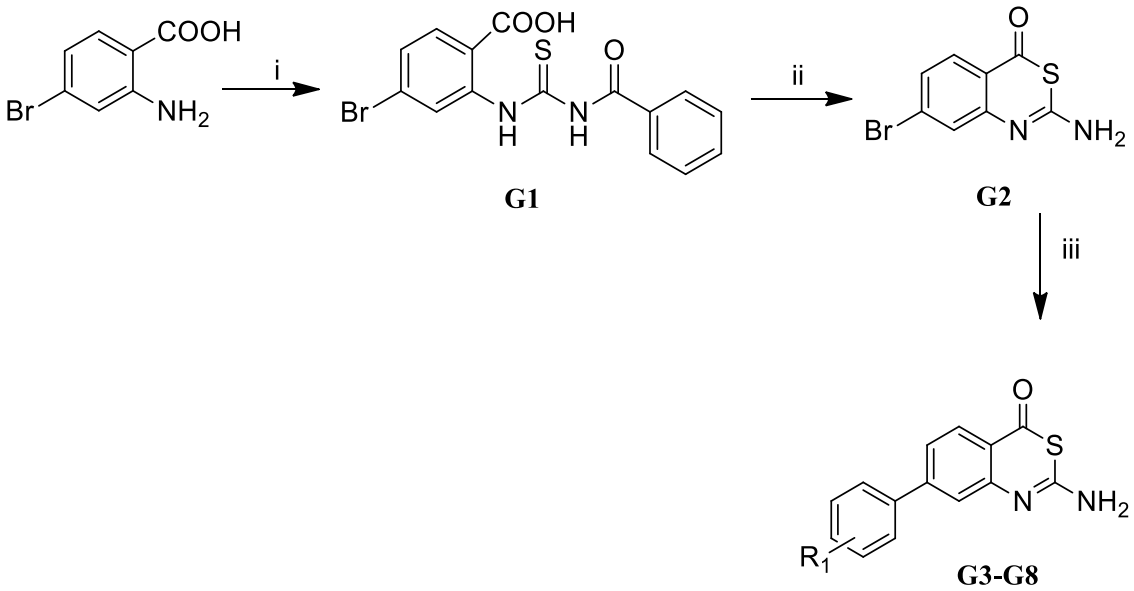

Scheme 21. Synthetic strategy for 4*H*-3,1-Benzothiazin-4-one-based compounds. *Reagents and conditions: i)Benzoyl isothiocyanate, acetone, r.t; ii)H_2SO_4, 48h, r.t.; iii) R-B(OH)$_2$, K_2CO_3, Pd[P(Ph$_3$)]$_4$, dioxane/H_2O, 80°C, over-night.*

3.3.3 Biophysical assay

An assay aimed at evaluating the ability of compounds **G3-G8** to interfere with the activity of mPGES-1 is now ongoing (in collaboration with Prof. Oliver Werz of the University of Jena (Germany). The biophysical assay consists of a cell-free assay, using the microsomal fractions of interleukin-1β (IL-1β)-stimulated A549 cells as a source for human mPGES-1.[124]

3.4. Application of the computational protocol for the generation of 6 libraries of compounds as mPGES-1/sEH potential inhibitors

3.4.1. 3-benzilquinossalin-2(1*H*)-one scaffold for mPGES-1 potential inhibition

One of the scaffolds selected for the generation of new large libraries of molecules on mPGES-1 enzyme is the quinoxalin-2(1*H*)-one building block (**Scheme 22**). The synthetic versatility and accessibility of this scaffold are noteworthy, and a wide range of chemical routes for the generation of derivatives has been explored and optimized.[126-127] Among them, the synthetic route reported in **Scheme 23** was selected as template for the *in silico* drug design. In light of this, the scaffold and the chemical route were chosen with the idea that we could modify positions 3 and 6/7, creating new molecules fitting in the mPGES-1 binding site. In particular, the benzyl group was placed in position 3 to improve the interaction with aromatic residues of the target binding site, according to the importance of these amino acids in the binding mode of known inhibitors. After that, these new nucleus were combined with all aromatic amine commercial available, placing them in position 6 and/or 7, generating two different libraries, each containing ~5400 molecules:

1) *3-benzyl-6-(phenylamino)quinoxalin-2(1H)-one* (**H-a**);

2) *3-benzyl-7-(phenylamino)quinoxalin-2(1H)-one* (**H-b**).

Then, the libraries were processed with LigPrep,[97] to generate all the possible stereoisomers, tautomers, and protonation states at a pH of 7.4 ± 1.0. The application of QikProp[98] for the determination of pharmacokinetic parameters and LigFilter[105] (150<MW<=logP O/ W<=6.5, logS >= –7, reactive groups=0) afforded the final libraries **H-a** and **H-b**.

After docking experiments, no significant differences were observed between the two isomer libraries generated *in silico* in terms of interactions with amino acids and docking score (between -9.91 and -6.84 kcal/mol). In both cases, the quinossalin-2(1*H*)-one structure established a hydrogen bond with $Thr131_{ChainA}$ and π-π stacking interactions with $Thr130_{ChainA}$, while the substituent could interact with $Ser127_{ChainA}$ and $His53_{ChainB}$ by hydrogen bonds. In addition, the benzyl group was close to $Ile32_{ChainB}$, $Ala31_{ChainB}$, $Gln134_{ChainA}$ with which it established hydrophobic interactions (**Figure 37**). In light of this, eleven pairs of molecules were selected (**Scheme 24**).

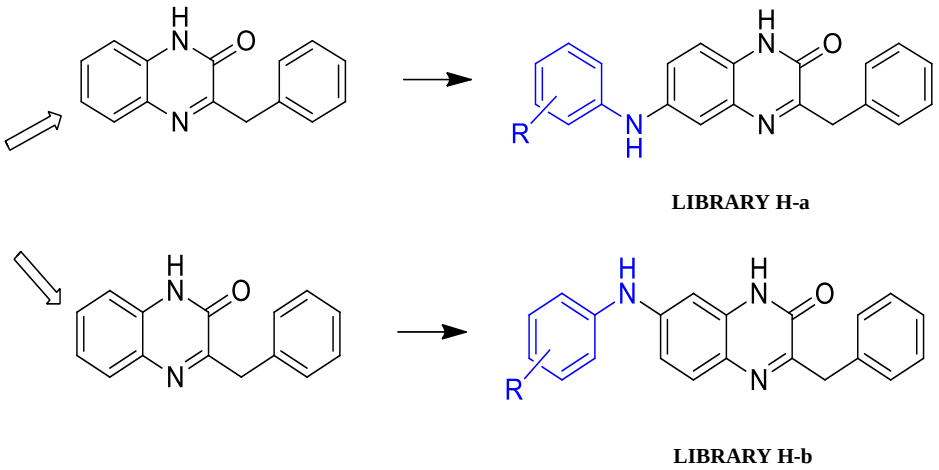

Scheme 22. Generation of two 3-benzilquinossalin-2(1*H*)-one libraries.

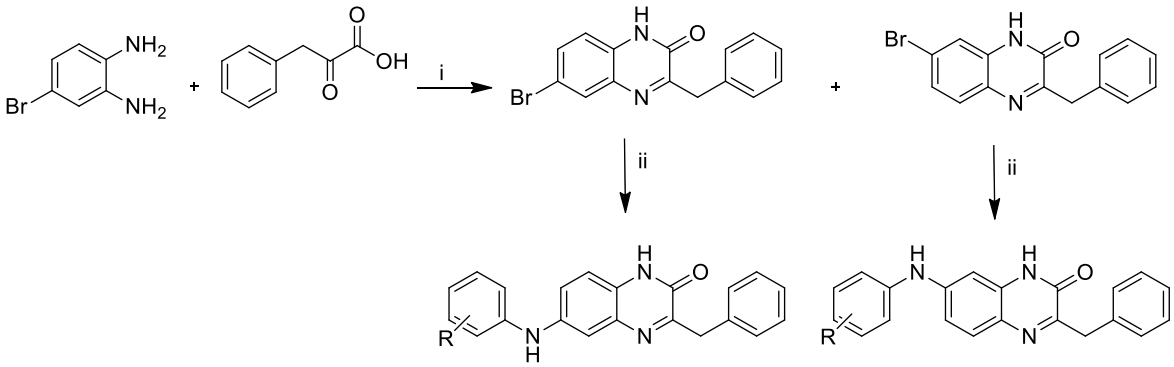

Scheme 23. Syntheticc strategy chosen as template for the *in silico* drug design of 3-benzilquinossalin-2(1*H*)-one libraries. *Reagent and conditions: i) EtOH, reflux, 5h;*[128] *ii) R(Ph)NH*$_2$*, Cu/Cu*$_2$*O, 2-ethoxyethanol, 130°C.*[129]

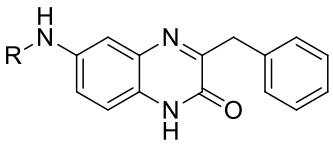

H-a

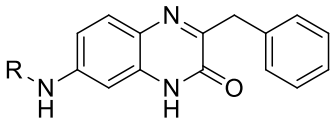

H-b

H1-a	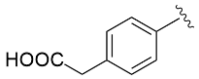
H1-b	
H2-a	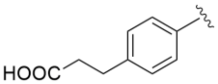
H2-b	
H3-a	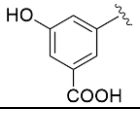
H3-b	
H4-a	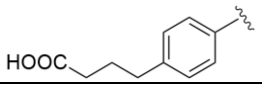
H4-b	
H5-a	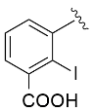
H5-b	
H6-a	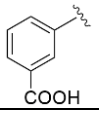
H6-b	
H7-a	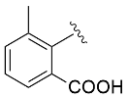
H7-b	
H8-a	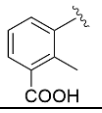
H8-b	
H9-a	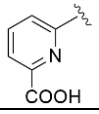
H9-b	
H10-a	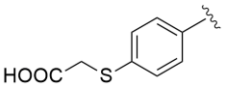
H10-b	
H11-a	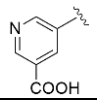
H11-b	

Scheme 24. Selected 3-benzilquinossalin-2(1*H*)-one-based compounds.

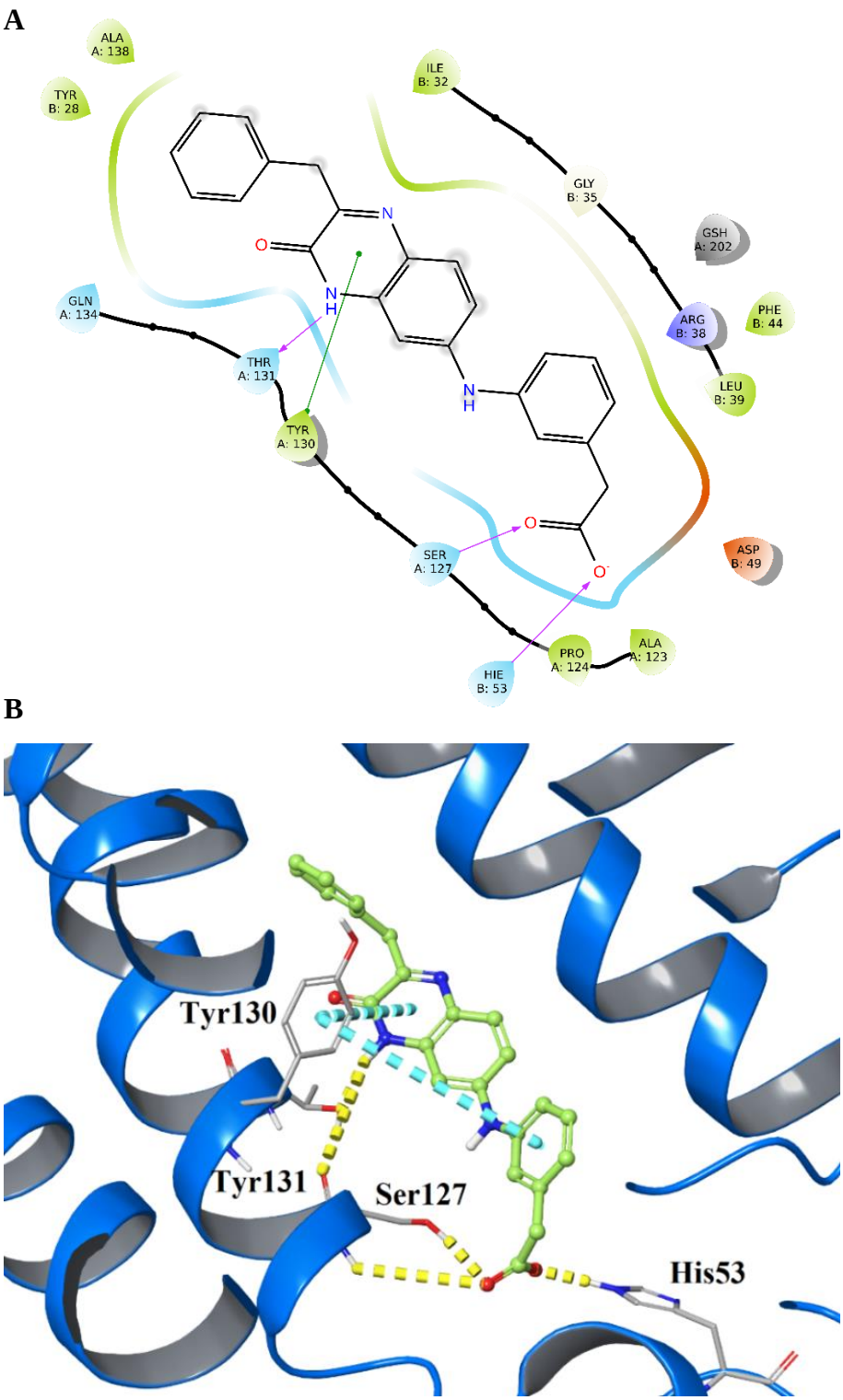

Figure 37. a) 2D dimensional panel representing interactions of compounds **H1-b** (violet arrows representing H-bonds, green arrows representing π-π stacking); b) 3D dimensional panel representing interactions of compounds **H1-b** (yellow arrows representing H-bonds, light-blue arrows representing π-π stacking.

3.4.2 2-benzo[*d*]oxazol-2(3*H*)-one scaffold for mPGES-1 potential inhibition

Starting from a phenylindole acetic known inhibitor of mPGES-1 enzyme (MK-866), the benzo[*d*]oxazol-2(3*H*)-one was used as structure-based, to evaluate if the presence of the carbamate could influence positively or negatively the binding with the idea that could interact with polar amino acid $His53_{ChianB}$, $Pro124_{ChianA}$, $Arg52_{ChianB}$ in place of the acid group (**Scheme 25**). The built nucleus was then replaced on the nitrogen with all acyl chlorides commercially available so as to guarantee the same shape of the known inhibitor in the mPGES-1 binding site. The acyl chlorides were used for the nitrogen substitution according to the selected chemical procedure (**Scheme 26**). A library of 1260 molecules was generated through Combiglide[96] (**Scheme 25**). LigPrep[97] calculations and the same filters enumerated above were applied, obtaining the resulting library **I**. After performing the Virtual Screening calculation, the obtained molecules were not selected for the successive synthesis step. In fact, the docking score value was around -5.0 kcal/mol and few interactions with the essential amino acids for the inhibition were present.

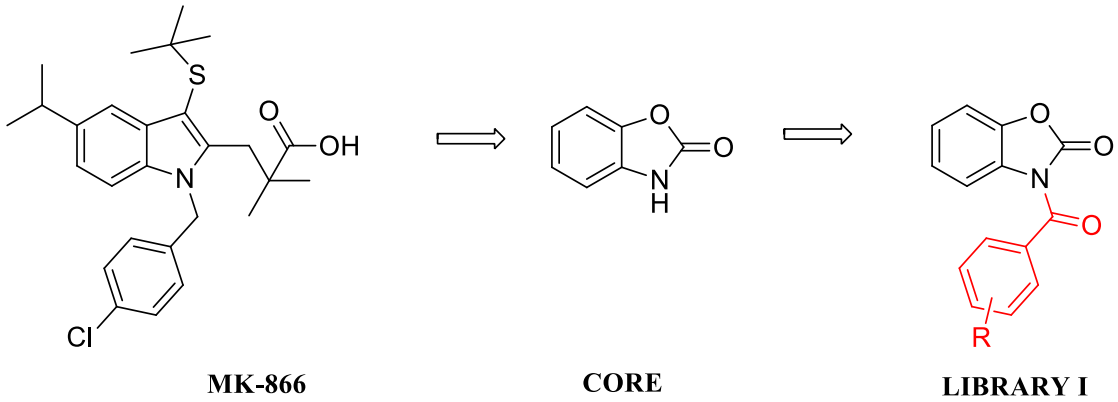

Scheme 25. Selection of the core starting from MK-866 and consequent generation of 2-benzo[*d*]oxazol-2(3*H*)-one library.

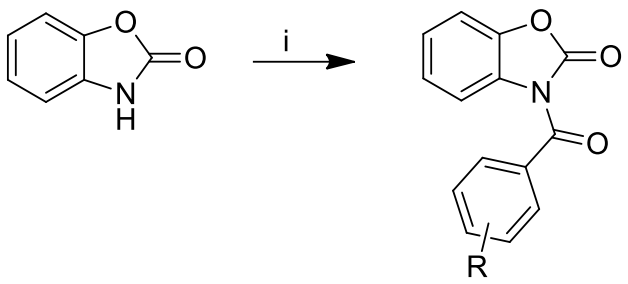

Scheme 26. Synthetic strategy chosen as template for the *in silico* drug design. *Reagent and conditions*: i*) NEt_3, acyl chloride, CH_3CN.*

3.4.3 Furoquinoline and furoquinolinone scaffolds for mPGES-1 potential inhibition

Furoquinoline and furoquinolinone scaffolds were also chosen as a new scaffold for promising mPGES-1 inhibitor considering a known imidazoquinoline-based compound inhibitor of mPGES-1, with an IC_{50} value of 9.1nM[57] (**Scheme 27**).

In detail, the modifications provided the variation of imidazole structure with a furane to obtain the first scaffold. On the second scaffold, the imidazole and the carbonyl group were replaced with an immine into a 1,4,5,6-tetrahydropyrimidine. Last, the third library was designed with the 5,6-dihydropyridine-4(3*H*)-one structure. In this way, three different scaffolds were selected:

- *5,9b-dihydrofuro[3,2-c]quinolin-4(3aH)-one* (**J-a**);
- *5,6,7,12b-tetrahydro-3aH-furo[3,2-c]pyrimido[1,2-a]quinoline* (**J-b**);
- *5,6-dihydro-3aH-furo[3,2-c]pyrimido[1,2-a]quinolin-7(12bH)-one* (**J-c**).

Considering that these structures coul be synthetically modify in a reaction with alkyl or aryl iodides/bromides (**Scheme 29**), all the commercially available aryl iodine and aryl bromide were used for the decoration by Combiglide (**Scheme 28**).[96] Then, as in the previous examples, on the three final libraries, LigPrep[97] calculation was performed to add all the tautomers, stereoisomers, and protonation states at physiological pH and QikProp[98] was used for the

estimation of pharmacokinetic parameters. Finally, specific filters were applied and the final libraries (**Ja**-**Jc**) were determined. As depicted in **Figure 39** the binding groove of the selected molecules is characterized by polar ($Ser127_{ChainA}$ and $His53_{ChainC}$) and aromatic ($Phe44_{ChainB}$ and $Tyr130_{ChainA}$) residues. In particular, the scaffold extended its interaction in a pocket binding area detectable toward the aromatic residue and $Tyr130_{ChainA}$, while the substituents were mainly involved in interactions with polar amino acids. Another parameter used to evaluate the molecules was the shape similarity. In this case, to increase the probability of binding, it may be useful to understand how the shape of the new potential inhibitors was similar to that of the known inhibitor,[59] from which the design was started. The shape similarity with the known inhibitor was 0.8. Indeed, fourteen molecules were selected belonging to the libraries **J-a** and **J-b**, with a value of binding energy between -7.56 and -6.11 kcal/mol (**Scheme 30**).

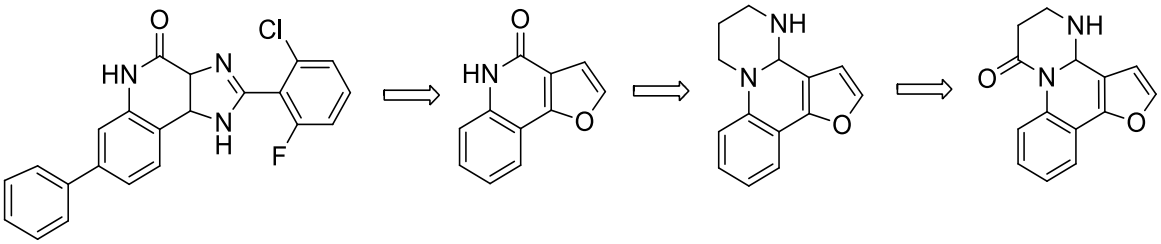

Scheme 27. Chosen scaffolds.

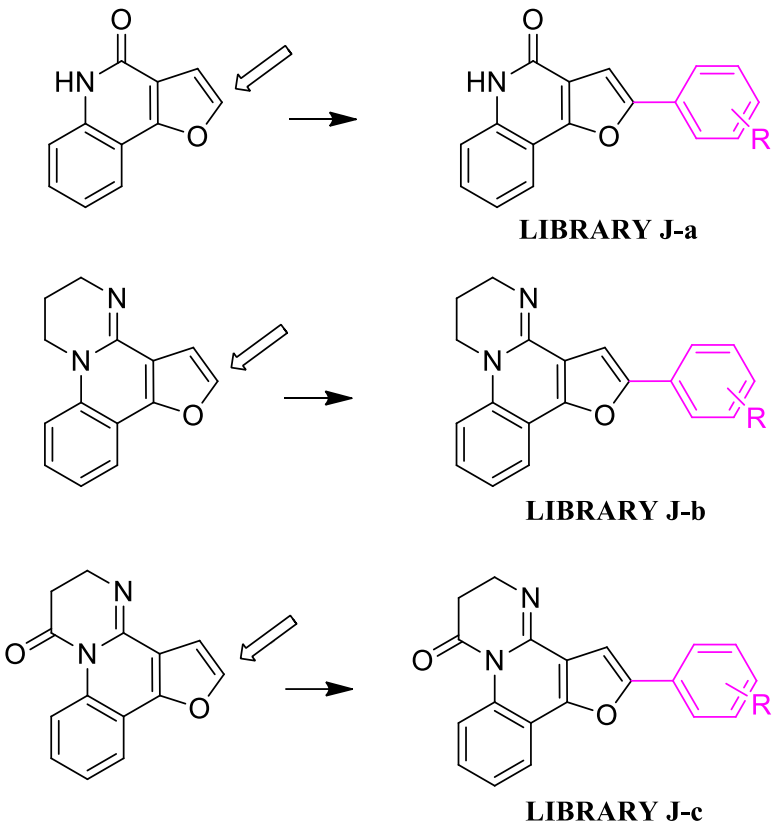

Scheme 28. Generation of furoquinoline and furoquinolinone libraries.

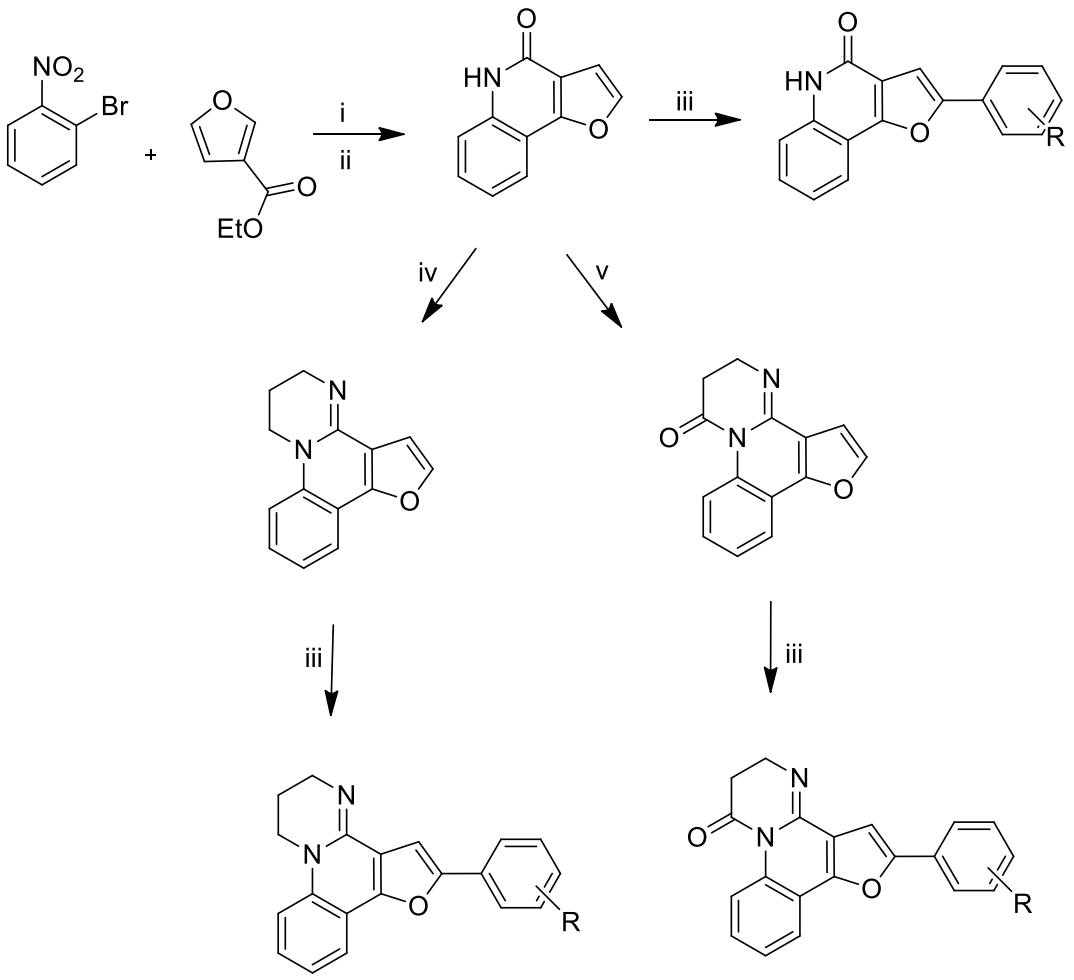

Scheme 29. Syntheticc strategy chosen as template for the *in silico* drug design. *Reagent and conditions*: i)*Pd(PPh$_3$)$_4$, toluene; ii) H$_2$, Pd/C;* [149] *iii) R(Ph)Br, Pd(PPh$_3$)$_4$, KOAc, toluene, 110 °C;*[149] *iv) a) Br(CH$_2$)$_3$NH$_2$, EtOH, 0 °C to rt; b) K$_2$CO$_3$, 0°C to rt, 6 h; v) a)3-aminopropanoic acid, POCl$_3$, CHCl$_3$, 15 min, r.t, b) after addition of starting material, 3h at reflux.*

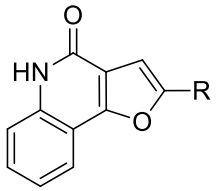

J-a

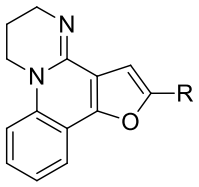

J-b

COMPOUND	R	COMPOUND	R
J1-a	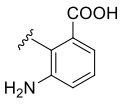	**J8-a**	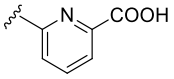
J2-a	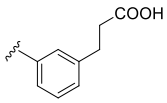	**J1-b**	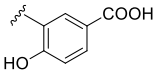
J3-a	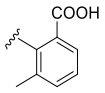	**J2-b**	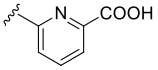
J4-a	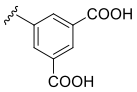	**J3-b**	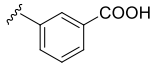
J5-a	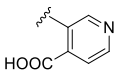	**J4-b**	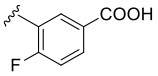
J6-a	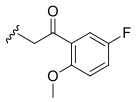	**J5-b**	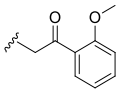
J7-a	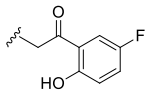	**J6-b**	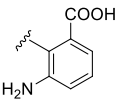

Scheme 30. Selected furoquinoline and furoquinolinone-based compounds.

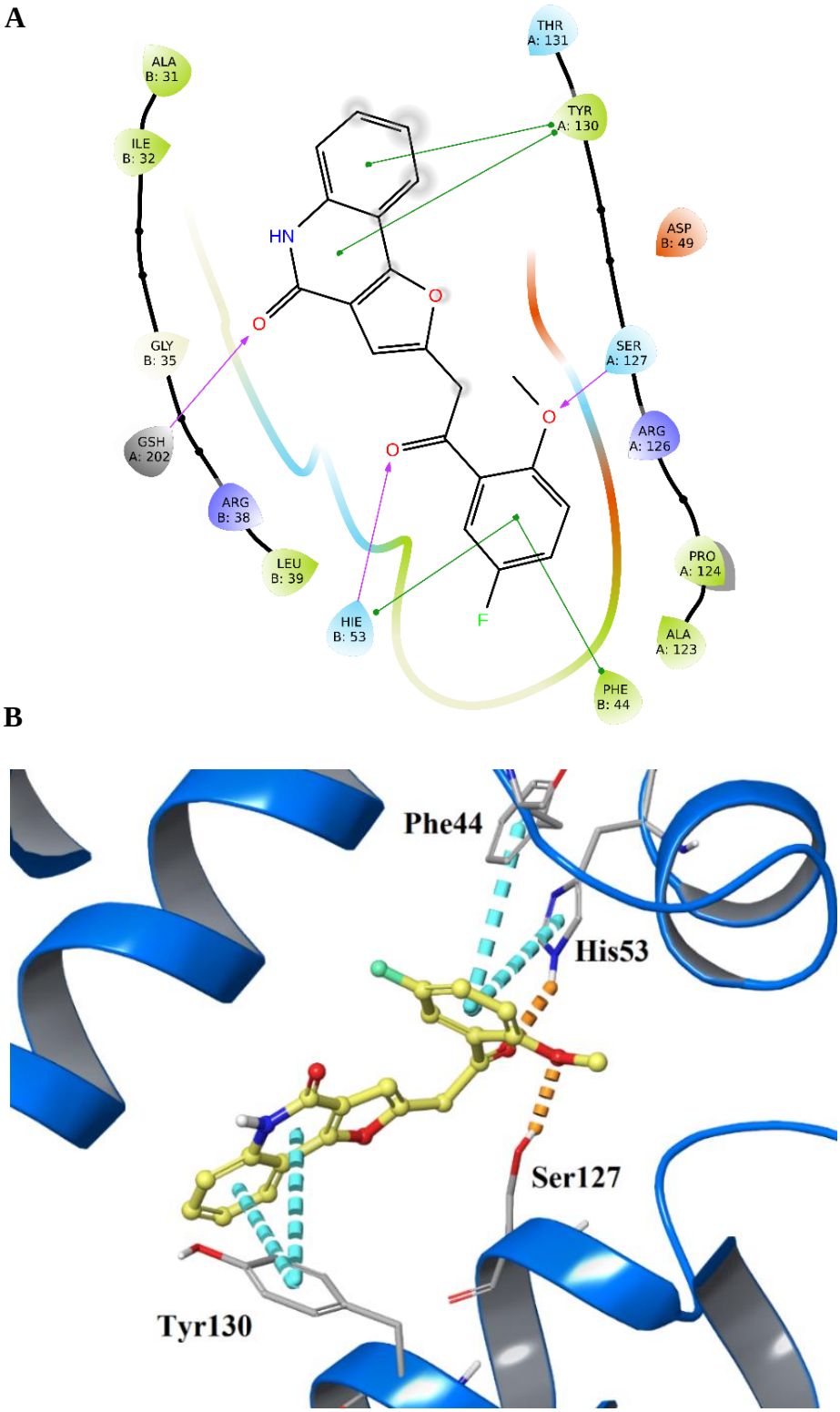

Figure 39. a) 2D dimensional panel representing interactions of compounds **J1-a** (violet arrows representing H-bonds, green arrows representing π-π stacking); b) 3D dimensional panel representing interactions of compounds **J1-a** (orange arrows representing H-bonds, light-blue arrows representing π-π stacking.

3.4.4 1,3,4-oxadiazole-based compounds for mPGES-1 potential inhibition

The 1,3,4-oxadiazole-based compounds were explored considering as a starting point 1,3,4-thiadiazole, already investigated by our research group on the same target (unpublished data) and presenting a good inhibitory activity against mPGES-1. In this work, the sulfur in position 1 was replaced with the oxygen, its isostere, and to keep the nitrogen atoms in the same positions. For the preparation and subsequent screening of molecular libraries, two cores were used:

- *2-(4-ethylphenyl)-1,3,4-oxadiazole* (**K-a**);
- *1-(4-(1,3,4-oxadiazol-2-yl)phenyl)ethanol* (**K-b**).

In both cases, position 5 was replaced with all commercially available aromatic esters, while the phenyl chain was functionalized with all aromatic and aliphatic amines (**Scheme 31**), according to the synthetic procedure chosen (**Scheme 32** and **33**). As a result, the generated molecules differed only for the presence of a carbonyl on the aromatic ring. Accordingly, it was possible to evaluate whether the interaction with the target could vary depending on the presence of a hydrogen binding acceptor group and on the different flexibility of the structure. After virtual screening experiments, all the selected molecules (**Schemes 34** and **35**) presented a value of binding energy in the range of –10.31 and -8.28 kcal/mol and demonstrated to be able to establish the key interactions with the receptor counterpart. The 1,3,4-oxadiazole scaffolds interacted by π-π interactions with $Tyr130_{ChainA}$, $Thr131_{ChainA}$, while the aromatic portion in position 2 of the oxadiazole was generally involved in hydrophobic interactions, given their spatial closeness to $Ala138_{ChainA}$ and $Leu135_{ChainA}$. In most of the compounds, the aromatic/aliphatic(R2) moiety deriving from the amine building block was involved in π-π interactions edge to face to face with $His53_{ChainC}$ and $Phe44_{ChainC}$ and *via* hydrogen bond with $Ser127_{ChainA}$ and $Asp49_{ChainB}$. Both scaffolds seemed promising: molecules of library **K-a** because bound the GSH with -NH of the ethanolamine portion, while in the scaffold **K-b** this

bond was made by the C=O. Moreover, molecule mobility did not influence the binding. Representative 2D and 3D binding modes of compound **K4-a** are reported in **Figure 40.**

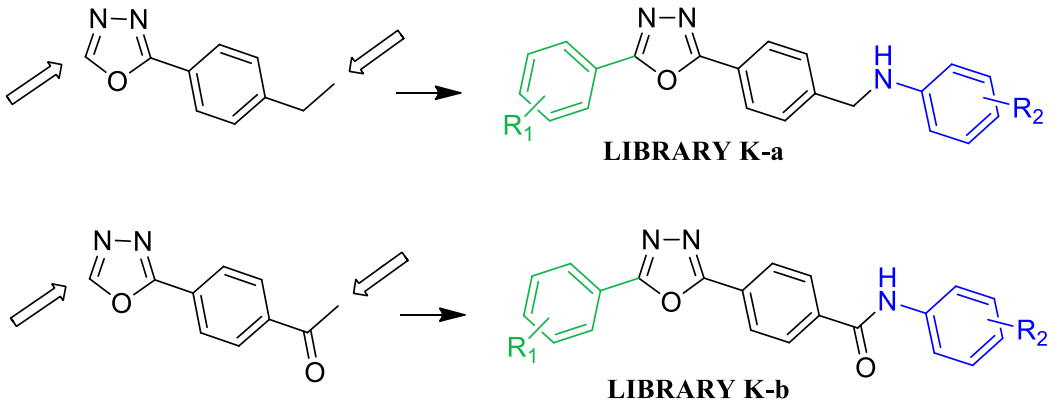

Scheme 31. Generation of the 1,3,4-oxadiazole libraries:

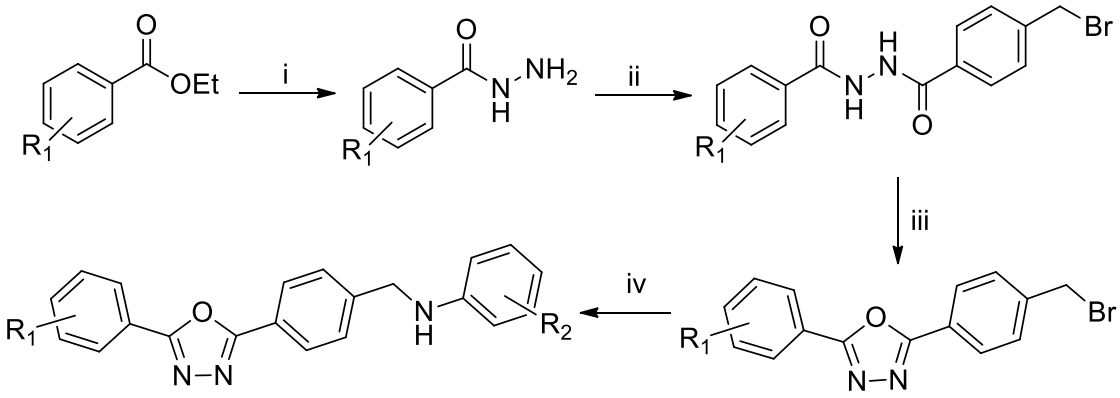

Scheme 32. Synthetic strategy chosen as template for the *in silico* drug design. *Reagent and conditions: i)NH_2NH_2, EtOH, reflux; ii) ethyl 4-(bromomethyl)benzoate, EtOH, reflux; iii) $ZnCl_2$, DCM, r.t.;*[130] *iv)$R_2(Ph)NH_2$, Cs_2CO_3, DMF, r.t.*[131]

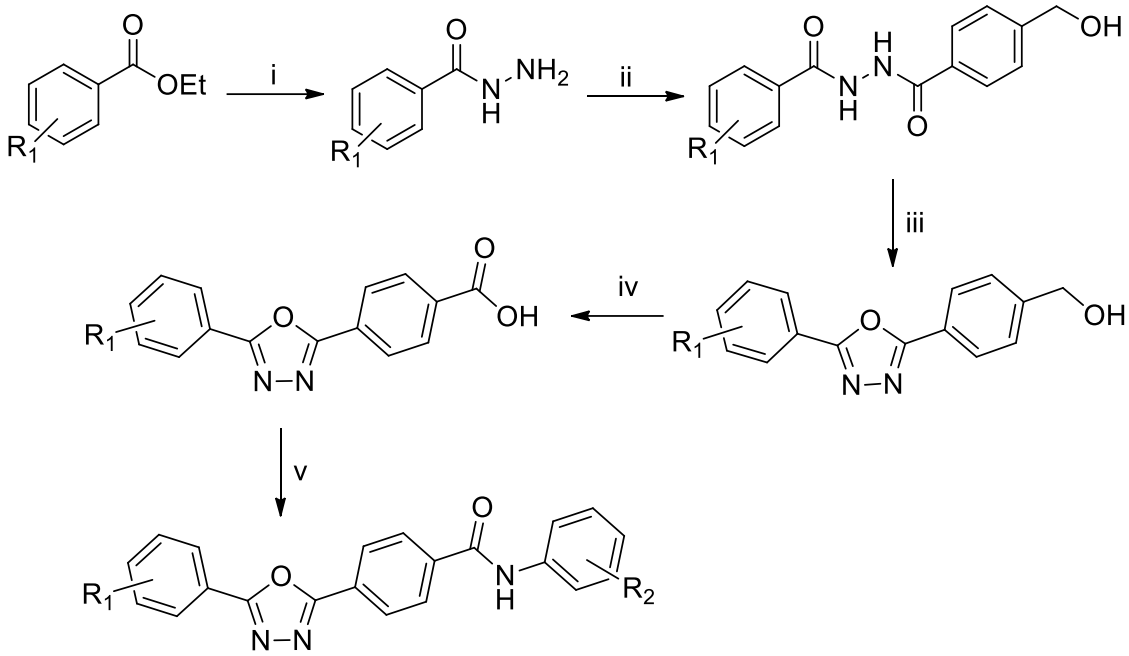

Scheme 33. Synthetic strategy chosen as template for the *in silico* drug design. *Reagent and conditions: i) NH_2NH_2, EtOH, reflux; ii) ethyl 4-(hydroxymethyl)benzoate, EtOH, reflux; iii) $ZnCl_2$, DCM, r.t.;*[130] *iv)$KMnO_4$, NaOH, H_2O, 25°C v)HOBt, HBTU, DIPEA, $R_2(Ph)NH_2$, DCM/DMF.*

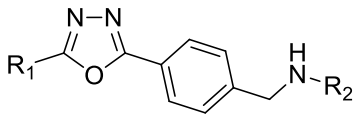

SCAFFOLD K-a

COMPOUND	R_1	R_2
K1-a	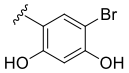	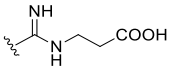
K2-a	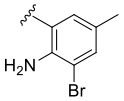	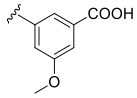
K3-a		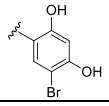
K4-a		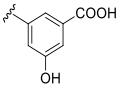
K5-a	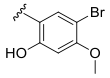	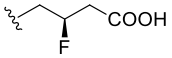
K6-a	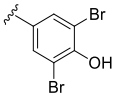	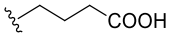
K7-a		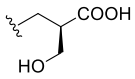
K8-a		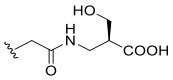
K9-a	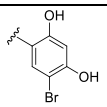	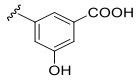
K10-a	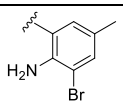	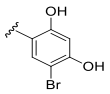
K11-a		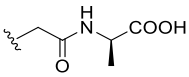
K12-a	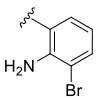	
K13-a		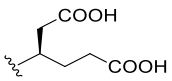

Scheme 34. Selected molecules amoung library M-a.

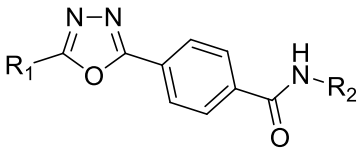

SCAFFOLD K-b

COMPOUND	R_1	R_2
K1-b		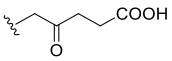
K2-b		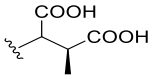
K3-b		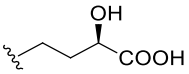
K4-b		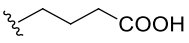
K5-b		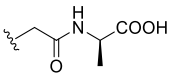
K6-b		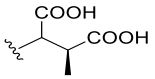
K7-b		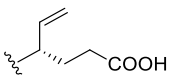
K8-b		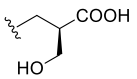
K9-b		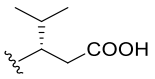
K10-b		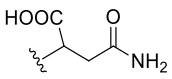

Scheme 35. Selected molecules amoung M-b library.

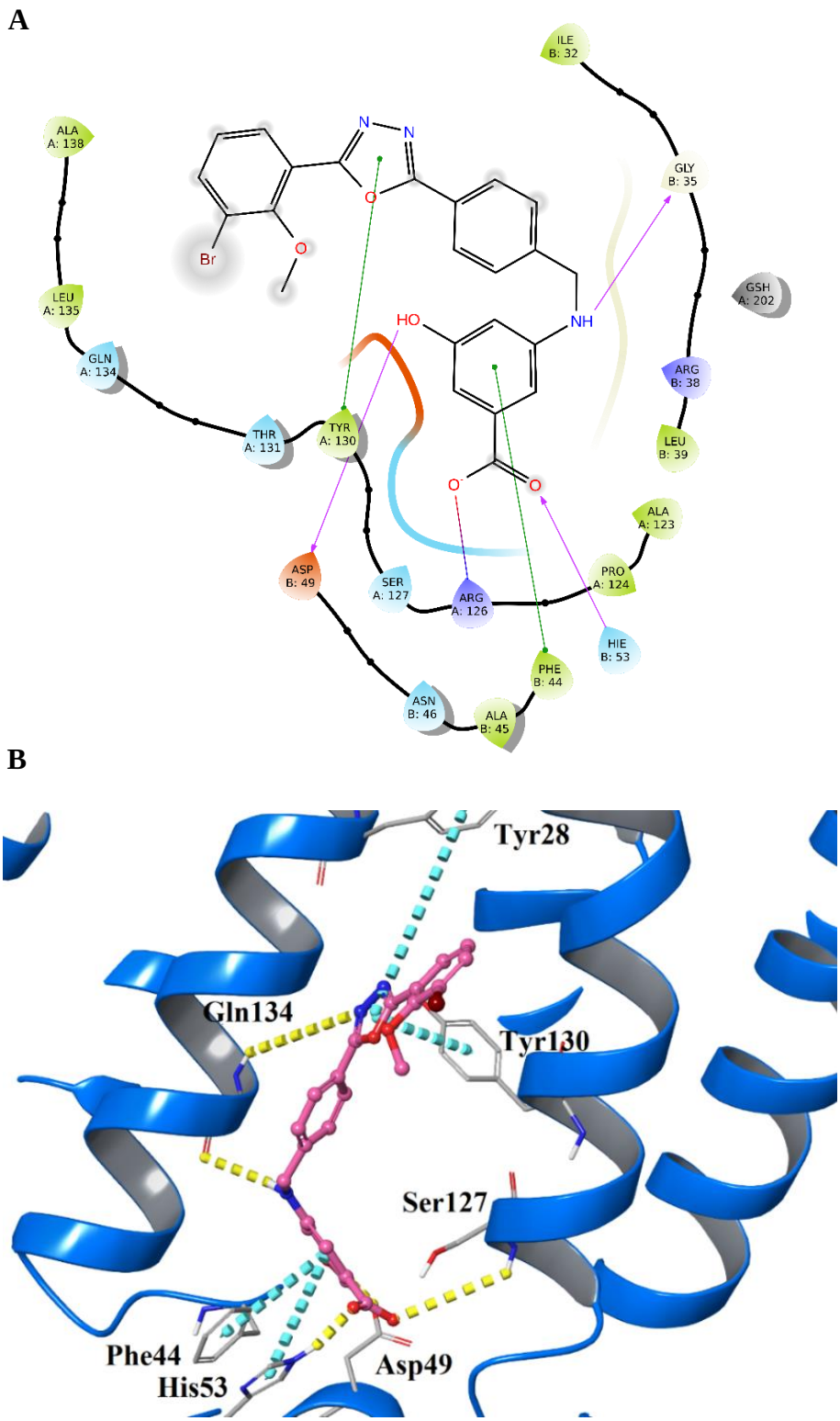

Figure 40. a) 2D dimensional panel representing interactions of compounds **K4-a** (violet arrows representing H-bonds, green arrows representing π-π stacking); b) 3D dimensional panel representing interactions of compounds **K4-a** (yellow arrows representing H-bonds, light-blue arrows representing π-π stacking.

3.4.5 4*H*-benzo[*b*]imidazo[1,5-*d*][1,4]oxazine-based compounds for mPGES-1 potential inhibition

For the design of these potential inhibitors a new scaffold, 4*H*-benzo[*b*]imidazo[1,5-*d*][1,4]oxazine, never evaluated on mPGES-1, was tried. Thus, four cores were built (**Scheme 36**):

- *8-methyl-4H-benzo[b]imidazo[1,5-d][1,4]oxazine-3-carbaldehyde* (**L-a**);
- *N-(2-bromophenyl)-8-methyl-4H-benzo[b]imidazo[1,5-d][1,4]oxazine-3-carboxamide* (**L-b**);
- *N-(2-chloro-4-fluorophenyl)-8-methyl-4H-benzo[b]imidazo[1,5-d][1,4]oxazine-3-carboxamide* (**L-c**);
- *N-(2-chloro-6-methylpyridin-4-yl)-8-methyl-4H-benzo[b]imidazo[1,5-d][1,4]oxazine-3-carboxamide* (**L-d**).

Starting from the chemical procedure reported in **Scheme 37**, positions 3 and 8 were modified with all amine commercial available, generating the first library.

For the other libraries, we arbitrarily decided to place in 3 the substituents recurrent in other inhibitors of the same target we previously discovered[124], considering that this part of the molecules could bind $His53_{ChainB}$, $Ser127_{ChainA}$, $Phe44_{ChainB}$, fundamental for mPGES-1 inhibition. Additionally, position 8 was functionalized using Combiglide[96] in order to increase the interaction with the aromatic amino acid $Tyr130_{ChainA}$, $Thr131_{ChainA}$.

Starting from these libraries, the filters mentioned above were applied. The molecules subjected to docking analysis were 916000 for the **L-a** scaffold and ~13000 for the **L-b**, **L-c** and **L-d** scaffolds.

The 4*H*-benzo[*b*]imidazo[1,5-*d*][1,4]oxazine derivatives selected in the virtual screening workflow could be classified into two different groups: the first group belonging to the library

L-a, where both positions 3 and 8 were replaced; the second one, which includes the molecules of the other libraries (**L-b**, **L-c**, **L-d**) where only the position 8 of the scaffold was replaced.

The derivatives of the first group, bearing different aminobenzoic acids in position 3 and amino pyrazoles in position 8 as coupling partner moiety (**Scheme 38)**, had a better docking score value (between -10.81 and -10.01 kcal/mol) than the others (between -8.11 and -6.94) (**Scheme 39)**. In fact, the derivatives of the second group, bearing different halogens on the aniline in position 3, lost the hydrogen bond resulting in a lower docking score.

For example, the compound **L1-a** was placed in the middle of the ligand binding site. In this case, the aminobenzoic acids group interacted with the key amino acids Ser127 $_{ChainA}$ and His53$_{ChainB}$ by hydrogen bonds. The scaffold was able to establish π-π stacking interactions with Tyr130 $_{ChainA}$ and to direct the substituent in position 8. The latter that in compound **L1-a** was an amino pyrazole established a π-π stacking interaction with Tyr28 $_{ChainB}$, a hydrogen bond with Tyr130 $_{ChainA}$ and hydrophobic interactions with Tyr130$_{ChainA}$, Tyr131 $_{ChainA}$, Gln 134 $_{ChainA}$ (**Figure 41**).

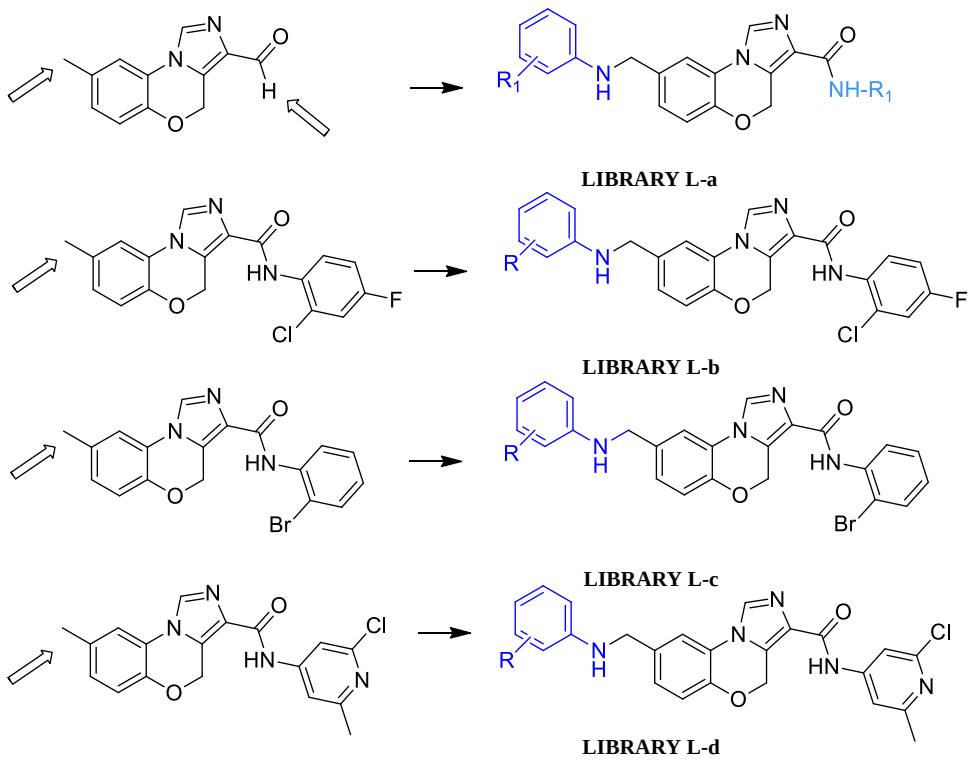

Scheme 36. Generation of the 4*H*-benzo[*b*]imidazo[1,5-*d*][1,4]oxazine libraries.

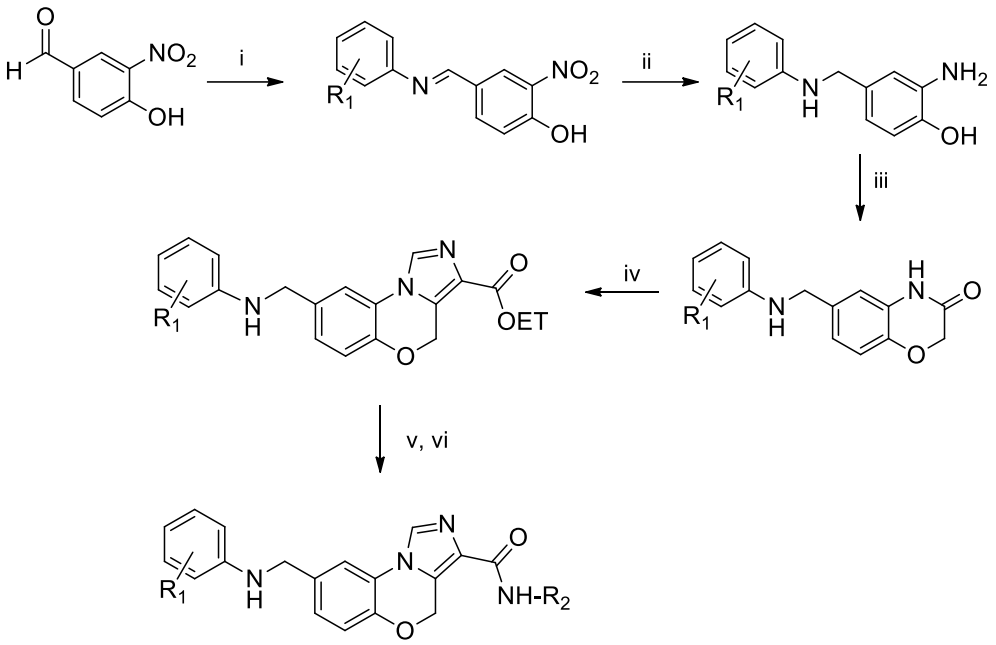

Scheme 37. Synthetic strategy chosen as template for the *in silico* drug design. *Reagent and conditions: i) $R_1(Ph)NH_2$, $Ti(OiPr)_4$, THF; ii) H_2, Pd/C; iii) chloroacetyl chloride, K_2CO_3, CH_3CN, r.t.*[150] *iv) KOtBu, diethyl chlorophosphate, DMF, 0°C, 10 min then ethyl isocyanoacetate, 60°C, 6 h;*[132] *v) NaOH, MeOH, 60°C, 30 min; vi) HOBt, HBTU, R_2-NH_2, DMF/DCM, r.t.*

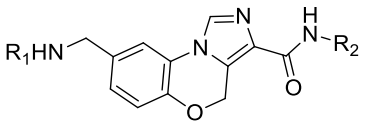

SCAFFOLD L-a

COMPOUND	R_1	R_2
L1-a	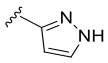	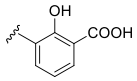
L2-a	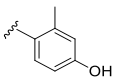	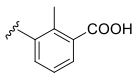
L3-a		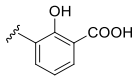
L4-a	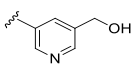	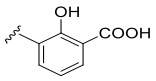
L5-a	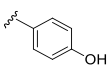	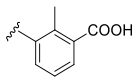
L6-a	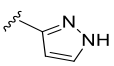	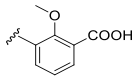
L7-a	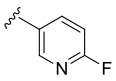	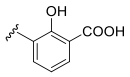
L8-a	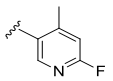	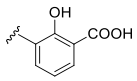
L9-a	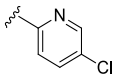	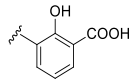
L10-a		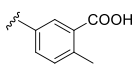
L11-a	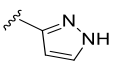	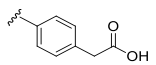
L12-a	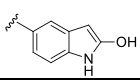	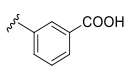

Scheme 38. Selected compounds within the L-a library.

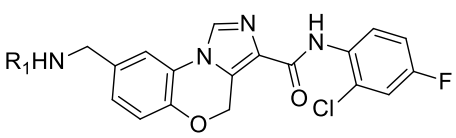

SCAFFOLD L-b

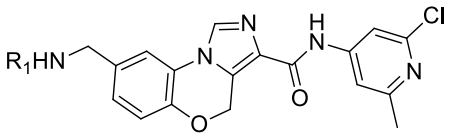

SCAFFOLD L-c

COMPOUND	R_1
L1-b	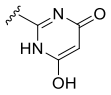
L2-b	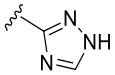
L3-b	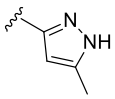
L1-d	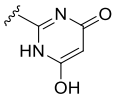
L2-d	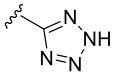

Scheme 39. Selected compounds within the L-b and L-d libraries.

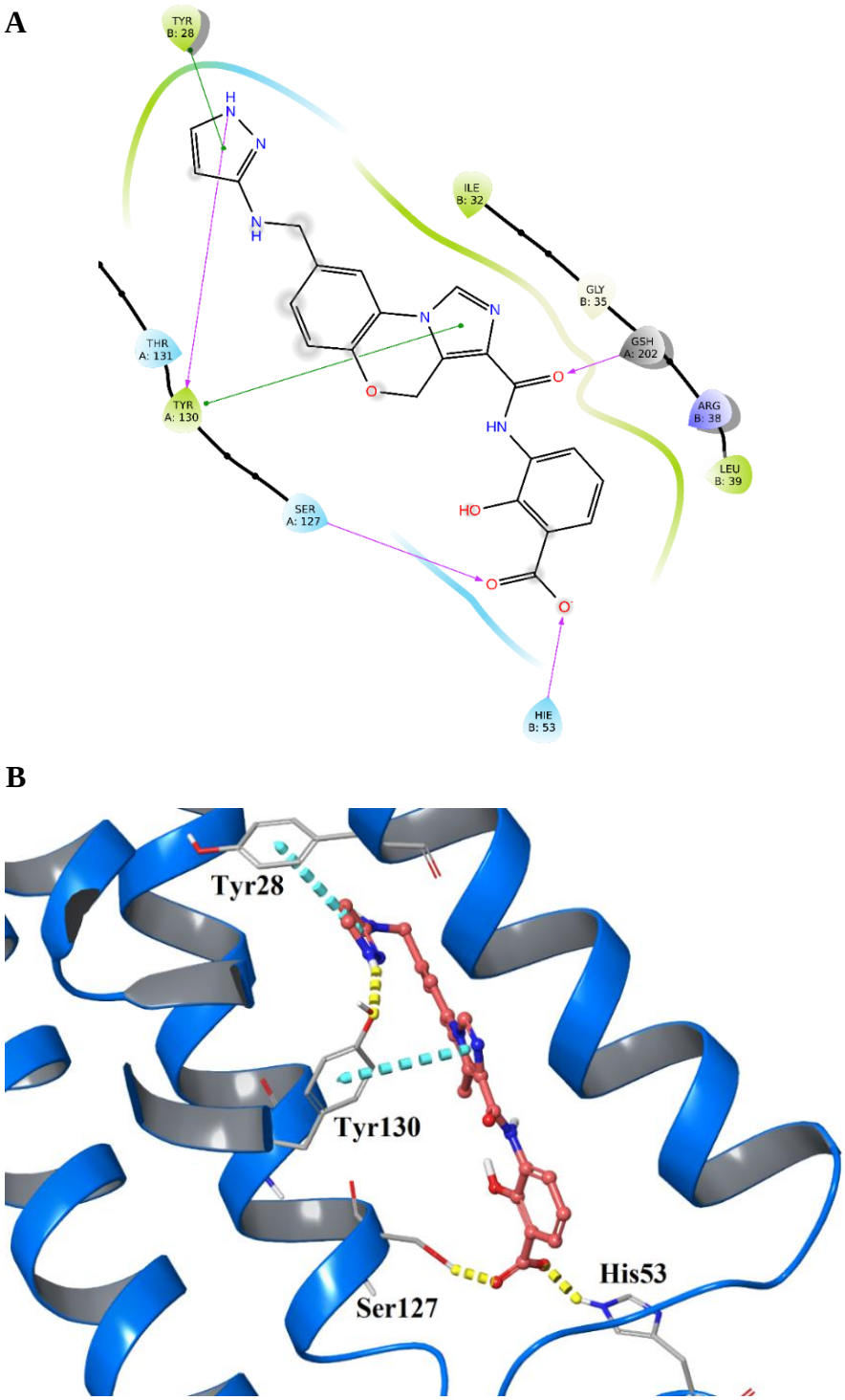

Figure 41. a) 2D dimensional panel representing interactions of compounds **L3-a** (violet arrows representing H-bonds, green arrows representing π-π stacking); b) 3D dimensional panel representing interactions of compounds **L3-a** (yellow arrows representing H-bonds, light-blue arrows representing π-π stacking).

3.4.6 Thiazole-based compounds for sEH potential inhibition

Thiazolyl-urea sEH inhibitors[133] have already been described. We, therefore, decided to modify the thiazoles nucleus in positions 2 and 5. All commercially available thioamides were replaced in position 2, and all the terminal alkynes in position 5, according with the synthetic procedure (**Scheme 41**).[151] A library of 3874 molecules was thus created (**Scheme 40**). The generated library was subjected to LigPrep,[97] QuikProp[98], and the final LigFilter[105] to obtain a filter library of 3408 molecules to process with docking experiments.

Thiazole-based compounds were evaluated on both mPGES-1 and sEH. The Docking calculations on mPGES-1 led us to too small molecules for the mPGES-1 binding site. Indeed, even if they were placed in an energetically favorable way, with the best docking score values around -9/-8 kcal/mol, they cannot give interaction with most of the binding site amino acids. The same library evaluated on soluble epoxide hydrolase gave the most promising results. The R_2 group always contained a carbamic/urea chemical portion capable of interacting with the amino acids implicated in sEH catalytic mechanism. In particular, hydrogen bond interactions were observed among the oxygen of the carbonyl group and both the tyrosine involved in the catalytic mechanism (Tyr343 and Tyr466).

The thiazole scaffold and the R_1 substituent, placed in the most apolar portion of the binding site, exhibited hydrophobic interactions with this part (**Figure 42**). Indeed, the docking score values (between -11.91 and -9.52 kcal/mol) confirmed the promising affinity of these molecules and the receptor counterpart. Thus, fifteen molecules (**Scheme 42**) were selected for the next synthesis and biological evaluation steps.

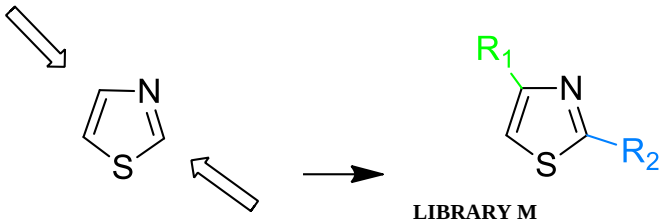

LIBRARY M

Scheme 40. Generation of the thiazole-based library.

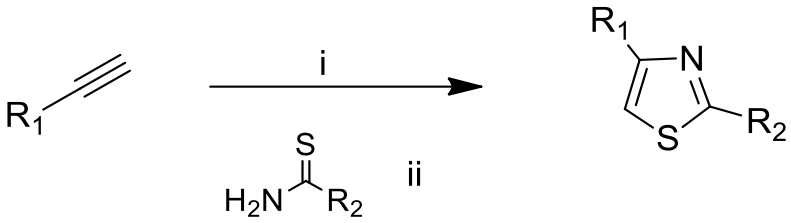

Scheme 41. Synthetic strategy chosen as template for the *in silico* drug design. *Reagent and conditions: i) Mor-DaIPhosAuOMs, MsOH, DCM, 6h, r.t. ii) 40°C, 16h.*[151]

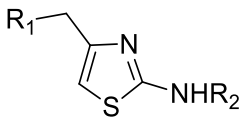

SCAFFOLD M

COMPOUND	R_1	R_2
M1	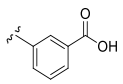	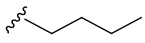
M2	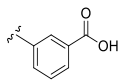	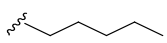
M3	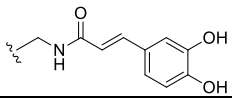	
M4	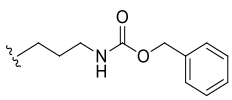	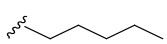

M5	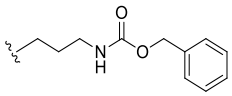	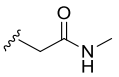
M6	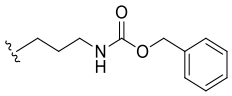	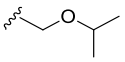
M7	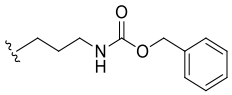	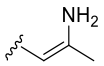
M8	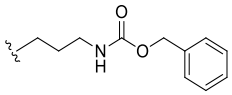	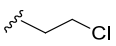
M9	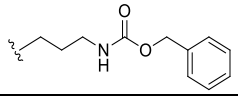	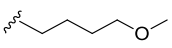
M10	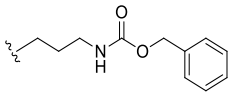	
M11	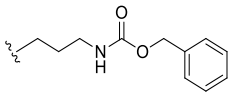	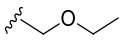
M12	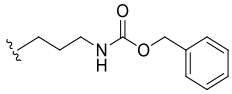	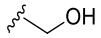
M13	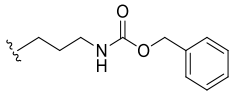	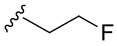
M14	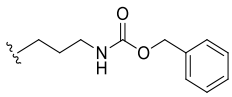	
M15	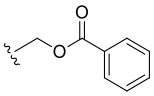	

Scheme 42. Selected compounds within M library.

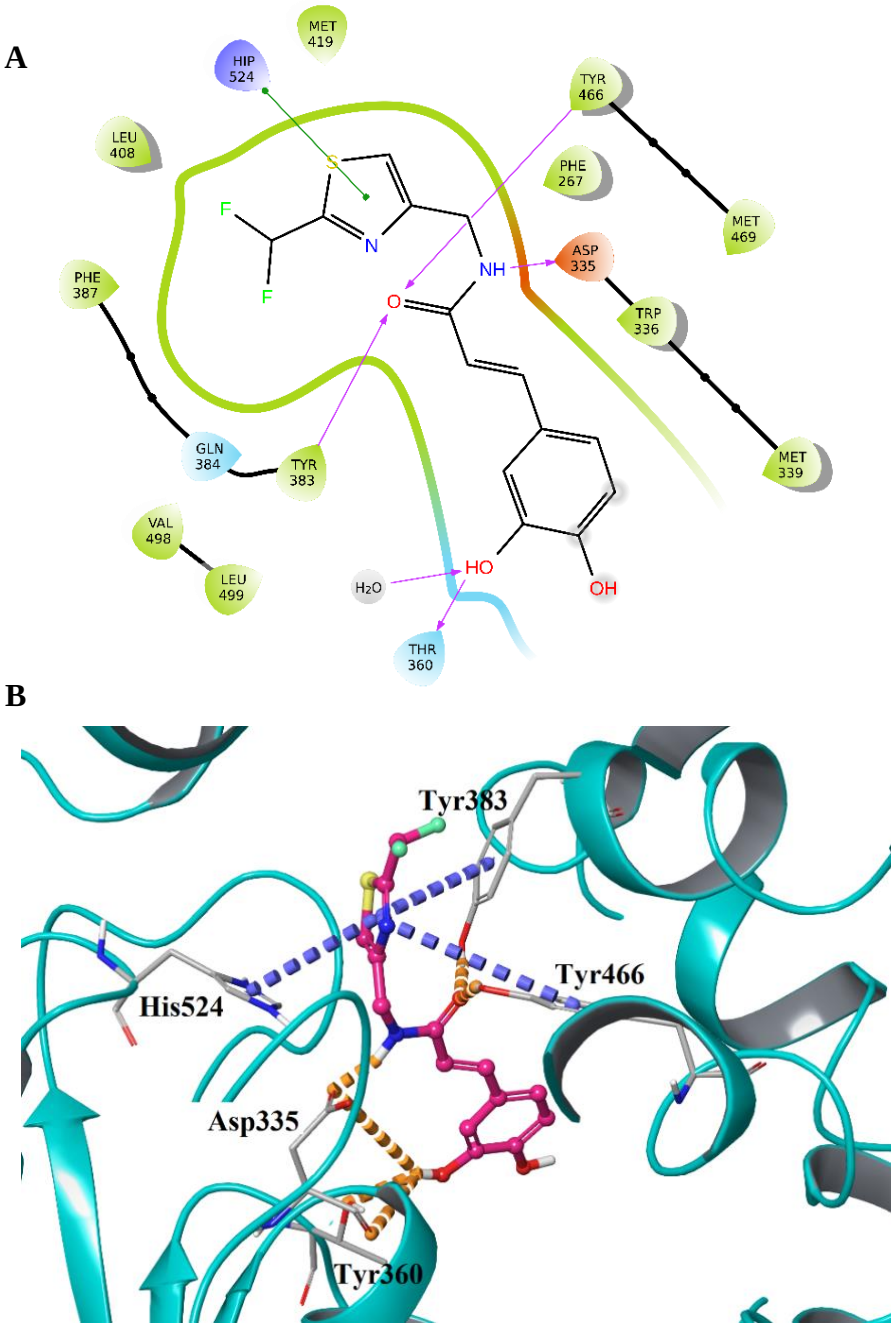

Figure 42. a) 2D dimensional panel representing interactions of compounds **M3-a** (violet arrows representing H-bonds, green arrows representing π-π stacking); b) 3D dimensional panel representing interactions of compounds **M3-a** (orange arrows representing H-bonds, violet arrows representing π-π stacking).

3.5 Summary

In conclusion, here we report that the new thiazolidin-4-one-based compounds can inhibit mPGES-1 with modest activity. Moreover, considering the increasing interest toward the identification of compounds able to interfere with the eicosanoid biosynthesis pathways, this

chemical core was tested against sEH, 5-LO, and COXs enzymes, focusing our attention on sEH due to the amide group belonging to the thiazolidin-4-one ring that is a typical pharmacophore of sEH inhibitors. Specifically, followed docking calculations, eleven compounds (**F2**-**F4**, **F7**-**F8**, **F10**-**F11, F13**, **F15**, **F22**-**F23**) of the small synthesized library were subjected to a cell-free assay against sEH, and three of them (**F2**, **F4**, **F8**) were able to interfere with the enzymatic activity. Finally, cell-free assays on COXs and 5-LO with the hits **F2**, **F4**, and **F8** revealed compound **F4** also as a promising 5-LO inhibitor, with somewhat reduced potencies for compounds **F2** and **F8**, expanded our investigations on interference with inflammation-related lipid mediator biosynthesis. Finally, the capability of the test compounds for reducing 5-LO-mediated LT production in intact human neutrophils was confirmed efficient inhibition of 5-LO in the cellular context.

Also, seven benzothiazinone-based compounds were synthesized starting from 2-amino-4-bromobenzoic acid through 3 synthetic steps, and the biological assays are now in progress in collaboration with Prof. Oliver Werz.

Finally, 6 series of molecules were designed *in silico* on mPGES-1 and/or sEH. After that, starting from an initial list of 10,904,538 virtual compounds, the Virtual Screening procedure permitted to limit the range to the most promising 88 ones, showing the great potential of computational methods in the drug discovery process**.**

CHAPTER 4
Synthesis of fluorinated dienes and their functionalization through enantioselective Diels-Alder

4.1 State of the art

Flurodienes, fluoropolyenes, and more in general, all the fluorinated compounds have recently attracted attention due to their biological activities.[134] Several synthetic methods for such fluoroolefins have been reported, although the stereoselectivity achieved with such methods is generally unsatisfactory.[134]

Schlosser and co-workers[135] showed that trimethylsilyl-2-chloro-2-fluorocyclopropanes can be transformed to fluorodienes by cleavage of the distal C1-C3 bond, when treated with activated zinc or with a fluoride source. Furthermore, Kobayashi et al.[136] reported the synthesis of fluorodienes starting from gem-difluorocyclopropanes bearing an electron-withdrawing group (-CO_2Me, -CN,-SO_2Ph) in the α-position when treated with a strong base, such as lithiumdiisopropyl amide (LDA). However, these fluorodienes were obtained in modest yields.

Another approach[137] described the preparation of fluorodienes with 1,1-bromo-fluoro-olefins in a palladium-catalyzed cross-coupling. However, the time-consuming preparation of the starting 1,1-bromofluoro-olefins represents the main limitation of such approach, along with the stereochemical purity.

In our study, we explored a stereospecific synthesis of fluorodienes utilizing different gem-difluorocyclopropane derivatives as substrates. The advantages of this method reside in the possibility to apply this method to different types of gem-diflurorocyclopropanes (not exclusively bearing an electron-withdrawing group) that can be easily synthesized from the analog alkene and in the quite high obtained yields.

Fu's group[138] described a general and efficient Pd-catalyzed activation of gem-difluorinated cyclopropanes that in the presence of boronic acids afford the corresponding arylated/alkenylated/alkylated 2-fluoroallylic scaffolds. Based on these results, our native idea

was to obtain a beta-hydride elimination in the absence of the boron reagent, due to the presence of beta-hydrogens on the starting gem-difluorinated cyclopropanes.

Applying the exact condition of Fu's work,[138] without using the boronic acid, the gem-diflurocyclopropane led to the formation of fluorodienes (**Scheme 43**). With the aim to optimize the conditions, ten chiral ligands were first examined in this transformation. In this context, the 2-dicyclohexylphosphino-2′-(N,N-dimethylamino)biphenyl ligand (DavePhos) gave the better results.

Using 1-(2,2-difluoro-3-methylcyclopropyl)-4-methoxybenzene as starting material, the yield improved to 80% in dry 1,4-dioxane. Finally, further investigation was applied to see the effect of decreasing the base amount, which resulted in a reduced yield.

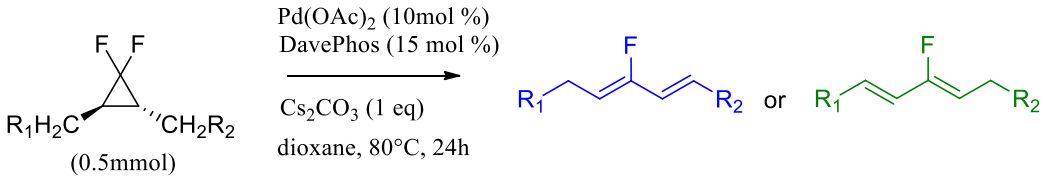

Scheme 43. Scheme of synthesis of the new chemical route for the synthesis of fluorodienes.

4.2 Improved substrate scope

4.2.1 First series of substrates: 2,2-difluorocyclopropylbenzene, pyrrolidines and piperidines derivatives

After this proof of the concept, we focused on the synthesis of more diverse fluorinated dienes through other gem-difluorocyclopropane.

The synthesis was first attempted on a group of eight (2,2-difluorocyclopropyl)benzene molecules featuring different substitutions on the aromatic ring (**Figure 43A**). These gem-difluorocyclopropanes were synthesized from the analog alkene through a reaction involving

the use of TMS-CF_3 as carbene source and NaI in THF at reflux[139-140] (Yield:68-89%). In this case, the amount and the time during which the TMS-CF_3 was added to the reaction varied depending on the reactivity of the used alkenes. If the alkene was not very reactive, an excess of TMS-CF_3 (5 equiv) and the addition of the split reagent in 12 hours would be needed to avoid the precipitation of the reactant as a siloxy adduct.

The subsequent palladium coupling on this synthesized gem-difluorocyclopropanes proceeded with high stereoselectivity and good yield (56-87%) (**Figure 43B**). We hypothesized that from a cyclopropane opening ring, a fluoroalkene in complex with the palladium and the ligand is formed as an intermediate. Thereafter, the proton in beta to the fluorine is torn to form the diene (**Scheme 44**). Selectivity depends on the nature of the gem-diflurocyclopropane. In fact, we suspected that after the cyclopropane ring-opening, the first proton to be torn is the most acidic, with the second being the most accessible.

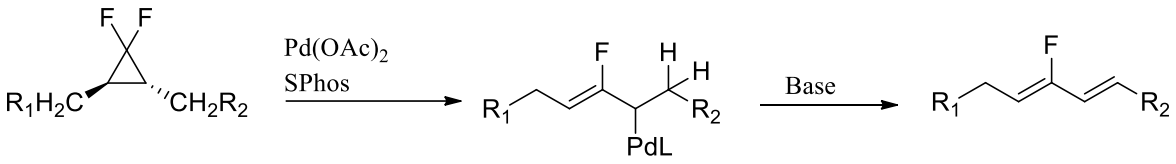

Scheme 44. Plausible mechanism.

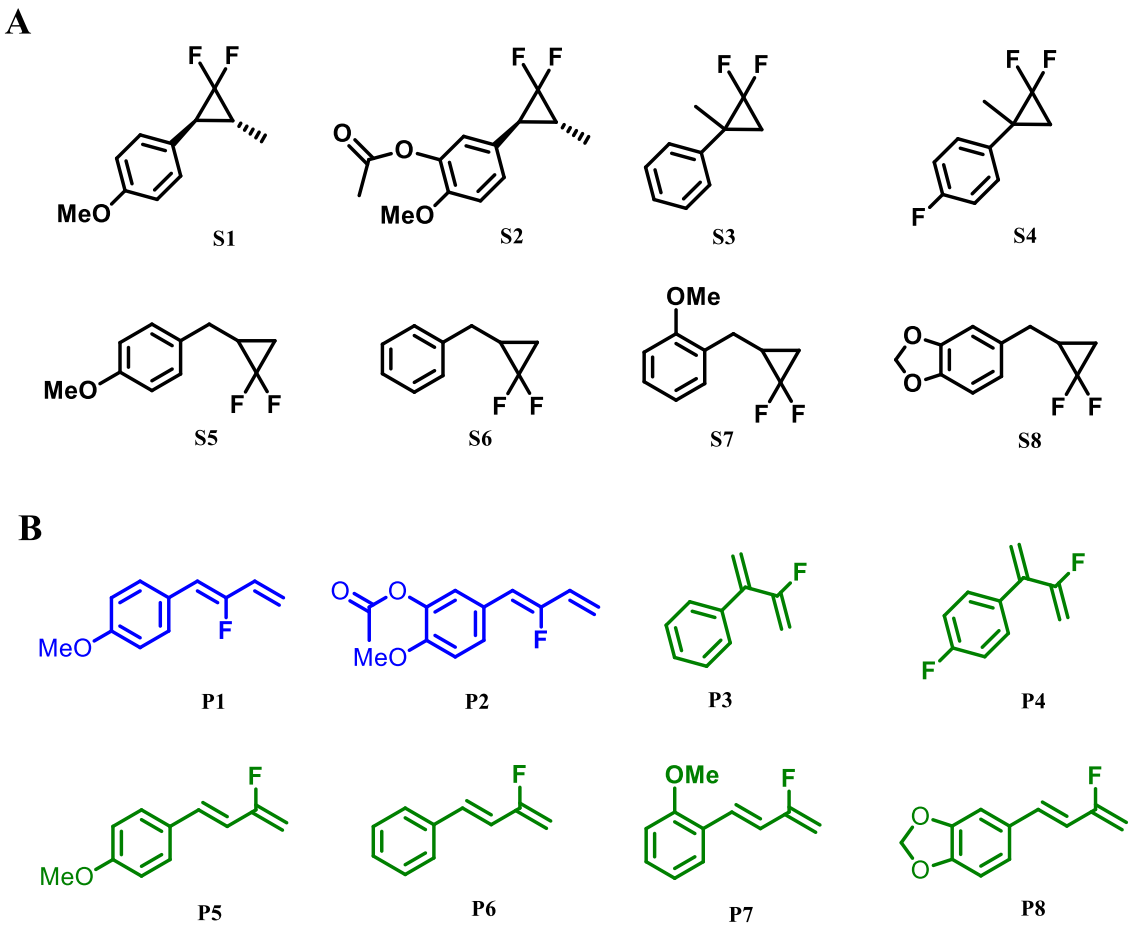

Figure 43. A) Gem-difluorocyclopropanes synthesized B) Alkenes resulting from new described coupling.

In addition, in the frame of the substrate improvement, pyrrolidines and piperidines derivatives with the difluorocyclopropane in their structure were synthesized. The reaction previously described was evaluated on these synthesized compounds (**Figure 44**).

First, we focused on the preparation of the difluorocyclopropane starting from lactam analogs through 4 synthetic steps (**Scheme 45**):

i) -Boc or -Tos protection of the lactam;

ii) reduction of the carbonyl group with DIBAL-H in THF at -78°C;

iii) dehydration with trifluoracetic anhydride and triethylamine from -78°C to r.t in DCM;

iv) formation of the gem-difluorocyclopropane in the same condition already discussed before.[139]

Overall, seven compounds were synthesized (**Figure 44**). Compound **S16** was the only one for which the synthesis was not successfully accomplished due to a failure of the last synthetic step, possibly related to the low reactivity of the corresponding alkene. However, the subsequent reaction on these substrates was successful, except for compounds **S9** and **S10**, both with the -Boc on the nitrogen atom. In these cases, the fluorodiene was very unstable, with further oxidation of the carbon carrier of fluorine.

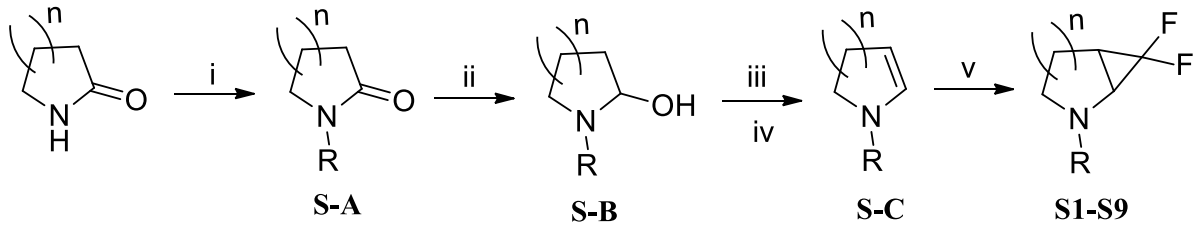

R= -Boc, -Tos,
n= 1, 2.

Scheme 45. General scheme of synthesis. *Reagents and conditions: i) BOC-anhydride, DMAP, CH_3CN, 0°C to r.t. or BuLi, benzenesulfonyl chloride, THF, -78°C to r.t.; ii) DIBAL-H, THF, -78°C; iii) $(CF_3CO)_2O$, DCM, -78°C; iv) NEt_3; v) NaI, $TMSCF_3$, THF, reflux.*

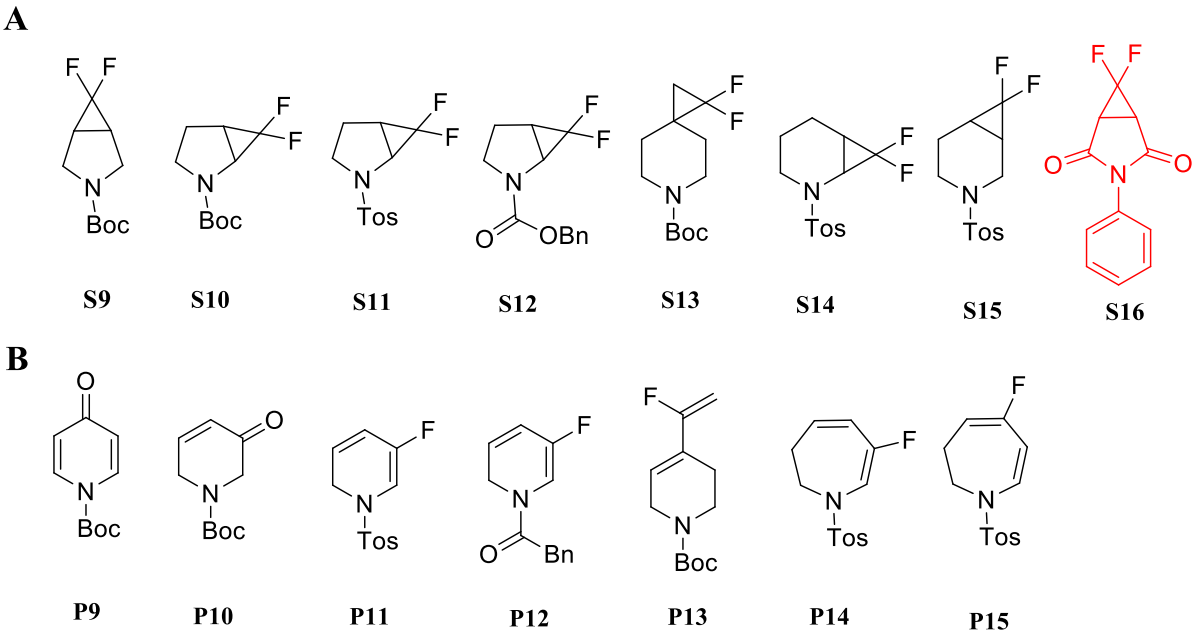

Figure 44. A) Second set of gem-difluorocyclopropanes synthesized; B) Dienes resulting from the new described coupling.

4.2.2 Third series of substrates: oxygenated compounds

We successively explored the scope of the reaction with various oxygenated compounds as substrates. After synthesizing compounds **S17**, **S18**, **S19,** the reaction was attempted. Unfortunately, only compound **S17** gave the expected product in good yield (75%); the formation of the other isomer was not observed. On the other hand, **S18** and **S19** resulted in 0% and 19% yield, respectively (**Figure 45A-45B**). Given these results, the reaction conditions on these oxygenated compounds were modified in order to increase the yield.

Compound **S19** was chosen for the following optimization step. First, due to the high compound volatility, the temperature was lowered at 50°C. Under these conditions, a similar yield was detected, but with a greater amount of starting material, thus being well suited to be optimized. Thereafter, the reaction conditions were modified, changing the base amount and then the base type. The yield with different carbonates remained similar; however, a slight improvement using a stronger base, such as NaOH or NaH, was observed (**Table 16**).

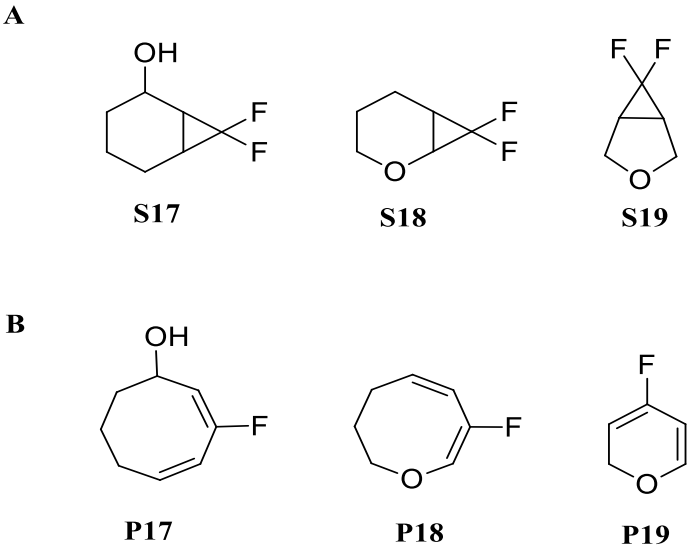

Figure 45. A) Set 3 of gem-difluorocyclopropanes synthesized B) Alkene resulting from the new described coupling.

Table 16. Reaction optimization.

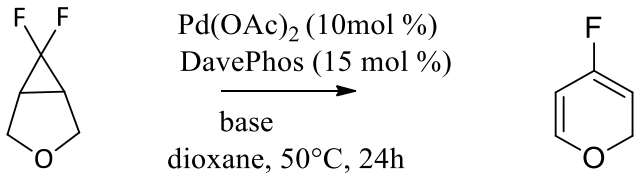

ENTRY	BASE	AMOUNT OF BASE (eq)	YIELD% (SM)
1	Cs_2CO_3	1	11% (71)
2	Cs_2CO_3	2	20% (65)
3	K_2CO_3	2	13% (73)
4	Na_2CO_3	2	17% (68)
5	NaH	1	30% (33)
6	NaOH	1	29% (25)

Last, phosphine ligand screening under improved conditions was made using the condition of entry 2 (**Table 16**). Indeed, we opted for this condition to have a greater amount of starting material despite a lower yield compared to the others (for example, entry 5 and 6 (**Table 16**).

Ligand screening was made using eighteen different phosphines (**Figure 46**). Unfortunately, the screening on the batch gave worst results than expected (Yield: 1-5%). Possibly the final results were influenced by the loss of solvent connected to the small amount used to have the same concentration of the previous trials.

The reaction was also attempted at room temperature without any success. Therefore, before performing the ligand screening again with a larger amount of solvent and a different concentration, some reaction trials were made with the microwave.

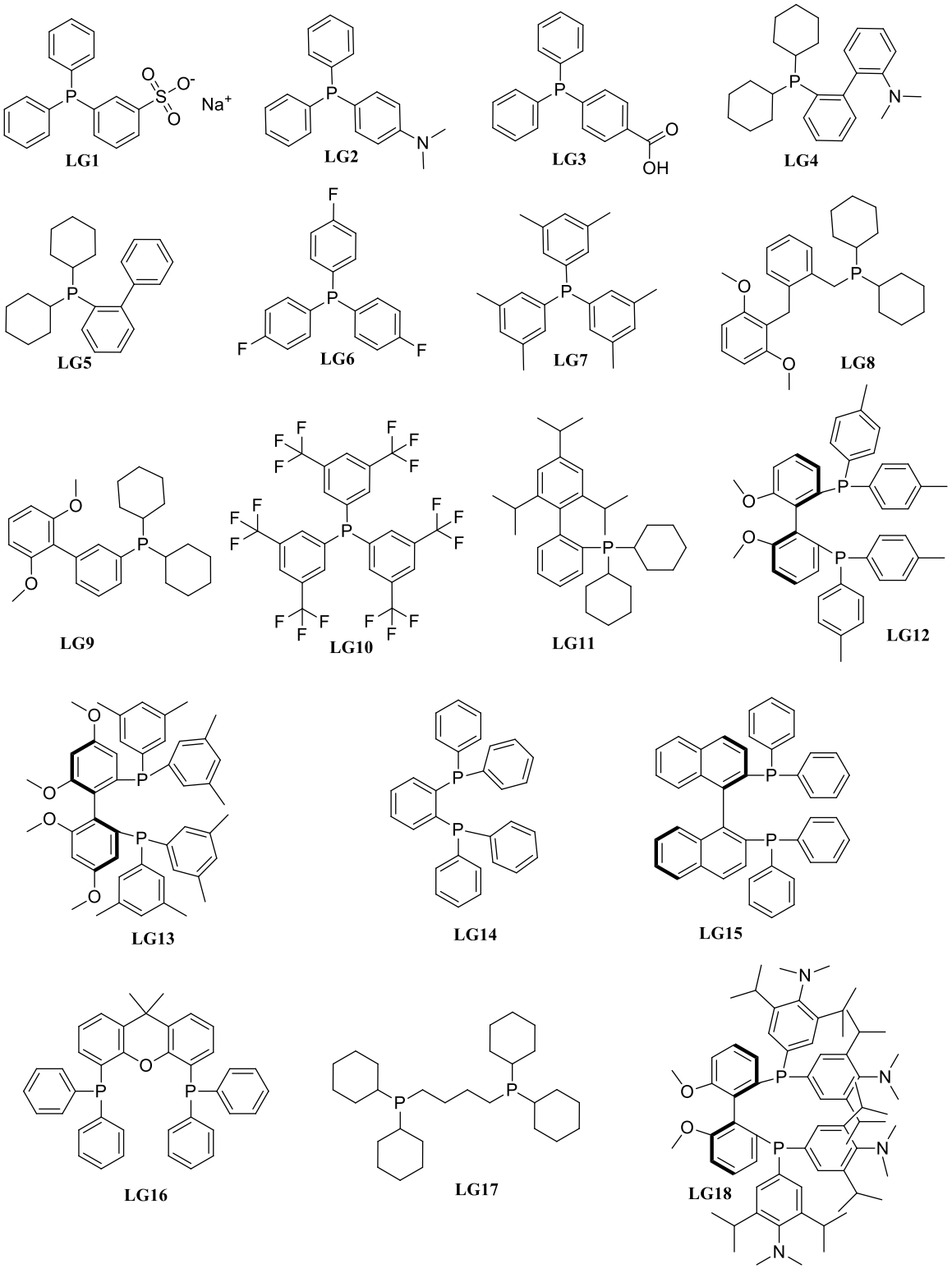

Figure 46. Phosphine ligands used for the screening.

In the microwave apparatus, we obtained a better result compared to the reaction with conventional heating, already after 1h. We observed no significant loss of solvent or of starting material compared to the bath. Moreover, the best results obtained with this new condition were in a reaction solvent-free for 1h using Cs_2CO_3 as base (**Entry 9**, **Table 17**). The microwave apparatus is particularly suitable for solvent-free reactions in a short time, and liquid substrate acting as solvent as in this case (as already described in **Chapter 2**). However, considering that the use of a solvent will hopefully allow us to try other non-liquid substrates in the future, we also tested the ligands under microwave irradiation in dioxane, using NaH as base (**Entry 8**, **Table 17**).

Better results were gathered with slightly more basic ligands. However, the difference in the ligand pK_a was not significant, resulting in a slight change in the final yield (**Table 18**). All the obtained results were sent to Sigman's group to:

i) assess (through computational technique) the possible influence of pK_a on the reaction;
ii) to evaluate the use of a ligand with different chemical-physio properties for these substrates.

Table 17. Summary of microwave trials.

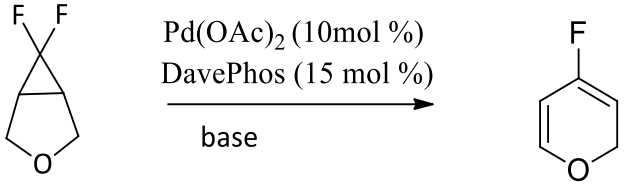

ENTRY	TEMPERATURE	BASE	SOLVENT	TIME	ABSORPTION	YIELD% (SM)
1	50°C	Cs_2CO_3	dioxane	10 min	normal	0%(100)
2	80°C	Cs_2CO_3	dioxane	10 min	normal	0%(100)
3	100°C	Cs_2CO_3	dioxane	10 min	normal	0%(100)
4	80°C	Cs_2CO_3	dioxane	30 min	normal	0%(100)
5	50°C	Cs_2CO_3	dioxane	5 h	high	4%(96)
6	100°C	Cs_2CO_3	dioxane	5 h	high	8%(91)
7	100°C	NaOH	dioxane	5 h	high	19%(80)
8	100°C	NaH	dioxane	5 h	high	24%(65)
9	100°C	Cs_2CO_3	Solvent free	1h	high	30%(70)
10	100°C	NaOH	Solvent free	1h	high	30%(15)
11	100°C	NaH	Solvent free	1h	high	36%(6)

Table 18. Summary of phosphine ligand screening.

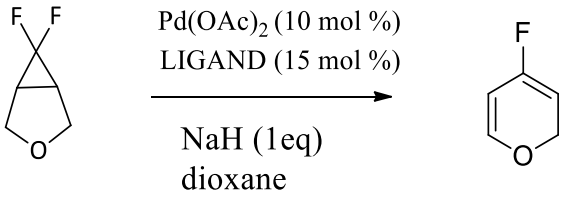

COMPOUND	YIELD% (SM)
L1	25% (65)
L2	25% (65)
L3	7% (83)
L4	21% (69)
L5	6% (84)
L6	1% (90)
L7	0% (90)
L8	0% (90)
L9	6% (80)
L10	20% (75)
L11	22% (70)
L12	11% (80)
L13	0% (100)
L14	26% (65)
L15	5% (90)
L16	11% (79)
L17	0% (90)
L18	24% (60)

4.3 Investigation of a new Diels-Alder (*DA*) reaction on fluorodienes

The Diels-Alder reaction is considered a fundamental finding in the field of organic chemistry. Nowadays, many reaction variants, either enantioselective or not, have been described; however, studies based on fluorodienes as reaction substrate are still quite rare. In 2010, Iio's group[141] reported an example of Diels-Alder reaction on fluorinate diene. Although described as a strongly activated diene, the reaction is not applicable to different types of fluorodienes. Moreover, the final products, obtained through the reaction of (*E*)-1-benzyloxy-3-fluoro-1,3-butadiene with different types of dienophiles, is a racemic mixture.

Therefore, our purpose was to investigate *DA* on fluorinate compounds in addition to an enantioselective mechanism.

Our first idea was to generate the fluorinated diene *in-situ* with the previously reported reaction and utilize it immediately for further functionalization.

((2,2-difluorocyclopropyl)methyl)benzene was chosen as substrate to give (3-fluorobuta-1,3-dien-1-yl)benzene. After obtaining the fluorodine we tried the next step under the standard Diels-Alder condition (dioxane, 100°C, 24h) with different dienophiles (**Scheme 46**). The reaction did not work for most of them, while dienophile A (maleic anhydride) and B (di-tert-butyl diazene-1,2-dicarboxylate) proceeded with 33% and 8% yield, respectively.

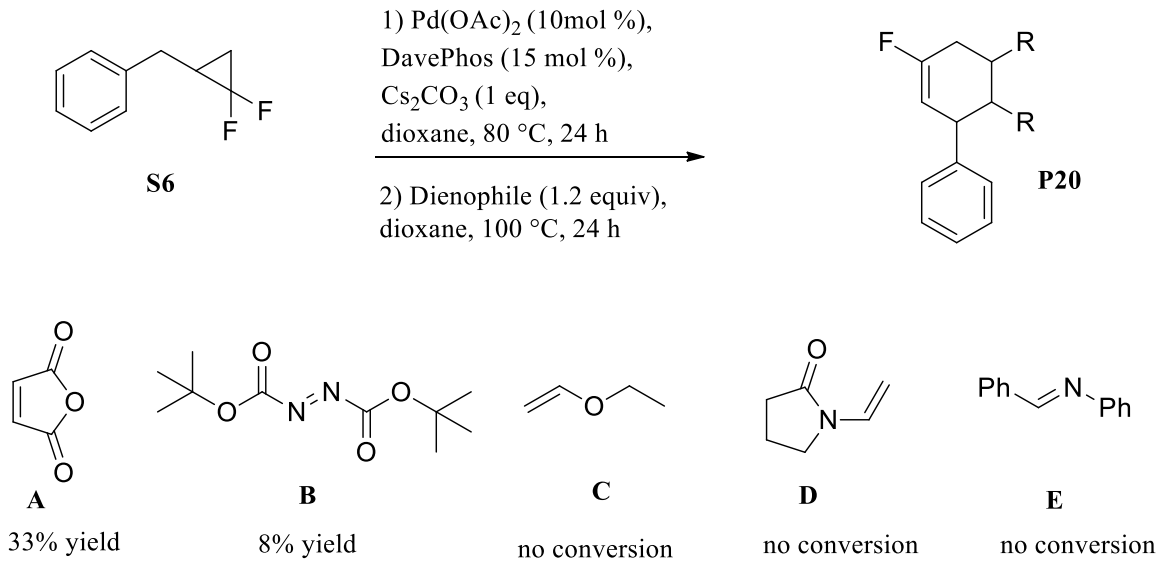

Scheme 46. Model choice for Diels-Alder reaction.

Considering the more reactivity of maleic anhydride in this reaction type, we opted for dienophile B for the next trials. This choice was made to guarantee conditions as general as possible and applicable to different substrates.

At this point, with the purpose of improving the yield of the reaction and obtain an enantiopure product, we decided to use a chiral catalyst. Different derivatives of (*S*)-BINOL phosphoric acid, either synthesized (**(*S*)-CT3**, **(*S*)-CT4**) (**Figure 47** and **Scheme 47**) or commercially available (**(*S*)-CT1**, **(*S*)-CT2**, **(*S*)-CT5**) (**Figure 47**), were used.

Catalyst **(*S*)-CT2** and **(*S*)-CT5** were chosen with the idea that the protonation of the transition state could enhance the reaction. In particular, the protonation could improve the energy of the diene HOMO (highest occupied molecular orbital) and facilitate the interaction with the dienophile LUMO (lowest unoccupied molecular orbital) due to the reduction of the energy gap between the two orbital. The *DA* reaction could therefore become a two-step process with a zwitterionic intermediate. Indeed, even if generally the process of bond breaking and bond formation in the *DA* reaction is considered to be concerted, it is not necessarily synchronous.

Thus, *DA* reaction can even become a two-step process with a zwitterionic intermediate in such cases, and this support our idea.

On the other hand, the idea to use other catalysts (**(*S*)-CT3** and **(*S*)-CT4**) was based on the principle that phosphamides are able to coordinate the dienophile, thereby lowering the LUMO energy of the dienophile and facilitating the interaction with the diene HOMO.

Finally, we used **(*S*)-CT1** considering that when a hydrogen bond is formed with such an activating group, its electron-withdrawing capacity is enhanced, resulting in a further lowering of the LUMO energy, a smaller HOMO-LUMO gap, and still a faster reaction.

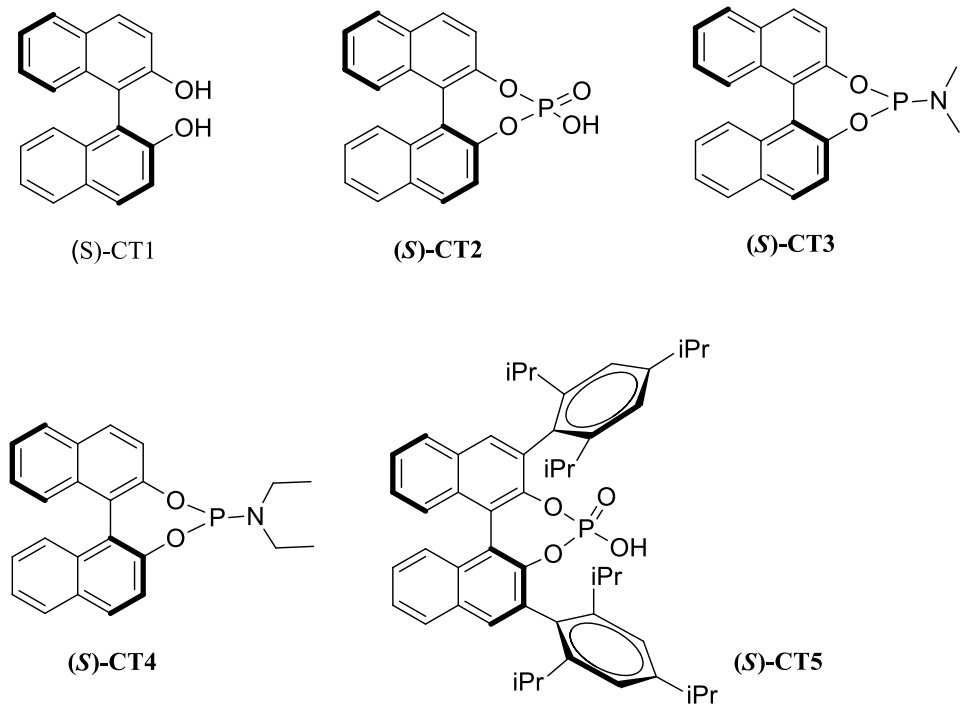

(S)-CT1 **(*S*)-CT2** **(*S*)-CT3**

(*S*)-CT4 **(*S*)-CT5**

Figure 47. First catalyst screening.

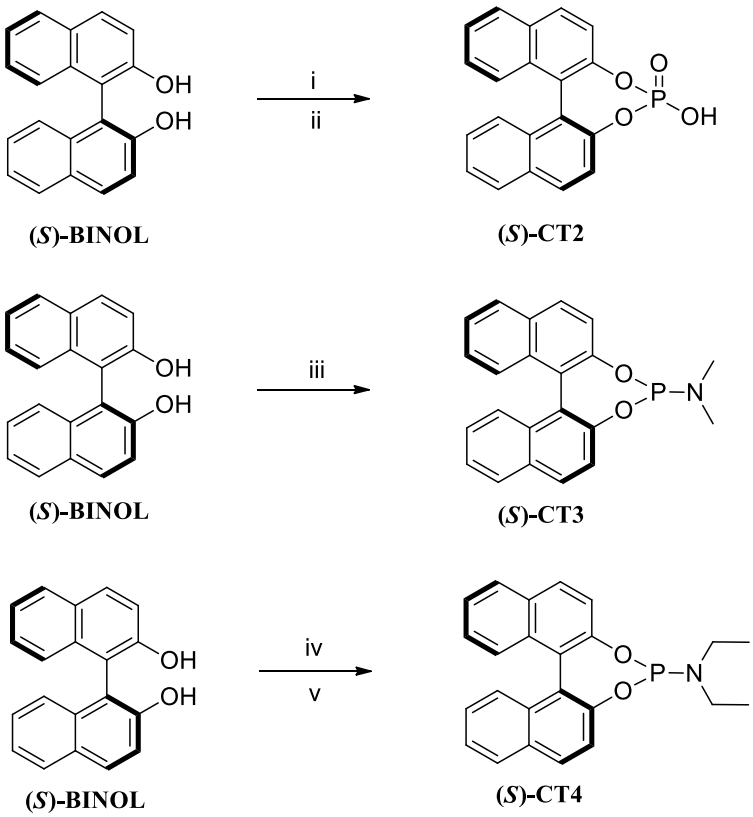

Scheme 47. Synthesis of catalyst **(*S*)-CT2**, **(*S*)-CT3**, **(*S*)-CT4**. *Reagent and conditions: i)$POCl_3$, pyridine, O°C 4h; ii)4N HCl; iii) $P(NMe_2)_3$, toluene, reflux; iv) $POCl_3$, NEt_3, toluene, O°C 6h, v) NEt_3, over-night.*

The five catalysts gave better results compared to the reaction without any catalyst addition (**Table 19**), except for **(*S*)-CT1**. In fact, in the latter case the formation of the product was not observed.

(*S*)-CT2 was the best catalyst; even if **(*S*)-CT4** gave comparable yields and better enantiomeric excess. Therefore, 0.1 equivalent of **(*S*)-CT2** were added to the reaction for the subsequent solvent screening.

Different solvents, or mixture of them, were tried (**Table 20**) in order to evaluate the yield and the enantiomeric excess. The use of a polar solvent, theoretically able to stabilize the reactant by hydrogen bond, was not successful.

Nine different solvents were tested, but none gave results better than dioxane. The yield was still low, so the dienophile's stability at the reaction temperature was evaluated.

Table 19. Summary of the first catalyst screening. SM_2 represent the amount of flurodiene residue.

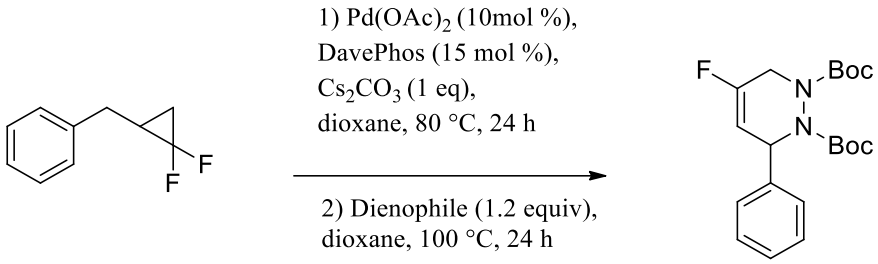

CATALYST	YIELD%(SM_2)	ee%
(*S*)-CT1	0% (10)	/
(*S*)-CT2	22%(19)	9
(*S*)-CT3	10%(7)	7
(*S*)-CT4	16% (21)	6
(*S*)-CT5	20% (10)	12

Table 20. Summary of the solvent screening.

ENTRY	CATALYST	SOLVENT	TEMPERATURE	YIELD% (SM2)
1	**(*S*)-CT2**	Dioxane + Toluene	100°C	19% (20)
2	**(*S*)-CT2**	Dioxane + Benzene	100°C	20% (15)
3	**(*S*)-CT2**	Dioxane + H_2O	100°C	1% (5)
4	**(*S*)-CT2**	Dioxane + DCM	100°C	7% (19)
5	**(*S*)-CT2**	Toluene	100°C	18% (18)
6	**(*S*)-CT2**	Benzene	100°C	20% (14)
7	**(*S*)-CT2**	Et_2O	reflux	18% (0)
8	**(*S*)-CT2**	Pentane	reflux	19% (0)
9	**(*S*)-CT2**	DCM	reflux	9% (4)

At 100°C, the dienophile was already unstable after 1/2h, while great stability was observed at room temperature and 50°C. However, at 80°C, the dienophile degraded after 16h (**Table 21**). Therefore, the Diels-Alder reaction was carried out at room temperature and 50°C.

In both cases, the product was not isolated, although the polymerization of the dienes was observed. Considering that the reaction worked only at high temperatures, it was performed with a larger amount of dienophile and a shorter time, obtaining a better but still not satisfactory yield improvement (**Table 22**). In addition, the enantiomeric excess (*ee*) was evaluated at 80°C and 100°C, with the idea that at 80°C the *ee* could improve. Lowering the temperature to 80°C we have obtained a better ***ee*** but it was not satisfactory as well as the reaction yield (**Table 22**).

Table 21. Trials to evaluate the stability of dienophile.

ENTRY	COMPOUNDS	TEMPERATURE	SOLVENT	TIME	STABILITY
1	Dienophile	100°C	Dioxane	1h	unstable
2	Dienophile + **(*S*)-CT2**	100°C	Dioxane	1h	unstable
3	Dienophile	100°C	Dioxane	1/2h	unstable
4	Dienophile + **(*S*)-CT2**	100°C	Dioxane	1/2h	unstable
5	Dienophile	80°C	Dioxane	16h	unstable
6	Dienophile + **(*S*)-CT2**	80°C	Dioxane	16h	unstable
7	Dienophile	50°C	Dioxane	24h	stable
8	Dienophile + **(*S*)-CT2**	50°C	Dioxane	24h	stable
9	Dienophile	r.t.	Dioxane	24h	stable
10	Dienophile + **(*S*)-CT2**	r.t.	Dioxane	24h	stable

Table 22. Trials conducted with a bigger amount of dienophile in a small reaction time.

ENTRY	TEMPERATURE	TIME	DIENOPHILE (eq)	YIELD%(SM_2)	*ee*(%)
1	80°C	20h	1.2	22% (19)	/
2	80°C	20h	4	25% (15)	/
3	80°C	20h	6	28% (10)	12%
4	100°C	5h	4	23% (18)	/
5	100°C	5h	6	26% (12)	7%

Last, in light of these results, further trials (**Table 23**) were conducted performing the second step on isolated diene, either with only the catalyst or with the catalyst plus the palladium, in order to understand the impact of each of the two catalysts on the reaction. Indeed, when the *DA* was conducted *in situ*, the palladium deriving from the first step was still present. However, a slightly better yield was obtained without the palladium. Given the still unsatisfactory yield, we decided to opt for a new approach.

Table 23. Trials conducted with the isolate diene.

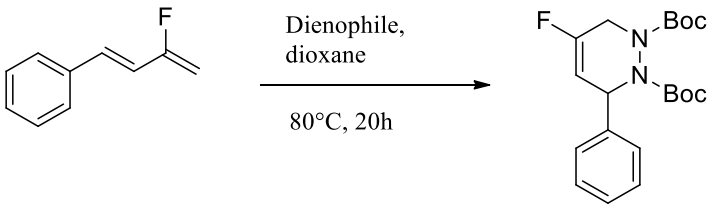

ENTRY	CATALYSTS	DIENOPHILE (eq)	YIELD (SM)
1	$Pd(OAc)_2$ + BINOL-PHOS	1.2	10% (9)
2	BINOL-PHOS	1.2	24% (9)
3	BINOL-PHOS	4	30% (0)
4	BINOL-PHOS	6	36% (0)

4.4 Investigation of a new Diels-Alder with different titanium catalysts

Essers.et al. [142] already reported the use of chiral titanium catalysts for the Diels-Alder reaction when the fluorine is neither on the dienophile nor on the diene. Thus, the catalyst could also coordinate the transition state of the reaction under-screening. In addition, catalyst **(*S*)-CT6** is a Lewis acid and could coordinate the diene in order to increase the energy level of the diene HOMO and allow the interaction with the dienophile LUMO, acting as the previous catalyst. The titanium catalyst was synthesized through a reaction of titanium(IV) tetrachloride and (*S*)-BINOL (**Scheme 49**) to give the final product **(*S*)-CT6**. Before this procedure was attempted, we tried to perform **(*S*)-CT6** from diisopropoxytitanium(IV) chloride and (*S*)-BINOL, as suggested by Essers.et al. [142]. However in this case we obtained a complex in which the chlorine (and not the isopropoxide group) was substituted with the hydroxyl of the (*S*)-BINOL.

We started from the previous ameliorated conditions for the trial with catalyst **(*S*)-CT6**. In particular, we still used 4 equivalent of dienophile in dioxane as solvent, and performed the experiment at room temperature, 50°C, and 80°C.

The use of catalyst **(*S*)-CT6** (0.1 eq) led to a 47% yield at 80°C, and 43% at 50°C. This result was particularly interesting, considering that under previous conditions catalyst **(*S*)-CT2** led to non-detectable yield at 50°C. The reaction did not work at room temperature, as in the previous cases (**Table 24**).

Therefore, the reaction was tested using a larger amount of titanium catalyst (0.3 eq) at 80°C and 50°C. The yield significantly increased, reaching a peak of 88% at 80°C. Nevertheless, the enantiomeric excess with this amount of catalyst was 6% at 80°C and 14% at 50°C (**Table 24).**

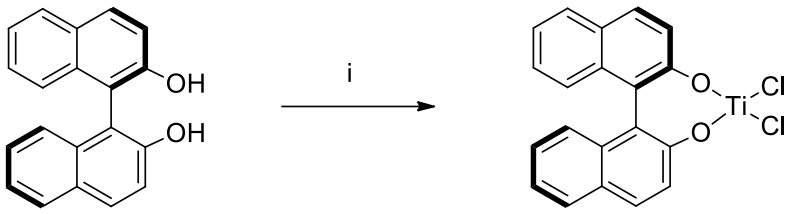

(S)-BINOL **(S)-CT6**

Scheme 49. Synthesis of titanium catalyst **(*S*)-CT6**. *Reagent and conditions: $TiCl_4$, pentane r.t.*

Table 24. Reaction condition optimization.

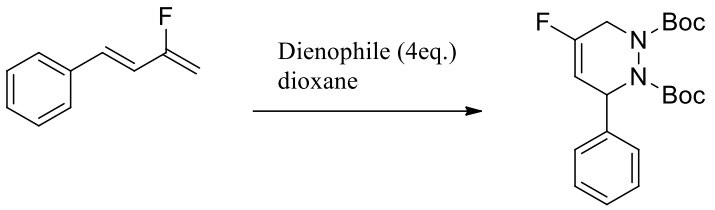

ENTRY	TEMPERATURE	TIME	CATALYST (eq)	YIELD(SM)	*ee* (%)
1	r.t.	24h	0.10	1% (10)	/
2	80°C	6h	0.10	26% (30)	/
3	80°C	16h	0.10	42% (15)	/
4	80°C	24h	0.10	47% (2)	4%
5	80°C	24h	0.30	88% (2)	6%
6	50°C	6h	0.10	5% (66)	/
7	50°C	24h	0.10	34% (37)	/
8	50°C	30h	0.10	43% (29)	12%
10	50°C	24h	0.30	50% (50)	14%

With the aim of improving the enantiomeric excess, the synthesis of other two chiral titanium catalysts were performed (**Scheme 50 and 51**). We opted for these catalysts since in the case of **(*S*)-CT7** the scaffold structure is similar to (*S*)-TRIP; this bulky portion may therefore

promote the formation of one enantiomer rather than the other. On the other hand, the choice of **(*S*)-CT8** was made to evaluate how the TADOLate could influence this reaction (**Figure 48**).

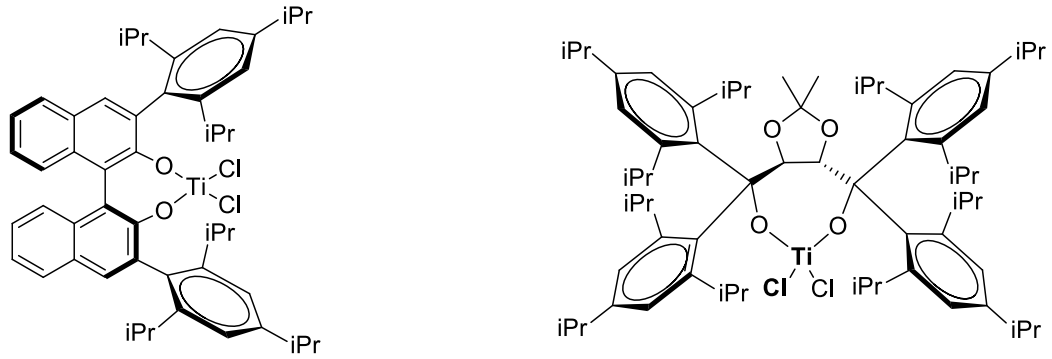

Figure 48. Structure of **(*S*)-CT7** and **(*S*,*S*)-CT8**

(*S*)-CT7 synthesis started from (*S*)-3,3'-dibromo-2,2'-bis(ethoxymethoxy)-1,1'-binaphthalene that, due to the Kumada cross-coupling, generates two carbon–carbon bonds through the reaction with the Grignard reagent. The intermediate **(*S*)-CT11** was thus deprotected by reaction with 4M HCl in dioxane at 70°C. The final compound **(*S*)-CT7** was obtained from the reaction between this intermediate and $TiCl_4$ in pentane at room temperature for 6h (**Scheme 50**).

For the synthesis of **(*S*,*S*)-CT8** we started to generate in situ the Grignard reagent from 2-bromo-1,3,5-triisopropylbenzene with magnesium tunings in THF at reflux. After 2h the mixture was cooled down to room temperature, and a solution of (4*S*,5*S*)-dimethyl 2,2-dimethyl-1,3-dioxolane-4,5-dicarboxylate in THF was added. The reaction refluxed for 12h gave the intermediate **(*S*,*S*)-CT14**. The final TADOLate was obtained at the same condition with $TiCl_4$ in pentane at room temperature for 6h (**Scheme 51**).

At this point, trials with this new catalyst and with **(*S*)-CT6** in different solvents were performed (**Table 25**).

Catalyst **(*S*)-CT6** gave better results in terms of yield and enantiomeric excess in benzene. These results highlighted the ability of the solvent to influence the enantiomeric excess in a different way depending on their polarity. Unfortunately, when we performed the reaction with **(*S*)-CT7**, we observed only the diene polymerization. This phenomenon is, in our understanding, related to the diene rather than the catalyst. We hypothesize that the fluorodiene in acid condition at room temperature tends to polymerize, and the reaction of polymerization is faster than *DA*. For this reason, it should be useful to avoid long periods under nitrogen at room temperature to create the nitrogen atmosphere before the reaction starts. Further experiments with this catalysts will be conducted in the future by Toste's group.

Last, the TADDOLate **(*S*,*S*)-CT8** gave a satisfactory yield, although the worst enantiomeric excess was recorded among the compounds tested.

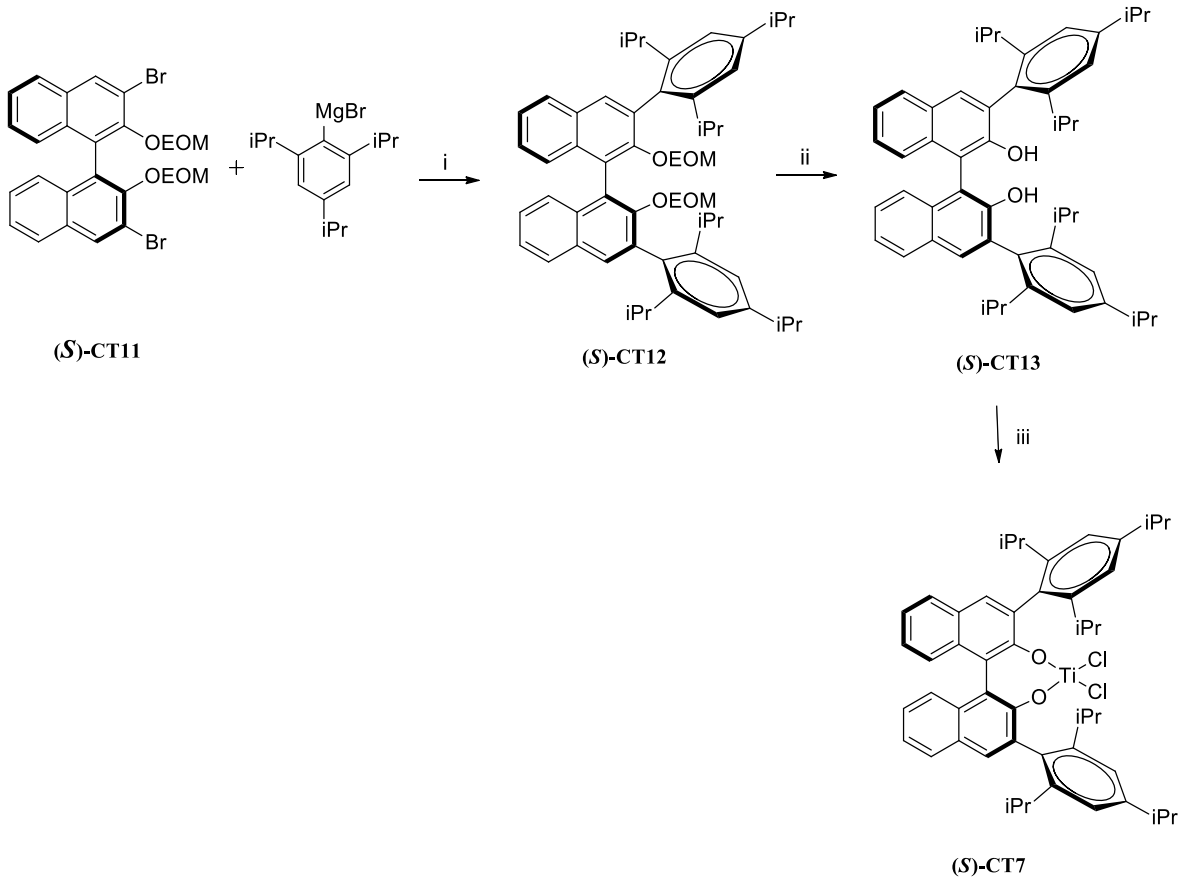

(*S*)-CT11 (*S*)-CT12 (*S*)-CT13 (*S*)-CT7

Scheme 50. Synthetic strategy for the synthesis of **(*S*)-CT7**. *Reagents and conditions: i) $Ni(PPh_3)_2Cl_2$, Et_2O, 6h, reflux; ii) HCl/dioxane (4M),70°C;iii)) $TiCl_4$, pentane, r.t.*

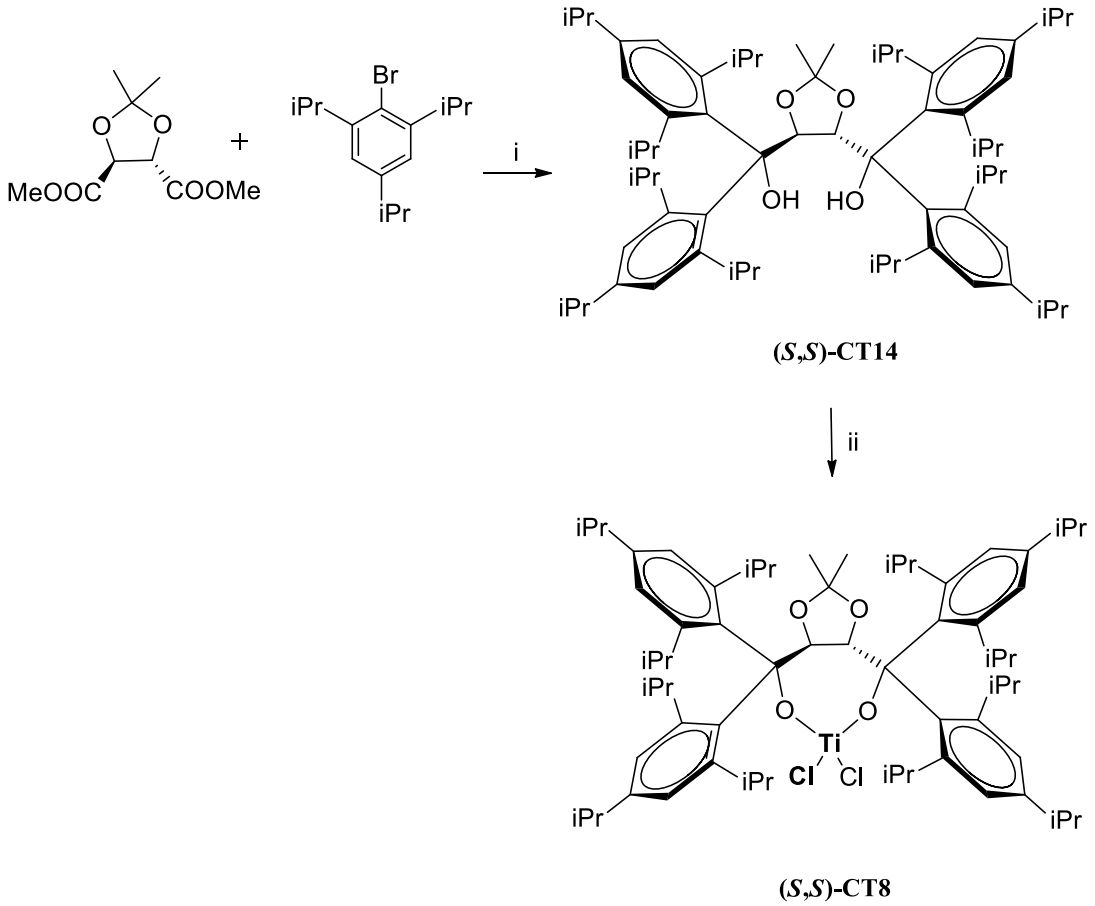

Scheme 51. Synthetic strategy for the synthesis of **(*S*,*S*)-CT8**. *Reagents and conditions: i) Mg, THF, reflux; ii) $TiCl_4$, pentane, r.t.*

Table 25. Summary of the solvent and catalyst screening.

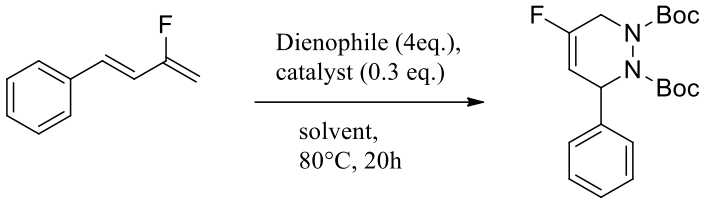

ENTRY	SOLVENT	CATALYST TYPE	YIELD (SM)	*ee* (%)
1	Toluene	**(*S*)-CT6**	80% (2)	38%
2	Benzene	**(*S*)-CT6**	93% (4)	38%
3	Dioxane	**(*S*)-CT7**	Polymerization	/
4	Toluene	**(*S*)-CT7**	Polymerization	/
5	Benzene	**(*S*)-CT7**	Polymerization	/
6	Dioxane	**(*S,S*)-CT8**	64% (5)	11%
7	Toluene	**(*S,S*)-CT8**	77% (11)	14%
8	Benzene	**(*S,S*)-CT8**	80% (10)	12%

4.5 Summary

In summary, we explored the feasibility of a new ring-opening of difluoro-cyclopropane procedure to form the corresponding flurodiene. The reaction led to high yields with different difluoro-cyclopropane types, except for tetrahydrofuran and tetrahydro-2*H*-pyran derivatives. Our trials to perform the reaction in a microwave led to yield not greater than 36% for the latter substrates. In addition, we functionalized the reaction through a new Diels-Alder reaction for flurodienes. After several trials aimed at ameliorating the reaction with the BINOL-phosphoric acids (**(*S*)-CT2**), we opted for using a titanium catalyst (**(*S*)-CT6**), which led to a yield of 93%, with an enantiomeric excess in benzene of 38%.

CONCLUSIONS

Conclusion

The research work carried out in the frame of my Ph.D. was focused on the development and the identification of new small molecules with potential application in the treatment of inflammation and cancer. Among the targets involved in these pathologies, bromodomain-containing protein 9 (BRD9), microsomal Prostaglandin E_2 Synthase-1 (mPGES-1), and soluble epoxide hydrolase (sEH) are of relevant interest, as described in **Chapters 1**. Considering their biological importance, this research project was mainly addressed to discovering new binders/inhibitors of these three biological targets.

Supported by computational approaches, nine 2,4,5-trisubstituted-2,4-dihydro-3*H*-1,2,4-triazol-3-one-based compounds (**D22**, **D25**, **D26**, **D28**, **D30**, **D31**, **D32**, **D34**, **D35**) were identified as BRD9 binders with IC_{50} in the low micromolar range and a good selectivity among the selected panel of bromodomains. Eventually, preliminary biological evaluation based on *in vitro* bioscreens disclosed compounds **D22** and **D25** endowed with a significant selectivity profile towards leukemia cells. This bioactivity data embodies a starting point for further developments to expand the collection of 2,4-dihydro-3*H*-1,2,4-triazol-3-one derivatives to identify more potent BRD9 binders. Importantly, these chemical items represent a precious starting point to the future design of PROTACs and/or SWI/SNF multi-target compounds preserving the binding to BRD9, which could likely show remarkable effects in cellular systems.

Based on the same drug design approach, quinazoline-4(3*H*)-one scaffold was also explored, synthesizing fourteen derivatives. In this case, AlphaScreen assay led us to two weak binders (**E7** and **E13**), whose structures were used as a template for synthesizing seven other derivatives.

The binding evaluation of the new derivatives against BRD9 is now ongoing. Positive results will make us investigate the selectivity of these compounds towards other bromodomains;

negative results will pave the way towards new modifications of **E7** and **E13** compounds to improve the binding with the target and reach our goal.

On the other hand, based on the *Interaction-based approach*, twenty-eight isoxazolo[2,3-*c*][1,3,5]thiadiazepin-2-one-based compounds, four 4-ethyl-benzo[*d*]thiazol-2-amine-based compounds and seven 1,8-naphthyridinone-based compounds were synthesized. After highlighting the inability of these compounds to inhibit BRD9, the *in silico*-driven repurposing disclosed a potential binding of a subset of items against estrogen receptor, soluble epoxide hydrolase (sEH), and tyrosine kinase proteins, respectively. Biophysical assays already corroborated this hypothesis for isoxazolo[2,3-*c*][1,3,5]thiadiazepin-2-one and for 4-ethyl-benzo[*d*]thiazol-2-amine-based compounds. In light of this, for the isoxazolo[2,3-*c*][1,3,5]thiadiazepin-2-one molecules, our future goal is to separate the two enantiomers of the active compounds **A17**, **A19**, **A20**, **A28**, in order to elucidate any difference in terms of activity on the estrogen receptor. Lastly, the best compounds, both in the form of pure racemic mixture and enantiomers, will be evaluated in different cell lines in which the estrogen receptor is overexpressed. Instead, among the 4-ethyl-benzo[*d*]thiazol-2-amine-based compound synthesized, after disclosing compound **B2** as a soluble epoxide hydrolase inhibitor, new potential inhibitors are being designed based on its chemical structure.

Also, the use of computational approaches allowed the discovery of new mPGES-1 inhibitors. This strategy led to the identification of the thiazolidin-4-one core as a new molecular platform for mPGES-1 modulation, yielding compounds **F1**, **F2**, **F4**, **F14**, **F22** with an inhibition percentage of around 50%. In addition, we assumed that the thiazolidin-4-one core might also represent a new template to target sEH, due to some structure analogies of the thiazolidin-4-one ring with sEH known inhibitors. Thus, the biological investigation was carried out on a group of eleven compounds among the twenty-three synthesized, disclosing compounds **F2**, **F4**, **F8** as the most promising (IC_{50}~6μM). Last, considering that dual inhibition of both

mPGES-1 and 5-LO can better resolve inflammatory/cancer disorders, we evaluated these compounds in cell-free assays on COXs and 5-LO. Thus, compound **F4** disclosed a favorable multi-target inhibitor profile, resulting in the first mPGES-1/sEH/5-LO multitarget inhibitor development. Even in this case, with the purpose to increase the activity of the compounds **F2**, **F4**, **F8**, our future perspectives are represented by the purification of each enantiomer and the evaluation of each one on the targets of the interest.

In addition, considering our effort to develop new inhibitors of arachidonic acid cascade enzymes, seven benzothiazinone-based compounds were designed and synthesized for mPGES-1 inhibition, and the biological assays are now in progress in collaboration with Prof. Oliver Werz of the University of Jena. On the other hand, we designed six libraries of molecules with the same scope, evaluated on the interest targets by computational chemistry tools. Following the generical workflow (see **Introduction**), the synthesis of the selected molecules is now in progress, and thy will be then evaluated on the arachidonic acid cascade enzymes.

Finally, given the increasing importance of both fluorinated and enantiopure compounds in medicinal chemistry, I spent the period at the University of California, Berkeley, working on the synthesis of new fluorodienes and their functionalization through new enantioselective Diels-Alder reactions.

In fact, considering that the fluorine could improve the pharmacokinetic properties compared to non fluorinate ones, and that a single enantiomer could show a better biological activity than a whole racemic mixture, new venues could be open towards the design and the synthesis of new potential anti-inflammatory and anticancer molecules.

EXPERIMENTAL SECTION

CHAPTER 5
Synthesis and biophysical assays of BRD9 designed molecules

5.1 Synthesis of isoxazole[2,3-*c*][1,3,5]thiadiazepin-2-one derivatives (A1-A28)

5.1.1 Chemistry general information

All commercially available starting materials were purchased from Sigma-Aldrich and used without purification. All solvents used for the synthesis were of HPLC grade; they were also purchased from Sigma-Aldrich. ^{1}H NMR spectra were recorded on 400 MHz or 500MHz Bruker Avance instrument. All compounds were dissolved in 0.5 mL of the following solvents: chloroform-d (Sigma-Aldrich, 99.8 Atom % D); methanol-d4 (Sigma-Aldrich, 99.8 Atom % D); DMSO-d6 (Aldrich, 99.8+ Atom% D). Coupling constants (J) are reported in Hertz, and chemical shifts are expressed in parts per million (ppm) on the delta (δ) scale relative to $CHCl_3$ (7.26 ppm for ^{1}H and 77.0 ppm for ^{13}C) or CH_3OH (3.31 ppm for 1H and 49.15 ppm for ^{13}C) or DMSO (2.50 ppm for ^{1}H and 39.52 ppm for ^{13}C) as internal reference. Multiplicities are reported as follows: s, singlet; d, doublet; t, triplet; m, multiplet; dd, doublet of doublets. ^{13}C NMR spectra were obtained at 100 MHz and referenced to the internal solvent signal. Electrospray mass spectrometry (ESMS) spectra were performed on a LCQ DECA ThermoQuest (San Josè, California, USA) mass spectrometer. Reactions were monitored on silica gel 60 F254 plates (Merck) and the spots were visualized under UV light. Analytical and semi-preparative reversed-phase HPLC was performed on Agilent Technologies 1200 Series high performance liquid chromatography using a NUCLEODUR® C8 reversed-phase column (250 × 4.60 mm, 4 μ, 80 Å, flow rate = 1 mL/min; 250 × 10.00 mm, 10 μ, 80 Å, flow rate = 4 mL/min respectively, Phenomenex®). The binary solvent system (A/B) was as follow: 0.1% TFA in water (A) and 0.1% TFA in CH_3CN (B); gradient conditions are reported for each product. The absorbance was detected at 280 nm. The purity of all tested compounds (>95%) was determined by HPLC analysis.

5.1.2 General scheme *a* of synthesis for compounds A1-A12, A16-A28.

The amino-isoxazole (1.0 equiv, 0.5 mmol) selected by docking calculation and mercaptoacetic acid (1.0 equiv, 0.5 mmol) in presence of para-toluenesulfonic acid (0.5 equiv, 0.25mmol) were stirred at reflux for 5h in dry CH_3CN (20mL). After the formation of the reaction intermediate, the aromatic aldehyde (1.0 equiv, 0.5 mmol) was added; the reaction proceeded over-night always at reflux (**Scheme 3, Chapter 2**). After cooling to room temperature, the reaction mixture was diluted with CH_2Cl_2 (20 mL) and washed with sat. $NaHCO_3$ (10 mL), brine (10mL) and 0.5N HCl (10ml). The organic lower was dried over anhydrous Na_2SO_4, filtered, and concentrated under reduced pressure to afford the crude product. The resulting residue was purified on a silica gel column chromatography in hexane/ethyl acetate. The purity of synthesized compounds was determined by HPLC. All compounds for biological testing were >95% pure.

5.1.3 General scheme *b* of synthesis for compound A13-A15 under microwave irradiation

Compounds **A13-A15** (**Scheme 2, Chapter 2**) were synthesized by microwave assisted synthesis (MW) rather than conventional heating. The amino-isoxazole(1.0 equiv, 0.5 mmol), mercaptoacetic acid (1.0 equiv, 0.5 mmol) and PTSA(0.5 equiv, 0.25mmol) were put to react at a temperature of 120°C to 200 W and pressure 300 PSI for 15 minutes under solvent-free conditions. After added aldehyde (1.0 equiv, 0.5 mmol), the reaction was carried out for 10 minutes respecting the previous parameters, diluted with CH_2Cl_2 (20 mL) ,and washed with washed with sat. $NaHCO_3$ (10 mL), brine (10mL) and 0.5N HCl (10ml).

The organic lower was dried over anhydrous Na_2SO_4, filtered, and concentrated under reduced pressure to afford the crude product. The resulting residue was purified on a silica gel column chromatography in hexane/ethyl acetate. The purity of synthesized compounds was determined by HPLC. All compounds for biological testing were >95% pure.

Synthesis of 5-(3-ethoxyphenyl)-3,5-dihydro-2*H*-isoxazolo[2,3-*c*][1,3,5]thiadiazepin-2-one (A1)

Compound **A1** was obtained following the general procedure *a*. Purification by silica gel (8:2 hexane/AcOEt) provided the product as a yellow solid (Yield: 43%).

^{1}H NMR (400 MHz, CD_3OD) δ 8.52 (d, *J* = 1.8 Hz, 1H); 7.21 (t, *J* = 7.9 Hz, 1H); 7.11 (d, *J* = 1.8 Hz, 1H); 6.82 (m, 3H); 6.35 (d, *J* = 1.2 Hz, 1H); 4.00 (m, 2H); 3.77 (d, *J* = 16.3 Hz, 2H); 1.35 (t, *J* = 6.9 Hz, 3H).

^{13}C NMR (100 MHz, DMSO-d_6) δ 171.3; 160.9; 158.7; 156.7; 142.3; 129.9; 117.3; 113.8; 111.8; 98.4; 63.1; 61.3; 31.5; 14.6.

HR-MS: *m/z* calcd for $C_{14}H_{14}N_2O_3S$ $[M+H]^+$ 291.0725, found $[M+Na]^+$ 313.0811.

Synthesis of 5-(3,4-dihydroxyphenyl)-3,5-dihydro-2*H*-isoxazolo[2,3-*c*][1,3,5]thiadiazepin-2-one (A2)

Compound **A2** was obtained following the general procedure *a*. Purification by silica gel (8:2 hexane/AcOEt) provided the product as a yellow solid (Yield: 38%).

^{1}H NMR (400 MHz, CD_3OD) δ 8.51 (d, *J* = 1.8 Hz, 1H); 7.04 (d, *J* = 1.8 Hz, 1H); 6.72 (s, 1H); 6.66 (m, 2H); 6.25 (s, 1H); 3.98 (d, *J* = 16.4 Hz, 1H); 3.76 (d, *J* = 16.3 Hz, 1H).

^{13}C NMR (100 MHz, DMSO-d_6) δ 171.6; 161.1; 157.0; 145.7; 145.6; 131.5; 117.4; 115.9; 113.4; 99.1; 62.1; 32.1.

HR-MS: *m/z* calcd for $C_{12}H_{10}N_2O_4S$ $[M+H]^+$ 279.2838, found $[M+Na]^+$ 301.2987.

Synthesis of 5-(3-hydroxy-4-nitrophenyl)-3,5-dihydro-2*H*-isoxazolo[2,3-*c*][1,3,5]thiadiazepin-2-one (A3)

Compound **A3** was obtained following the general procedure *a*. Purification by silica gel (8:2 hexane/AcOEt) provided the product as a yellow solid (Yield: 45%).

^{1}H NMR (400 MHz, DMSO-d_6) δ 8.86 (d, *J* = 1.8 Hz, 1H); 7.86 (d, *J* = 8.6 Hz, 1H); 7.14 (d, *J* = 1.6 Hz, 1H); 7.04 (s, 1H); 6.97 (dd, *J* = 8.6, 1.9 Hz, 1H); 6.45 (s, 1H); 4.09 (d, *J* = 16.4 Hz, 1H); 4.09 (d, *J* = 16.4 Hz, 1H).

^{13}C NMR (100 MHz, DMSO-d_6) δ 171.2; 161.2; 156.6; 152.3; 148.3; 136.2; 126.1; 116.3; 115.5; 98.1; 60.3; 31.4.

HR-MS: *m/z* calcd for $C_{12}H_9N_3O_5S$ $[M+H]^+$ 308.0363, found $[M+Na]^+$ 330.0694.

Synthesis of 5-(2-bromo-5-hydroxy-4-methoxyphenyl)-3,5-dihydro-2*H*-isoxazolo[2,3-*c*][1,3,5]thiadiazepin-2-one (A4)

Compound **A4** was obtained following the general procedure *a*. Purification by silica gel (6:4 hexane/AcOEt) provided the product as a brown solid (Yield: 43%).

^{1}H NMR (500 MHz, CD_3OD) δ 8.56 (d, *J* = 1.8 Hz, 1H); 8.51 (s, OH); 7.17 (d, *J* = 1.8 Hz, 1H); 7.13 (s, 1H); 6.50 (s, 2H); 3.89 (d, *J* = 16.4 Hz, 1H); 3.83 (s, 3H); 3.73 (d, *J* = 16.4 Hz, 1H).

^{13}C NMR (125 MHz, CD_3OD) δ 173.5; 161.5; 158.4; 149.9; 147.9; 132.4; 117.7; 112.9; 111.7; 99.3; 63.1; 56.9; 32.3.

HR-MS: *m/z* calcd for $C_{13}H_{11}BrN_2O_4S$ $[M+H]^+$ 372.9623, found $[M+Na]^+$ 393.0041, 395.0041.

Synthesis of 5-(3-chloro-5-fluoro-2-hydroxyphenyl)-3,5-dihydro-2*H*-isoxazolo[2,3-*c*][1,3,5]thiadiazepin-2-one (A5)

Compound **A5** was obtained following the general procedure *a*. Purification by silica gel (8:2 hexane/AcOEt) provided the product as a yellow solid (Yield: 47%).

^{1}H NMR (400 MHz, CD_3OD) δ 8.54 (d, *J* = 1.8 Hz, 1H); 7.18 (d, *J* = 1.8 Hz, 1H); 7.08 (dd, *J* = 8.1, 3.0 Hz, 1H); 6.75 (dd, *J* = 8.7, 3.0 Hz, 1H); 6.51 (s, 1H); 4.00 (dd, *J* = 16.1, 1.2 Hz, 1H); 3.73 (d, *J* = 16.2 Hz, 1H).

^{13}C NMR (100 MHz, DMSO-d_6) δ 171.4; 161.1; 156.6; 154.8 (d, *J* = 239.3 Hz); 146.5; 131.1 (d, *J* = 7.3 Hz); 121.7 (d, *J* = 11.0 Hz); 115.9 (d, *J* = 26.1 Hz); 111.2 (d, *J* = 24.2 Hz); 98.0; 57.3; 31.6.

HR-MS: *m/z* calcd for $C_{12}H_8ClFN_2O_3S$ $[M+H]^+$ 314.7199, found $[M+Na]^+$ 337.7203.

Synthesis of 5-(2-bromo-5-hydroxyphenyl)-3,5-dihydro-2*H*-isoxazolo[2,3-*c*][1,3,5]thiadiazepin-2-one (A6)

Compound **A6** was obtained following the general procedure *a*. Purification by silica gel (7:3 hexane/AcOEt) provided the product as a brown solid (Yield: 37%).

^{1}H NMR (400 MHz, CD_3OD) δ 8.55 (d, *J* = 2.0 Hz, 1H); 7.39 (d, *J* = 8.6 Hz, 1H); 7.20 (d, *J* = 1.9 Hz, 1H); 6.63 (dd, *J* = 8.5, 2.9 Hz, 1H); 6.50 (s, 1H); 6.47 (d, *J* = 2.8 Hz, 1H); 3.87 (dd, *J* = 16.1, 1.2 Hz, 1H); 3.71 (d, *J* = 16.1 Hz, 1H).

^{13}C NMR (100 MHz, CD_3OD) δ 173.5; 161.5; 158.8; 158.3; 140.9; 135.4; 117.9; 112.9; 11.7; 99.1; 63.2; 32.1.

HR-MS: *m/z* calcd for $C_{12}H_9BrN_2O_3S$ $[M+H]^+$ 339.9517, found $[M+Na]^+$ 363.0129.

Synthesis of 5-(8-hydroxyquinolin-2-yl)-3,5-dihydro-2*H*-isoxazolo[2,3-*c*][1,3,5]thiadiazepin-2-one (A7)

Compound **A7** was obtained following the general procedure *a*. Purification by silica gel (9:1 hexane/AcOEt) provided the product as an orange solid (Yield: 51%).

^{1}H NMR (400 MHz, CD_3OD) δ 8.52 (d, *J* = 1.8 Hz, 1H); 8.33 (d, *J* = 8.6 Hz, 1H); 7.89 (s, OH); 7.56 (d, *J* = 8.6 Hz, 1H); 7.46 (t, *J* = 7.9 Hz, 1H); 7.39 (dd, *J* = 8.3, 1.3 Hz, 1H); 7.23 (d,

J = 1.8 Hz, 1H); 7.14 (dd, *J* = 7.5, 1.3 Hz, 1H); 6.64 (s, 1H); 4.14 (d, *J* = 16.3Hz, 1H); 3.81 (d, *J* = 16.3 Hz, 1H).

^{13}C NMR (100 MHz, DMSO-d$_6$) δ 171.9; 161.0; 157.6; 157.1; 152.7; 137.9; 137.7; 128.4; 127.8; 118.9; 118.0; 112.2; 98.1; 62.4; 31.8.

HR-MS: *m/z* calcd for $C_{15}H_{11}N_3O_3S$ $[M-H]^-$ 312.3311, found $[M-H]^-$ 312.3208.

Synthesis of 5-(quinolin-4-yl)-3,5-dihydro-2*H*-isoxazolo[2,3-*c*][1,3,5]thiadiazepin-2-one (A8)

Compound **A8** was obtained following the general procedure *a*. Purification by silica gel (7:3 hexane/AcOEt) gave the pure product (Yield: 65%). An analytic sample of the product was obtained through purification with HPLC using CH_3CN/H_2O as eluent (From 5% to 100% in 50 minutes, flow rate 3 mL/min) (t_R = 22.5 min).

^{1}H NMR (400 MHz, CD$_3$OD) δ 9.00 (d, *J* = 5.5 Hz, 1H); 8.61 (d, *J* = 1.9 Hz, 1H); 8.46 (d, *J* = 8.5 Hz, 1H); 8.26 (d, *J* = 8.5 Hz, 1H); 8.15 (ddd, *J* = 8.4, 7.0, 1.2 Hz, 1H); 8.00 (ddd, *J* = 8.4, 6.9, 1.2 Hz, 1H); 7.68 (d, *J* = 5.5 Hz, 1H); 7.38 (s, 1H); 7.32 (d, *J* = 1.8 Hz, 1H); 4.07 (d, *J* = 16.3, Hz, 1H); 3.91 (d, *J* = 16.4 Hz, 1H).

^{13}C NMR (100 MHz, DMSO-d$_6$) δ 171.4; 161.3; 156.6; 150.1; 147.4; 145.4; 130.0; 129.3; 127.4; 124.2; 123.3; 114.9; 97.9; 57.3; 31.4.

HR-MS: *m/z* calcd for $C_{15}H_{11}N_3O_2S$ $[M+H]^+$ 298.3317, found $[M+H]^+$ 298.0483.

Synthesis of 5-(benzo[*c*][1,2,5]oxadiazol-5-yl)-8-methyl-3,5-dihydro-2*H*-isoxazolo[2,3-*c*][1,3,5]thiadiazepin-2-one (A9)

Compound **A9** was obtained following the general procedure *a*. Purification by silica gel (9:1 hexane/AcOEt) gave the pure product (Yield: 73%).

^{1}H NMR (400 MHz, CD_3OD) δ 8.41 (s, 1H), 7.90 (d, *J* = 9.4 Hz, 1H); 7.72 (s, 1H); 7.54 (dd, *J* = 9.5, 1.6 Hz, 1H); 6.86 (s, 1H); 6.47 (s, 1H); 4.06 (dd, *J* = 16.4, 1.3 Hz, 1H); 3.81 (d, *J* = 16.3 Hz, 1H); 2.36 (s, 3H).

HR-MS: *m/z* calcd for $C_{13}H_{10}N_4O_3S$ $[M+H]^+$ 303.3085, found $[M+H]^+$ 303.0949.

Synthesis of 5-(4-hydroxynaphthalen-1-yl)-8-methyl-3,5-dihydro-2*H*-isoxazolo[2,3-*c*][1,3,5]thiadiazepin-2-one (A10)

Compound **A10** was obtained following the general procedure *a*. Purification by silica gel (7:3 hexane/AcOEt) gave the pure product (Yield: 36%). An analytic sample of the product was purified by HPLC on using the gradient conditions from 5% B to 100% B over 50 min, flow rate of 4 mL/min, λ = 240 nm (t_R = 32.0 min).

^{1}H NMR (400 MHz, DMSO-d_6) δ 8.20 (d, *J* = 8.3 Hz, 1H); 8.02 (d, *J* = 8.4 Hz, 1H); 7.60 (t, *J* = 7.4 Hz, 1H); 7.52 (t, *J* = 7.6 Hz, 1H); 7.06 (s, 1H); 6.96 (d, *J* = 7.9 Hz, 1H); 6.90 (s, 1H); 6.75 (d, *J* = 7.9 Hz, 1H); 3.88 (q, *J* = 16.4 Hz, 2H); 2.36 (s, 3H).

^{13}C NMR (100 MHz, DMSO-d_6) δ 171.5; 170.5; 157.1; 143.4; 130.5; 126.7; 125.0; 124.8; 124.7; 122.8; 122.6; 121.5; 107.1; 95.4; 58.6; 31.5; 12.1.

HR-MS: *m/z* calcd for $C_{17}H_{14}N_2O_3S$ $[M+H]^+$ 327.3697, found $[M+Na]^+$ 349.0966.

Synthesis of 8-methyl-5-(quinolin-4-yl)-3,5-dihydro-2*H*-isoxazolo[2,3-*c*][1,3,5]thiadiazepin-2-one (A11)

Compound **A11** was obtained following the general procedure *a*. Purification by silica gel (7:3 hexane/AcOEt) gave the pure **A11** (Yield: 66%).

^{1}H NMR (400 MHz, CD_3OD) δ 8.74 (d, *J* = 4.8 Hz, 1H); 8.14 (d, *J* = 8.6 Hz, 1H); 8.10 (d, *J* = 8.6 Hz, 1H); 7.84 (t, *J* = 7.5 Hz, 1H); 7.73 (t, *J* = 7.6 Hz, 1H); 7.18 (d, *J* = 4.9 Hz, 1H); 7.16 (s, 1H); 6.96 (s, 1H); 3.96 (d, *J* = 16.3 Hz, 1H); 3.81 (d, J = 16.3 Hz, 1H); 2.38 (s, 3H).

^{13}C NMR (100 MHz, CD_3OD) δ 173.1; 172.5; 159.1; 151.2; 149.3; 147.9; 131.4; 130.3; 128.8; 126.4; 124.2; 116.2; 96.3; 58.9; 32.8; 12.4.

HR-MS: *m/z* calcd for $C_{16}H_{13}N_3O_2S$ $[M+H]^+$ 312.3583, found $[M+H]^+$ 312.0562.

Synthesis of 5-(3-bromo-5-fluoro-4-hydroxyphenyl)-8-methyl-3,5-dihydro-2*H*-isoxazolo[2,3-*c*][1,3,5]thiadiazepin-2-one (A12)

Compound **A12** was obtained following the general procedure *a*. Purification by silica gel (7:3 hexane/ethyl acetate) gave the pure product as a yellow solid (Yield: 72%). An analytic sample of the product was obtained through purification with HPLC using CH_3CN/H_2O as eluent (From 5% to 100% in 50 minutes, flow rate 3 mL/min) (t_R = 19.0 min).

^{1}H NMR (400 MHz, CD_3OD) δ 7.25 (s, 1H); 7.07 (d, *J* = 11.1 Hz, 1H); 6.76 (s, 1H); 6.25 (s, 1H); 4.02 (d, *J* = 16.2 Hz, 1H); 3.76 (d, *J* = 16.2 Hz, 1H); 2.36 (s, 3H).

^{13}C NMR (100 MHz, CD_3OD) δ 172.9; 172.2; 158.9; 153.0 (d, J = 243.5 Hz); 145.3 (d, J = 16.2 Hz); 134.4 (d, *J* = 6.3 Hz); 127.2; 114.1 (d, *J* = 20.9 Hz); 112.5 (d, *J* = 3.3 Hz); 96.9; 62.4; 32.9; 12.4.

HR-MS: *m/z* calcd for $C_{13}H_{10}BrFN_2O_3S$ $[M+H]^+$ 374.1975, found $[M+Na]^+$ 396.9869.

Synthesis of 5-(3-chloro-4-hydroxy-5-methoxyphenyl)-8-methyl-3,5-dihydro-2*H*-isoxazolo[2,3-*c*][1,3,5]thiadiazepin-2-one (A13)

Compound **A13** was obtained following the general procedure *b*. Purification by silica gel (DCM 100%) gave the pure compound (Yield: 66%). An analytic sample of the product was obtained through purification with HPLC using CH_3CN/H_2O as eluent (From 5% to 100% in 50 minutes, flow rate 3 mL/min) (t_R = 22.0 min).

^{1}H NMR (400 MHz, CD_3OD) δ 6.84 (d, *J* = 2.1 Hz, 1H); 6.82 (d, *J* = 2.0 Hz, 1H); 6.74 (s, 1H); 6.26 (s, 1H); 4.01 (dd, *J* = 16.3, 1.2 Hz, 1H); 3.84 (s, 3H); 3.76 (d, *J* = 16.3 Hz, 1H); 2.36 (s, 3H).

^{13}C NMR (100 MHz, CD_3OD) δ 173.0; 172.1; 159.0; 150.3; 144.6; 133.2; 121.4; 120.3; 109.3; 97.1; 63.3; 56.9; 33.0; 12.4.

HR-MS: *m/z* calcd for $C_{14}H_{13}ClN_2O_4S$ $[M+H]^+$ 341.7820, found $[M+Na]^+$ 363.0972.

Synthesis of 5-(3,5-dibromo-4-hydroxyphenyl)-8-methyl-3,5-dihydro-2*H*-isoxazolo[2,3-*c*][1,3,5]thiadiazepin-2-one (A14)

Compound **A14** was obtained following the general procedure *b*. Purification by silica gel (4:6 hexane/DCM) gave the pure product as a brown solid (Yield: 32%). An analytic sample of the product was obtained through purification with HPLC using CH_3CN/H_2O as eluent (From 5% to 100% in 50 minutes, flow rate 3 mL/min) (t_R = 26.0 min).

^{1}H NMR (400 MHz, CD_3OD) δ 7.44 (s, 2H); 6.76 (s, 1H); 6.24 (s, 1H); 4.03 (dd, *J* = 16.4, 1.2 Hz, 1H); 3.77 (d, *J* = 16.4 Hz, 1H); 2.37 (s, 3H).

^{13}C NMR (100 MHz, CD_3OD) δ 172.8; 172.2; 158.9: 136.0; 131.3 (2 C); 129.6; 112.3 (2 C); 96.9; 62.1; 32.9; 12.4.

HR-MS: *m/z* calcd for $C_{13}H_{10}Br_2N_2O_3S$ $[M+H]^+$ 433.1031, found $[M+Na]^+$ 456.9094.

Synthesis of 5-(3,4-dihydroxyphenyl)-8-methyl-3,5-dihydro-2*H*-isoxazolo[2,3-*c*][1,3,5]thiadiazepin-2-one (A15)

Compound **A15** was obtained following the general procedure *b*. Purification by silica gel (7:3 hexane/ethyl acetate) gave the pure product as a yellow solid (Yield: 70%). An analytic sample of the product was obtained through purification with HPLC using CH_3CN/H_2O as eluent (From 5% to 100% in 50 minutes, flow rate 3 mL/min) (t_R = 17.0 min).

^{1}H NMR (400 MHz, DMSO-d_6) δ 6.76 (s, 1H); 6.68 (d, *J* = 2.1 Hz, 1H); 6.64 (d, *J* = 8.1 Hz, 1H); 6.57 (dd, J = 8.2, 2.1 Hz, 1H); 6.22 (s, 1H); 4.00 (d, *J* = 16.3 Hz, 1H); 3.81 (d, *J* = 16.4 Hz, 1H); 2.35 (s, 3H).

^{13}C NMR (100 MHz, DMSO-d_6) δ 170.6; 169.9; 156.7; 145.0; 144.8; 130.9; 116.4; 115.0; 112.6; 95.4; 60.9; 31.2; 11.7.

HR-MS: *m/z* calcd for $C_{13}H_{12}N_2O_4S$ $[M+H]^+$ 293.3103, found$[M+Na]^+$ 315.0548.

Synthesis of 8,9-dimethyl-5-(quinolin-4-yl)-3,5-dihydro-2*H*-isoxazolo[2,3-*c*][1,3,5]thiadiazepin-2-one (A16)

Compound **A16** was obtained following the general procedure *a*. Purification by silica gel (7:3 hexane/ethyl acetate) gave the pure product as a yellow solid (Yield: 73%). An analytic sample of the product was obtained through purification with HPLC using CH_3CN/H_2O as eluent (From 5% to 100% in 50 minutes, flow rate 3 mL/min) (t_R = 23.0 min).

^{1}H NMR (400 MHz, CD_3OD) δ 9.10 (d, *J* = 5.6 Hz, 1H); 8.45 (d, *J* = 8.6 Hz, 1H); 8.24 (d, *J* = 8.7 Hz, 1H); 8.14 (t, *J* = 7.5 Hz, 1H); 7.99 (d, *J* = 7.8 Hz, 1H); 7.96 (d, *J* = 5.8 Hz, 1H); 7.30 (s, 1H); 4.07 (dd, *J* = 16.3, 1.2 Hz, 1H); 3.96 (d, *J* = 16.2 Hz, 1H); 2.28 (s, 3H); 2.04 (s, 3H).

^{13}C NMR (100 MHz, CD_3OD) δ 173.1; 169.5; 159.9; 148.8; 133.9; 130.3; 126.8; 126.6; 124.8; 121.5; 121.1; 118.7; 108.8; 60.4; 33.0; 11.0; 8.0.

HR-MS: *m/z* calcd for $C_{17}H_{15}N_3O_2S$ $[M+H]^+$ 326.3849, found$[M+H]^+$ 326.1799.

Synthesis of 5-(3-chloro-5-fluoro-2-hydroxyphenyl)-8-phenyl-3,5-dihydro-2*H*-isoxazolo[2,3-*c*][1,3,5]thiadiazepin-2-one (A17)

Compound **A17** was obtained following the general procedure *a*. Purification by silica gel (8:2 hexane/ethyl acetate) gave the pure product as a white solid (Yield: 46%).

^{1}H NMR (400 MHz, $CDCl_3$) δ 7.69 (dd, *J* = 6.7, 3.0 Hz, 2H); 7.38 (m, 4H); 6.98 (dd, *J* = 7.6, 2.9 Hz, 1H); 6.73 (dd, *J* = 8.5, 2.9 Hz, 1H); 6.49 (s, 1H); 3.93 (d, *J* = 16.2 Hz, 1H); 3.68 (d, *J* = 16.2 Hz, 1H).

^{13}C NMR (100 MHz, $CDCl_3$) δ 171.2; 170.6; 157.6; 155.9 (d, *J* = 243.4 Hz); 145.1; 130.6; 129.0 (2 C); 128.8; 126.9 (2 C); 121.4 (d, *J* = 10.9 Hz); 116.1 (d, *J* = 26.3 Hz); 111.8 (d, *J* = 24.2 Hz); 92.8; 57.7; 32.5.

HR-MS: *m/z* calcd for $C_{18}H_{12}ClFN_2O_3S$ $[M+H]^+$ 391.8159; found$[M+Na]^+$ 413.8607.

Synthesis of 5-(3-hydroxy-4-nitrophenyl)-8-phenyl-3,5-dihydro-2*H*-isoxazolo[2,3-*c*][1,3,5]thiadiazepin-2-one (A18)

Compound **A18** was obtained following the general procedure *a*. Purification by silica gel (7:3 hexane/ethyl acetate) gave the pure product as a white solid (Yield: 57%).

^{1}H NMR (400 MHz, $CDCl_3$) δ 10.54 (s, 1H); 8.02 (d, *J* = 8.7 Hz, 1H); 7.66 (m, 2H); 7.36 (m, 3H); 7.32 (s, 1H); 6.98 (d, *J* = 1.8 Hz, 1H); 6.85 (d, *J* = 8.7 Hz, 1H); 6.25 (s, 1H); 3.91 (d, *J* = 16.3 Hz, 1H); 3.70 (d, *J* = 16.3 Hz, 1H).

^{13}C NMR (100 MHz, $CDCl_3$) δ 170.7; 170.5; 157.6; 155.5; 150.7; 133.2; 130.6; 128.9 (2 C); 126.8; 126.2; 125.7 (2 C); 117.1; 116.2; 92.8; 60.8; 32.2.

HR-MS: *m/z* calcd for $C_{18}H_{13}N_3O_5S$ $[M - H]^-$ 383.3779, found$[M - H]^-$ 382.0685.

Synthesis of 5-(3-chloro-2-hydroxyphenyl)-8-phenyl-3,5-dihydro-2*H*-isoxazolo[2,3-*c*][1,3,5]thiadiazepin-2-one (A19)

Compound **A19** was obtained following the general procedure *a*. Purification by silica gel (8:2 hexane/ethyl acetate) gave the pure product as a white solid (Yield: 45%). An analytic sample of the product was obtained through purification with HPLC using CH_3CN/H_2O as eluent (From 5% to 100% in 50 minutes, flow rate 3 mL/min) (t_R = 32.5 min).

^{1}H NMR (400 MHz, CD_3OD) δ 7.81 (m, 2H); 7.48 (m, 4H); 7.21 (d, *J* = 8.0 Hz, 1H); 7.12 (s, 1H); 6.83 (t, *J* = 7.9 Hz, 1H); 5.78 (s, 1H); 3.47 (dd, *J* = 23.4, 15.4 Hz, 2H).

^{13}C NMR (100 MHz, DMSO-d_6) δ 170.8; 168.7; 158.5; 149.8; 130.6; 129.3 (2 C); 129.1; 128.4; 126.8; 126.6; 125.5 (2 C); 121.0; 120.3; 94.4; 47.4; 35.5.

HR-MS: *m/z* calcd for $C_{18}H_{13}ClN_2O_3S$ $[M+H]^+$ 373.8256; found$[M+Na]^+$ 395.2074.

Synthesis of 5-(2-isopropyl-2,5-dihydrooxazol-4-yl)-8-phenyl-3,5-dihydro-2*H*-isoxazolo[2,3-*c*][1,3,5]thiadiazepin-2-one (A20)

Compound **A20** was obtained following the general procedure *a*. Purification by silica gel (9:1 hexane/ethyl acetate) gave the pure product as a yellow solid (Yield: 72%).

^{1}H NMR (400 MHz, $CDCl_3$) δ 7.68 (m, 2H); 7.60 (d, *J* = 0.8 Hz, 1H); 7.37 (m, 3 H); 7.16 (s, 1H); 5.42 (d, *J* = 0.8 Hz, 1H); 3.65 (d, *J* = 15.5 Hz, 1H); 3.32 (d, *J* = 15.7 Hz, 1H); 2.98 (hept, *J* = 7.0 Hz, 1H); 1.20 (d, *J* = 7.0 Hz, 3H); 1.19 (d, *J* = 7.0 Hz, 3H).

^{13}C NMR (100 MHz, $CDCl_3$) δ 173.3; 170.4; 170.1; 167.7; 158.0; 137.9; 136.1; 130.5; 128.9 (2 C); 127.0; 125.5 (2 C); 94.0; 45.9; 33.5; 28.5; 19.9 (2 C).

HR-MS: *m/z* calcd for $C_{18}H_{19}N_3O_3S$ $[M+H]^+$ 357.4268; found$[M+Na]^+$ 379.4211.

Synthesis of 5-(2-fluoro-4-methoxyphenyl)-8-phenyl-3,5-dihydro-2*H*-isoxazolo[2,3-*c*][1,3,5]thiadiazepin-2-one (A21)

Compound **A21** was obtained following the general procedure *a*. Purification by silica gel (9:1 hexane/ethyl acetate) gave the pure product as yellow solid (Yield: 52%).

^{1}H NMR (400 MHz, $CDCl_3$) δ 7.69 (m, 2H); 7.37 (m, 2H); 7,18 (s, 1H); 6.95 (t, *J* = 9.5 Hz, 1H); 6.70 (m, 1H); 6.70 (m, 1H); 6.61 (dd, *J* = 6.1, 3.0 Hz, 1H); 6.46 (s, 1H); 3.95 (d, *J* = 16.1 Hz, 1H); 3.66 (s, 3H); 3.65 (d, *J* = 16.1 Hz, 1H).

^{13}C NMR (100 MHz, $CDCl_3$) δ 171.1; 170.4; 157.7; 155.7; 154.3 (d, *J* = 240.9 Hz); 130.5; 128.9 (2 C); 128.2 (d, *J* = 13.5 Hz); 127.1; 125.7 (2 C); 116.8 (d, *J* = 22.8 Hz); 114.1 (d, *J* = 8.2 Hz); 112.1 (d, *J* = 2.9 Hz); 92.9; 57.2; 55.7; 32.4.

HR-MS: *m/z* calcd for $C_{19}H_{15}FN_2O_3S$ $[M + H]^+$ 370.3974; found$[M+Na]^+$ 393.2000.

Synthesis of 5-(3,4-dihydroxyphenyl)-8-phenyl-3,5-dihydro-2*H*-isoxazolo[2,3-*c*][1,3,5]thiadiazepin-2-one (A22)

Compound **A22** was obtained following the general procedure *a*. Purification by silica gel (6:4 hexane/ethyl acetate) gave the pure product as a yellow solid (Yield: 35%). An analytic sample of the product was obtained through purification with HPLC using CH_3CN/H_2O as eluent (From 5% to 100% in 50 minutes, flow rate 3 mL/min) (t_R = 23.0min).

^{1}H NMR (400 MHz, CD_3OD) δ 7.78 (m, 2 H); 7.47 (m, 3 H); 7.34 (s, 1H); 6.77 (d, *J* = 2.1 Hz, 1H); 6.69 (m, 2 H); 6.29 (s, 1H); 4.00 (d, *J* = 16.3 Hz, 1H); 3.78 (d, *J* = 16.3 Hz, 1H).

^{13}C NMR (100 MHz, , CD_3OD) δ 177.0, 156.7, 146.9, 145.3, 144.6, 131.7, 129.9, 128.6, 128.5(2C), 127.8(2C), 120.0, 116.0, 115.4, 97.7, 64.1, 34.8.

HR-MS: *m/z* calcd for $C_{18}H_{14}N_2O_4S$ $[M + H]^+$ 355.3798; found $[M-H]^+$ 355,3780.

Synthesis of 5-(3,5-difluoro-2-hydroxyphenyl)-8-phenyl-3,5-dihydro-2*H*-isoxazolo[2,3-*c*][1,3,5]thiadiazepin-2-one (A23)

Compound **A23** was obtained following the general procedure *a*. Purification by silica gel (7:3 hexane/ethyl acetate) gave the pure product as a yellow solid (Yield: 84%). An analytic sample of the product was obtained through purification with HPLC using CH_3CN/H_2O as eluent (From 5% to 100% in 50 minutes, flow rate 3 mL/min) (t_R = 28.2 min).

^{1}H NMR (400 MHz, CD_3OD) δ 7.81 (d, *J* = 7.0 Hz, 2H); 7.48 (m, 3H); 7.15 (s, 1H); 7.07 (d, *J* = 8.9 Hz, 1H); 6.83 (m, 1H); 5.78 (s, 1H); 3.64 (d, *J* = 15.1 Hz, 1H); 3.32 (d, *J* = 15.1 Hz, 1H).

^{13}C NMR (100 MHz, CD_3OD) δ 171.2; 170.1: 159.9; 156.5 (dd, *J* = 238.9, 11.6 Hz); 152.7 (dd, *J* = 242.1, 12.5 Hz); 140.2 (d, *J* = 15.0 Hz); 131.7; 130.9 (m); 130.3 (2 C); 128.8; 126.8 (2 C); 110.9 (d, *J* = 26.8 Hz); 104.7 (dd, *J* = 27.0, 23.7 Hz); 95.3; 47.9; 37.3.

HR-MS: *m/z* calcd for $C_{18}H_{12}F_2N_2O_3S$ $[M + H]^+$ 374.0578; found $[M-H]^+$ 373.0588.

Synthesis of 5-(4-fluorophenyl)-8-phenyl-3,5-dihydro-2*H*-isoxazolo[2,3-*c*][1,3,5]thiadiazepin-2-one (A24)

Compound **A24** was obtained following the general procedure *a*. Purification by silica gel (6:4 hexane/ethyl acetate) gave the pure product as a white solid (Yield: 60%).

^{1}H NMR (400 MHz, $CDCl_3$) δ 7.67 (m, 2H); 7.67 (m, 3H); 7.30 (s, 1H); 7.26 (dd, *J* = 8.6, 5.2 Hz, 2H); 6.97 (t, *J* = 8.6 Hz, 2H); 6.31 (s, 1H); 3.94 (d, *J* = 16.3 Hz, 1H); 3.71 (d, *J* = 16.3 Hz, 1H).

^{13}C NMR (100 MHz, $CDCl_3$) δ 170.8; 170.4; 162.6 (d, *J* = 248.0 Hz); 157.7; 135.9; 130.5; 128.96 (2 C); 127.6 (d, *J* = 8.4 Hz, 2 C); 127.1; 125.7 (2 C); 115.9 (d, *J* = 22.0 Hz, 2 C); 93.2; 61.7; 32.5.

HR-MS: *m/z* for $C_{18}H_{13}FN_2O_2S$ $[M+ H]^+$ 340.07; found $[M+Na]^+$ 363.1671.

Synthesis of 5-(4-chlorophenyl)-8-phenyl-3,5-dihydro-2*H*-isoxazolo[2,3-*c*][1,3,5]thiadiazepin-2-one (A25)

Compound **A25** was obtained following the general procedure *a*. Purification by silica gel (6:4 hexane/ethyl acetate) gave the pure product as a white solid (Yield: 62%).

^{1}H NMR (400 MHz, $CDCl_3$) δ 7.67 (m, 2H); 7.37 (m, 3H); 7.30 (s, 1H); 7.25 (d, *J* = 8.6 Hz, 2H); 7.20 (d, *J* = 8.6 Hz, 2H); 6.29 (s, 1H); 3.92 (d, *J* = 16.3 Hz, 1H); 3.71 (d, *J* = 16.3 Hz, 1H).

^{13}C NMR (100 MHz, $CDCl_3$) δ 170.8; 170.4; 157.7; 138.8; 134.5; 130.5; 129.2 (2 C); 128.9 (2 C); 127.0 (2 C); 125.7 (2 C); 119.9; 93.1; 61.6; 32.5.

HR-MS: *m/z* calcd for $C_{18}H_{13}ClN_2O_2S$ $[M+H]^+$ 356.0682; found $[M+Na]^+$ 379.1979.

Synthesis of 5-(4-bromophenyl)-8-phenyl-3,5-dihydro-2*H*-isoxazolo[2,3-*c*][1,3,5]thiadiazepin-2-one (A26)

Compound **A26** was obtained following the general procedure *a*. Purification by silica gel (7:3 hexane/ethyl acetate) gave the pure product as a white solid (Yield: 74%).

^{1}H NMR (400 MHz, $CDCl_3$) δ 7.72 (m, 2H); 7.46 (m, 3H); 7.30 (s, 1H); 7.48 (d, *J* = 8.5 Hz, 2H); 7.30 (d, *J* = 8.5 Hz, 2H); 6.39 (s, 1H); 3.92 (d, *J* = 16.3 Hz, 1H); 3.71 (d, *J* = 16.3 Hz, 1H).

^{13}C NMR (100 MHz, $CDCl_3$) δ 170.8; 170.0; 156.7; 135.5; 131.8 (2 C); 131.0; 129.9, 129.1 (2 C); 128.8 (2C); 127.8 (2C); 121.8, 97.7; 64.2; 34.8.

HR-MS: *m/z* calcd for $C_{18}H_{13}BrN_2O_2S$ $[M+H]^+$ 400.8891; found $[M+H]^+$ 400.8888.

Synthesis of 5-(2-bromo-5-hydroxy-4-methoxyphenyl)-8-phenyl-3,5-dihydro-2*H*-isoxazolo[2,3-*c*][1,3,5]thiadiazepin-2-one (A27)

Compound **A27** was obtained following the general procedure *a*. Purification by silica gel (7:3 hexane/ethyl acetate) gave the pure product as a white solid (Yield: 47%). An analytic sample of the product was obtained through purification with HPLC using CH_3CN/H_2O as eluent (From 5% to 100% in 50 minutes, flow rate 3 mL/min) (t_R = 37.3 min).

^{1}H NMR (400 MHz, $CDCl_3$) δ 7.69 (m, 2H); 7.27 (m, 4 H); 7.19 (s, 1H); 7.01 (s, 1H); 6.58 (s, 1H); 6.52 (s, OH); 3.83 (d, *J* = 16.3 Hz, 1H); 3.81 (s, 3H); 3.62 (d, *J* = 16.3 Hz, 1H).

^{13}C NMR (100 MHz, $CDCl_3$) δ 171.4; 171.5; 157.6; 146.9; 145.4; 131.4; 130.4; 128.9 (2 C); 127.1; 125.7 (2 C); 115.8; 111.3; 110.7; 92.9; 61.7; 56.3; 31.8.

HR-MS: *m/z* calcd for $C_{19}H_{15}BrN_2O_4S$ $[M + H]^+$ 447.9936; found $[M+Na]^+$ 469.1575.

Synthesis of 5-(2-chloro-3-hydroxyphenyl)-8-phenyl-3,5-dihydro-2*H*-isoxazolo[2,3-*c*][1,3,5]thiadiazepin-2-one (A28)

Compound **A28** was obtained following the general procedure *a*. Purification by silica gel (6:4 hexane/ethyl acetate) gave the pure product as a white solid (Yield: 57%). An analytic sample of the product was obtained through purification with HPLC using CH_3CN/H_2O as eluent (From 5% to 100% in 50 minutes, flow rate 3 mL/min) (t_R = 38.0 min).

^{1}H NMR (400 MHz, $CDCl_3$) δ 7.69 (m, 2H); 7.38 (m, 4H); 7.19 (s, 1H); 7.05 (t, *J* = 8.0 Hz, 1H); 6.92 (d, *J* = 8.2 Hz, 1H); 6.57 (s, 1H); 3.82 (d, *J* = 16.3 Hz, 1H); 3.64 (d, *J* = 16.3 Hz, 1H).

^{13}C NMR (100 MHz, $CDCl_3$) δ 171.4; 170.6; 157.6; 152.3; 137.6; 130.5; 128.9 (2 C); 128.1; 127.0; 125.7; 118.0; 116.2; 116.1; 92.7; 59.6; 31.7.

HR-MS: *m/z* calcd for $C_{17}H_{13}ClN_2O_3S$ $[M+H]^+$373.8254; found $[M+Na]^+$ 395.1634.

5.2 Synthesis of 4-ethylbenzothiazole molecules

5.2.1 Chemistry general information

Chemicals were purchased from Aldrich Chemicals (Milan, Italy) and used without further purification. Reactions and purity of products were estimated by TLC, using precoated silica gel glass plates 60 F254 plates (Merck), and the spots were visualized under UV light. Preparative separations were performed by silica gel, analytical and semi-preparative purifications were carried out by reversed-phase HPLC on Agilent Technologies 1200 Series

high performance liquid chromatography using a Synergi Fusion C18 reversed-phase column (250 x 4.60mm, 4µ, 80 Å, flow rate = 1 mL/min; 250 x 10.00mm, 10µ, 80 Å, flow rate = 4 mL/min respectively, Phenomenex®). The binary solvent system (A/B) was as follows: 0.1% TFA in water (A) and 0.1% TFA in CH_3CN (B); gradient condition: from 5% B to 100 % B in 50 min. The absorbance was detected at 280 nm. All tested compounds were obtained with high purity (> 98% detected by HPLC analysis) and were fully characterized by HRMS, and NMR spectra.

NMR spectra (^1H, ^{13}C) were recorded using a Bruker Avance DRX400 at T=298K. The compounds were dissolved in 0.5 mL of d-$CHCl_3$ (Aldrich, 99.8+ Atom% D). Coupling constants (*J*) are reported in Hertz, and chemical shifts are expressed in parts per million (ppm) on the delta (δ) scale relative to $CDCl_3$ (7.16 ppm for ^1H and 77.20 ppm for ^{13}C) as internal reference. Multiplicities are reported as follows: s, singlet; d, doublet; t, triplet; m, multiplet; dd, doublet of doublets. ^{13}C NMR spectra were obtained at 100 MHz and referenced to the internal solvent signal. DEPTQ experiments (deptpolarization transfer with decoupling during acquisition using shaped pulse for 180 degree pulse onf1channel) were acquired at 100 MHz. Mass spectra (MS) were recorded on Q-Tof Premier Mass Spectrometer, using electrospray ionization (ESI).

5.2.2 General procedure *c* for the synthesis of compound B1

6-bromo-4-ethylbenzo[*d*]thiazol-2-amine (1.0 equiv, 1.94 mmol), (3,5-dimethylisoxazol-4-yl)boronic acid (1.5 equiv, 2.92 mmol), K_2CO_3 (3.0 equiv, 5.83 mmol) and tetrakis(triphenylphosphine)palladium(0) (0.2 equiv, 0.39 mmol) were dissolved in a previous degassed mixture of 1,4-dioxane (80%) and water (20%) (20 mL) and stirred over-night at 80 °C under argon atmosphere (**Scheme 6**, **Chapter 2**). After the completion of the reaction, the mixture was diluted with dichloromethane and washed with brine (3x10mL). The organic lower

was dried over anhydrous Na_2SO_4, filtered and concentrated under reduced pressure to afford the crude product.

5.2.3 General procedure *d* for the synthesis of compounds B2-B3

To a solution of 6-(3,5-dimethylisoxazol-4-yl)-4-ethylbenzo[*d*]thiazol-2-amine (1.0 equiv, 0.18 mmol) in dry acetonitrile (10 mL), pyridine was added (30.0 equiv, 5.4 mmol). After 10 minutes, the proper acyl chloride was added (1.5 equiv, 0.27mmol), the reaction mixture was stirred overnight at room temperature (**Scheme 6**, **Chapter 2**). The mixture was diluted with dichloromethane, washed with 0.5 N HCl (10 mL x 3) and brine (10 mL), and dried (Na_2SO_4). The solvent was removed under reduced pressure and the residue was purified on a silica gel column chromatography in hexane/ethyl acetate, followed by semi-preparative reversed-phase HPLC. Yields are reported below for each compound.

Synthesis of 6-(3,5-dimethylisoxazol-4-yl)-4-ethylbenzo[*d*]thiazol-2-amine (B1)

Compound **B1** was obtained following the general procedure *c*. The resulting residue was purified on a silica gel column chromatography eluting with a 65:35 hexane/ethyl acetate mixture to give the final product (Yield: 78%).

^{1}H NMR (400 MHz, CDCl3) δ 7.24 (d, *J* = 1.9 Hz, 1 H); 6.97 (d, *J* = 1.9 Hz, 1 H); 2.92 (q, *J* = 7.6 Hz, 2 H); 2.34 (s, 3 H); 2.20 (s, 3 H); 1.28 (t, *J* = 7.6 Hz, 3 H).

^{13}C NMR (100 MHz, CDCl3) δ 165.6, 165.1, 159.0, 149.5 135.3, 131.8, 126.4, 124.6, 118.9, 116.7, 25.4, 14.2, 11.7, 11,0. **HR-MS:** *m/z* calcd for $C_{14}H_{15}N_3OS$ $[M+H]^+$ 274.35, $[M+H]^+$ found 274.06.

Synthesis of N-(6-(3,5-dimethylisoxazol-4-yl)-4-ethylbenzo[*d*]thiazol-2-yl)-3-fluorobenzamide (B2)

Compound **B2** was obtained following the general procedure *d* Purification by silica gel (9:1 hexane/ ethyl acetate) gave compound **B2** (Yield: 62%). An analytic sample of **B2** was further purified by HPLC, gradient condition from 5% B to 100 % B in 50 min (t_R = 35.0 min).

^{1}H NMR (400 MHz, CDCl3) δ 7.75 (d, *J* = 7.3 Hz, 1H); 7.64 (d, *J* = 7.3 Hz, 1H); 7.46 (m, 1H); 7.25 (m, 2H); 7.05 (s, 1H); 2.77 (m, 2H); 2.36 (s, 3H); 2.22 (s, 3H); 1.28 (t, *J* = 7.2Hz, 3H).

^{13}C NMR (100 MHz, $CDCl_3$) δ 167.9 (d, *J*=248.4Hz), 167.6, 163.7, 158.7, 158.5,133.4,130.6, 128.4, 127.8, 127.6, 127.3, 125.0, 122.5, 120.5,119.9(d, *J*=19.8Hz), 116.0. 114.1 (d, *J*=22.4Hz), 24.7, 13.9, 11.8, 10.9.

HR-MS: *m/z* calcd for $C_{21}H_{18}FN_3O_2S$ $[M+H]^+$ 396.11, $[M+H]^+$ found 396.04.

Synthesis of 4-chloro-N-(6-(3,5-dimethylisoxazol-4-yl)-4-ethylbenzo[*d*]thiazol-2-yl)butanamide (B3)

Compound **B3** was obtained following the general procedure *d*. Purification by silica gel (8:2 hexane/ ethyl acetate) gave the pure product (Yield: 50%). An analytic sample of **B3** was further purified by HPLC, gradient condition from 5% B to 100 % B in 50 min (t_R = 39.0 min).

^{1}H NMR (400 MHz, CDCl3) δ 7.49 (s, 1H); 7.19 (s, 1H); 3.64 (t, *J* = 6.3 Hz, 2H); 3.04 (q, *J* = 7.5 Hz, 2H); 2.82 (t, *J* = 7.0 Hz, 2H); 2.39 (s, 3H); 2.24 (m, 5H); 1.32 (t, *J* = 7.5 Hz, 3H).

^{13}C NMR (100 MHz, CDCl3) δ 171.6; 165.6; 161.4; 158.4; 138.6; 135.1; 129.2, 128.7; 128.4; 128.2; 119.6; 43.6; 33.1; 27.1; 24.9; 14.5; 11.6; 10.8.

HR-MS: *m/z* calcd for $C_{18}H_{20}ClN_3O_2S$ $[M+H]^+$ 378.89, $[M+H]^+$ found 378.08.

5.2.4 General procedure *e* for the synthesis of compounds B4-B5

To a solution of 6-(3,5-dimethylisoxazol-4-yl)-4-ethylbenzo[d]thiazol-2-amine (1.0 equiv, 0.18 mmol) in dry acetonitrile (10 mL), pyridine was added (30.0 equiv, 5.4 mmol). After 10 minutes, the sulfonyl chloride was added (1.5 equiv, 0.27mmol), and the reaction mixture was stirred overnight at reflux (**Scheme 6**, **Chapter 2**). The mixture was diluted with dichloromethane, washed with 0.5N HCl (10 mL x 3) and brine (10 mL), and dried (Na_2SO_4). The solvent was removed under reduced pressure, and the residue was purified on a silica gel column chromatography in hexane/ethyl acetate and then on semi-preparative reversed-phase HPLC. Yields are reported below for each compound.

Synthesis of N-(6-(3,5-dimethylisoxazol-4-yl)-4-ethylbenzo[*d*]thiazol-2-yl)-2,4,6-trifluorobenzenesulfonamide (B4)

Compound **B4** was obtained following the general procedure *e*. Purification by silica gel (8:2 hexane/ ethyl acetate) gave compound **B4** (Yield: 69%). An analytic sample of **B4** was further purified by HPLC gradient condition from 5% B to 100 % B in 50 min (t_R = 35.0 min).

^{1}H NMR (400 MHz, CDCl3) δ 7.23 (s, 1H); 7.05 (s, 1H); 6.69 (t, *J* = 8.8 Hz, 2H); 2.80 (q, *J* = 7.6 Hz, 2H); 2.35 (s, 3H); 2.21 (s, 3H); 1.30 (t, *J* = 7.5 Hz, 3H).

^{13}C NMR (100 MHz, CDCl3) δ 168.8; 166.2(t, *J* = 24.0 Hz); 165.7, 164.7 (dt, *J* = 254.0, 14.4 Hz); 161.9 (dd, *J* = 259.4, 15.4 Hz); 159.6(ddd, *J* = 259.4, 15.4 Hz); 158.5, 133.4; 129.1; 127.7; 127.4; 124.9; 120.2; 115.7; 101.9 (dt, *J* = 26.5, 3.6 Hz, 2 C); 24.4; 13.7; 11.5; 10.7.

HR-MS: *m/z* calcd for $C_{20}H_{16}F_3N_3O_3S_2$ $[M+H]^+$ 468.06, $[M+H]^+$ found 468.03.

Synthesis of 5-chloro-N-(6-(3,5-dimethylisoxazol-4-yl)-4-ethylbenzo[*d*]thiazol-2-yl)thiophene-2-sulfonamide (B5)

Compound **B5** was obtained following the general procedure *e*. Purification by silica gel (9:1 hexane/ ethyl acetate) gave the pure compound **B5** (Yield: 72%).

^{1}H NMR (400 MHz, $CDCl_3$) δ 7.45 (d, *J* = 4.0 Hz, 1H); 7.23 (s, 1H); 7.03 (s, 1H); 6.84(d, *J* = 4.0 Hz, 1H); 2.79 (q, *J* = 7.5 Hz, 2H); 2.35 (s, 3H); 2.20 (s, 3H); 1.30 (t, *J* = 7.5 Hz, 3H)

^{13}C NMR (100 MHz, $CDCl_3$) δ 168.2; 165.7; 158.6; 145.4; 144.8; 141.3, 133.2; 130.6; 128.9; 127.7; 127.3; 126.4; 125.1; 120.3; 24.4; 13.7; 11.5; 10.7.

HR-MS: *m/z* calcd for $C_{18}H_{16}ClN_3O_3S_3$ [M+H]+ 454.00, [M+H]+ found 454.05.

5.3 Synthesis of 1,8-naphthyridone molecules

5.3.1 Chemistry general information

All commercially available starting materials were purchased from SigmaAldrich and were used as received. Solvents used for the synthesis were of HPLC grade and were purchased from Sigma-Aldrich or Fluorochem. NMR spectra were recorded on Bruker Avance 400 MHz instruments. Compounds were dissolved in 0.5 ml of CD_3OD, $CDCl_3$, or DMSO-d_6. Coupling constants (J) are reported in Herz, and chemical shifts are expressed as parts per million (ppm) on the delta (δ) scale relative to the solvent peak as internal reference. Multiplicities are reported as follows: s, singlet; d, doublet; t, triplet; m, multiplet; dd, doublet of doublets. Chemical reactions were monitored on silica gel 60 F254 plates (Merck) and the spots were visualized under UV light. Analytical and semi-preparative reversed-phase HPLC were performed on an Agilent Technologies 1200 Series high performance liquid chromatography system using C18 Synergi Fusion reversed-phase columns ((a) 250 x 4.60mm, 4 μ, 90 Å, flow rate = 1 ml/min; (b) 250 x 10.00 mm, 10 μ, 90 Å, flow rate = 4 ml/min respectively, Phenomenex®). The binary solvent system (A/B) was as follows: 0.1% TFA in water (A) and 0.1% TFA in CH_3CN (B). Absorbance was detected at 240 nm. The purity of all tested compounds (> 95%) was

determined by HPLC analysis. Microwave irradiation reactions were carried out in a dedicated CEM-Discover® Focused Microwave Synthesis apparatus, operating with continuous irradiation power from 0 to 200 W utilizing the standard absorbance level of 300 W maximum power. Reactions were carried out in 10 ml sealed microwave glass vials. The DiscoverTM system also included controllable ramp time, hold time (reaction time) and uniform stirring. After the irradiation period, reaction vessels were cooled rapidly (60- 120 s) to ambient temperature by air jet cooling.

5.3.2 General procedure *f* for the synthesis of compound C1

A mixture of 2-chloronicotinoyl chloride (1 equiv, 0.5mmol), (*Z*)-ethyl 3-(dimethylamino)acrylate (0.9 equiv, 0.45mmol), and triethylamine (4 equiv, 2mmol) was placed in a 10 mL microwave glass vial equipped with a small magnetic stirring bar, without any addition of solvents. The mixture was then stirred under microwave irradiation at 100°C for 10 minutes, setting the maximum power and pressure that can be reached according to the selected temperature (**Scheme 10**, **Chapter 2**). After irradiation, the reaction mixture was cooled to ambient temperature by air jet cooling, the orange precipitate was solubilized in DCM (20ml) and washed with a solution of HCl 0.5N (3x10ml). The resulting crude was dried over anhydrous Na_2SO_4 and concentrated under vacuum to give the pure product in good yields (84%). This intermediate was purified by silica gel using a mixture of 8/2 hexane/AcOEt as eluent.

5.3.3 General procedure *g* for the synthesis of compounds C2-C9

The (*Z*)-ethyl 2-(2-chloronicotinoyl)-3-(dimethylamino)acrylate (1 equiv, 0.3mmol) was dissolved in toluene (30ml). The amine (1 equiv, 0.3 mmol) was added to this mixture and the

reaction was stirred over-night at reflux (**Scheme 10, Chapter 2**). After the completion of the reaction, it was quenched with water and the aqueous layer was extracted three times with dichloromethane. The combined organic layers were dried with anhydrous Na_2SO_4 and concentrated under vacuum. The crude mixture was purified by silica gel using different mixtures of hexane/ethyl acetate. Only a small amount of compound was then purify with HPLC to obtain a purity > 95% in order to evaluate the biological assay.

Synthesis of (*Z*)-ethyl 2-(2-chloronicotinoyl)-3-(dimethylamino)acrylate (C1)

Compound **C1** was obtained as an orange powdery solid following the general procedure *f* (Yield: 84%).

^{1}H NMR (400 MHz, CD_3OD) δ 8.45 (dd, J = 4.9, 1.9 Hz, 1H); 7.82 (dd, J = 7.6, 1.8 Hz, 1H); 7.48 (dd, J = 7.6, 4.9 Hz, 1H); 3.12 (s, 3H); 2.90 (s, 3H).

^{13}C NMR (100 MHz, CD_3OD) δ 190.8, 165.2, 162.6, 152.3, 151.3, 141.4, 136.2, 123.2, 102.0, 60.3, 44.9(2C), 14.14.

Synthesis of ethyl 4-oxo-1-(1*H*-pyrazol-5-yl)-1,4-dihydro-1,8-naphthyridine-3-carboxylate (C2)

Compound **C2** was obtained as a yellow powdery solid following the general procedure *g*, and then purified by silica gel using a mixture of 7/3 hexane/ethyl acetate (Yield: 66%). An analytic sample of **C2** was further purified by HPLC, using a gradient condition from 5% B to 100 % B in 50 min (t_R = 30.0 min).

^{1}H NMR (400 MHz, $CDCl_3$) δ 9.10 (s, 1H, NH); 8.57 (dd, *J* = 4.9, 2.1 Hz, 2H); 8.16 (d, *J* = 2.4 Hz, 1H); 7.72 (dd, *J* = 7.5, 2.1 Hz, 2H); 7.42 (dd, *J* = 7.6, 4.7 Hz, 2H); 6.83 (d, *J* = 2.4 Hz, 1H); 4.17 (m, 2H); 1.06 (t, *J* = 7.0 Hz, 3H).

^{13}C NMR (100 MHz, $CDCl_3$) δ 163.3; 150.8; 150.0; 149.4; 149.2; 147.7; 145.2; 138.8; 127.3; 122.1; 111.6; 98.6; 61.8; 13.7.

Synthesis of ethyl 1-(3-ethyl-1*H*-pyrazol-5-yl)-4-oxo-1,4-dihydro-1,8-naphthyridine-3-carboxylate (C3)

Compound **C3** was obtained as a brown solid following the general procedure *g* (Yield: 78%). An analytic sample of **C3** was purified with HPLC, using a gradient condition from 5% B to 100 % B in 50 min (t_R = 35.0 min).

^{1}H NMR (400 MHz, $CDCl_3$) δ 9.02 (s, 1H); 8.55 (dd, *J* = 4.9, 1.9 Hz, 1H); 7.70 (dd, *J* = 7.6, 1.9 Hz, 1H); 7.40 (dd, *J* = 7.6, 4.9 Hz, 1H); 6.62 (s, 1H); 4.15 (m, 2H); 2.75 (q, *J* = 7.6 Hz, 2H); 1.24 (t, *J* = 7.6 Hz, 3H); 1.05 (t, *J* = 7.2 Hz, 3H).

^{13}C NMR (100 MHz, $CDCl_3$) δ 164.2; 163.6; 150.5; 149.9; 149.6; 149.2; 144.7; 139.0; 127.5; 122.0; 110.6; 96.6; 61.6; 22.5; 13.7; 13.3.

Synthesis of ethyl 1-(4-cyano-1*H*-pyrazol-5-yl)-4-oxo-1,4-dihydro-1,8-naphthyridine-3-carboxylate (C4)

Compound **C4** was obtained as brown solid following the general procedure *g* (Yield: 79%). An analytic sample of **C4** was purified by HPLC, using a gradient condition from 5% B to 100 % B in 50 min (t_R = 28.0 min).

^{1}H NMR (400 MHz, $CDCl_3$) δ 9.05 (s, 1H); 8.69 (dd, *J* = 4.9, 1.9 Hz, 1H); 7.74 (dd, *J* = 7.6, 1.9 Hz, 1H); 7.55 (s, 1H); 7.52 (dd, *J* = 7.6, 4.9 Hz, 1H); 4.20 (m, 2H); 1.10 (t, *J* = 7.1 Hz, 3H).

^{13}C NMR (100 MHz, $CDCl_3$) δ 161.9; 152.3; 151.5; 149.0; 143.2; 141.8; 138.8; 126.5; 125.4; 122.8; 113.8; 113.1; 105.5; 62.6; 13.7.

Synthesis of ethyl 4-oxo-1-(1*H*-pyrazolo[3,4-*b*]pyridin-3-yl)-1,4-dihydro-1,8-naphthyridine-3-carboxylate (C5)

Compound **C5** was obtained as a yellow solid following the general procedure *g* and then purified by silica gel using a mixture of 99/1 dichloromethane/methanol (Yield: 50%). An analytic sample of **C5** was obtained through purification with HPLC, gradient condition from 5% B to 100 % B in 50 min (t_R = 27.0 min).

^{1}H NMR (400 MHz, DMSO-d_6) δ 9.37 (s, 1H, NH); 8.98 (dd, *J* = 4.3, 1.8 Hz, 1H); 8.84 (dd, *J* = 8.2, 1.8 Hz, 1H); 8.72 (dd, *J* = 4.9, 1.9 Hz, 1H); 8.19 (dd, *J* = 7.6, 1.9 Hz, 1H); 7.75 (dd, *J* = 7.6, 4.9 Hz, 1H); 7.45 (dd, *J* = 8.3, 4.3 Hz, 1H); 4.20 (qd, *J* = 7.1, 2.0 Hz, 2H).

^{13}C NMR (100 MHz, DMSO-d_6) δ 162.6; 160.5; 155.6; 151.8; 148.0; 147.5; 143.5; 143.4; 140.3; 130.8; 127.2; 123.1; 118.1; 116.1; 105.6; 61.8; 13.4.

Synthesis of 3-acetyl-1-(2-hydroxy-1*H*-indol-4-yl)-1,8-naphthyridin-4(1*H*)-one (C6)

Compound **C6** was obtained as a brown solid following the general procedure *g* and then purified by silica gel using a mixture of 8/2 hexane/ethyl acetate (Yield: 54%). An analytic sample of **C6** was obtained through purification with HPLC, gradient condition from 5% B to 100 % B in 50 min (t_R = 27.0 min).

Synthesis of ethyl 4-oxo-1-(7*H*-pyrrolo[2,3-*d*]pyrimidin-4-yl)-1,4-dihydro-1,8-naphthyridine-3-carboxylate (C7)

Compound **C7** was obtained as a brown solid following the general procedure *g* (Yield: 55%). An analytic sample of **C7** was obtained through purification with HPLC, gradient condition from 5% B to 100 % B in 50 min (t_R = 27.0 min).

^{1}H NMR (400MHz, $CDCl_3$) δ 9.25 (d, *J* = 6.4 Hz, 1H), 8.61 (s, 1H), 8.52 (dd, *J* = 4.8, 2.2 Hz, 1H), 8.17 (d, *J* = 2.2 Hz, 1H), 7.45 (dd, *J* = 8.2, 4.8 Hz, 1H), 7.08 (dd, *J* = 6.4, 5.7 Hz, 1H), 6.56 (d, *J* = 5.7 Hz, 1H), 4.27 (q, *J* = 7.1 Hz, 2H), 1.24 (t, *J* = 7.1 Hz, 3H).

^{13}C NMR (100 MHz, $CDCl_3$) δ 173.8, 165.4; 150.2; 149.7; 148.6; 144.7; 140.8; 134.2; 127.6; 123.2; 122.8; 120.1; 123.1; 102.9; 99.9; 60.8; 15.0.

Synthesis of ethyl 4-oxo-1-(3-(thiophen-2-yl)-1*H*-pyrazol-5-yl)-1,4-dihydro-1,8-naphthyridine-3-carboxylate (C8)

Compound **C8** was obtained as a white solid following the general procedure *g* and then purified by silica gel using a mixture of 8/2 hexane/ethyl acetate (Yield: 79%). An analytic sample of **C8** was obtained through purification with HPLC, gradient condition from 5% B to 100 % B in 50 min (t_R = 34.0 min).

^{1}H NMR (400 MHz, $CDCl_3$) δ 9.05 (s, 1H); 8.59 (dd, *J* = 4.9, 1.9 Hz, 1H); 7.76 (dd, *J* = 7.6, 1.9 Hz, 1H); 7.49 (dd, *J* = 3.6, 1.2 Hz, 1H); 7.44 (dd, *J* = 7.6, 4.9 Hz, 1H); 7.31 (dd, *J* = 5.0, 1.2 Hz, 1H); 7.04 (dd, *J* = 5.0, 3.6 Hz, 1H); 6.98 (s, 1H); 4.16 (m, 2H); 1.07 (t, *J* = 7.1 Hz, 3H).

^{13}C NMR (100 MHz, $CDCl_3$) δ 163.0; 154.4; 150.3; 150.1; 149.7; 149.0; 144.9; 139.8; 134.6; 127.9; 127.8; 127.3; 127.2; 122.3; 111.3; 94.9; 61.9; 13.8.

Synthesis of ethyl 1-(3-(4-bromophenyl)-1*H*-pyrazol-5-yl)-4-oxo-1,4-dihydro-1,8-naphthyridine-3-carboxylate (C9)

Compound **C9** was obtained as an orange solid following the general procedure *g* and then purified by silica gel using a mixture of 8/2 hexane/ethyl acetate (Yield: 74%). An analytic sample of **C9** was obtained through purification with HPLC gradient condition from 5% B to 100 % B in 50 min (t_R = 37.0 min).

^{1}H NMR (400 MHz, $CDCl_3$) δ 9.07 (s, 1H); 8.60 (dd, *J* = 4.9, 1.9 Hz, 1H); 7.76 (dd, *J* = 7.6, 1.9 Hz, 1H); 7.69 (d, *J* = 8.6 Hz, 2H); 7.49 (d, *J* = 8.6 Hz, 2H); 7.44 (dd, *J* = 7.6, 4.9 Hz, 1H); 7.08 (s, 1H); 4.15 (m, 2H); 1.08 (t, *J* = 7.1 Hz, 3H).

^{13}C NMR (100 MHz, $CDCl_3$) δ 163.3; 157.7; 150.6; 150.5; 150.2; 149.3; 144.9; 139.2; 131.9 (2 C); 130.8; 128.4 (2 C); 127.3; 124.0; 122.1; 111.5; 95.2; 61.8; 13.8.

5.4 Synthesis of 2,4,5-trisubstituted-2,4-dihydro-3*H*-1,2,4-triazol-3-one-based molecules (D3-D36)

5.4.1 Chemistry general information

All commercially available starting materials were purchased from Sigma-Aldrich and used as received. The solvents used for the synthesis were of HPLC grade (Sigma-Aldrich). NMR spectra were recorded on a Bruker Avance 400 MHz or 600MHz instrument at T = 298 K.

Compounds **D3**-**D36** were dissolved in 0.5 mL of $CDCl_3$, MeOD, DMSO-d_6 (Sigma-Aldrich, 99.98 Atom % D). Coupling constants (J) are reported in Hertz, and chemical shifts are expressed in parts per million (ppm) on the delta (δ) scale relative to solvent peak as internal reference. Electrospray mass spectrometry (ESI-MS) was performed on a LCQ DECA TermoQuest (San Jose, CA, USA) mass spectrometer. Reactions were monitored on silica gel 60 F plates (Merck) and visualized under UV light (λ = 254 nm, 365 nm). Analytical and semi-preparative reversed-phase HPLC was performed on Agilent Technologies 1200 Series high

performance liquid chromatography using a Fusion-RP, C reversed-phase column (100 × 2 mm, 4 µm, 80 Å, flow rate = 1 mL/min; 250 ×10.00 mm, 4 µm, 80 Å, flow rate= 4 mL/min respectively, Phenomenex). The binary solvent system (A/B) was as follows: 0.1 % TFA in water (A) and 0.1% TFA in CH_3CN (B). The absorbance was detected at 240 nm. The purity of all tested compound (>96%) were determined by HPLC analysis and NMR data.

5.4.2 General method *h* for the synthesis of compounds 5-methyl-4-phenyl-2,4-dihydro-3*H*-1,2,4-triazol-3-one 3*H*-1,2,4-triazol-3-one

The synthetic routes of the identified molecules were graphed in **Scheme 13** (**Chapter 2**). To a solution of ethyl acetate (1.0 equiv, 50mmol) in ethanol, an excess of hydrazine hydrate (1.3equiv, 65mmol) was added before over-night stirring under reflux. The solvent was removed under vacuum, and the desired compound was obtained through purification on a silica gel column chromatography using hexane/ethyl acetate 9/1 as eluent. A mixture of acetyl hydrazine (1.0 equiv, 2 mmol), aromatic isocyanate (1.0 equiv, 2 mmol), and ethanol (20 mL) was placed in a 50 ml bottom flask. The reaction mixture was continuously stirred and refluxed overnight. At the end of the reaction, the ethanol was removed in vacuum, the crude was extracted with AcOEt (3×20 mL) and the organic phases were combined, dried over anhydrous $NaSO_4$, filtered, and concentrated in vacuo. The obtained urea derivatives were used without further purification for the next step. Compounds were dissolved in MeOH (5ml) and reacted with an excess of NaOH 2% (20ml) under reflux for 3 hours. The reactions were quenched by solution neutralization with HCl (1N), then the methanol was evaporated in vacuo, and the water solution extracted by $CHCl_3$. HPLC purification of the crude product was performed by semi-preparative reversed-phase HPLC (Fusion-RP, C-18 reversed-phase column: 250 ×10.00 mm, 4 µm, 80 Å, flow rate = 4 mL/min) using the gradient conditions reported below.

5.4.3 General method *i* for synthesis of compounds 5-ethyl-4-phenyl-2,4-dihydro-3*H*-1,2,4-triazol-3-one

Hydrazine hydrate (1 equiv, 2 mmol) was added to a solution of phenyl isocyanate (1 equiv, 2 mmol) in dry dichloromethane (25mL) at 0°C. After 10 minutes, the reaction was allowed to warm to room temperature and stirred for 24h. After completion of the reaction, the organic phase was washed with water (3x 20.0 mL), dried over anhydrous $NaSO_4$, filtered, and concentrated in vacuo. The obtained compounds (1 equiv, 1.6 mmol) (Yield=80-90%) were dissolved in dry $CHCl_3$ (25mL) and propionic anhydride (1 equiv, 1.6 mmol) was added to the solution under nitrogen atmosphere, at 0°C. The reactions were stirred at room temperature from 5h to 24h. After the end of the reaction, the crudes were washed with water (20.0 mL), dried over anhydrous $NaSO_4$, filtered, and concentrated in vacuo. The urea derivatives were obtained in good yield and used for the next step without any purifications. Compounds were dissolved in MeOH (5ml) with an excess of NaOH 2% (20ml) and stirred under reflux for 3 hours. The reactions were quenched by solution neutralization with HCl (1N), the methanol was removed, and the water solution extracted by $CHCl_3$. HPLC purification of the crude products was performed by semi-preparative reversed-phase HPLC (Fusion-RP, C-18 reversed-phase column: 250 ×10.00 mm, 4 µm, 80 Å, flow rate = 4 mL/min) using the gradient conditions reported below.

5.4.4 General method *j* for synthesis of compounds 5-alkyl-2-methyl-4-phenyl-2,4-dihydro-3*H*-1,2,4-triazol-3-one

Compounds 5-alkyl-2-methyl-4-phenyl-3H-1,2,4-triazol-3-one were obtained from their analogous through N-methylation in position 2. At first, 1.0 equiv of compound 5-alkyl-4-phenyl-1,2,4-triazol-3-one was dissolved in anhydrous DMF, and NaH (1.5 equiv) and CH_3I (1.5equiv) were added under nitrogen atmosphere, allowing the solution to warm 0°C to room

temperature for 5 hours. The mixture was diluted with 10 mL of water, extracted with $CHCl_3$ (3 ×20 mL), and the combined organic layers were dried over anhydrous sodium sulphate. The final compounds were obtained with yields from 61% to 77%. Compounds **D24**-**D26**, **D30**-**D32** instead were obtained with a higher amount of NaH (2 equiv) (**Scheme 13, Chapter 2**). In these cases, yields were increased from 91 to 99%. HPLC purification was performed by semi-preparative reversed-phase HPLC (Fusion-RP, c-18 reversed-phase column: 250 ×10.00 mm, 4 µm, 80 Å, flow rate = 4 mL/min) using the gradient conditions reported below.

5.4.5 General method *k* for synthesis of compounds 5-alkyl-2-ethyl-4-phenyl-2,4-dihydro-3*H*-1,2,4-triazol-3-one

NaH (2 equiv) and CH_3CH_2I (1.5equiv) were added to a solution of 5-alkyl-2-ethyl-4-phenyl-3H-1,2,4-triazol-3-one (1.0 equiv) in dry DMF under nitrogen atmosphere, allowing the solution to warm from 0°C to room temperature for 5 hours (**Scheme 13, Chapter 2**). Then, the solution was diluted with chloroform (20mL) and extracted with H_2O (3x10mL). The organic lower was treated with Na_2SO_4 and concentration in vacuo. The final products were obtained with yields from 70 to 90%. HPLC purification was performed by semi-preparative reversed-phase HPLC (Fusion-RP, C-18 reversed-phase column: 250 ×10.00 mm, 4 µm, 80 Å, flow rate = 4 mL/min) using the gradient conditions reported below.

Synthesis of 5-methyl-4-(p-tolyl)-2,4-dihydro-3*H*-1,2,4-triazol-3-one (D3) Compound **D3** was obtained by following the general procedure *h* as a white solid (Yield: 90%). An analytical sample was purified by HPLC; RP-HPLC t_R= 18.0 min, condition 35 % B over 40 min, flow rate of 3 mL/min, λ = 240 nm.

^{1}H NMR (400 MHz, DMSO-d$_6$) δ 11.49, 7.38 (d, *J* = 8.0 Hz, 2H), 7.02 (d, *J* = 8.0 Hz, 2H), 2.37 (s, 3H), 2.15 (s, 3H).

^{13}C NMR (100 MHz, DMSO-d$_6$) δ 153.2, 147.2, 139.8, 130.5, 129.2(2C), 118.2(2C), 22.3, 14.0.

HR-MS: m/z calcd for $C_{10}H_{11}N_3O$ $[M+H]^+$ 190.2138; found $[M+H]^+$ 190.1098.

Synthesis of 5-methyl-4-(m-tolyl)-2,4-dihydro-3*H*-1,2,4-triazol-3-one (D4) Compound **D4** was obtained by following the general procedure *h* as a white solid (Yield: 95%). An analytical sample was purified by HPLC; RP-HPLC t_R= 17.1 min, condition 35 % B over 40 min, flow rate of 3 mL/min, λ = 240 nm.

^{1}H NMR (400 MHz, DMSO-d$_6$) δ 11.59 (s, 1H), 7.41 (t, *J* = 7.7 Hz, 1H), 7.27 (d, *J* = 7.5 Hz, 1H), 7.22 (s, 1H), 7.19 (d, *J* = 7.9 Hz, 1H), 2.37 (s, 3H), 2.05 (s, 3H).

^{13}C NMR (100 MHz, DMSO-d$_6$) δ 154.1, 143.5, 139.0, 133.0, 129.1, 129.0, 123.9, 127.5, 20.4, 12.4.

HR-MS: m/z calcd for $C_{10}H_{11}N_3O$ $[M+H]^+$ 190.0902; found $[M+H]^+$ 190.1098.

Synthesis of 5-methyl-4-(4-(tert-butyl)phenyl)-2,4-dihydro-3*H*-1,2,4-triazol-3-one (D5)

Compound D**5** was obtained by following the general procedure *h* as an orange oil (Yield: 98%) An analytical sample was purified by HPLC; RP-HPLC t_R= 32.7 min, gradient condition: from 5 % B to 100 % B over 50 min, flow rate of 3 mL/min, λ= 240 nm.

^{1}H NMR (400 MHz, DMSO-d$_6$) δ 11.53 (s, 1H), 7.48 (d, *J* = 8.4 Hz, 2H), 7.26 (d, *J* = 8.4 Hz, 2H), 2.01 (s, 9H).

^{13}C NMR (100 MHz, DMSO-d$_6$) δ 154.2, 150.7, 143.7, 130.3, 126.5(2C), 126.0(2C), 34.2, 30.8 (3C), 12.40.

HR-MS: m/z calcd for $C_{13}H_{17}N_3O$ $[M+H]^+$ 232.1372; found $[M+Na]^+$ 254.1322.

Synthesis of 4-(4-fluoro-3-methylphenyl)-5-methyl-2,4-dihydro-3*H*-1,2,4-triazol-3-one (D6)

Compound **D6** was obtained by following the general procedure *h* as an orange oil (Yield: 98%). An analytical sample was purified by HPLC; RP-HPLC t_R= 7.5 min, gradient condition: from 38 % B to 100 % B over 50 min, flow rate of 3 mL/min, λ= 240 nm

^{1}H NMR (400 MHz, DMSO-d*6*) δ 11.60 (s, 1H), 7.35 (d, *J* = 7.4 Hz, 1H), 7.28 (m, 2H), 2.25 (s, 3H), 2.06 (s, 3H).

^{13}C NMR (100 MHz, DMSO-d*6*) δ 160.1 (d, *J* = 248.4 Hz), 154.3, 143.8, 130.4 (d, *J* = 5.6 Hz), 128.9, 126.6 (d, *J* = 8.3Hz), 125.5 (d, *J* = 18.9 Hz), 115.7 (d, *J* = 21.3 Hz), 14.3, 12.3.

HR-MS: m/z calcd for $C_{10}H_{10}FN_3O$ $[M+H]^+$ 208.0808; found $[M+H]^+$ 208.0901.

Synthesis of 4-(4-fluoro-3-(trifluoromethyl)phenyl)-5-methyl-2,4-dihydro-3*H*-1,2,4-triazol-3-one (D7)

Compound **D7** was obtained by following the general procedure *h* as a white solid (Yield: 98%). An analytical sample was purified by HPLC purification; RP-HPLC t_R= 14.9 min, condition: from 40 % B to 80 % B over 50 min, flow rate of 3 mL/min, λ = 240 nm

^{1}H NMR (400 MHz, DMSO-d$_6$) δ 11.70 (s, 1H), 7.97 – 7.91 (m, 1H), 7.88 (dd, J = 8.2, 3.6 Hz, 1H), 7.71 (t, J = 9.6 Hz, 1H), 2.08 (s, 3H).

^{13}C NMR (100 MHz, DMSO-d$_6$) δ 158.0 (d, *J*=255.3 Hz)), 154.2, 143.9, 134.1 (d, *J* = 9.3 Hz), 129.9 (d, *J*=7.0 Hz), 126.3, 122.0 (q, *J* = 272.3 Hz), 118.4 (d, *J* = 21.8 Hz), 117.2 (m), 12.1.

HR-MS: m/z calcd for $C_{10}H_7F_4N_3O$ $[M+H]^+$ 262.0525; found $[M+Na]^+$ 283.2645.

Synthesis of 4-(3,4-dimethoxyphenyl)-5-methyl-2,4-dihydro-3*H*-1,2,4-triazol-3-one (D8)

Compound **D8** was obtained by following the general procedure *h* as a brown powder (Yield: 60%). An analytical sample was purified by HPLC; RP-HPLC t_R= 19.5 min, gradient condition: from 5 % B to 100 % B over 50 min, flow rate of 3 mL/min, λ = 240 nm.

^{1}H NMR (400 MHz, DMSO-d_6) δ 11.51 (s, 1H), 7.05 (d, *J* = 8.5 Hz, 1H), 6.98 (d, *J* = 2.0 Hz, 1H), 6.90 (dd, *J* = 8.4, 2.0 Hz, 1H), 3.80 (s, 3H), 3.76 (s, 3H), 2.02 (s, 3H).

^{13}C NMR (100 MHz, DMSO-d_6) δ 154.5, 149.1, 148.7, 144.3, 125.7, 119.7, 111.7, 111.3, 55.8, 55.2, 12.3.

HR-MS: m/z calcd for $C_{11}H_{13}N_3O_3$ $[M+H]^+$ 236.0957; found $[M+Na]^+$ 258.0851.

Synthesis of 4-(3,4-dimethylphenyl)-5-ethyl-2,4-dihydro-3*H*-1,2,4-triazol-3-one (D11)

Compound **D11** was obtained by following the general procedure *i* as a brown powder (Yield: 98%). An analytical sample was purified by HPLC; RP-HPLC t_R= 28.0 min, gradient condition: from 5 % B to 100 % B over 50 min, flow rate of 3 mL/min, λ = 240 nm.

^{1}H NMR (400 MHz, DMSO-d_6) δ 11.56 (s, 1H), 7.26 (d, *J* = 7.9 Hz, 1H), 7.14 (s, 1H), 7.07 (d, *J* = 7.8 Hz, 1H), 2.36 (q, *J* = 7.4 Hz, 2H), 2.25 (s, 6H), 1.00 (t, *J* = 7.4 Hz, 3H).

^{13}C NMR (100 MHz, DMSO-d_6) δ 154.6, 148.1, 137.7, 137.0, 130.7, 130.3, 128.2, 124.7, 19.7, 19.4, 19.1, 10.0.

HR-MS: m/z calcd for $C_{12}H_{15}N_3O$ $[M+H]^+$ 218.1215; found $[M+Na]^+$ 240.1124.

Synthesis of 5-ethyl-4-(4-ethylphenyl)-2,4-dihydro-3*H*-1,2,4-triazol-3-one (D12)

Compound **D12** was obtained by following the general procedure *i* as a yellow powder (Yield: 87%). An analytical sample was purified by HPLC; RP-HPLC t_R= 26.7 min, gradient condition: from 5 % B to 100 % B over 50 min, flow rate of 3 mL/min, λ = 240 nm.

^{1}H NMR (400 MHz, DMSO-d_6) δ 11.57 (s, 1H), 7.35 (d, *J* = 8.2 Hz, 2H), 7.28 (d, *J* = 8.3 Hz, 2H), 2.66 (q, *J* = 7.6 Hz, 2H), 2.37 (q, *J* = 7.4 Hz, 2H), 1.21 (t, *J* = 7.6 Hz, 3H), 1.00 (t, *J* = 7.4 Hz, 3H).

^{13}C NMR (100 MHz, DMSO-d_6) δ 154.7, 148.2, 144.1, 130.5, 129.0(2C), 127.1 (2C), 28.3, 19.4, 15.3, 9.8.

HR-MS: m/z calcd for $C_{12}H_{15}N_3O$ $[M+H]^+$ 218.1215; found $[M+Na]^+$ 240.1124.

Synthesis of 4-(3-chloro-4-fluorophenyl)-5-ethyl-2,4-dihydro-3*H*-1,2,4-triazol-3-one (D13)

Compound **D13** was obtained by following the general procedure *i* as a white powder (Yield: 98%) An analytical sample was purified by HPLC; RP-HPLC t_R= 27.2 min, gradient condition: from 5 % B to 100 % B over 50 min, flow rate of 3 mL/min, λ = 240 nm.

^{1}H NMR (400 MHz, DMSO-d_6) δ 11.67 (s, 1H), 7.81 – 7.77 (m, 1H), 7.62 – 7.56 (m, 1H), 7.52 –7.46 (m, 1H), 2.42 (dt, *J* = 12.1, 5.0 Hz, 2H), 1.09 – 0.91 (m, 3H). **^{13}C NMR (100 MHz, DMSO-d_6) δ** 157.0 (d, *J* =248.4), 154.3, 147. (d, *J* = 3.4 Hz), 130.11(d, *J* = 3.3Hz), 129.8, 128.5 (d, *J* = 7.9 Hz), 120.0 (d, *J* = 18.8 Hz), 117.5 (d, *J* = 22.3 Hz), 19.3, 9.6.

HR-MS: m/z calcd for $C_{10}H_9ClFN_3O$ $[M+H]^+$ 242.0418; found $[M+H]^+$ 242.0503.

Synthesis of 4-(3-chloro-4-methylphenyl)-5-ethyl-2,4-dihydro-3*H*-1,2,4-triazol-3-one (D14)

Compound **D14** was obtained by following the general procedure *i* as a yellow solid (Yield: 66%). An analytical sample was purified by HPLC; RP-HPLC t_R= 19.5 min, gradient condition: from 5 % B to 100 % B over 50 min, flow rate of 3 mL/min, λ = 240 nm.

^{1}H NMR (400 MHz, CD_3OD) δ 7.49 (d, *J* = 8.2 Hz, 1H), 7.48 (d, *J* = 2.1 Hz, 1H), 7.26 (dd, *J* = 8.1, 2.2 Hz, 1H), 2.50 (q, *J* = 7.5 Hz, 2H), 2.46 (s, 3H), 1.15 (t, *J* = 7.5 Hz, 3H).

^{13}C NMR (100 MHz, CD_3OD) δ 156.7, 150.5, 139.4, 136.3, 133.5, 133.1, 129.7, 127.3, 20.2, 19.9, 10.5.

HR-MS: m/z calcd for $C_{11}H_{12}ClN_3O$ $[M+H]^+$ 237.0669, found $[M+Na]^+$ 237.0712.

Synthesis of 5-ethyl-4-(4-fluoro-3-methylphenyl)-2,4-dihydro-3*H*-1,2,4-triazol-3-one (D15)

Compound **D15** was obtained by following the general procedure *i* as a white powder (Yield: 85%). An analytical sample was purified by HPLC; RP-HPLC t_R= 34.1 min, gradient condition: from 5 % B to 100 % B over 50 min, flow rate of 3 mL/min, λ = 240 nm.

^{1}H NMR (400 MHz, $CDCl_3$) δ 7.49 (d, *J* = 8.2 Hz, 1H), 7.48 (d, *J* = 2.1 Hz, 1H), 7.26 (dd, *J* = 8.1, 2.2 Hz, 1H), 2.50 (q, *J* = 7.5 Hz, 2H), 2.46 (s, 3H), 1.15 (t, *J* = 7.5 Hz, 3H).

^{13}C NMR (100 MHz, $CDCl_3$) δ 161.1 (d, *J* = 248.3 Hz), 155.3, 149.1, 130.5(d, *J* = 6.0 Hz), 128.2, 126.9(d, *J* = 19.0 Hz), 126.2(d, *J* = 8.8 Hz), 116.3(d, *J* = 24.2 Hz), 19.3, 9.2

HR-MS: m/z calcd for $C_{11}H_{12}ClN_3O$ $[M+H]^+$ 222.0964; found $[M+Na]^+$ 244.0923.

Synthesis of 5-ethyl-4-(3-(trifluoromethyl)phenyl)-2,4-dihydro-3*H*-1,2,4-triazol-3-one (D16)

Compound **D16** was obtained by following the general procedure *i* as a white powder (Yield: 75%). An analytical sample was purified by HPLC; RP-HPLC t_R= 27.0 min, gradient condition: from 5 % B to 100 % B over 50 min, flow rate of 3 mL/min, λ = 240 nm.

^{1}H NMR (400 MHz, DMSO-d$_6$) δ 11.73 (s, 1H), 7.89 – 7.82 (m, 2H), 7.81 – 7.73 (m, 2H), 2.43 (q, J = 7.4 Hz, 2H), 1.02 (t, J = 7.4 Hz, 3H).

^{13}C NMR (100 MHz, DMSO-d$_6$) δ 154.3, 147.5, 133.9, 131.5, 130.7, 130.1 (q, *J* =32.2 Hz), 125.2, 124.7 (q, *J* = 32.2 Hz), 124.2 (q, *J* = 272.3 Hz), 19.7, 9.5.

HR-MS: m/z calcd for $C_{11}H_{10}F_3N_3O$ $[M+H]^+$ 257.0776, found [M+Na]+ 280.0668.

Synthesis of 4-(3,4-dimethoxyphenyl)-5-ethyl-2,4-dihydro-3*H*-1,2,4-triazol-3-one (D17)

Compound **D17** was obtained by following the general procedure *i* as a brown powder (Yield: 83%). An analytical sample was purified by HPLC; RP-HPLC t_R= 22.5 min, gradient condition: from 5 % B to 100 % B over 50 min, flow rate of 3 mL/min, λ = 240 nm.

^{1}H NMR (400 MHz, DMSO-d$_6$) δ 11.53 (s, 1H), 7.06 (d, *J* = 8.5 Hz, 1H), 6.99 (d, *J* = 1.9 Hz, 1H), 6.90 (dd, *J* = 8.1, 1.8 Hz, 1H), 3.81 (s, 3H), 3.76 (s, 3H), 2.38 (q, *J* = 7.5 Hz, 3H), 1.02 (t, *J* = 7.5 Hz, 3H).

^{13}C NMR (100 MHz, DMSO-d$_6$) δ 154.9, 149.0, 148.9, 148.3, 125.8, 119.9, 111.8, 111.5, 55.8 , 55.7, 19.3, 10.0.

HR-MS: m/z calcd for $C_{12}H_{15}N_3O_3$ $[M+H]^+$ 250.1113; found $[M+H]^+$ 250.1167.

Synthesis of 4-(benzo[*d*][1,3]dioxol-5-yl)-5-ethyl-2,4-dihydro-3*H*-1,2,4-triazol-3-one (D18)

Compound **D18** was obtained by following the general procedure *i* as a brown powder (Yield: 89%). An analytical sample was purified by HPLC; RP-HPLC t_R= 22.5 min, gradient condition: from 5 % B to 100 % B over 50 min, flow rate of 3 mL/min, λ = 240 nm.

^{1}H NMR (400 MHz, DMSO-d_6) δ 11.54 (s, 1H), 8.44 (d, *J*=7.4Hz, 1H), 8.03 (dd, *J* = 7.7 Hz, 1,4Hz, 1H), 7.04(s, 1H), 6.11 (s, 2H), 2.37 (q, 7.4 Hz, 2H), 1.02 (t, *J* = 7.4 Hz, 3H).

^{13}C NMR (100 MHz, DMSO-d_6) δ 154.6, 148.1, 147.7, 147.3, 126.6, 121.3, 108.6, 108.3, 101. , 19.19, 9.6.

HR-MS: m/z calcd for $C_{11}H_{11}N_3O_3$ $[M+H]^+$ 234,0800; found $[M+H]^+$ 234,0845.

Synthesis of 2,5-dimethyl-4-(m-tolyl)-2,4-dihydro-3*H*-1,2,4-triazol-3-one (D19)

Compound **D19** was obtained from compound **D11** by following the general procedure *j* as a white solid (Yield: 77.0%). An analytical sample was purified by HPLC; RP-HPLC t_R= 21.8 min, gradient condition: from 5 % B to 100 % B over 50 min, flow rate of 3 mL/min, λ = 240 nm.

^{1}H NMR (400 MHz, $CDCl_3$) δ 7.37 (t, J = 7.8 Hz, 1H), 7.26 (d, *J* = 7.8 Hz, 1H), 7.11 (s, 1H), 7.06 (d, *J* = 7.9 Hz, 1H), 3.50 (s, 3H), 2.40 (s, 3H), 2.13 (s, 3H).

^{13}C NMR (100 MHz, $CDCl_3$) δ 153.5. 142.8, 139.9, 132.9, 129.9, 129.5, 127.6, 124.0, 32.5, 21.5, 12.1.

HR-MS: m/z calcd for $C_{11}H_{13}N_3O$ $[M+H]^+$ 204.1059; found $[M+H]^+$ 204.1059.

Synthesis of 2,5-dimethyl-4-(4-(tert-butyl)phenyl)-2,4-dihydro-3*H*-1,2,4-triazol-3-one (D20)

Compound **D20** was obtained from compound **D5** by following the general procedure *j* as a brown powder (Yield: 61%). An analytical sample was purified by HPLC; RP-HPLC t_R= 34.0 min, gradient condition: from 5 % B to 100 % B over 50 min, flow rate of 3 mL/min, λ = 240 nm.

^{1}H NMR (400 MHz, $CDCl_3$) δ 7.44 (d, *J* = 6.2 Hz, 1H), 7.15 – 7.13 (m, 1H), 7.16 (d, *J* =6.2 Hz, 1H), 3.43 (s, 3H), 2.08 (s, 3H), 1.28 (s, 9H).

^{13}C NMR (100 MHz, $CDCl_3$) δ 153.7, 152.3, 143.1, 130.5, 126.9(2C), 126.6(2C), 45.6, 32.5, 31.2, 12.8.

HR-MS: m/z calcd for $C_{14}H_{19}N_3O$ $[M+H]^+$ 246.1528, found $[M+H]^+$ 246.1532.

Synthesis of 2,5-dimethyl-4-(4-fluoro-3-(trifluoromethyl)phenyl)-2,4-dihydro-3*H*-1,2,4-triazol-3-one (D21)

Compound **D21** was obtained from compound **D7** by following the general procedure *j* as a yellow solid (Yield: 75%). An analytical sample was purified by HPLC; RP-HPLC t_R= 22.2 min, gradient condition: from 5 % B to 100 % B over 50 min, flow rate of 3 mL/min, λ = 240 nm.

1H NMR (600 MHz, $CDCl_3$) δ 7.51 (dd, *J* = 8.9, 2.7 Hz, 1H), 7.45 (m, 1H), 7.30 (t, *J* = 9.1 Hz, 1H), 3.44 (s, 3H), 2.10 (s, 3H).

^{13}C NMR (150 MHz, $CDCl_3$) δ 159.5(d, *J*=259.4Hz), 153.0, 141.3, 132.5(d, *J*=9.0Hz), 126.2(d, J=6.3Hz), 121.8(q, *J*=273.0Hz), 119.9(q, *J*=33.6Hz), 118.4(d, *J*=22.1Hz), 113.4, 32.2, 11.9.

HR-MS: m/z calcd for $C_{11}H_9F_4N_3O$ $[M+H]^+$ 276.0682, found $[M+H]^+$276.0651.

Synthesis of 2,5-dimethyl-4-(3,4-dimethoxyphenyl)-2,4-dihydro-3*H*-1,2,4-triazol-3-one (D22)

Compound **D22** was obtained from compound **D8** by following the general procedure *j* as an orange oil (Yield: 74%). An analytical sample was purified by HPLC; RP-HPLC t_R = 23.0 min, gradient condition: from 5 % B to 100 % B over 50 min, flow rate of 3 mL/min, λ = 240 nm.

^{1}H NMR (400 MHz, $CDCl_3$) δ 6.94 (d, *J* = 8.4 Hz, 1H), 6.82 (dd, *J* = 8.4, 2.4 Hz, 1H), 6.79 (d, *J* = 2.3 Hz, 1H), 3.92 (s, 3H), 3.88 (s, 3H), 3.49 (s, 3H), 2.12 (s, 3H).

^{13}C NMR (100 MHz, $CDCl_3$) δ 153.9, 149.9, 149.9, 143.4, 125.8, 120.2, 112.1, 110.7, 56.2 (2C), 32.7, 12.3.

HR-MS: m/z calcd for $C_{12}H_{15}N_3O_3$ $[M+H]^+$ 250.2658, found $[M+Na]^+$ 272.1031.

Synthesis of 4-(3,4-dimethylphenyl)-5-ethyl-2-methyl-2,4-dihydro-3*H*-1,2,4-triazol-3-one (D23)

Compound **D23** was obtained from compound **D11** by following the general procedure *j* as an orange solid (Yield: 77%). An analytical sample was purified by HPLC; RP-HPLC t_R= 30.9 min, gradient condition: from 5 % B to 100 % B over 50 min, flow rate of 3 mL/min, λ = 240 nm.

^{1}H NMR (400 MHz, CD_3OD) δ 7.39 (d, *J* = 2.2 Hz, 1H), 7.31 (dd, *J* = 8.4, 1.8 Hz, 1H), 7.02 (d, *J*=8.4, 1.0 Hz, 1H)3.66(s, 6H), 2.75(q, *J*=7.5Hz, 2H), 2.80(s, 3H), 1.66 (t, *J* = 7.5 Hz, 2H).

^{13}C NMR (100 MHz, CD_3OD) δ 155.5, 151.5, 139.9, 139.5, 131.8,131.6, 129.9, 125.0, 35.4, 32.3, 20.1, 18.8, 10.4.

HR-MS: m/z calcd for $C_{13}H_{17}N_3O$ $[M+H]^+$ 232.1372; found $[M+Na]^+$254.2815.

Synthesis of 5-ethyl-2-methyl-4-(3-(trifluoromethyl)phenyl)-2,4-dihydro-3*H*-1,2,4-triazol-3-one (D24)

Compound **24** was obtained by following the general procedures *i* and *j* as a yellow powder (Yield: 95%). An analytical sample was purified by HPLC; RP-HPLC t_R= 28.5 min, gradient condition: from 5 % B to 100 % B over 50 min, flow rate of 3 mL/min, λ = 240 nm.

^{1}H NMR (400 MHz, CD_3OD) δ 7.84 (d, *J* = 7.7 Hz, 1H), 7.81 – 7.75 (m, 2H), 7.69 (d, *J* =7.8 Hz, 1H), 3.48 (s, 3H), 2.51 (q, *J* = 7.2 Hz, 2H), 1.15 (t, *J* = 7.5 Hz, 3H).

^{13}C NMR (100 MHz, CD_3OD) δ 155.0, 148.7, 135.1, 133.2(q, *J* = 33.2 Hz), 132.4, 131.9, 127,1 (d, *J*=3.4Hz), 125.1 (q, *J*= 102.0 Hz), 124.6 (d, *J*=3.8Hz), 32.5, 20.7, 10.3.

HR-MS: m/z calcd for $C_{12}H_{12}F_3N_3O$ $[M+H]^+$ 272.0932, found $[M+H]^+$294.0923.

Synthesis of 4-(benzo[d][1,3]dioxol-5-yl)-5-ethyl-2-methyl-2,4-dihydro-3*H*-1,2,4-triazol-3-one (D25)

Compound **D25** was obtained from compound **D18** by following the general procedure *j* as a pink powder (Yield: 91%). An analytical sample was purified by HPLC; RP-HPLC t_R= 11.8 min, gradient condition: from 25 % B to 100 % B over 50 min, flow rate of 3 mL/min, λ = 240 nm.

^{1}H NMR (400 MHz, $CDCl_3$) δ 7.77 (s, 1H), 7.38(d; *J*=7.8 Hz, 1H), 7.23 (d, *J* = 2.1 Hz,1H), 6.56 (s, 2H), 4.01 (s, 2H), 2.97 (q, *J*=7.5Hz, 2H), 1.66 (t, *J* = 7.5 Hz, 2H).

^{13}C NMR (100 MHz, $CDCl_3$) δ 154.1. 148.8, 148.7, 147.7, 121.5, 108.9, 108.6, 102.3, 32.7, 20.0, 10.2.

HR-MS: m/z calcd for $C_{12}H_{13}N_3O_3$ $[M+H]^+$ 248.0957, found $[M+Na]^+$ 270.2435.

Synthesis of 4-(3,4-dimethoxyphenyl)-5-ethyl-2-methyl-2,4-dihydro-3*H*-1,2,4-triazol-3-one (D26)

Compound **D26** was obtained from compound **D17** by following the general procedure *j* as an orange powder (Yield: 91%). An analytical sample was purified by HPLC; RP-HPLC t_R= 21.0 min, gradient condition: from 5 % B to 100 % B over 50 min, flow rate of 3 mL/min, λ = 240 nm.

^{1}H NMR (400 MHz, $CDCl_3$) δ 6.93 (d, *J* = 8.5 Hz, 1H), 6.82 (dd, *J* = 8.4, 2.3 Hz, 1H), 6.77 (d, *J* = 2.4 Hz, 1H), 3.91 (s, 3H), 3.87 (s, 3H), 3.49 (s, 2H), 2.43 (dd, *J* = 15.0, 7.5 Hz, 2H), 1.14 (t, *J* = 7.5 Hz, 4H).

^{13}C NMR (100 MHz, $CDCl_3$) δ 1154.1, 150.2, 149.8, 149.1, 125.0, 119.9, 111.5, 110.7, 56.2, 56.0, 32.8, 20.2, 10.4.

HR-MS: m/z calcd for $C_{13}H_{17}N_3O_3$ $[M+H]^+$ 263.1260, found $[M+Na]^+$286.2044.

Synthesis of 2,5-diethyl-4-(3,4-dimethoxyphenyl)-2,4-dihydro-3*H*-1,2,4-triazol-3-one (D27)

Compound **D27** was obtained from compound **D17** by following the general procedure *k* as a brown powder (Yield: 97%). An analytical sample was purified by HPLC; RP-HPLC t_R= 24.9 min, gradient condition: from 5 % B to 100 % B over 50 min, flow rate of 3 mL/min, λ = 240 nm.

^{1}H NMR (400 MHz, CD_3OD) δ 7.10 (d, *J* = 8.5 Hz, 1H), 6.99 (d, *J* = 2.4 Hz, 1H), 6.93 (dd, *J* = 8.5, 2.4 Hz, 1H), 3.90 (s, 3H), 3.89-3.83(m, 5H) 2.50 (q, *J*=7.5Hz, 2H), 1.37 (t, *J* = 7.2 Hz, 3H), 1.15 (t, *J* = 7.5 Hz, 3H).

^{13}C NMR (100 MHz, CD_3OD) δ 154.9, 151.4, 151.2, 149.6, 121.3, 113.0, 112.5, 56.7, 56.6, 41.2, 20.7, 13.9, 14.3, 10.7.

HR-MS: m/z calcd for $C_{13}H_{19}N_3O_3$ $[M+H]^+$ 278.1426, found $[M+Na]^+$300.1322.

Synthesis of 4-(3,4-dimethoxyphenyl)-2-ethyl-5-methyl-2,4-dihydro-3*H*-1,2,4-triazol-3-one (D28)

Compound **D28** was obtained from compound **D8** by following the general procedure *k* as a brown solid (Yield: 88%). An analytical sample was purified by HPLC; RP-HPLC t_R= 21.9 min, gradient condition: from 5 % B to 100 % B over 50 min, flow rate of 3 mL/min, λ = 240 nm.

^{1}H NMR (400 MHz, CD_3OD) δ 7.10 (d, *J* = 8.5 Hz, 1H), 7.00 (d, *J* = 2.5 Hz, 1H), 6.93 (dd, *J* = 8.5, 2.4 Hz, 1H), 3.90 (s, *3*H), 3.88-3.83(m, 5H) 2.14 (s, 3H), 1.37 (t, *J* = 7.2 Hz, 3H), 1.36 (t, *J* = 7.2 Hz, 3H).

^{13}C NMR (100 MHz, CD_3OD) δ 154.6, 151.4, 151.2, 145.5, 121.0, 113.0, 112.4, 56.7, 56.6, 41.2, 14.3, 11.8.

HR-MS: m/z calcd for $C_{13}H_{17}N_3O_3$ $[M+H]^+$ 263.1260, found $[M+Na]^+$ 286.2044.

Synthesis of 4-(benzo[*d*][1,3]dioxol-5-yl)-2,5-diethyl-2,4-dihydro-3*H*-1,2,4-triazol-3-one (D29)

Compound **D29** was obtained from compound **D18** by following the general procedure *k* as a brown solid (Yield: 98%). An analytical sample was purified by HPLC; RP-HPLC t_R= 24.0 min, gradient condition: from 5 % B to 100 % B over 50 min, flow rate of 3 mL/min, λ = 240 nm.

^{1}H NMR (400 MHz, CD_3OD) δ 6.85 (d, *J* = 8.2 Hz, 1H), 6.77 (d, *J* = 2.1 Hz, 1H), 6.72 (dd, *J* = 8.2, 2.1 Hz, 1H), 5.95 (s, 2H) 3.73 (q, *J* = 7.2 Hz, 2H), 2.37 (q, *J* = 7.5 Hz, 2H), 1.23 (t, *J* = 7.2 Hz, 3H), 1.03 (t, J = 7.5 Hz, 3H).

^{13}C NMR (100 MHz, CD_3OD) δ 154.9, 150.0, 149.9, 149.5, 127.5, 122.6, 109.6, 109.5, 103.6, 41.3, 19.9, 13.9, 10.3.

HR-MS: m/z calcd for $C_{13}H_{15}N_3O_3$ $[M+H]^+$ 261.1113, found $[M+Na]^+$ 284.1015.

Synthesis of 4-(4-(tert-butyl)phenyl)-2,5-dimethyl-2,4-dihydro-3*H*-1,2,4-triazol-3-one (D30)

Compound **D30** was obtained by following the general procedures *h* and *j* as a brown solid (Yield: 94%). An analytical sample was purified by HPLC; RP-HPLC t_R= 21.8 min, gradient condition: from 5 % B to 100 % B over 50 min, flow rate of 3 mL/min, λ = 240 nm.

^{1}H NMR (400 MHz, $CDCl_3$) δ 6.88 (d, *J* = 8.1 Hz, 1H), 6.74 (d, *J* = 1.8 Hz, 1H), 6.72 (dd, *J* = 8.1, 1.9 Hz, 1H), 6.04 (s, 2H), 3.47 (s, 3H), 2.11 (s, 3H).

^{13}C NMR (100 MHz, $CDCl_3$) δ 153.7. 148.7, 148.5, 143.2, 126.6, 121.1, 108.8, 108.3, 102.3, 32.5, 12.6.

HR-MS: m/z calcd for $C_{11}H_{11}N_3O_3$ $[M+H]^+$ 246.1528, found $[M+Na]^+$268.2179.

Synthesis of 4-(benzo[*d*][1,3]dioxol-5-yl)-5-ethyl-2-methyl-2,4-dihydro-3*H*-1,2,4-triazol-3-one (D31)

Compound **D31** was obtained by following the general procedures *i* and *j* as a brown solid (Yield: 87%). An analytical sample was purified by HPLC; RP-HPLC t_R= 22.5 min, gradient condition: from 5 % B to 100 % B over 50 min, flow rate of 3 mL/min, λ = 240 nm.

^{1}H NMR (400 MHz, $CDCl_3$) δ 6.88 (d, *J* = 8.0 Hz, 1H), 6.76 – 6.70 (m, 2H), 5.06 (s, 2H), 3.89 (q, *J* = 7.2 Hz, 2H), 2.13 (s, 3H), 1.39 (t, *J* = 7.2 Hz, 3H).

^{13}C NMR (100 MHz, $CDCl_3$) δ 153.2, 148.6, 148.3, 142.7, 126.8, 120.86, 108.6, 108.2, 102.3, 50.9, 40.3, 13.7.

HR-MS: m/z calcd for $C_{12}H_{13}N_3O_3$ $[M+H]^+$ 247.0957, found $[M+Na]^+$ 270.2435.

Synthesis of 4-(3-chloro-4-fluorophenyl)-5-ethyl-2-methyl-2,4-dihydro-3*H*-1,2,4-triazol-3-one (D32)

Compound **D32** was obtained from compound **D13** by following the general procedure *j*. Purification by silica gel (1:1 hexane/AcOEt) gave the pure compound as a yellow solid (Yield: 88%).

^{1}H NMR (400 MHz, $CDCl_3$) δ 7.65 (dd, *J* = 6.5, 2.5 Hz, 1H), 7.46 (t, *J* = 8.7 Hz, 1H), 7.43 – 7.39 (m, 1H), 3.46 (s, 3H), 2.50 (q, *J* = 7.5 Hz, 2H), 1.17 (t, *J* = 7.5 Hz, 3H).

^{13}C NMR (100 MHz, $CDCl_3$) δ 158.4 (d, *J* = 252.2 Hz), 153.4, 146.6, 129.8, 127.1 (d, *J* = 8.1 Hz), 122.5 (d, *J* = 19.0 Hz), 117.54 (d, *J* = 22.6 Hz), 32.4, 19.6, 10.0.

HR-MS: m/z calcd for $C_{11}H_{11}ClFN_3O$ $[M+H]^+$ 255.0575, found $[M+H]^+$278.0507.

Synthesis of 4-(3-chloro-4-fluorophenyl)-2,5-diethyl-2,4-dihydro-3*H*-1,2,4-triazol-3-one (D33):

Compound **D33** was obtained from compound **D13** by following the general procedure *k* as a yellow oil (Yield: 80.0%). An analytical sample was purified by HPLC; RP-HPLC t_R= 30.0 min.

^{1}H NMR (600 MHz, $CDCl_3$) δ 7.35 (dd, *J* = 6.4, 2.5 Hz, 1H), 7.21 (t, *J* = 8.6 Hz, 1H), 7.15 (dtd, *J* = 8.7, 2.6, 1.3 Hz, 1H), 3.81 (q, *J* = 7.2 Hz, 2H), 2.40 (q, *J* = 7.5 Hz, 2H), 1.31 (t, *J* = 7.2 Hz, 3H), 1.11 (t, J = 7.5 Hz, 3H).

^{13}C NMR (150 MHz, $CDCl_3$) δ 158.3 (d, *J* = 252.1 Hz), 155.6, 153.2, 129.8 (d, *J* = 13.1 Hz), 127.3 (d, *J* = 7.7 Hz), 127.2(d, *J* = 5.2 Hz),, 122.4 (d, J = 19.4 Hz), 117.7 (d, *J* = 22.2 Hz), 39.9, 19.6, 13.8, 10.1.

HR-MS: m/z calcd for $C_{12}H_{13}ClFN_3O$ $[M+H]^+$ 269.0731, found $[M+Na]^+$292.0618.

Synthesis of 4-(3-chloro-4-fluorophenyl)-2-ethyl-5-methyl-2,4-dihydro-3*H*-1,2,4-triazol-3-one (D34)

Compound **D34** was obtained by following the general procedures *h* and *k*. Purification by silica gel (1:1 hexane/AcOEt) gave the pure compound as a yellow oil (Yield: 73%).

^{1}H NMR (400 MHz, $CDCl_3$) δ 7.42 (dd, *J* = 6.4, 2.6 Hz, 1H), 7.30 – 7.27 (m, 1H), 7.21 (ddd, *J* = 8.8, 4.2, 2.5 Hz, 1H), 3.86 (q, *J* = 7.2 Hz, 2H), 2.16 (s, 3H), 1.38 (t, *J* = 7.2 Hz, 3H).

^{13}C NMR (100 MHz, $CDCl_3$) δ 158.3 (d, *J* = 252.0 Hz), 152.7, 142.2, 129.8, 129.6, 127.1, 122.5, 117.7, 40.54, 14.1, 12.7.

HR-MS: m/z calcd for $C_{11}H_{11}ClFN_3O$ $[M+H]^+$ 255.0575, found $[M+Na]^+$ 278.0507.

Synthesis of 2,5-diethyl-4-(3-(trifluoromethyl)phenyl)-2,4-dihydro-3*H*-1,2,4-triazol-3-one (D35)

Compound **D35** was obtained from compound **D16** by following the general procedure *k* as a brown solid (Yield: 89 %). An analytical sample was purified by HPLC; RP-HPLC t_R= 27.5 min, gradient condition: from 5 % B to 100 % B over 50 min, flow rate of 3 mL/min, λ = 240 nm.

^{1}H NMR (400 MHz, CD_3OD) δ 7.87 – 7.84 (m, 1H), 7.81 (s, 1H), 7.78 (dt, *J* = 7.7, 0.8 Hz, 1H), 7.71 (dt, *J* = 7.8, 1.7 Hz, 1H), 3.88 (q, *J* = 7.2 Hz, 2H), 2.54 (q, *J* = 7.5 Hz, 2H), 1.38 (t, *J* = 7.2 Hz, 3H), 1.16 (t, *J* = 7.5 Hz, 3H).

^{13}C NMR (100 MHz, CD_3OD) δ 152.9, 147.3, 133.7, 131.8 (q, *J* = 33.1 Hz), 125.7 (q, *J*=5,1 Hz), 124.2 (q, *J*= 4.9Hz), 123.5 (q, *J* = 105.0 Hz), 40.1, 19.2, 12.7, 8.7.

HR-MS: m/z calcd for $C_{13}H_{14}F_3N_3O$ $[M+H]^+$ 286.1089, found $[M+Na]^+$ 209.1120.

5.5 Synthesis of quinazolin-4(3*H*)-one derivatives

5.5.1 Chemistry general information

All commercially available starting materials were purchased from Sigma-Aldrich and were used as received. The solvents used for the synthesis were of HPLC grade (Sigma-Aldrich). NMR spectra were recorded on a Bruker Avance 400 MHz or 600MHz instrument at T = 298 K.

All the compounds were dissolved in 0.5 mL of $CDCl_3$, CD_3OD or DMSO-d_6 (Sigma-Aldrich, 99.98 Atom % D). Coupling constants (*J*) are reported in Hertz, and chemical shifts are expressed in parts per million (ppm) on the delta (δ) scale relative to solvent peak as internal reference. Reactions were monitored on silica gel 60 F plates (Merck) and visualized under UV light (λ = 254 nm, 365 nm). Analytical and semi-preparative reversed-phase HPLC was

performed on Agilent Technologies 1200 Series high performance liquid chromatography using a Fusion-RP, C reversed-phase column (100 × 2 mm, 4 µm, 80 Å, flow rate = 1 mL/min; 250 ×10.00 mm, 4 µm, 80 Å, flow rate= 4 mL/min respectively, Phenomenex). The binary solvent system (A/B) was as follows: 0.1 % TFA in water (A) and 0.1% TFA in CH_3CN (B). The absorbance was detected at 240 nm. The purity of all tested compound (>96%) were determined by HPLC analysis and NMR data.

5.5.2 General procedure *l* for the synthesis of compound E1

A solution of 2-amino-3-bromo-5-methylbenzoic acid (1 equiv, 2.2 mmol), EDC HCl (1.5 equiv, 13.0 mmol) and HOBt (1.65 equiv, 14.3 mmol) in dry DCM/DMF(10/1, 100ml) was treated with DIPEA (6.5 equiv, 56.7 mmol). The resulting mixture was stirred for 5 hours at room temperature under N2 atmosphere. After that NH_4Cl was added (3.25 equiv, 7.05 mmol), the reaction continued for 20h in the same conditions (**Scheme 15, Chapter 2**). The organic layer was washed with HCl 1N (3x15ml), dried over Na_2SO_4 and concentrated to obtain the final products. The crude was pure to use for the next step without any purification.

5.5.3 General procedure *m* for the synthesis of compounds E2A-E2J

A solution of 2-amino-3-bromo-5-methylbenzamide **(E1)** (1.0 equiv, 1 mmol) and selected benzaldehyde (1.2equiv, 1.2 mmol) in dry THF (30 mL) was stirred for 5h at reflux; then molecular I_2 (5 equiv, 5mmol) was added. The reaction was stirred over-night at reflux (**Scheme 15, Chapter 2**). Then, the mixture was diluted with DCM (20mL) and washed with a water solution of thiosulfate (2x10mL) and brine(2x10mL)., dried over anhydrous Na_2SO_4, filtered, and concentrated in vacuo.

The desired compounds were purified by silica gel using different mixtures of hexane/acetate depending on the polarity of the molecule.

5.5.4 General procedure *n* for the synthesis of compound E3

To a solution of 2-amino-3-bromo-5-methylbenzamide (**E1**) (1.0 equiv, 0.4mmol) in EtOH, *tert*-butyl hydroperoxide (3.85 equiv, 1.54 mmol) was added. The mixture was stirred over-night at reflux (**Scheme 15, Chapter 2**). After the competition of the reaction, the mixture was concentrated, diluted with CH_3Cl and washed for three times (3x10mL). The organic lower was dried over anhydrous Na_2SO_4, filtered and concentrated under reduced pressure to afford the crude product. The final product was obtained by silica gel purification using a mixture 65/35 hexane/ AcOEt.

5.5.5 General procedure *o* for the synthesis of compounds E4-15, E18-E24

8-bromo-6-methylquinazolin-4(3*H*)-one (1.0 equiv, 0.32 mmol), the selected boronic acid (1.5 equiv, 0.48 mmol), K_2CO_3 (3.0 equiv, 0.96 mmol) and tetrakis(triphenylphosphine)palladium(0) (0.2equiv, 0.064 mmol) were dissolved in a previously degassed mixture of 1,4-dioxane (80%) and water (20%) (20 mL) and stirred over-night at 80 °C under argon atmosphere (**Scheme 15, Chapter 2**). After the competition of the reaction, the mixture was diluted with dichloromethane and washed with brine (3x10mL). The organic lower was dried over anhydrous Na_2SO_4, filtered, and concentrated under reduced pressure to afford the crude product. The resulting residue was purified on a silica gel column chromatography eluting with different hexane/ethyl acetate mixture to give the final product.

5.5.6 General procedure *p* for the synthesis of compounds E16-E17

To solution of 6-methyl-2,8-diphenylquinazolin-4(3*H*)-one compound (1.0 equiv, 0.08mmol) in anhydrous DMF, NaH (1.5 equiv, 1.2 mmol) and CH_3I (1.5 equiv, 1.2 mmol) were added under nitrogen atmosphere. The reaction was stirred for 5 hours from 0°C to room temperature (**Scheme 15, Chapter 2**). After the competition of the reaction, the mixture solution was diluted with chloroform (20ml) and extracted with H_2O (3x10ml). After anhydrification and concentration in vacuo, the final products were obtained with 70-90% yield. HPLC purification was performed by semi-preparative reversed-phase HPLC (Fusion-RP, C-18 reversed-phase column: 250 ×10.00 mm, 4 µm, 80 Å, flow rate = 4 mL/min) using the gradient conditions reported below.

Synthesis of 2-amino-3-bromo-5-methylbenzamide (E1)

Compound **E1** was obtained by following the general procedure *l* as white solid (Yield: 97%).

^{1}H NMR (400 MHz, $CDCl_3$) δ 7.93 (s, 1H), 2.79 (s, 3H).

Synthesis of intermediate 8-bromo-2-(2-methoxyphenyl)-6-methylquinazolin-4(3*H*)-one (E2A)

Compound **E2A** was obtained from compound **E1** by following the general procedure *m* and purified by silica gel using a mixture of 6/4 hexane/ethyl acetate as eluent (Yield: 63%).

^{1}H NMR (400 MHz, CD_3OD) δ 8.29 (dd, *J* = 7.9, 1.8 Hz, 1H); 8.00 (s, 1H); 7.99 (s, 1H); 7.57 (ddd, *J* = 8.8, 7.3, 1.8 Hz, 1H); 7.23 (d, *J* = 8.4 Hz, 1H); 7.58 (t, *J* = 7.6 Hz, 1H); 4.04 (s, 3H); 2.48 (s, 3H).

Synthesis of 8-(3,5-difluorophenyl)-2-(2-methoxyphenyl)-6-methylquinazolin-4(3*H*)-one (E4)

Compound **E4** was obtained from compound **E2A** by following the general procedure *o* and purified by silica gel using a mixture of 1/1 hexane/ethyl acetate as eluent (Yield: 66%). A small sample for biological testing was further purified in HPLC, t_R=41.9 min, gradient condition: from 5 % B to 100 % B over 50 min, flow rate of 4 mL/min, λ=240nm.

^{1}H NMR (400 MHz, $CDCl_3$) δ 8.30 (dd, *J* = 8.0, 1.8 Hz, 1H); 8.12 (dd, *J* = 2.1, 1.0 Hz, 1H); 7.57 (d, *J* = 2.1 Hz, 1H); 7.44 (ddd, *J* = 8.3, 7.3, 1.8 Hz, 1H); 7.22 (m, 2H); 7.07 (ddd, *J* = 8.0, 7.3, 1.0 Hz, 1H); 7.01 (d, *J* = 8.3 Hz, 1H); 6.81 (tt, *J* = 9.0, 2.4 Hz, 1H); 4.02 (s, 3H); 2.56 (s, 3H).

^{13}C NMR (100 MHz, $CDCl_3$) δ 162.4 (dd, *J*= 246.0, 13.0 Hz, 2 C); 161.8; 157.9; 149.4; 144.2; 142.0 (t, *J*= 9.3 Hz); 136.8; 136.5; 136.3; 133.1; 131.5; 126.4; 122.0; 121.6; 119.8; 113.5 (d, *J*= 25.0 Hz, 2 C); 111.8; 102.5 (t, *J*= 25.0 Hz); 56.2; 21.3.

Synthesis of 8-(2-chloropyridin-4-yl)-2-(2-methoxyphenyl)-6-methylquinazolin-4(3*H*)-one (E5)

Compound **E5** was obtained from compound **E2A** by following the general procedure *o* and purified by silica gel using a mixture of 1/1 hexane/ethyl acetate as eluent (Yield:78%). A small sample for biological testing was further purified in HPLC, t_R=41.0min, gradient condition: from 5 % B to 100 % B over 50 min, flow rate of 4mL/min, λ=240nm.

^{1}H NMR (400 MHz, $CDCl_3$) δ 8.44 (dd, *J* = 5.1, 0.7 Hz, 1H); 8.29 (dd, *J* = 8.0, 1.8 Hz, 1H); 8.16 (dd, *J* = 2.1, 0.7 Hz, 1H); 7.70 (dd, *J* = 1.5, 0.7 Hz, 1H); 7.60 (dd, *J* = 2.2, 0.7 Hz, 1H); 7.53 (dd, *J* = 5.1, 1.5 Hz, 1H); 7.46 (ddd, *J* = 8.3, 7.3, 1.8 Hz, 1H); 7.08 (ddd, *J* = 8.0, 7.3, 1.0 Hz, 1H); 7.03 (d, *J* = 8.3 Hz, 1H); 4.03 (s, 3H); 2.51 (s, 3H).

^{13}C NMR (100 MHz, $CDCl_3$) δ 161.6; 158.0; 151.1; 149.8; 149.7; 148.8; 144.3; 136.4; 136.3; 134.9; 133.3; 131.5; 127.4; 125.8; 124.2; 122.0;121.7; 119.5; 111.9; 56.2; 21.3.

Synthesis of 8-(3-hydroxyphenyl)-2-(2-methoxyphenyl)-6-methylquinazolin-4(3*H*)-one (E6)

Compound **E6** was obtained from compound **E2A** by following the general procedure *o* and purified by methanol crystallization (Yield:54%).

^{1}H NMR (400 MHz, DMSO-d_6) δ 11.97 (s, 1H), 9.39 (s, 1H), 7.98 – 7.95 (m, 1H), 7.69 (dd, *J* = 7.6, 1.7 Hz, 1H), 7.63 (d, *J* = 2.0 Hz, 1H), 7.50 (ddd, *J* = 9.0, 7.5, 1.8 Hz, 1H), 7.22 (t, *J* = 7.8 Hz, 1H), 7.18 (d, *J* = 8.3 Hz, 1H), 7.07 – 7.03 (m, 3H), 6.75 (ddd, *J*=4.9, 2.3, 0.9 Hz 1H), 3.87 (s, 3H), 2.50 (s, 3H).

^{13}C NMR (100 MHz, DMSO-d_6) δ 161.6, 157.2, 156.7, 150.4, 143.9, 139.7, 139.0, 136.5, 135.9, 132.3, 130.6, 128.5, 124.6, 122.5, 121.3, 121.2, 120.5, 117.5, 114.1, 111.9, 55.8, 20.7.

Synthesis of intermediate 8-bromo-2-(furan-2-yl)-6-methylquinazolin-4(3*H*)-one (E2B)

Compound **E2B** was obtained from compound **E1** by following the general procedure *m* and purified by silica gel using a mixture of 7/3 hexane/ethyl acetate as eluent (Yield: 41%).

^{1}H NMR (400 MHz, $CDCl_3$) δ 7.87 (d, *J* = 1.0 Hz, 1H), 7.72 (d, *J* = 1.7 Hz, 1H), 7.48 (d, *J* = 1.0 Hz, 1H), 7.34 (d, *J* = 3.2 Hz, 1H), 6.49 (dd, *J* = 3.2, 1.7 Hz, 1H), 2.31 (s, 3H).

Synthesis of 2-(furan-2-yl)-8-(3-hydroxyphenyl)-6-methylquinazolin-4(3*H*)-one (E7)

Compound **E7** was obtained from compound **E2B** by following the general procedure *o* and purified by silica gel using a mixture of 1/1 hexane/ethyl acetate as eluent (Yield: 55%).

^{1}H NMR (400 MHz, CD_3OD) δ 8.00 (s, 1H); 7.74 (s, 1H); 7.65 (s, 1H); 7.26 (t, *J* = 7.8 Hz, 1H); 7.20 (d, *J* = 3.4 Hz, 1H); 7.12 (m, 2H); 6.82 (m, 1H); 6.63 (m, 1H); 2.50 (s, 3H).

^{13}C NMR (100 MHz, CD_3OD) δ 160.5; 154.0; 145.6; 143.7; 143.2; 140.4; 138.9; 137.5; 136.1; 135.6; 127.8; 124.7; 122.1; 120.6; 116.7; 113.2; 122.5; 112.0; 20.3.

Synthesis of intermediate 8-bromo-2-(isoquinolin-5-yl)-6-methylquinazolin-4(3*H*)-one (E2C)

Compound **E2C** was obtained from compound **E1** by following the general procedure *m* and purified by silica gel using a mixture of 6/4 hexane/ethyl acetate as eluent (Yield: 44%).

^{1}H NMR (400 MHz, MeOD) δ 9.19 (s, 1H), 8.40 (d, *J* = 6.2 Hz, 1H), 8.32 (d, *J* = 6.2 Hz, 1H), 8.06 (dd, *J* = 8.1, 1.2 Hz, 1H), 7.90 (dd, *J* = 7.3, 1.2 Hz, 1H), 7.85 – 7.79 (m, 1H), 7.60 (dd, *J* = 8.3, 7.2 Hz, 1H), 7.55 (dd, *J* = 2.0, 0.9 Hz, 1H), 7.37 (d, *J* = 2.0 Hz, 1H), 2.18 (s, 3H).

Synthesis of 8-(3-hydroxyphenyl)-2-(isoquinolin-5-yl)-6-methylquinazolin-4(3*H*)-one (E8)

Compound **E8** was obtained from compound **E2C** by following the general procedure *o* and purified by silica gel using ethyl acetate as eluent (Yield: 62%).

^{1}H NMR (400 MHz, DMSO-d_6) δ 12.69 (s, 1H), 9.41 (d, *J* = 9.6 Hz, 1H), 8.57 (d, *J* = 6.1 Hz, 1H), 8.34 (d, *J* = 6.0 Hz, 1H), 8.30 (d, *J* = 8.3 Hz, 1H), 8.11 (d, *J* = 7.2 Hz, 1H), 8.05 (s, 1H), 7.79 (t, *J* = 7.7 Hz, 1H), 7.67 (d, *J* = 2.1 Hz, 1H), 7.27 – 7.16 (m, 1H), 7.12 (s, 1H), 7.01 (d, *J* = 7.2 Hz, 2H), 6.76 – 6.69 (m, 1H), 3.17 (s, 3H), 2.54 (s, 3H).

^{13}C NMR (100 MHz, DMSO-d_6) δ 160.7, 158.3, 153.2, 151.2, 144.4, 144.2, 138.4, 137.6, 135.6, 136.6, 132.7, 130.8, 129.0, 126.8, 123.1, 123.0, 121.5, 118.1, 114.3,49.1, 20.9.

Synthesis of intermediate 8-bromo-2-cyclopropyl-6-methylquinazolin-4(3*H*)-one (E2D)

Compound **E2D** was obtained from compound **E1** by following the general procedure *m* and purified by silica gel using a mixture of 8/2 hexane/ethyl acetate as eluent (Yield: 56%).

^{1}H NMR (400 MHz, DMSO) δ 12.60 (s, 1H), 7.97 (d, *J* = 2.0 Hz, 1H), 7.91 (dd, *J* = 2.0 Hz, 1H), 2.48 (s, 3H), 2.03 (m, 1H), 1.19 (m, 2H), 1.11 (m, 2H).

Synthesis of 2-cyclopropyl-8-(3-hydroxyphenyl)-6-methylquinazolin-4(3*H*)-one (E9)

Compound **E9** was obtained from compound **E2D** by following the general procedure *o* (Yield: 61%) and purified by HPLC, t_R=25.0 min, gradient condition: from 5 % B to 100 % B over 50 min, flow rate of 4mL/min, λ=240nm

^{1}H NMR (400 MHz, $CDCl_3$) δ 7.97 (s, 1H), 7.51 – 7.44 (m, 1H), 7.44 – 7.34 (m, 1H), 7.11 – 7.04 (m, 1H), 7.04 – 6.95 (m, 1H), 6.81 – 6.71 (m, 1H), 2.41 (s, 3H), 0.94 (dq, *J* = 7.3, 4.0 Hz, 1H), 0.84 – 0.67 (m, 4H).

^{13}C NMR (100 MHz, DMSO-d_6) δ 162.9, 160.1, 158.4, 144.4, 138.2, 137.4, 131.6, 130.6, 125.6, 123.6, 120.5,115.7, 114.3, 29.8, 20.9, 9.4.

Synthesis of 8-(2-chlorophenyl)-2-cyclopropyl-6-methylquinazolin-4(3*H*)-one (E10)

Compound **E11** was obtained from compound **E2D** by following the general procedure *o* and purified by silica gel using a mixture of 7/3 hexane/ethyl acetate as eluent (Yield: 52%).

^{1}H NMR (400 MHz, DMSO-d_6) δ 12.37 (s, 1H), 7.92 (d, *J* = 2.1 Hz, 1H), 7.51 (dt, *J* = 6.9, 3.0 Hz, 1H), 7.48 (d, *J* = 2.2 Hz, 1H), 7.42 – 7.31 (m, 2H), 7.35 – 7.27 (m, 1H), 2.43 (s, 3H), 1.87 (qd, *J* = 7.3, 5.0 Hz, 1H), 0.94 – 0.67 (m, 4H).

^{13}C NMR (100 MHz, DMSO-d_6) δ 162.1, 157.9, 144.7, 137.8, 136.3, 135.8, 134.10, 133.3,131.9, 128.9, 128.7, 126.4, 125.2, 120.5, 20.2, 12.7, 9.4, 8.9

Synthesis of intermediate 2-(2-(benzyloxy)ethyl)-8-bromo-6-methylquinazolin-4(3*H*)-one (E2E)

Compound **E2E** was obtained from compound **E1** by following the general procedure *m* and purified by silica gel using a mixture of 7/3 hexane/ethyl acetate as eluent (Yield: 88%).

^{1}H NMR (400 MHz, DMSO) δ 12.36 (s, 1H), 7.96 (d, *J* = 2.0 Hz, 1H), 7.93 – 7.87 (d, *J* = 2.0 Hz, 1H), 7.35 – 7.16 (m, 5H), 4.52 (s, 2H), 3.90 (t, *J* = 6.4 Hz, 2H), 2.94 (t, *J* = 6.5 Hz, 2H), 2.42 (s, 3H).

Synthesis of compound 2-(2-(benzyloxy)ethyl)-8-(2-chloropyridin-4-yl)-6-methylquinazolin-4(3*H*)-one (E11)

Compound **E11** was obtained from compound **E2E** by following the general procedure *o* and purified by silica gel using a mixture of 8/2 hexane/ethyl acetate as eluent (Yield: 50%).

^{1}H NMR (400 MHz, DMSO-d$_6$) δ 12.38 (s, 1H), 8.51 – 8.45 (m, 1H), 8.10 – 8.05 (m, 1H), 7.86 (dd, *J* = 13.2, 1.8 Hz, 2H), 7.71 (dd, *J* = 5.1, 1.5 Hz, 1H), 7.38 – 7.23 (m, 5H), 4.53 (s, 2H), 3.89 (t, *J* = 6.3 Hz, 3H), 2.94 (t, *J* = 6.3 Hz, 3H), 2.55 (s, 4H), 2.49 (s, 0H), 1.29 (s, 1H).

^{13}C NMR (100 MHz, DMSO-d$_6$) δ 161.9, 155., 150.4, 149.8, 149.5, 144.2, 138.7, 136.7, 136.2, 133.7, 128.6(2C), 127.9(2C),127.8, 127.2, 125.7, 124.9, 121.9, 72.3, 66.9, 35.2, 21.2.

Synthesis of compound 2-(2-(benzyloxy)ethyl)-8-(2'-chloro-[2,4'-bipyridin]-4-yl)-6-methylquinazolin-4(3*H*)-one (E12)

Compound **E12** was obtained from compound **E2E** by following the general procedure *o* and purified by silica gel using a mixture of 7/3 hexane/ethyl acetate as eluent (Yield: 50%).

^{1}H NMR (400 MHz, DMSO-d$_6$) δ 12.37 (s, 1H), 8.80 (d, *J* = 5.0 Hz, 1H), 8.59 (d, *J* = 5.2 Hz, 1H), 8.46 (d, *J* = 1.5 Hz, 1H), 8.28 (d, *J* = 1.5 Hz, 1H), 8.19 (dd, *J* = 5.2, 1.5 Hz, 1H), 7.97 (d,

J = 2.1 Hz, 1H), 7.82 (dd, *J* = 5.0, 1.5 Hz, 1H), 7.38 – 7.24 (m, 3H), 7.21 (dd, *J* = 7.3, 2.2 Hz, 2H), 4.44 (s, 2H), 3.85 (t, *J* = 6.4 Hz, 3H), 2.61 – 2.53 (m, 6H).

^{13}C NMR (100 MHz, DMSO-d$_6$) δ 162.3, 152.1, 151.8, 151.1, 150.0, 149.7, 147.9, 144.2, 138.6, 136.8, 136.1, 134.7, 128.5(2C), 127.8, 127.7(2C), 126.8, 126.7, 123.5, 121.8, 121.6, 120.6, 72.2, 67.3, 35.3, 21.0.

Synthesis of intermediate 8-bromo-2-(2-chloro-3-hydroxyphenyl)-6-methylquinazolin-4(3*H*)-one (E2F)

Compound **E2F** was obtained from compound **E1** by following the general procedure *m* and purified by silica gel using a mixture of 6/4 hexane/ethyl acetate as eluent (Yield: 66%).

^{1}H NMR (400 MHz, DMSO-d$_6$) δ 12.76 (s, 1H), 10.58 (s, 1H), 8.07 (d, *J*=0.6Hz, 1H), 8.03 (d, *J*=0.6 Hz, 1H), 7.35 (td, *J* = 8.1, 1.7 Hz, 2H), 7.21 (d, *J* = 8.2 Hz, 1H), 7.13 (d, *J* = 7.5 Hz, 1H), 3.23 (d, *J* = 1.5 Hz, 3H).

Synthesis of compound 2-(2-chloro-3-hydroxyphenyl)-8-(3,5-dimethoxyphenyl)-6-methylquinazolin-4(3*H*)-one (E13)

Compound **E13** was obtained from compound **E2F** by following the general procedure *o* and purified by silica gel using a mixture of 6/4 hexane/ethyl acetate as eluent (Yield: 66%).

^{1}H NMR (400 MHz, DMSO-d$_6$) δ 8.00 (d, *J* = 2.0 Hz, 1H); 7.71 (d, *J* = 2.0 Hz, 1H); 7.24 (t, *J* = 7.8 Hz, 1H); 7.10 (dd, *J* = 8.2, 1.4 Hz, 1H); 7.03 (dd, *J* = 7.5, 1.4 Hz, 1H); 6.77 (d, *J* = 2.2 Hz, 2H); 6.46 (s, 1H); 3.74 (s, 6H); 2.50 (s, 3H).

^{13}C NMR (100 MHz, DMSO-d$_6$) δ 161.4; 159.7; 159.6; 153.4; 150.7; 143.5; 140.1; 138.5; 136.36; 136.30; 135.3; 127.4; 124.8; 121.6; 120.6; 118.4; 117.5; 108.5 (2 C); 99.3; 55.1 (2 C); 20.8.

Synthesis of intermediate 8-bromo-2,6-dimethylquinazolin-4(3*H*)-one (E3)

Compound **E3** was obtained from compound **E1** by following the general procedure *n* as white solid. Purification by silica gel using 65/35 hexane/ AcOEt gave the pure product (60%).

^{1}H NMR (400 MHz, DMSO) δ 7.94 (d, *J* = 2.0 Hz, 1H), 7.88 (d, *J* = 1.9 Hz, 1H), 2.43 (s, 3H), 2.40 (s, 3H).

Synthesis of compound 8-(furan-3-yl)-2,6-dimethylquinazolin-4(3*H*)-one (E14)

Compound **E14** was obtained from compound **E3** by following the general procedure *o* and purified by silica gel using a mixture of 6/4 hexane/ethyl acetate as eluent (Yield: 72%).

^{1}H NMR (400 MHz, DMSO-d$_6$) δ 12.21 (s, 1H), 8.66 (s, 1H), 7.92 (s, 1H), 7.82 – 7.72 (m, 2H), 7.17 (s, 1H), 2.45 (s, 3H), 2.41 (s, 3H).

^{13}C NMR (100 MHz, DMSO-d$_6$) δ 162.4, 152.8, 144.3, 143.4, 143.1, 135.6, 133.9, 128.7, 124.0, 122.4, 121.6, 110.5, 31.2, 22.2, 21.2.

Synthesis of compound 8-(3,5-dimethylisoxazol-4-yl)-2,6-dimethylquinazolin-4(3*H*)-one (E15)

Compound **E15** was obtained from compound **E3** by following the general procedure *o* (Yield: 55%) and purified by HPLC, t_R=26.0 min, gradient condition: from 5 % B to 100 % B over 50 min, flow rate of 4 mL/min, λ=240nm.

^{1}H NMR (400 MHz, CDCl$_3$) δ 9.39 (s, 1H), 7.93 (s, 1H), 7.03 (s, 1H), 3.13(s, *3*H), 2.65 (s, *3*H), 2.56 (s, 3H), 2,42(s, 3H).

^{13}C NMR (100 MHz, CDCl$_3$) δ 168.5, 160.7, 156.3, 154.5, 146.8, 137.2, 131.2, 124.7, 123.5, 120.2, 113.6, 21.3, 21.1,11.8,10.8.

Synthesis of compound 8-(3,5-dimethylisoxazol-4-yl)-2,3,6-trimethylquinazolin-4(3*H*)-one (E16)

Compound **E16** was obtained from compound **E15** by following the general procedure *p* and purified by silica gel using a mixture of 1/1 hexane/ethyl acetate as eluent (Yield: 57%). An analytical sample was further purified by HPLC, t_R=20.0 min, gradient condition: from 5 % B to 100 % B over 50 min, flow rate of 4 mL/min, λ=240nm.

^{1}H NMR (400 MHz, $CDCl_3$) δ 6.90 (d, *J* = 2.2 Hz, 1H), 6.82 (d, *J* = 2.2 Hz, 1H), 3.09 (s, 3H), 2.91 (s, 3H), 2.22 (s,3H), 2.21 (s,3H).

^{13}C (100 MHz, $CDCl_3$) δ 172.4, 165.4, 163.8, 162.2,159.4, 134.3,133.2,131.2, 128.8, 126.3, 39.7, 35.3, 20.5, 11.3,10.2.

Synthesis of compound 2-(2-(benzyloxy)ethyl)-8-(2-chloropyridin-4-yl)-3,6-dimethylquinazolin-4(3*H*)-one (E17)

Compound **E17** was obtained from compound **E11** by following the general procedure *p* and purified by methanol crystallization (Yield: 90%).

^{1}H NMR (400 MHz, DMSO-d_6) δ 8.46 (d, *J* = 5.2 Hz, 1H), 8.06 (s, 1H), 7.88 (s, 1H), 7.84 (s, 1H), 7.70 (d, *J* = 5.2 Hz, 1H), 7.25 – 7.13 (m, 5H), 4.48 (s, 2H), 3.78 – 3.69 (m, 2H), 3.63 (s, 3H), 2.82 – 2.70 (m, 2H), 2.48 (s,3H).

Synthesis of compound 2-(2-chloro-3-hydroxyphenyl)-8-(3-hydroxyphenyl)-6-methylquinazolin-4(3*H*)-one (E18)

Compound **E18** was obtained from compound **E2F** by following the general procedure *o* and purified by silica gel using 8/2 hexane/ethyl acetate as eluent (Yield: 72%). An analytical

sample was further purified by HPLC, t_R=36.0 min, gradient condition: from 5 % B to 100 % B over 50 min, flow rate of 4mL/min, λ=240nm.

^{1}H NMR (400 MHz, CD_3OD) δ 7.99 (d, *J* = 2.2 Hz, 1H), 7.59 (d, *J* = 2.1 Hz, 1H), 7.13 (td, *J* = 7.9, 5.7 Hz, 2H), 7.07 – 6.93 (m, 4H), 6.71 – 6.64 (m, 1H), 2.45 (s, 3H).

^{13}C (100 MHz, $CDCl_3$) δ 162.9, 156.6, 153.5,151.1, 143.5, 139.6, 139.5, 137.1, 136.9, 134.6, 128.5, 127.3, 124.5, 121.5, 121.1,117.8,117.1, 114.0,19.3.

Synthesis of compound 8-(3,5-dimethoxyphenyl)-2-(furan-2-yl)-6-methylquinazolin-4(3*H*)-one (E19)

Compound **E19** was obtained from compound **E2B** by following the general procedure *o* and purified by silica gel using 7/3 hexane/ethyl acetate as eluent (Yield: 80%).

^{1}H NMR (400 MHz, $CDCl_3$) δ 8.05 (dd, *J* = 2.1, 1.0 Hz, 1H), 7.61 (d, *J* = 2.2 Hz, 1H), 7.52 (dd, *J* = 1.8, 0.8 Hz, 1H), 7.14 (dd, *J* = 3.6, 0.8 Hz, 1H), 6.78 (d, *J* = 2.3 Hz, 2H), 6.52 (dd, *J* = 3.5, 1.7 Hz, 1H), 6.47 (t, *J* = 2.3 Hz, 1H), 3.79 (s, 6H), 2.46 (s, 3H).

^{13}C (100 MHz, $CDCl_3$) δ 162.1, 160.1(2C), 146.4, 144.8, 144.2, 141.5, 140.1, 137.3, 136.8, 125.8, 121.3, 113.5, 112.9, 108.7, 100.0, 91.8, 54.9(2C), 20.7.

Synthesis of compound 2-(2-(benzyloxy)ethyl)-8-(3,5-dimethoxyphenyl)-6-methylquinazolin-4(3*H*)-one (E20)

Compound **E20** was obtained from compound **E2E** by following the general procedure *o* and purified by silica gel using 7/3 hexane/ethyl acetate as eluent (Yield: 75%).

^{1}H NMR (400 MHz, CD_3OD) δ 8.08 (dd, *J* = 2.0, 1.0 Hz, 1H), 7.72 (d, *J* = 2.1 Hz, 1H), 7.24 (m, 3H), 7.17 (dd, *J* = 6.9, 2.7 Hz, 2H), 6.69 (d, *J* = 2.3 Hz, 2H), 6.55 (t, *J* = 2.3 Hz, 1H), 4.48 (s, 2H), 3.88 (t, *J* = 5.8 Hz, 2H), 3.80 (s, 6H), 3.07 (t, *J* = 5.9 Hz, 2H), 2.55 (s, 3H).

^{13}C NMR (100 MHz, CD_3OD) δ 161.3, 156.9, 138.8, 138.7,137.8, 137.7, 137.5, 137.2, 136.3, 128.0, 127.5, 127.4(2C), 125.2, 120.4, 107.9(2C),99.6, 72.5, 65.6, 54.6(2C), 33.1, 19.6.

Synthesis of intermediate 8-bromo-2-(3-hydroxy-4-nitrophenyl)-6-methylquinazolin-4(3*H*)-one (E2G)

Compound **E2G** was obtained from compound **E1** by following the general procedure *m* and purified by ethyl acetate crystallization (Yield: 89%).

^{1}H NMR (400 MHz, DMSO) δ 8.06 (d, *J* = 2.0 Hz, 1H), 8.03 (d, *J* = 8.6 Hz, 1H), 7.97 (d, *J* = 1.9 Hz, 1H), 7.94 (d, *J* = 1.8 Hz, 1H), 7.70 (dd, *J* = 8.7, 1.9 Hz, 1H), 2.47 (s, 3H).

Synthesis of compound 8-(3,5-dimethoxyphenyl)-2-(3-hydroxy-4-nitrophenyl)-6-methylquinazolin-4(3*H*)-one (E21)

Compound **E21** was obtained from compound **E2G** by following the general procedure *o* and purified by methanol crystallization (Yield: 82%).

^{1}H NMR (400 MHz, DMSO-d_6) δ 8.03 – 7.95 (m, 2H), 7.76 (d, *J* = 2.7 Hz, 2H), 7.58 (d, *J* = 8.8 Hz, 1H), 6.86 (d, *J* = 2.3 Hz, 2H), 6.59 – 6.50 (m, 1H), 3.80 (s, 6H), 2.52 (s, 3H).

^{13}C NMR (100 MHz, DMSO-d_6) δ 167.5, 160.2,(2C), 149.6, 149.4, 143.8, 140.6, 139.3, 139.2, 138.6, 137.7, 137.1, 137.0, 125.9, 125.4, 119.9, 117.7, 109.2(2C), 100.3, 55.3(2C), 21.3.

Synthesis of intermediate 8-bromo-2-(4-hydroxyphenyl)-6-methylquinazolin-4(3*H*)-one (E2H)

Compound **E2H** was obtained from compound **E1** by following the general procedure *m* and purified by silica gel using 1/1 hexane/ethyl acetate as eluent (Yield: 66%).

^{1}H NMR (400 MHz, $CDCl_3$) δ 7.92 (d, *J* = 2.1 Hz, 1H), 7.78 – 7.74 (m, 2H), 7.72 – 7.70 (m, 1H), 6.96 – 6.92 (m, 2H), 2.46 (s, 3H).

Synthesis of compound 8-(3,5-dimethoxyphenyl)-2-(4-hydroxyphenyl)-6-methylquinazolin-4(3*H*)-one (E22)

Compound **E22** was obtained from compound **E2H** by following the general procedure *o* and purified by methanol crystallization (Yield: 90%).

^{1}H NMR (400 MHz, DMSO-d_6) δ 8.07 – 8.00 (m, 2H), 7.94 (s, 1H), 7.67 (s, 1H), 6.90 (t, *J* = 2.1 Hz, 2H), 6.83 (dt, *J* = 8.7, 2.3 Hz, 2H), 6.54 (q, *J* = 2.2 Hz, 1H), 3.82 – 3.73 (m, 6H), 2.48 (s, 3H).

^{13}C NMR (100 MHz, DMSO-d_6) δ 161.8, 161.7, 160.6, 158.6, 154.8, 144.5, 139.1, 137.7, 133.9, 130.2, 129.6, 126.2, 125.3, 124.2, 123.2, 116.2, 116.1, 102.4(2C), 97.4(2C), 55.8, 21.1.

Synthesis of intermediate 8-bromo-2-(4-methoxyphenyl)-6-methylquinazolin-4(3*H*)-one (E2I)

Compound **E2I** was obtained from compound **E1** by following the general procedure *m* and purified by silica gel using 1/1 hexane/ethyl acetate as eluent (Yield: 75%).

^{1}H NMR (400 MHz, DMSO-d_6) δ 7.92 (d, *J* = 2.2 Hz, 0H), 7.76 – 7.73 (m, 1H), 7.71 – 7.69 (m, 0H), 7.07 – 7.02 (m, 1H), 3.80 (s, 1H), 2.46 (s, 1H).

Synthesis of compound 8-(3,5-dimethoxyphenyl)-2-(4-methoxyphenyl)-6-methylquinazolin-4(3*H*)-one (E23)

Compound **E23** was obtained from compound **E2I** by following the general procedure *o* and purified by silica gel using 6/4 hexane/ethyl acetate as eluent (Yield: 80%).

^{1}H NMR (400 MHz, DMSO-d_6) δ 9.95 (s, 1H), 7.99 (s, 1H), 7.72 (d, *J* = 2.1 Hz, 1H), 7.53 – 7.48 (m, 2H), 6.86 (d, *J* = 8.6 Hz, 2H), 6.84 (d, *J* = 2.3 Hz, 2H), 6.48 (t, *J* = 2.3 Hz, 1H), 4.04 (dt, *J* = 1.7, 0.9 Hz, 3H), 3.77 (s, 6H), 3.43 (s, 4H).

^{13}C NMR (100 MHz, DMSO-d_6) δ 162.7, 159.9, 151.3, 150.5, 143.2, 143.1, 138.2, 136.2, 133.7, 130.7 (2C), 128.3, 125.6, 115.5 (2C), 108.9(2C), 101.4, 99.5, 55.1(2C), 34.2, 20.7.

Synthesis of compound 8-(3,5-dimethoxyphenyl)-2,6-dimethylquinazolin-4(3*H*)-one (E24)

Compound **E24** was obtained from compound **E3** by following the general procedure *o* and purified by silica gel using 8/2 hexane/ethyl acetate as eluent (Yield: 72%).

^{1}H NMR (400 MHz, DMSO-d_6) δ 12.15 (s, 1H), 7.89 (dd, *J* = 2.1, 1.0 Hz, 1H), 7.61 (t, *J* = 2.3 Hz, 1H), 6.73 (d, *J* = 2.3 Hz, 2H), 6.50 (t, *J* = 2.3 Hz, H), 3.77 (s, 6H), 2.44 (s, 3H), 2.28 (s, 3H).

^{13}C NMR (100 MHz, DMSO-d_6) δ 162.3, 160.1(2C), 152.9, 144.3, 140.9, 138.0, 136.7, 135.4, 125.1, 109.04(2C), 99.5, 55.5(2C), 22.2, 21.2.

5.6 In vitro Alpha Screen assay

The binding of synthesized compounds against BRD9 has been measured by Alpha Screen Technology through BRD9 (BD1) Inhibitor Screening Assay Kit (BSP-32519). Anti-GST-coated acceptor beads were used to capture the GST-fusion BRD9, whereas the biotinylated-H4 peptide (BET bromodomain ligand) was captured by the streptavidin donor beads. Upon illumination at 680 nm, chemical energy is transferred from donor to acceptor beads across the complex streptavidin-donor/H4-biotin/GST-BRD9/anti-GST-acceptor and a signal is

produced. The assay has been performed in white, 384-well Optiplates (Perkin Elmer) using a final volume of 30 µL containing final concentrations of 50 nM of purified GST-tagged BRD9 protein (BSP-31091), 1 µL of BET bromodomain ligand (BSP-33000), 10 µL of 250-fold diluted Glutathione AlphaLISA Acceptor Beads (PerkinElmer #AL109C) and 10µL of 15-fold diluted Streptavidin Donor Bead (PerkinElmer #6760002). The concentration of DMSO in each well was maintained at a final concentration of 2%. The stimulation times with 10 µL of tested compound (each at final concentrations of 10 and 1 µM) were fixed to 30 min at room temperature. After the addition of the detection acceptor bead,s the plates were incubated in the dark for 30 min at room temperature and finally read in an Enspire microplate analyzer (Perkin Elmer).

CHAPTER 6
Computational details and synthetic procedures of new inhibitors of the arachidonic acid cascade enzyme

6.1 Synthesis of thiazolidin-4-one-based compounds

6.1.1 Chemistry general information

NMR spectra (^{1}H, ^{13}C) were recorded on a Bruker Avance DRX400, Bruker Avance DRX500, Bruker Avance DRX600 and Varian Inova500 NMR spectrometers at T=298K. The compounds were dissolved in 0.5 mL of $CDCl_3$ (Aldrich, 99.8+ Atom% D), DMSO-d_6 (Aldrich, 99.8+ Atom% D). Coupling constants (*J*) are reported in Hertz, and chemical shifts are expressed in parts per million (ppm) on the delta (δ) scale relative to $CDCl_3$ (7.16 ppm for ^{1}H and 77.20 ppm for ^{13}C) or DMSO-d_6 (2.50 ppm for ^{1}H and 39.52 ppm for ^{13}C) as the internal reference. Multiplicities are reported as follows: s, singlet; d, doublet; t, triplet; m, multiplet; dd, doublet of doublets. ^{13}C DEPTQ experiments (dept polarization transfer with decoupling during acquisition using shaped pulse for 180 degree pulse on f1channel) were acquired at 100 MHz or 125MHz and referenced to the internal solvent signal. High Resolution Mass Spectrometry spectra (HRMS) were performed on a LTQ-Orbitrap XL (Thermo Fisher Scientific, Bremen, Germany) mass spectrometer, with electrospray ionization (ESI). HPLC was performed using a Waters Model 510 pump equipped with Waters Rheodine injector and a differential refractometer, model 401. All the solvents used for the synthesis were HPLC grade; they were purchased from Aldrich and VWR. The reagents for the synthesis were purchased from Sigma Aldrich and Zentek S.r.l. and used as received. Toluene was distilled from calcium hydride immediately prior to use.

Reaction progress was monitored via thin-layer chromatography (TLC) on Alugram® silica gel G/UV254 plates.

6.1.2 General procedure *q* for the synthesis of compounds F1-F23

The synthetic strategy of the targeted molecules involves a one-pot multicomponent reaction as depicted in **Scheme 18** (**Chapter 3**). 2-amino-1-phenylethanone (1 equiv, 0.30 mmol), an

excess of 2-mercaptoacetic acid and substituted-benzaldehyde (1 equiv, 0.30 mmol) were dissolved in dry toluene (10 mL) and stirred under reflux. The reaction time and the excess of 2-mercaptoacetic acid used are shown in (**Chapter 3**). After the competition of the reaction, the solvent was evaporated, the mixture was diluted with ethyl acetate and washed with sat. $NaHCO_3$ (10 mL), brine (10mL) and 0.5N HCl (10ml).

The organic lower was dried over anhydrous Na_2SO_4, filtered, and concentrated under reduced pressure to afford the crude product. The resulting residue was purified on a silica gel column chromatography using different mixtures of hexane/ethyl acetate as eluent. The purity of synthesized compounds was determined by HPLC. All compounds for biological testing were >95% pure.

Synthesis of 3-(2-(4-bromophenyl)-2-oxoethyl)-2-(2,6-dichlorophenyl)thiazolidin-4-one (F1)

Purification by silica gel (95:5 hexane/AcOEt) gave compound F**1** (Yield: 92%). An analytic sample of F**1** was obtained through purification with HPLC on a Phenomenex C18 (5 μm; 10 mm i.d. x 250 mm), with MeOH/H_2O (95:5) as eluent (flow rate 3 mL/min) (t_R = 5.0 min).

^{1}H NMR (400 MHz, DMSO-d_6) δ 7.91 (d, *J* = 8.5 Hz, 2H), 7.71 (d, *J* = 8.5 Hz, 2H), 7.54 (dd, *J* = 7.8 Hz, 1.3 Hz, 1H), 7.48 (dd, *J* = 8.0, 1.3 Hz, 1H), 7.42 (t, *J* = 8.0 Hz, 1H), 6.63 (s, 1H), 5.10 (d, *J* = 18.2 Hz, 1H), 4.13 (d, *J* = 18.2 Hz, 1H), 3.91 (s, 2H).

^{13}C NMR (100 MHz, DMSO-d_6) δ 193.3, 171.6, 135.6, 134.8, 133.7, 132.3 (2C), 132.0, 131.7, 131.7, 130.6 (2C), 129.6, 128.7, 58.4, 49.3, 33.7.

HR-MS: m/z calcd for $C_{17}H_{12}BrCl_2NO_2S$ $[M+H]^+$445.9129; $[M+Na]^+$467.9006.

Synthesis of 3-(2-(4-bromophenyl)-2-oxoethyl)-2-(3,5-dibromo-4-hydroxyphenyl)thiazolidin-4-one (F2)

Purification by silica gel (9:1 hexane/AcOEt) gave compound **F2** (Yield: 89%). An analytic sample of **F2** was obtained through purification with HPLC on a Nucleodur 100-5 (5 μm; 10 mm i.d. x 250 mm), with hexane/AcOEt (40:60) as eluent (flow rate 3 mL/min) (t_R = 6.0 min).

^{1}H NMR (400 MHz, DMSO-d$_6$) δ 7.88 (d, *J* = 8.4 Hz, 2H), 7.73 (d, *J* = 8.3 Hz, 2H), 7.59 (s, 2H), 5.69 (s, 1H), 4.94 (d, *J* = 15.4 Hz, 1H), 4.25 (d, *J* = 14.3 Hz, 1H), 4.02 (d, *J* = 15.6 Hz, 1H) 3.74 (d, *J* = 15.6 Hz, 1H).

^{13}C NMR (100 MHz, DMSO-d$_6$) δ 192.7, 171.6, 151.4, 134.2, 133.7, 132.0 (2C), 131.5 (2C), 130.2 (2C), 128.2, 112.1 (2C), 61.1, 49.5, 32.3.

HR-MS: m/z calcd for $C_{17}H_{12}Br_3NO_3S$ [M+H]+ 551.8047; found $[M+Na]^+$ 573.7986.

Synthesis of 3-(2-(4-bromophenyl)-2-oxoethyl)-2-(3-chloro-5-fluoro-4-hydroxyphenyl)thiazolidin-4-one (F3)

Purification by silica gel (85:15 hexane/AcOEt) gave compound **F3** (Yield: 77%). An analytic sample of **F3** was obtained through purification with HPLC on a Nucleodur 100-5 (5 μm; 10 mm i.d. x 250 mm), with hexane/AcOEt (40:60) as eluent (flow rate 3 mL/min) (t_R = 6.0 min).

^{1}H NMR (400 MHz, DMSO-d$_6$) δ 7.88 (d, *J* = 8.5 Hz, 2H), 7.73 (d, *J* = 8.5 Hz, 2H), 7.28 (s, 2H), 5.71 (s, 1H), 4.95 (d, *J* = 18.2 Hz, 1H), 4.25 (d, *J* = 18.2 Hz, 1H), 4.06 (d, *J* =15.6, 1H), 3.74 (d, *J* = 15.6 Hz, 1H).

^{13}C NMR (100 MHz, DMSO-d$_6$) δ 192.1, 171.1, 152.2 (d, *J* = 242.6 Hz), 141.9 (d, *J* = 16.5 Hz), 133.5, 131.9 (2C), 131.4(d, *J* = 6.4 Hz), 130.1 (2C), 128.0, 124.4, 121.9 (d, *J* = 4.5 Hz), 114.8 (d, *J* = 20.02 Hz), 61.8, 49.11, 31.08.

HR-MS: m/z calcd for $C_{17}H_{12}BrClFNO_3S$ [M+H]+ 445.9394; found $[M+Na]^+$467.9250.

Synthesis of 3-(2-(4-bromophenyl)-2-oxoethyl)-2-(4-hydroxy-3-(trifluoromethyl)phenyl)thiazolidin-4-one (F4)

Purification by silica gel (85:15 hexane/AcOEt) gave compound **F4** (Yield: 71%). An analytic sample of **F4** was obtained through purification with HPLC on a Nucleodur 100-5 (5 μm; 10 mm i.d. x 250 mm), with hexane/AcOEt (40:60) as eluent (flow rate 3 mL/min) (t_R = 9.0 min).

^{1}H NMR (500 MHz, $CDCl_3$) δ 7.64 (d, *J* = 8.5 Hz, 2H), 7.53 (d, *J* = 8.5 Hz, 2H), 7.42 (s, 1H), 7.34 (m, 1H), 6.90 (d, *J* = 8.4 Hz, 1H), 5.81 (s, 1H), 5.05 (d, *J* = 17.8 Hz, 1H), 3.85 (d, *J* = 15.8 Hz, 1H), 3.78 (m, 2H).

^{13}C NMR (125 MHz, $CDCl_3$) δ 193.9, 172.3, 155.4, 133.3, 133.1, 132.4(2C), 132.3,129.6(2C), 126.7, 126.6(q, *J*=103.6 Hz), 119.09, 118.0.(q, *J*=52.2 Hz),118.4, 63.5, 52.8, 33.5.

HR-MS: m/z calcd for $C_{18}H_{13}BrF_3NO_3S$ $[M+H]^+$ 461.9752; found $[M+Na]^+$ 483.9687.

Synthesis of 3-(2-(4-bromophenyl)-2-oxoethyl)-2-(4-chlorophenyl)thiazolidin-4-one (F5)

Purification by silica gel (9:1 hexane/AcOEt) gave compound **F5** (Yield: 87%). An analytic sample of **F5** was obtained through purification with HPLC on a Nucleodur 100-5 (5 μm; 10 mm i.d. x 250 mm), with hexane/AcOEt (40:60) as eluent (flow rate 3 mL/min).

^{1}H NMR (400 MHz, $CDCl_3$) δ 7.63 (d, *J* = 8.6 Hz, 2H), 7.52 (d, , *J* = 8.6 Hz, 2H), 7.28 (d, *J* = 7.9 Hz, 2H), 7.21 (d, *J* = 7.9 Hz, 2H), 5.80 (s, 1H), 5.07 (d, *J* = 17.8 Hz, 1H), 3.81 – 3.79 (m, 1H), 3.75 (d, *J* = 7.0 Hz, 1H).

^{13}C NMR (100 MHz, $CDCl_3$) δ 191.9, 172.5, 136.5, 135.5, 133.2, 133.2, 132.2 (2C), 129.5 (2C), 129.4 (2C), 129.2 (2C), 63.3, 48.6, 29.8.

HR-MS: m/z calcd for $C_{17}H_{13}BrClNO_2S$ $[M+H]^+$ 411.9539; found $[M+K]^+$ 450.9351.

Synthesis of 3-(2-(4-bromophenyl)-2-oxoethyl)-2-(2-chloro-4-methylphenyl)thiazolidin-4-one (F6)

Purification by silica gel (9:1 hexane/AcOEt) gave compound **F6** (Yield: 91%). An analytic sample of **F6** was obtained through purification with HPLC on a Nucleodur 100-5 (5 μm; 10 mm i.d. x 250 mm), with hexane/AcOEt (40:60) as eluent (flow rate 3 mL/min) (t_R = 6.5 min).

^{1}H NMR (400 MHz, $CDCl_3$) δ 7.76 (d, *J* = 8.6 Hz, 2H), 7.61 (d, *J* = 8.5 Hz, 2H), 7.29 (m, 2H), 7.15 (d, *J* = 7.8 Hz, 1H), 6.29 (s, 1H), 5.11 (d, *J* = 17.7 Hz, 1H), 3.94 (d, *J* = 17.7 Hz, 1H), 3.86 (m, 2H), 2.26 (s, 3H).

^{13}C NMR (100 MHz, $CDCl_3$) δ 192.1, 172.7, 140.9, 133.5, 133.4, 132.8, 132,4 (2C), 131.0, 129.7 (2C), 129.4, 128.8, 128.5, 60.5, 49.2, 32.0, 20.6.

HR-MS: m/z calcd for $C_{18}H_{15}BrClNO_2S$ [M+ H] 425.9695; found $[M+H]^+$ 426.0074.

Synthesis of 3-(2-(4-bromophenyl)-2-oxoethyl)-2-(4-(dimethylamino)phenyl)thiazolidin-4-one (F7)

Pure compound **F7** was obtained through purification with HPLC on a Nucleodur 100-5 (5 μm; 10 mm i.d. x 250 mm), with hexane/AcOEt (40:60) as eluent (flow rate 3 mL/min) (t_R = 7.0 min) (Yield= 45%).

^{1}H NMR (400 MHz, $CDCl_3$) δ 7.63 (d, *J* = 8.4 Hz, 2H), 7.51 (d, *J* = 8.3 Hz, 2H), 7.12 (d, *J* = 8.5 Hz, 2H), 6.59 (d, *J* = 8.5 Hz, 2H), 5.78 (s, 1H), 5.02 (d, *J* = 17.7 Hz, 1H), 3.84 (d, *J* = 8.2 Hz, 1H), 3.81 (d, *J* = 6.3 Hz, 1H), 3.73 (d, *J* = 17.5 Hz, 1H), 2.90 (s, 6H).

^{13}C NMR (100 MHz, $CDCl_3$) δ 190.7, 172.4, 147.2, 132.7(2C), 129.7(2c), 124.8(2C), 117.7(2C), 114.3(2C),63.8, 51.4, 43.8(2C), 32.7.

HR-MS: m/z calcd for $C_{19}H_{19}BrN_2O_2S$ $[M+ H]^+$ 419.0351; found $[M+Na]^+$ 442.0286.

Synthesis of 3-(2-(4-bromophenyl)-2-oxoethyl)-2-(3-((2-chlorobenzyl)oxy)-4-methoxyphenyl)thiazolidin-4-one (F8)

Purification by silica gel (85:15 hexane/AcOEt) gave compound **F8** (Yield: 68%). An analytic sample of **F8** was obtained through purification with HPLC on a Phenomenex C18 (5 μm; 10 mm i.d. x 250 mm), with MeOH/H_2O (95:5) as eluent (flow rate 3 mL/min) (t_R = 5.0 min).

^{1}H NMR (500 MHz, $CDCl_3$) δ 7.59 (d, *J* = 8.4 Hz, 2H), 7.51 (d, *J* = 8.6 Hz, 2H), 7.32 (d, J = 2.3 Hz, 1H), 7.20, 7.17 (m, 4H), 6.81 (dd, *J* = 8.1 Hz, 2.3 Hz, 1H), 6.76 (d, *J* = 8.1 Hz, 1H), 5.74 (s, 1H), 5.23 (d, *J* = 5.1 Hz, 2H), 4.99 (d, *J* = 17.7 Hz, 1H), 3.89 (s, 3H), 3.87 (d, *J* = 17.6 Hz, 2H), 3.76 (t, *J* = 17.1 Hz, 2H).

^{13}C NMR (125 MHz, $CDCl_3$) δ 193.7, 172.1, 149.2, 147.7, 135.3, 134.1, 133.2, 132.2(2C), 131.5(2C), 129.8,129.5, 129.3, 126.8, 121.3, 113.7,112.9, 70.2, 62.1, 55.9, 51.7, 33.3.

HR-MS: m/z calcd for $C_{25}H_{21}BrClNO_4S$ $[M+H]^+$ 548.0063; found $[M+K]^+$ 570.0099.

Synthesis of 2-(2,4-dichlorophenyl)-3-(2-(4-methoxyphenyl)-2-oxoethyl)thiazolidin-4-one (F9)

Purification by silica gel (8:2 hexane/AcOEt) gave compound **F9** (Yield: 95%). An analytic sample of **F9** was obtained through purification with HPLC with hexane/acetate (40:60) as eluent (flow rate 3mL/min) (t_R = 5.5 min).

^{1}H NMR (400 MHz, DMSO-d_6) δ 7.98 (d, *J* = 6.7, 2H), 7.58 (d, *J* = 6.2, 2H), 7.56 (dd, *J* = 4.5, 1.5 Hz, 1H), 7.50 (dd, *J* = 4.5, 1.5 Hz, 1H), 7.41 (m, 1H), 6.62 (s, 1H), 5.10 (d, *J* = 18.2 Hz, 1H), 4.14 (d, *J* = 18.2 Hz, 1H), 3.91 (s, 2H).

^{13}C NMR (100 MHz, DMSO-d_6) δ 192.8, 171.1, 139.0, 135.1, 134.3, 132.9, 131.5, 131.3, 131.2, 130.0 (2C), 129.1, 128.9 (2C), 57.9, 48.8, 32.7.

HR-MS: m/z calcd for $C_{17}H_{12}Cl_3NO_2S$ [M+H]+ 401.9654; found $[M+Na]^+$423.9598.

Synthesis of 3-(2-(4-chlorophenyl)-2-oxoethyl)-2-(3-fluoro-4-hydroxy-5-methoxyphenyl)thiazolidin-4-one (F10)

Purification by silica gel (85:15 hexane/AcOEt) gave compound **F10** (Yield: 74%).

^{1}H NMR (400 MHz, DMSO-d_6) δ 7.97 (d, *J* = 10.0 Hz 2H), 7.59 (d, *J* = 9.8 Hz 2H), 6.87 (d, *J* = 1.9 Hz, 1H), 6.84 (s, 1H), 5.73 (s, 1H), 5.00 (d, *J* = 18.7 Hz, 1H), 4.19 (d, *J* = 18.7 Hz, 1H), 3.99 (d, *J* = 9.7 Hz, 1H), 3.93 (d, *J* = 9.7 Hz, 1H), 3.77 (s, 3H).

^{13}C NMR (100 MHz, DMSO-d_6) δ 192.3, 171.4, 170.6, 151.2 (d, *J* = 238.7 Hz), 149.5 (d, *J* = 6.4 Hz), 138.8, 134.8 (d, *J* = 14.2 Hz), 133.2, 130.3 (2C), 129.9 (2C), 129.5 (d, *J* = 7.7 Hz), 128.9 (2C), 107.7 (d, *J* = 20.3 Hz), 107.1, 62.6, 56.1, 49.2, 31.7.

HR-MS: m/z calcd for $C_{18}H_{15}ClFNO_4S$ $[M+H]^+$ 396.0394; found $[M+Na]^+$ 418.1628.

Synthesis of 2-(3-((2-chloro-6-fluorobenzyl)oxy)-4-methoxyphenyl)-3-(2-(4-chlorophenyl)-2-oxoethyl)thiazolidin-4-one (F11)

Purification by silica gel (9:1 hexane/AcOEt) gave compound **F11** (Yield: 89%).

^{1}H NMR (400 MHz, $CDCl_3$) δ 7.61 (d, *J* = 8.3 Hz, 2H), 7.25 (d, *J* = 8.2 Hz, 2H), 7.09 (dd, *J* = 8.6,1.9 Hz, 1H), 7.08 – 7.01 (m, 1H), 6.87 (s, 1H), 6.84 (t, *J* = 8.6 Hz, 1H), 6.73 (d, *J* = 8.1 Hz, 1H), 6.63 (d, *J* = 8.2 Hz, 1H), 5.67 (s, 1H), 5.06 (s, 2H), 4.91 (d, *J* = 17.8 Hz, 1H), 3.73 (dd, *J* = 15.3, 6.3 Hz, 2H), 3.69, 3.61 (m, 4H).

^{13}C NMR (100 MHz, $CDCl_3$) δ 191.9, 172.2, 164.2, 161.0, 150.0(d, *J* = 280.3 Hz), 140.8, 136.5(d, *J* = 5.1 Hz), 130.7(d, *J* = 9.9 Hz), 129.4(2C), 129.2(2C), 125.6(d, *J* = 3.6 Hz), 122.3(d, *J* = 5.8 Hz), 122.1, 114.4, 114.3, 111.8, 64.2, 62.9, 55.9, 48.8, 32.9.

HR-MS: m/z calcd for $C_{25}H_{20}Cl_2FNO_4S$ $[M+ H]^+$ 520.0474, found $[M+H]^+$ 520.0500.

Synthesis of 2-(3,5-dibromo-4-hydroxyphenyl)-3-(2-(4-methoxyphenyl)-2-oxoethyl)thiazolidin-4-one (F12)

Purification by silica gel (8:2 hexane/AcOEt) gave compound **F12** (Yield: 86%).

^{1}H NMR (400 MHz, DMSO-d_6) δ 7.92 (d, *J* =8.7 Hz, 2H), 7.58 (s, 2H), 7.02 (d, *J* =8.7, 2H), 5.70 (s, 1H), 4.93 (d, *J* = 18.0 Hz, 1H), 4.16 (d, *J* = 18.0 Hz, 1H), 4.00 (d, *J* = 15.6 Hz, 1H), 3.83 (s, 3H), 3.71 (d, *J* = 15.6 Hz, 1H).

^{13}C NMR (100 MHz, DMSO-d_6) δ 191.2, 171.4, 163.7, 151.3, 133.9, 131.6 (2C), 130.5 (2C), 127.5, 114.1 (2C), 112.1(2C), 61.6, 55.5, 48.9, 31.8.

HR-MS: m/z calcd for $C_{18}H_{15}Br_2NO_4S$ [M+H]+ 501.9068; found $[M+Na]^+$523.8943.

Synthesis of 2-(3-chloro-5-fluoro-4-hydroxyphenyl)-3-(2-(4-methoxyphenyl)-2-oxoethyl)thiazolidin-4-one (F13)

Purification by silica gel (8:2 hexane/AcOEt) gave compound **F13** (Yield: 90 %).

^{1}H NMR (400 MHz, DMSO-d_6) δ 7.97 (d, *J* = 6.8, 2H), 7.32 (s, 2H), 7.06 (d, *J* = 8.9 Hz, 1H), 5.75 (s, 1H), 4.98 (d, *J* = 18.0 Hz, 1H), 4.18 (d, *J* = 6.5 Hz, 1H), 4.04 (dd, *J* = 15.6, 18 Hz, 1H), 3.87 (s, 3H), 3.80 (d, J=6.8Hz, 1H).

^{13}C NMR (100 MHz, DMSO-d_6) δ 191.2, 171.1, 163.6, 151.9 (d, *J* = 242.7 Hz), 141.9 (d, *J* = 16.5 Hz), 131.5 (d, *J* = 6.4 Hz), 130.5 (2C), 127.4, 124.4 (d, *J* = 2.0Hz), 121.9 (d, *J* = 4.4 Hz). 114.0 (2C), 114.0 (d, *J* = 7.3Hz), 66.6, 60.5, 53.8, 36.4.

HR-MS: m/z calcd for $C_{18}H_{15}ClFNO_4S$ $[M+H]^+$ 396.0394; found $[M+H]^+$ 396.0378.

Synthesis of 2-(3-bromo-5-fluoro-4-hydroxyphenyl)-3-(2-(4-methoxyphenyl)-2-oxoethyl)thiazolidin-4-one (F14)

Purification by silica gel (8:2 hexane/AcOEt) gave compound **F14** (Yield: 89%). An analytic sample of **F14** purified with HPLC on a Nucleodur 100-5 (5 μm; 10 mm i.d. x 250 mm), with hexane/AcOEt (40:60) as eluent (flow rate 3 mL/min) (t_R = 8.5 min).

^{1}H NMR (500 MHz, $CDCl_3$) δ 7.85 (d, *J* = 8.8 Hz, 2H), 7.25 (s, 1H),7.10 (d, *J* = 10.3 Hz, 2H), 6.92 (d, *J* = 8.7 Hz, 1H), 5.82 (s, 1H), 5.19 (d, *J* = 17.6 Hz, 1H), 3.92 – 3.80 (m, 3H).3.82 (s, 3H).

^{13}C NMR (100 MHz, DMSO-d_6) δ 191.1, 171.0, 163.6, 151.6 (d, *J*= 243.2Hz), 144.4, 131.6, 130.3 (2C), 127.3, 127.1, 114.4, (d, *J* = 20.3Hz), 113.8 (2C), 111.7 (d, *J* = 14.0 Hz), 61.8, 55.5, 48.7, 31.7.

HR-MS: m/z calcd for $C_{18}H_{15}BrFNO_4S$ $[M+H]^+$ 439.9889; found $[M+H]^+$ 439.9982.

Synthesis of 2-(4-hydroxy-3-(trifluoromethyl)phenyl)-3-(2-(4-methoxyphenyl)-2-oxoethyl)thiazolidin-4-one (F15)

Purification by silica gel (8:2 hexane/AcOEt) gave compound **F15** (Yield: 88%). An analytic sample of **10** was obtained through purification with HPLC on a Nucleodur 100-5 (5 μm; 10 mm i.d. x 250 mm), with hexane/AcOEt (40:60) as eluent (flow rate 3 mL/min) (t_R = 13.0 min).

^{1}H NMR (500 MHz, $CDCl_3$) δ 7.84 (d, *J* = 8.9 Hz, 2H), 7.49 (s, 1H), 7.42 (d, *J* = 8.3 Hz, 1H), 6.97 (d, *J* = 8.3 Hz, 1H), 6.91 (d, *J* = 8.9 Hz, 2H), 5.90 (s, 1H), 5.15 (d, *J* = 17.5 Hz, 1H), 3.91 (d, *J* = 17.0 Hz, 1H), 3.86 (s, 3H), 3.86 (d, *J* = 7.8 Hz, 2H), 3.83 (d, *J* = 8.2 Hz, 1H).

^{13}C NMR (100 MHz, DMSO-d_6) δ 191.4, 171.4, 169.3, 164.0, 156.3, 133.5, 130.2 (2C), 128.5 (q, *J* = 129.7 Hz), 126.5, 121.8 (q, *J* = 96.5 Hz), 117.4, 114.1 (2C), 62.2, 55.5, 48.8, 31.8.

HR-MS: m/z calcd for $C_{19}H_{16}F_3NO_4S$ $[M+ H]^+$ 412.0752; found $[M+H]^+$ 412.0635.

Synthesis of 2-(4-chlorophenyl)-3-(2-(4-methoxyphenyl)-2-oxoethyl)thiazolidin-4-one (F16)

Purification by silica gel (9:1 hexane/AcOEt) gave compound **F16** (Yield: 73%). An analytic sample of **F16** was obtained through purification with HPLC on a Nucleodur 100-5 (5 μm; 10 mm i.d. x 250 mm), with hexane/AcOEt (40:60) as eluent (flow rate 3 mL/min) (t_R = 8.5 min).

^{1}H NMR (400 MHz, $CDCl_3$) δ 7.76 (d, *J* = 8.9 Hz, 2H), 7.28 (d, *J* = 8.2 Hz, 2H), 7.23 (d, *J* = 8.1 Hz, 2H), 6.84 (d, *J* = 8.8 Hz, 2H), 5.85 (s, 1H), 5.11 (d, *J* = 17.4 Hz, 1H), 3.86-3.71(m, 6H).

^{13}C NMR (100 MHz, $CDCl_3$) δ 191.1, 172.3, 164.3, 136.9, 135.8, 130.5 (2C), 129.6 (2C), 129.4 (2C), 127.8, 114.2 (2C), 63.9, 56.2, 48.8, 33.0.

HR-MS: m/z calcd for $C_{18}H_{16}ClNO_3S$ $[M+ H]^+$ 362.0539; found $[M+H]^+$ 362.0484.

Synthesis of 3-(2-(4-methoxyphenyl)-2-oxoethyl)-2-(p-tolyl)thiazolidin-4-one (F17)

Purification by silica gel (9:1 hexane/AcOEt) gave compound F**17** (Yield: 78%). An analytic sample of F**17** was obtained through purification with HPLC on a Nucleodur 100-5 (5 μm; 10 mm i.d. x 250 mm), with hexane/AcOEt (40:60) as eluent (flow rate 3 mL/min) (t_R = 8.0 min).

^{1}H NMR (400 MHz, $CDCl_3$,) δ 7.84 (d, *J* = 8.7 Hz, 2H), 7.25 (d, *J* = 7.6 Hz, 2H), 7.19 (d, *J* = 7.7 Hz, 2H), 6.91 (d, *J* = 8.8 Hz, 2H), 5.91 (s, 1H), 5.18 (d, *J* = 17.6 Hz, 1H), 3.87 (s, 3H), 3.91 – 3.82 (m, 3H), 2.37 (s, 3H).

^{13}C NMR (100 MHz, $CDCl_3$) δ 191.2, 172.2, 164.1, 139.5 (2C), 135.1, 130.72 (2C), 129.8 (2C), 127.9 (2C), 113.9 (2C), 63.9, 55.5, 47.8, 32.9, 21.4.

HR-MS: m/z calcd for $C_{19}H_{19}NO_3S$ $[M+H]^+$ 341.1086; found $[M+Na]^+$ 364.0979.

Synthesis of 2-(2-chloro-4-methylphenyl)-3-(2-(4-methoxyphenyl)-2-oxoethyl)thiazolidin-4-one (F18)

Purification by silica gel (85:15 hexane/AcOEt) gave compound F**18** (Yield: 90%). An analytic sample of F**18** was obtained through purification with HPLC on a Nucleodur 100-5 (5 μm; 10 mm i.d. x 250 mm), with hexane/AcOEt (40:60) as eluent (flow rate 3 mL/min) (t_R = 8.5 min).

^{1}H NMR (400 MHz, $CDCl_3$) δ 7.80 (d, *J* = 8.3 Hz, 2H), 7.21 (d, *J* = 7.8 Hz, 1H), 7.12 (s, 1H), 7.06 (d, *J* = 7.7 Hz, 1H), 6.84 (d, *J* = 8.2 Hz, 2H), 6.23 (s, 1H), 5.15 (d, *J* = 17.5 Hz, 1H), 3.86 (d, *J* = 17.5 Hz, 1H), 3.79 (s, 3H), 3.77 (d, *J* = 6.0 Hz, 2H), 2.27 (s, 3H).

^{13}C NMR (100 MHz, $CDCl_3$,) δ 191.0, 172.8, 164.6, 141.0, 140.7, 133.2, 130.9, 130.6, 130.5 (2C), 128.7, 127.9, 114.4 (2C), 60.5, 55.5, 48.8, 32.7, 21.6.

HR-MS: m/z calcd for $C_{19}H_{18}ClNO_3S$ $[M+H]^+$ 376.0696; found $[M+H]^+$ 376.0687.

Synthesis of 2-(2-chloro-4-hydroxyphenyl)-3-(2-(4-methoxyphenyl)-2-oxoethyl)thiazolidin-4-one (F19)

Purification by silica gel (9:1 hexane/AcOEt) gave compound F**19** (Yield: 58%). An analytic sample of F**19** was obtained through purification with HPLC on a Nucleodur 100-5 (5 μm; 10 mm i.d. x 250 mm), with hexane/AcOEt (40:60) as eluent (flow rate 3 mL/min) (t_R = 9.0 min).

^{1}H NMR (600 MHz, $CDCl_3$) δ 7.80 (d,J=8.0, 2H), 7.23 (d,J=7.7Hz, 1H), 7.09 ((d,J=7.7Hz , 1H), 6.84, 6.81 (m, 3H), 6.13 (s, 1H), 5.13 (d, J = 17.5 Hz, 1H), 3.87 (d, J = 17.5 Hz, 1H), 3.76(m, 5Hz).

^{13}C NMR (150 MHz, $CDCl_3$) δ 191.0, 172.6, 164.2, 149.9, 130.5(2C), 129.8, 127.8, 127.0, 126.3, 121.4, 121.2, 114.1(2C), 59.0, 55.3, 48.7, 32.5.

HR-MS: m/z calcd for $C_{18}H_{16}ClNO_4S$ [M+ H]+ 378.0532; found [M+Na]+400.0381.

Synthesis of 2-(2,4-dichlorophenyl)-3-(2-(4-methoxyphenyl)-2-oxoethyl)thiazolidin-4-one (F20)

Purification by silica gel (85:15 hexane/AcOEt) gave compound **F20** (Yield: 91%).

^{1}H NMR (400 MHz, DMSO-d_6) δ 7.94 (d, *J* = 8.9 Hz, 2H), 7.66 (d, *J* = 2.0 Hz, 1H), 7.51 (dd, *J* = 8.4, 2.0 Hz, 1H), 7.44 (d, *J* = 8.4 Hz, 1H), 7.03 (d, *J* = 8.9 Hz, 2H), 6.04 (s, 1H), 5.11 (d, *J* = 18.0 Hz, 1H), 4.26 (d, *J* = 18 Hz, 1H), 3.88 (dd, *J* = 15.8, 1H), 3.84 (s, 3H), 3.77 (d, *J* = 15.8 Hz, 1H).

^{13}C NMR (100 MHz, DMSO-d_6) δ 191.2, 171.8, 163.7, 136.4, 133.7, 133.0, 130.4 (2C), 129.4, 128.1 (2C), 127.4, 114.1 (2C), 59.2, 55.8, 49.5, 31.4.

HR-MS: m/z calcd for $C_{18}H_{15}Cl_2NO_3S$ $[M+H]^+$ 396.0150 , found $[M+Na]^+$ 418.0041.

Synthesis of 2-(4-(dimethylamino)phenyl)-3-(2-(4-methoxyphenyl)-2-oxoethyl)thiazolidin-4-one (F21)

Pure compound F**21** was obtained through purification with HPLC on a Nucleodur 100-5 (5 μm; 10 mm i.d. x 250 mm), with hexane/AcOEt (40:60) as eluent (flow rate 3 mL/min) (t_R = 9.0 min) (Yield= 49%).

^{1}H NMR (400 MHz, $CDCl_3$) δ 7.75 (d, J = 8.7 Hz, 2H), 7.32 (d, J = 8.7 Hz, 2H), 7.16 (d, J = 8.3 Hz, 2H), 6.83 (d, J = 8.3 Hz, 2H), 5.85 (s, *1*H), 5.09 (d, *J* = 17.6 Hz, 1H), 3.80 (m, 3H), 3.78 (s, 3H), 3.03 (s, 6H).

^{13}C NMR (100 MHz, $CDCl_3$) δ 190.7, 172.4, 164.0, 147.4, 133.8, 130.5(2c), 129.6(2C), 117.7(2C), 114.3(2C),63.9, 55.6, 51.3, 43.8(2C), 32.7.

HR-MS: m/z calcd for $C_{20}H_{22}N_2O_3S$ $[M+H]^+$ 370.1371, found $[M+Na]^+$ 393.1236.

Synthesis of 3-(2-(4-fluorophenyl)-2-oxoethyl)-2-(4-hydroxy-3-(trifluoromethyl)phenyl)thiazolidin-4-one (F22)

Purification by silica gel (8:2 hexane/AcOEt) gave compound **F22** (Yield: 62%). An analytic sample of **F22** was obtained through purification with HPLC on a Nucleodur 100-5 (5 μm; 10 mm i.d. x 250 mm), with hexane/AcOEt (40:60) as eluent (flow rate 3 mL/min) (t_R = 10.0 min).

^{1}H NMR (500 MHz, $CDCl_3$) δ 8.06 – 7.99 (m, 2H), 7.54 (s, 1H), 7.52 (d, J = 8.5 Hz, 1H), 7.33 (t, J = 8.8 Hz, 1H), 7.01 (d, J = 8.3 Hz, 2H), 5.79 (s, 1H), 4.95 (d, J = 18.1 Hz, 1H), 4.20 (d, J = 18.1 Hz, 1H), 3.96 (d, J = 15.7 Hz, 1H), 3.77 (d, J = 15.5 Hz, 1H).

^{13}C NMR (100 MHz, DMSO-d_6) δ 191.4, 171.0, 160.1(d, J = 250.8 Hz), 144.2, 132.8, 130.7(d, J=5.2, 2C), 128.5, 126.2, 123.7, 117.3, 115.8(d, J=8.9, 2C), 110.7 (q, J = 129.0 Hz), 73.7(q, J=55.6 Hz), 61.9, 48.9, 31.95.

HR-MS: m/z calcd for $C_{18}H_{13}F_4NO_3S$ $[M+H]^+$ 400.0552, found $[M+H]^+$ 400.0536.

Synthesis of 2-(3-((2-chloro-6-fluorobenzyl)oxy)-4-methoxyphenyl)-3-(2-(4-fluorophenyl)-2-oxoethyl)thiazolidin-4-one (F23)

Purification by silica gel (85:15 hexane/AcOEt) gave compound F**23** (Yield: 84%).

^{1}H NMR (400 MHz, $CDCl_3$) δ 7.86 (dd, *J* = 8.6, 5.4 Hz, 2H), 7.28 – 7.23 (m, 1H), 7.20 (d, *J* = 8.0 Hz, 1H), 7.10 (t, *J* = 8.5 Hz, 2H), 7.04 (d, *J* = 1.6 Hz, 1H), 6.99 (t, *J* = 8.6 Hz, 1H), 6.89 (d, *J* = 8.3 Hz, 1H), 6.79 (d, *J* = 8.2 Hz, 1H), 5.84 (s, 1H), 5.21(s, 1H), 5.07 (d, *J* = 17.7 Hz, 1H), 3.89 (d, *J* = 14.1 Hz, 1H), 3.85 – 3.77 (m, 5H).

^{13}C NMR (100 MHz, DMSO-d_6) δ 191.6, 171.2, 165.4 (d, *J* = 252.8 Hz), 161.5 (d, *J* = 250.1 Hz), 149.9, 147.6, 135.5 (d, *J* = 5.1 Hz), 131.8 (d, *J* = 9.8 Hz), 131.2 (d, *J* = 2.5 Hz), 131.1, 131.0 (d, *J* = 9.4 Hz) (2C), 125.7 (d, *J* = 2.8 Hz), 121.9 (d, *J* = 10.2 Hz), 121.2, 115.9 (d, *J* = 22.0 Hz) (2C), 114.7 (d, *J* = 22.4 Hz), 113.0, 112.0. 62.8, 61.5, 55.5, 49.1, 31.7.

HR-MS: m/z calcd for $C_{25}H_{20}ClF_2NO_4S$ $[M+H]^+$ 504,0670; found $[M+Na]^+$526.0657.

6.2 Synthesis of 2-amino-4*H*-benzo[*d*][1,3]thiaz-4-one-based compounds

6.2.1 Chemistry general information

NMR spectra (^{1}H, ^{13}C) were recorded on a Bruker Avance DRX400 spectrometers at T=298K. The compounds were dissolved in 0.5 mL of d-$CHCl_3$ (Aldrich, 99.8+ Atom% D), MeOD (Aldrich, 99.8+ Atom% D). Coupling constants (*J*) are reported in Hertz, and chemical shifts are expressed in parts per million (ppm) on the delta (δ) scale relative to $CHCl_3$ (7.16 ppm for ^{1}H and 77.2 ppm for ^{13}C) or MeOD (3.33 ppm for ^{1}H and 49.3 ppm for ^{13}C) as the internal reference. Multiplicities are reported as follows: s, singlet; d, doublet; t, triplet; m, multiplet; dd, doublet of doublets. ^{13}C DEPTQ experiments (dept polarization transfer with decoupling during acquisition using shaped pulse for 180 degree pulse on f1channel) were acquired at 100 MHz or 125MHz and referenced to the internal solvent signal. HPLC was performed using a Waters Model 510 pump equipped with Waters Rheodine injector and a differential

refractometer, model 401. All the solvents used for the synthesis were HPLC grade; they were purchased from Aldrich. The reagents for the synthesis were purchased from Sigma Aldrich and used as received.

Reaction progress was monitored via thin-layer chromatography (TLC) on Alugram® silica gel G/UV254 plates.

6.2.2 General procedure *r* for the synthesis of compound G1

2-amino-4-bromobenzoic acid (1 equiv, 0.23 mmol) and N-(phenyl carbamoyl)methanethioamide (1 equiv, 0.23 mmol) were solubilized in acetone, the mixture was stirred at room temperature for 30 minutes. After the completion, the reaction was quacked with MeOH and the solvent was evaporated under vacuum (**Scheme 21, Chapter 3**). The pure product was obtained through methanol crystallization.

6.2.3 General procedure *s* for the synthesis of compound G2

To a solution of 2-(3-benzoylthioureido)-4-bromobenzoic acid (**G1**) (1.0 equiv., 0.20mmol) HCl 37N (1 mL) was added dropwise and the mixture was stirred for 48h at room temperature. Then the mixture was poured into ice-cold water and a precipitate was formed. The precipitate is the pure product (**Scheme 21, Chapter 3**).

6.2.4 General procedure *t* for the synthesis of compounds G3-G8

2-amino-7-bromo-4*H*-benzo[*d*][1,3]thiazin-4-one (1.0 equiv, 1.6 mmol), a commercial avaible boronic acid (1.5 equiv, 2.4 mmol), K_2CO_3 (3.0 equiv, 4.8 mmol) and tetrakis(triphenylphosphine)palladium(0) (0.2equiv, 0.32 mmol) were dissolved in a previous degassed mixture of 1,4-dioxane (80%) and water (20%) (20 mL) and stirred overnight at 80 °C under argon atmosphere (**Scheme 21, Chapter 3**). After the completion of the reaction, the

mixture was diluted with dichloromethane and washed with a solution of $NaHCO_3$ (1x10mL). The organic lower was dried over an anhydrous Na_2SO_4, filtered, and concentrated under reduced pressure to afford the crude product.

Synthesis of intermediate 2-(3-benzoylthioureido)-4-bromobenzoic acid (G1)

Compound **G1** was obtained by following the general procedure *r* as a white solid (Yield: 92%).

^{1}H NMR (400 MHz, CD_3OD) δ 8.32 (d, *J* = 8.8 Hz, 1H), 8.14 (d, *J* = 2.2 Hz, 1H), 7.97 (d, J = 7.6 Hz, 2H), 7.71 (dd, *J* = 8.8, 2.2 Hz, 1H), 7.65 (d, *J* = 7.5 Hz, 1H), 7.55 (t, *J* = 7.7 Hz, 2H).

Synthesis of 2-amino-7-bromo-4*H*-benzo[*d*][1,3]thiazin-4-one (G2)

Compound **G2** was obtained by following the general procedure *s* as a white precipitate (Yield: 80%).

^{1}H NMR (400 MHz, CD_3OD) δ 8.18 (d, *J* = 2.1 Hz, 1H), 8.02 (dd, *J* = 8.4, 1.9 Hz, 1H), 7.51 (d, *J* = 8.8 Hz, 1H).

Synthesis of 2-amino-6-(4-fluoro-3-(1*H*-tetrazol-5-yl)phenyl)-4*H*-benzo[*d*][1,3]thiazin-4-one(G3)

Compound **G3** was obtained by following the general procedure *t* as a brown solid (Yield: 61%). An analytic sample of the product was obtained through purification by HPLC using CH_3CN/H_2O as eluent (From 5% to 100% in 50 minutes, flow rate 3 mL/min) (t_R = 12.2min).

^{1}H NMR (400 MHz, CD_3OD) δ 7.96 (td, *J* = 7.5, 1.8 Hz, 1H), 7.48 – 7.39 (m, 1H), 7.32 – 7.21 (m, 3H), 7.04 (ddd, *J* = 11.1, 8.4, 6.2 Hz, 1H).

^{13}C NMR (100 MHz, CD_3OD) δ 185.2, 161.0, 159.0 (d, *J* = 220.1 Hz), 155.1, 149.40, 144.7, 137.4 (d, *J* = 3.6 Hz), 130.6 (d, *J* = 7.4 Hz), 130.2 (d, *J* = 6.9 Hz), 127.2, 120.4, 120.2,120.1, 114.9 (d, *J* = 27.9 Hz), 114.6 (d, *J* = 27.9 Hz).

Synthesis of 2-amino-6-(naphthalen-2-yl)-4*H*-benzo[*d*][1,3]thiazin-4-one (G4)

Compound **G4** was obtained by following the general procedure *t* as a brown solid (Yield: 86%). An analytic sample of the product was obtained through purification by HPLC using CH_3CN/H_2O as eluent (From 5% to 100% in 50 minutes, flow rate 3 mL/min) (t_R = 30.0min).

^{1}H NMR (400 MHz, $CDCl_3$) δ 8.06 – 8.01 (m, 3H), 7.95 – 7.90 (m, 1H), 7.82 (t, *J* = 2.1 Hz, 1H), 7.76(s, 1H), 7.72 – 7.66 (m, 2H), 7.65 (d, *J* = 1.8 Hz, 1H), 7.58 (ddd, *J* = 8.8, 7.1, 1.2 Hz, 1H), 7.51 (ddd, *J* = 8.0, 6.8, 1.1 Hz, 1H).

^{13}C NMR (100 MHz, $CDCl_3$) δ 185.1, 160.9, 149.4, 145.1, 137.7, 133.7, 132.6, 128.5, 128.1, 127.8, 127.2, 127.1, 126.8, 126.5, 126.1, 125.8, 120.3, 120.2.

Synthesis of 2-amino-6-(3-fluoro-4-methylphenyl)-4*H*-benzo[*d*][1,3]thiazin-4-one (G5)

Compound **G5** was obtained by following the general procedure *t* as a brown precipitate (Yield: 87%). An analytic sample of the product was obtained through purification by HPLC using CH_3CN/H_2O as eluent (From 5% to 100% in 50 minutes, flow rate 3 mL/min) (t_R = 23.7min).

^{1}H NMR (400 MHz, $CDCl_3$) δ 8.20 (d, *J*= 7.7 Hz, 1H), 7.76 (dd, *J* = 7.7, 2.0 Hz, 1H), 7.61 (d, *J* = 1.9 Hz, 1H), 7.42 – 7.32 (m, 3H), 2.29 (s, 3H).

^{13}C NMR (100 MHz, $CDCl_3$) δ 185.3, 161.0, 160.8 (d, J = 222.0 Hz), 149.5, 143.4, 143.4, 138.3, 138.2, 131.5 (d, *J* = 7.4 Hz), 127.7, 127.4, 123.6 (d, *J* = 4.3 Hz), 120.4(d, *J* = 7.4 Hz), 118.8 (d, *J* = 34.4 Hz), 14.4.

Synthesis of 2-amino-6-(2,4,6-trifluorophenyl)-4*H*-benzo[*d*][1,3]thiazin-4-one(G6)

Compound **G6** was obtained by following the general procedure *t* (Yield: 80%). Purification by silica gel using hexane/ethyl acetate (6:4) as eluent gave the pure product.

^{1}H NMR (400 MHz, $CDCl_3$) δ 8.01 (d, *J* = 7.2 Hz, 1H), 7.76 (s, 2H), 7.63-7.58 (m, 1H), 7.523-7.50 (m, 1H), 6.93-6.86 (m, 2H).

Synthesis of 2-amino-6-(3-isopropoxyphenyl)-4*H*-benzo[*d*][1,3]thiazin-4-one (G7)

Compound **G7** was obtained by following the general procedure *t* as a yellow solid (Yield: 85%). An analytic sample of the product was obtained through purification by HPLC using CH_3CN/H_2O as eluent (From 5% to 100% in 50 minutes, flow rate 3 mL/min) (t_R = 23.8min).

1H NMR (400 MHz, $CDCl_3$) δ 7.97 (d, *J* = 7.3 Hz, 1H), 7.76 (s, 2H), 7.66 (dd, *J* = 7.3, 2.0 Hz, 1H), 7.60 (d, *J* = 1.9 Hz, 1H), 7.56-7.52 (m, 1H), 7.36 – 7.31 (m, 2H), 6.94 (dd, *J* = 8.2, 2.3 Hz 1H), 4.68-4.61 (m, 1H), 1.29 (d, *J* = 5.7 Hz, 6H).

Synthesis of 3-(2-amino-4-oxo-4*H*-benzo[*d*][1,3]thiazin-6-yl)benzoic acid (G8)

Compound **G8** was obtained by following the general procedure *t* as a yellow solid (Yield: 40%). An analytic sample of the product was obtained through purification by HPLC using CH_3CN/H_2O as eluent (From 5% to 100% in 50 minutes, flow rate 3 mL/min) (t_R = 22.3min).

^{1}H NMR (400 MHz, MeOD) δ 8.08 (d, J = 1.6 Hz, 1H), 7.99 – 7.93 (m, 1H), 7.72 (dd, *J* = 7.6, 1.6 Hz, 1H), 7.63 (d, *J* = 7.3 Hz, 1H), 7.44 – 7.33 (m, 1H), 7.23-7.18 (m, 2H).

^{13}C NMR (100 MHz, MeOD) δ 185.3, 170.6, 161.0, 149.5, 144.1, 139.4, 132.3, 131.7, 129.8, 129.7, 129.0, 127.9, 123.7, 121.5, 120.6.

6.3 Computational details

6.3.1 Reagent Preparation

Reagent Preparation is a function that allows the preparation of several fragments for the decoration of the core. It works by the generation of SMARTS (representation of chemical structures through text string), and it defines precisely the fragment and the functional group that will be removed with Combiglide (Schrödinger, LLC)[96] in the successive step, to perform the connection to the core. Using the SMARTs it is possible to determine the breaking point of the collection of reagents, indicating the atom of the molecule that has to be preserved (rpc1) and the one that has to be removed (rpc2) (**Figure 49**).

To perform the virtual libraries design (**Chapter 3**), commercially available reactants were subjected to the Reagent Preparation phase, which provided the building blocks for the next step.

AddGNAcid_Chloride_C_C[#6][CX3](=O)(C1) 1:rpc1 2:rpc2

AddGNAcid_Chloride_C_C1[CX3](=O)(C1)[#6] 1:rpc1 3:rpc2

Figure 49. Commercially available compound and correspondents SMARTs for the two possible fragments.

6.3.2 Combiglide and libraries generation

Chemical structures of the scaffolds were built with Maestro's Build Panel (v. 9.6; Schrödinger, LLC, 2015). Combiglide[96] was used for the generation of the final libraries.

CombiGlide[96] allows the choice of the specific points on the scaffold for the addition of the prepared fragments, applying the interactive enumeration function. The latter works following a combinatorial chemistry approach to obtain all the possible combinations of the different reagents with the core, starting from the synthons of a selected synthetic strategy. The links scaffold-fragments are not necessarily the bonds that are cleaved in the real chemical reactions, taking into account that Combiglide considers the final product synthesizable using the selected synthetic strategy, generating all the possible final compounds. This is an important tool for the design of very large libraries of molecules.

Finally, LigPrep (Schrödinger, LLC)[97] software was used to perform:

- energetic minimization of the whole library using Optimized Potentials for Liquid Simulations (OPLS) 2005 force field;[143]
- considering all the energetic components, preparation of each compound, by the calculation of the stereoisomers, the tautomeric and ionization states, and the determination of three-dimensional ring conformations at physiological pH;
- eliminate possible mistakes in the structures of the molecules.

6.3.3 Calculation of pharmacokinetic parameters and filters application

Pharmacokinetic parameters have fundamental importance to evaluate if a molecule is a right candidate to become a drug, or if its properties are not appropriate to consider in the development of new hit compounds. With a prediction of these properties, it is possible to select drug-like compounds exclusively by discarding the remaining ones from the calculation. In this field, the hydrophobic/hydrophilic balance in a compound influences its intestinal adsorption, or the distribution in the several compartments of the organism, the metabolism (higher hydrophobic properties make more difficult the metabolic processes), and the elimination.

For the calculation of the pharmacokinetic parameters, LigFilter[105] was applied. Several filtering types are possible; however, we referred to the rule of Lipinski,[144] considered one of the most important to estimate the drug-like valid candidates in medicinal chemistry. The researcher Christopher Lipinski[99] in 1997 defined this rule according to which a molecule must:

1. not have a molecular weight higher than 500 (MW < 5);
2. have no more than 5 hydrogen bond donors; -
3. have no more than 10 hydrogen bond acceptors;
4. have a logP less than 5 (logP< 5).

By applying these filters, it is possible to eliminate the compounds unable to comply with some important rules and parameters.

The second step of this pharmacokinetic evaluation is the prediction of ADME (absorption, distribution, metabolism, elimination) properties of molecules (e.g. belonging to the filtered library obtained using QikProp[98] function).

Some of the properties calculated by the software are:

- QPlogBB, an index of the permeability of the blood-brain barrier (BEE);
- QPlogPo/w, the octanol/water partition coefficient;
- QPlogS predicts aqueous solubility;
- QPPC indicates the permeability through the Caco-2 cells, as a model of human intestinal barrier
- QPPMDCK indicates permeability through MDCK cells;
- QikProp predictions consider non-active transport;
- QPlogHERG, predicts IC_{50} value for blockage of HERG K+ channels;
- RtvFG, the number of reactive functional groups;
- SASA, the surface accessible to the solvent, expressed in Angstrom (Å);

- FISA, a hydrophilic component of the solvent-accessible surface area (SASA) on N, O, H bound to hetero-atoms and carbonyl C;
- HumanOralAbsorption, predicts human oral absorption, with values 1 (low), 2 (medium), and 3 (high), which can also be expressed as a percentage.

At the end of the calculation, only drug-like molecules were selected from the previous libraries resulting from Combiglide.[96]

6.3.4 Virtual screening workflow and docking analysis

Virtual screening workflow (VSW, Glide software) [105-145-146] is a computational method for the screening of large libraries of ligands versus one or more biological targets. Generally, the ligand files for the docking analysis are prepared using several software described above. The docking path works at three different levels, which operate with a gradually increasing precision:

- HTVS, high throughput virtual screening;
- SP, standard precision;
- XP, extra precision;

For each level, it is possible to keep a percentage of top-ranked poses using docking score as a selection parameter. The selected parameters are then submitted to the next docking step, which outperforms the previous for both sampling and scoring. The analysis of the final screened compounds is based on the interactions with the receptor counterpart, binding energy, superimposition with a known binder that is co-crystallized in the three-dimensional crystal structure of the protein available in the protein data bank (PDB) database.

In the structure-based molecular docking experiments, the same mPGES-1 three-dimensional crystal structure (PDB code: 4BPM) and sEH crystal structure were (PDB code: 5AI5) used for the calculation.[147] Also, in this specific case, Glide software[148] was used for docking analysis and the Virtual Screening Workflow[146] was applied in the same size receptor grid focused onto the co-crystallized ligand binding site (LVJ) and (5AI5), respectively for mPGES-1 and sEH.

HTVS was set keeping 10,000 poses in the starting phase of docking and selecting 800 poses for energy minimization. Specifically, one output structure was saved for each binder, with a scaling factor of 0.8 related to van der Waals radii with a partial charge cutoff of 0.15. Basing on a 0.5 kcal/mol rejection cutoff for the obtained minimized poses, a maximum of one pose was chosen in the post-docking optimization phase. The 50% of the best outputs were then submitted to the SP mode setting the same parameters in the previous HTVS-docking experiments. Finally, the 50% of the best SP outputs were subjected to XP mode, setting always the same parameters previous applied with the difference in the output file. This time 20 poses for each compound were saved, and in the post-docking optimization of the docking poses, a maximum of 20 poses was selected.

CHAPTER 7
General procedure for the synthesis of fluorinated dienes and their functionalization

7.1 Chemistry general information

All air-sensitive manipulations were conducted under an inert by standard Schlenk techniques. Vessels used in air-free reactions were oven-dried and cooled under dynamic vacuum (once at ambient temperature, vessels were refilled with nitrogen and evacuated two more times) prior to use. Reagents were purchased from commercial suppliers and used without further purification. Commercial grade solvents were used for reactions without further purification. Thin layer chromatography analysis was performed using Merck 60 pre-coated silica gel plates with F254 indicator. Visualization was accomplished by iodine, p-anisaldehyde, potassium permanganate, Dragendorff-Munier, cerium ammonium molybdate, and/or UV light (254 nm). Proton nuclear magnetic resonance (^{1}H NMR) spectra were recorded on Bruker Neo-500 and AV-600 instruments with 500 and 600 MHz frequencies. Carbon-13 nuclear magnetic resonance (^{13}C NMR) spectra were recorded on Bruker Neo-500 and AV-600 instruments with a ^{13}C operating frequency of 126 and 150 MHz. Fluorine-19 nuclear magnetic resonance (^{19}F NMR) spectra were recorded on Bruker DRX-500, Neo-500, and AV-600 instruments with 471, and 565 MHz frequencies. The proton signal for the residual non-deuterated solvent (δ 7.26 for $CHCl_3$, δ 7.16 for C_6H_6) was used as an internal reference for ^{1}H spectra. For ^{13}C spectra, chemical shifts are reported relative to the δ 77.16 resonance of $CDCl_3$ and relative to the δ 128.06 for C_6D_6. For ^{19}F spectra, chemical shifts are reported in relative to the δ -63.72 resonance of $PhCF_3$. Microwave reactions were run with a Biotage® Initiator + Microwave System with Robot Eight. Enantioselectivity was determined by chiral HPLC using Daicel OJ-H columns (0.46 x 25 cm) and a mixture 99:1 hexane/isopropanol as eluent mixture.

7.2 General procedures

7.2.1 General procedure *u* for the synthesis of compounds S1-S19

A mixture of alkene (1 equiv), sodium iodine (0.2 equiv) and THF (30mL) was put under nitrogen. TMS-CF_3 (2.5 equiv.)was added last via syringe and the reaction was stirred at 65 °C for 2 hours for compounds **S1**, **S5**, **S7**, **S8**. For the synthesis of all the other compounds, NaI (0.35 equiv.) and TMS-CF_3 (5 equiv) were used. The amount of TMS-CF_3 was split in 12h with a syringe pump, and the reaction was stirred for 24h (**Scheme 45**, **Chapter 4**). At the end of the reaction, the mixture was diluted with diethyl ether and washed with water(3x10mL). The organic layer was dried over magnesium sulfate, filtered and concentrated to give a crude oil. Compounds **S17-S19** were concentrated at 0°C to avoid the evaporation of the products.

7.2.2 General procedure v for the synthesis of compounds P1-P19

The gem-diflurocyclopropane (1 eq, 0.4 mmol), $Pd(OAc)_2$ (0.10 eq, 0.02 mmol), DavePhos (0.15 eq, 0.03 mmol) and Cs_2CO_3 (1 eq, 0.4 mmol) were dissolved in dry dioxane (2mL), the reaction was stirred at 80°C for 24h (**Scheme 43**, **Chapter 4**). After the completion of the reaction, the mixture was filtered on celite and concentrated under vacuum. Purification by silica using different mixtures n-hexane/ EtOAc gave the pure product with different yields.

7.2.3 General procedure *w* for the synthesis of compound P19 for the microwave ligand screening

Each ligand (**LG1-LG18**) (0.15 eq, 0.003 mmol) and NaH (1 eq, 0.04 mmol) were put in a microwave vessel. Thereafter, 100µL of a solution of **S19** in dioxane (0.04 mmol/100µL), and 100µL of a solution of $Pd(OAc)_2$ in dioxane (0.002 mmol/100µL), both previously prepared in

a stock solution, were added. The reaction run in a microwave apparatus for 5h at 100°C (**Table 17**, **Chapter 4**).

7.2.4 General procedure *x* for the synthesis of compound S10A

To a solution of 2-pyrrolidone (1 equiv, 20 mmol) and N,N-(dimethylamino)pyridine (0.05 equiv, l mmol) in CH_3CN, di-tert-butyl dicarbonate (1 equiv, 20 mmol) was added and the mixture was stirred at room temperature for 16h. After the reaction was complete, the residue was diluted with EtOAc. and washed with H_2O (2x 10mL) and brine (1x 10mL). The organic layer was dried over Na_2SO_4, filtered and concentrated under vacuum. The crude was used without any purification (Yield:100-95%).

7.2.5 General procedure *y* for the synthesis of compound S11A, S14A, S15A

To a round bottom flask under nitrogen atmosphere, dry THF and the lactam (1 equiv, 20 mmol) were added. The flask was cooled at -78°C, and n-butyllithium (1.05 equiv, 21 mmol) was added dropwise via syringe. The reaction was stirred for 1h at -78°C. Then, p-toluene sulfonyl chloride (1.05 eq, 21 mmol), dissolved in dry THF (10mL), was added. The reaction was allowed to warm at room temperature and stirred over-night (**Scheme 45**, **Chapter 4**). After the completion of the reaction, it was quenched with saturated NH_4Cl and the aqueous layer was extracted with EtOAc (3x 20ml). The organic layer was dried over Na_2SO_4, filtered and concentrated under vacuo. The crude was used without any purification (Yield: 95-100%).

7.2.6 General procedure *z* for the synthesis of compounds S10B, S11B, S14B, S15B.

To a stirred solution of compounds **SA** (1 eq, 10 mmol) in dry THF (30mL) a solution of DIBAL-H 1M in hexane (3 eq., 30 mmol) was slowly added at -78°C under nitrogen atmosphere. After 2h, the solution was transferred to a flask containing saturated NH_4Cl/diethyl ether (1/3). The solution was warmed at room temperature and stirred until a thick white gel formed at the bottom.

The mixture was filtered on celite and washed with a solution of NH_4Cl. The organic layer was dried over Na_2SO_4, filtered and concentrated under vacuo. The crude was purified by silica gel using different mixtures of n-hexane/ EtOAc (Yield:85-90%)(**Scheme 45**, **Chapter 4**).

7.2.7 General procedure *a2* for the synthesis of compound S10C, S11C, S14C, S15C.

A mixture of **SB** (1eq., 8 mmol) in dry DCM(100mL) was cooled at -78°C under nitrogen atmosphere. Trifluoroacetic anhydride was added in a period of 15 minutes and the reaction was stirred at this temperature. After 7h NEt_3 was added to the mixture and stirred over-night at room temperature. After the completion of the reaction, the mixture was washed with $NaHCO_3$, dried over Na_2SO_4, filtered and concentrated under vacuum. Purification by silica gel gave the pure product (Yield:72-90%).

7.2.8 General procedure *b2* for Diels-Alder reaction in situ after the Pd-cross-coupling

To the solution of fluorodiene (1 equiv, 0.32 mmol), just generated by *d2* general procedure, a mixture of di-tert-butyl diazene-1,2-dicarboxylate and catalyst (0.1 equiv, 0.016mmol) in dioxane (1mL) was added. The amount of di-tert-butyl diazene-1,2-dicarboxylate, the reaction time and the temperature varied according to the experimental phase (**Chapter 4**).

After the completion of the reaction, the mixture was filtered on celite and purified by silica gel using a mixture 9:1 n-hexane/acetate as eluent.

7.2.9 General procedure *c2* for Diels-Alder reaction on diene isolate

To an 5mL vessel, (*E*)-(3-fluorobuta-1,3-dien-1-yl)benzene (1 equiv, 0.32 mmol), di-tert-butyl diazene-1,2-dicarboxylate (4 equiv, 1.28 mmol) and catalyst (0.1 or 0.3 equiv) were added- The flask was evacuated and backfilled quickly with nitrogen three times, the mixture was solubilized in the solvent choice (3mL), and then the reaction was wormed at 50°C or at 80°C for 20h (**Chapter 4**).

7.2.10 General procedure *d2* for the synthesis of compound of (*S*)-CT2

To an oven-dried 100-mL round bottom flask, (*S*)-BINOL (1.0 equiv, 15mmol) was added. The flask was evacuated and backfilled with nitrogen three times. Anhydrous pyridine (50 mL) was added to the flask via syringe and the reaction was set to stir before the slow addition of 2mL (1.4 equiv) phosphorus(V) oxychloride (2.1 equiv, 31.5mmol). The reaction mixture was heated at 95 °C for 16 hours before cooling to room temperature and added by dropwise addition of 50 mL of water via syringe. A solid white precipitate initially formed and required vigorous stirring during the addition of water. The reaction was then heated to 105°C and stirred at this temperature for 5 hours with vigorous stirring (**Scheme 47**, **Chapter 4**). After this time, the mixture was cooled to room temperature and diluted with dichloromethane. The organic layer was washed with aqueous 1N HCl (3 x 50 mL), collected, dried over anhydrous Na_2SO_4, filtered and concentrated under reduced pressure. The resulting crude material was purified by flash column chromatography.

7.2.11 General procedure *e2* for the synthesis of compound (*S*)-CT3

To a 100 mL round-bottom flask containing (*S*)-BINOL (1 equiv, 5 mmol) in toluene (30 mL), tris(dimethylamino)phosphine was added (1 equiv, 5 mmol) under nitrogen atmosphere. The mixture was stirred for 9 hours at reflux. (**Scheme 47**, **Chapter 4**). After this time, the mixture was cooled to room temperature and diluted with dichloromethane. The organic layer was washed with aqueous 1N HCl (3 x 50 mL), collected, dried over anhydrous Na_2SO_4, filtered and concentrated under reduced pressure. The resulting crude material was purified by flash column chromatography.

7.2.12 General procedure *f2* for the synthesis of compound (*S*)-CT4

To a 100 mL round-bottom flask containing (*S*)-BINOL (1 equiv, 5 mmol) in toluene (30 mL) phosphorus chloride (1 equiv, 5 mmol) and triethylamine (1.23 equiv, 6,15 mmol) were added at 0 °C under a nitrogen atmosphere. The mixture was stirred for 6 hours.

Then, a solution of diethylamine (1.1 equiv, 5.5 mmol) and triethylamine (1.23 equiv, 6,15 mmol) was added to the flask and the mixture continued to stir over-night (**Scheme 47**, **Chapter 4**). After this time, the mixture was cooled to room temperature and diluted with dichloromethane. The organic layer was washed with aqueous 1N HCl (3 x 50 mL), collected, dried over anhydrous Na_2SO_4, filtered and concentrated under reduced pressure. Finally, the crude was purified by silica gel.

7.2.13 General procedure *g2* for synthesis of compounds (*S*)-CT6 - (*S*)-CT8

To a solution of the substrate (1 equiv, 2 mmol) in dry pentane (15mL), $TiCl_4$(1 equiv, 2 mmol) was added and the reaction was stirred at room temperature for 6h under nitrogen atmosphere. The crude was concentrated under vacuum without air exposure, and then precipitated with dry

pentane. The supernatant contained the pure product. All the NMR spectra were obtained with previously dried $CDCl_3$ (**Schemes 49-51**, **Chapter 4**).

7.2.14 General procedure *h2* for synthesis of compounds (*S*)-CT12

To an oven-dried 500-mL round bottom flask, (*S*)-BINOL (1.0 equiv, 20 mmol), and [1,3-[Bis(diphenylphosphino)propane]dichloronickel(II) (2 mmol, 0.10 equiv) were added. The flask was evacuated and backfilled with nitrogen three times, and dry diethyl ether (50 mL) was added via syringe. The flask was cooled to 0 °C in an ice bath, and (2,4,6-triisopropylphenyl)magnesium bromide (2 M solution in diethyl ether, 100 mmol, 5.0 equiv) was added dropwise via syringe with stirring over 5 minutes. The reaction mixture was stirred at room temperature for 1 hour, and then diluted with hexanes (200 mL). The reaction mixture was cooled to 0 °C and 100 mL of a saturated ammonium chloride solution was added slowly. The reaction mixture was then stirred vigorously at room temperature for 10 minutes, transferred into a 1-L separatory funnel, and diluted with water (100 mL). The organic layer was separated, and the aqueous layer was extracted with diethyl ether (3 x 100 mL). The combined organic layers were dried over sodium sulfate, filtered, and concentrated under reduced pressure (**Scheme 50**, **Chapter 4**).

.

7.2.15 General procedure *i2* for the synthesis of compounds (*S*)-CT13

To an oven-dried 50-mL round bottom flask, **(*S*)-CT12** (1.0 equiv, 2 mmol) and HCl 4M in dioxane (18ml) were added. The reaction was heated at 70°C and stirred for 20h. The reaction was then cooled to room temperature and concentrated under reduced pressure. The resulting mixture was diluted with dichloromethane (50 mL) and washed with saturated $NaHCO_3$(1 x 20

mL) and brine (20 mL). The organic lower was dried over sodium sulfate, filtered, and concentrated under reduced pressure (**Scheme 50**, **Chapter 4**).

7.2.16 General procedure *j2* for synthesis of compounds (*S*,*S*)-CT14

To an oven-dried 100-mL round bottom flask, aryl bromide (4.4 equiv, 22mmol) and magnesium turnings (4.6 equiv, 23 mmol) were added. The flask was evacuated and backfilled with nitrogen three times, and dry THF(50 mL) was added via syringe. The reaction mixture was heated to reflux and stirred for 2h. After 2h, the mixture was cooled, (4*S*,5*S*)-dimethyl 2,2-dimethyl-1,3-dioxolane-4,5-dicarboxylate (1 equiv, 5 mmol) was added, and the reaction was refluxed for other 2h. After that the mixture was quenched with saturated NH_4Cl (10mL) and extracted with EtOAc (2x 30mL) (**Scheme 51**, **Chapter 4**).

Synthesis of 1-(2,2-difluoro-3-methylcyclopropyl)-4-methoxybenzene (S1)

Compound **S1** was obtained following the general procedure *u*. Purification by silica gel (8:2 hexane/ethyl acetate) gave the pure product a yellow oil (Yield: 70%).

^{1}H NMR (500 MHz, $CDCl_3$) δ 6.98 – 6.94 (d, *J* = 8.1 Hz, 2H), 6.72 – 6.67 (d, *J* = 8.1 Hz, 2H), 3.63 (s, 3H), 2.07 (ddd, *J* = 11.2, 7.5, 3.0 Hz, 0H), 1.65 – 1.53 (m, 0H), 1.21 – 1.13 (m, 3H).

^{13}C NMR (125 MHz, $CDCl_3$) δ 158.6, 128.9 (2C), 126.2, 115.9 (t, *J* = 289.6 Hz), 113.9(2C), 55.3, 33.2(t, *J* = 10.2 Hz), 24.1 (t, *J* = 9.9 Hz), 11.5 (d, *J* = 4.2 Hz).

^{19}F NMR (470 MHz, $CDCl_3$) δ -137.65 – -138.50 (m, 2F).

Synthesis of (*Z*)-1-(2-fluorobuta-1,3-dien-1-yl)-4-methoxybenzene (P1)

Compound **P1** was obtained following the general procedure *v*. Purification by silica gel (8:2 hexane/ethyl acetate) gave the pure product a yellow oil (Yield: 56%).

^{1}H NMR (500 MHz, $CDCl_3$) δ 7.27 – 7.24 (d, *J*=8.2Hz, 2H), 6.94 (d, *J*=8.2Hz, 2H), 6.61 (m, 1H), 5.77 (dd, *J* = 34.2, 1.3 Hz, 1H), 5.56 – 5.50 (m, 2H), 3.80 (s, 3H).

^{13}C NMR (125 MHz, $CDCl_3$) δ 160.2, 156.5 (d, *J* = 252.3 Hz), 130.4 (2C), 126.7 (d, *J* = 13.1 Hz), 119.9 (d, *J* = 23.0 Hz), 118.2 (d, *J* = 11.0 Hz), 115.9 (d, *J* = 21.9 Hz), 114.5(2C), 55.3.

^{19}F NMR (472 MHz, $CDCl_3$) δ 123.35 – -123.53 (m).

Synthesis of 5-(2,2-difluoro-3-methylcyclopropyl)-2-methoxyphenyl acetate (S2)

Compound **S2** was obtained following the general procedure *u*. Purification by silica gel (8:2 hexane/ethyl acetate) gave the pure product a yellow oil (Yield: 54%).

^{1}H NMR (600 MHz, $CDCl_3$) δ 6.89 (d, *J* = 8.1 Hz, 1H), 6.74 – 6.68 (m, 2H), 3.75 (s, 3H), 2.23 (s, 3H), 2.22 – 2.15 (m, 1H), 1.73 (dddd, *J* = 14.0, 7.7, 6.3, 1.6 Hz, 1H), 1.27 (ddd, *J* = 6.4, 2.5, 1.2 Hz, 3H).

^{13}C NMR (150 MHz, $CDCl_3$) δ 169.0, 150.9, 138.7, 133.3, 122.7, 120.1 (t, *J* = 207.0 Hz), 114.5, 112.2, 55.9, 33.8 (t, *J* = 11.0 Hz), 25.8 (t, *J* = 12.0 Hz), 20.6, 11.4 (d, *J* = 4.6 Hz).

^{19}F NMR (565 MHz, $CDCl_3$) δ -137.02 – -138.10 (m, 2F).

Synthesis of (*Z*)-5-(2-fluorobuta-1,3-dien-1-yl)-2-methoxyphenyl acetate (P2)

Compound **P2** was obtained following the general procedure *v*. Purification by silica gel (8:2 hexane/ethyl acetate) gave the pure product a brown oil (Yield: 58%).

^{1}H NMR (500 MHz, $CDCl_3$) δ 7.07-7.04 (m, 2H), 6.87 (d, J = 8.9 Hz, 1H), 6.61 (dddd, *J* = 19.9, 16.8, 11.9, 1H), 5.77 (dd, *J* = 34.1, 1.4 Hz, 1H), 5.58 – 5.45 (m, 2H), 3.80 (s, 3H), 2.27 (s, 3H).

^{13}C NMR (125 MHz, $CDCl_3$) δ 172.1, 156.9 (d, *J* = 250.1 Hz), 147.2, 143.5, 127.9 (d, *J* = 14.3 Hz), 124.3, 123.1, 119.6 (d, *J* = 32.2 Hz), 118.2 (d, *J* = 11.0 Hz), 115.9 (d, *J* = 21.9 Hz), 112.1, 55.95, 25.5.

^{19}F NMR (470 MHz, $CDCl_3$) δ -120.90 (dd, *J* = 38.6, 26.3 Hz).

Synthesis of (2,2-difluoro-1-methylcyclopropyl)benzene (S3)

Compound **S3** was obtained following the general procedure *u*. Purification by silica gel (9:1 hexane/ethyl acetate) gave the pure product as a yellow oil (Yield: 62%).

^{1}H NMR (500 MHz, $CDCl_3$) δ 7.22 – 7.12 (m, 3H), 6.97 – 6.89 (m, 2H), 1.54 (ddd, *J* = 13.6, 7.6, 3.6 Hz, 1H), 1.41 (dd, *J* = 2.9, 1.8 Hz, 3H), 1.31 (ddd, *J* = 12.3, 7.6, 4.5 Hz, 1H).

^{13}C NMR (125 MHz, $CDCl_3$) δ 130.0 (2C), 127.1, 115.5 (2C), 30.5 (t, *J* = 20.2 Hz), 22.7 (t, *J* = 10.0 Hz), 21.4 (t, *J* = 22.0 Hz).

^{19}F NMR (470 MHz, $CDCl_3$) δ -132.22 – -132.86 (m), -137.74 (dd, *J* = 150.5, 12.2 Hz).

Synthesis of (3-fluorobuta-1,3-dien-2-yl)benzene (P3)

Compound **P3** was obtained following the general procedure *v*. Purification by silica gel (8:2 hexane/ethyl acetate) gave the pure product a brown oil (Yield: 69%).

^{1}H NMR (500 MHz, $CDCl_3$) δ 7.55 – 7.27 (m, 5H), 5.63 (dd, *J* = 4.6, 2.0 Hz, 1H), 5.38 (dd, *J* = 4.6, 2.0 Hz, 1H), 4.51-4.46 (m, 2H).

^{13}C NMR (125 MHz, $CDCl_3$) δ 165.3 (d, *J* = 248.0 Hz), 141.1 (d, *J* = 34.1 Hz), 132.9 (d, *J* = 6.2 Hz), 130.3 (2C), 128.5, 127.8 (2C), 116.2 (d, *J* = 7.9 Hz), 94.1 (d, *J* = 20.3 Hz).

^{19}F NMR (470 MHz, $CDCl_3$) δ -123.90 (m).

Synthesis of 1-(2,2-difluoro-1-methylcyclopropyl)-4-fluorobenzene (S4)

Compound **S4** was obtained following the general procedure *u*. Purification by silica gel (9:1 hexane/ethyl acetate) gave the pure product as a yellow oil (Yield: 65%).

^{1}H NMR (500 MHz, $CDCl_3$) δ 7.13 – 7.04 (m, 2H), 6.97 – 6.86 (m, 2H), 2.76 – 2.61 (m, 2H), 1.68 (dddt, *J* = 14.1, 11.3, 7.9, 7.0 Hz, 1H), 1.51 – 1.34 (m, 2H), 1.00 (dtd, *J* = 12.9, 7.5, 3.5 Hz, 1H).

^{13}C NMR (125 MHz, $CDCl_3$) δ 161.6 (d, *J* = 244.1 Hz), 135.2 (d, *J* = 3.0 Hz)(2C), 129.6 (d, *J* = 8.0 Hz)(2C), 115.4 (d, *J* = 21.2 Hz), 114.1 (t, *J* = 284.7 Hz), 32.1 (d, *J* = 4.3 Hz), 23.3, 16.4.

^{19}F NMR (470 MHz, $CDCl_3$) δ -116.81 (p, *J* = 6.8 Hz), -128.31 (dt, *J* = 156.3, 13.2 Hz), -143.10 (ddd, *J* = 156.4, 12.9, 4.1 Hz).

Synthesis of 1-fluoro-4-(3-fluorobuta-1,3-dien-2-yl)benzene (P4)

Compound **P4** was obtained following the general procedure *v*. Purification by silica gel (95:5 hexane/ethyl acetate) gave the pure product as a brown oil (Yield: 56%).

^{1}H NMR (500 MHz, $CDCl_3$) δ 7.24 – 7.18 (m, 2H), 7.09 – 7.03 (m, 2H), 5.63 (dd, *J* = 4.6, 2.0 Hz, 1H), 5.38 (dd, *J* = 4.6, 2.0 Hz, 1H), 4.51-4.38 (m, 2H).

^{13}C NMR (125 MHz, $CDCl_3$) δ 165.3(d, *J* = 250.2 Hz), 163.9 (d, *J* = 253.4 Hz), 132.1 (2C) (dd, *J* = 9.1, 2.6 Hz), 130.6 (d, *J* = 33.9 Hz), 129.5 (dd, *J* = 9.1, 2.6 Hz), 117.2 (d, *J* = 7.6 Hz), 113.4 (2C) (d, *J* = 22.7 Hz), 94.3 (d, *J* = 20.3 Hz).

^{19}F NMR (470 MHz, $CDCl_3$) δ -112.72 (ddd, *J* = 49.3, 25.1, 16.5 Hz).

Synthesis of 1-(2,2-difluorocyclopropyl)-4-methoxybenzene (S5)

Compound **S5** was obtained following the general procedure *u*. Purification by silica gel (8:2 hexane/ethyl acetate) gave the pure product as a yellow oil (Yield: 81%).

^{1}H NMR (500 MHz, $CDCl_3$) δ 7.05 (d, *J* = 8.1, 2H), 6.75 (d, *J* = 8.1, 2H), 3.69 (s, 3H), 2.60 (ddd, *J* = 13.4, 11.7, 8.0 Hz, 1H), 1.67 (dddd, *J* = 12.5, 11.6, 7.8, 4.7 Hz, 1H), 1.44 (dtd, *J* = 12.7, 7.9, 3.8 Hz, 1H).

^{13}C NMR (125 MHz, $CDCl_3$) δ 158.8, 129.2(2C), 125.6, 113.9(2C), 112.7(t, *J* = 285.5 Hz) 55.3, 26.5 (t, *J* = 11.5 Hz), 16.9 (t, *J* = 10.6 Hz).

^{19}F NMR (470 MHz, $CDCl_3$) δ -126.22 (dtd, *J* = 153.4, 13.1, 3.9 Hz), -142.51 (dd, *J* = 12.7, 4.8 Hz).

Synthesis of (*E*)-1-(3-fluorobuta-1,3-dien-1-yl)-4-methoxybenzene (P5)

Compound **P5** was obtained following the general procedure *v*. Purification by silica gel (8:2 hexane/ethyl acetate) gave the pure product as a brown oil (Yield: 87%).

^{1}H NMR (500 MHz, $CDCl_3$) δ 7.60 (d, *J* = 8.1, 2H), 7.05 (d, *J* = 8.1, 2H), 5.93 – 5.86 (m, 1H), 5.87 – 5.83 (m, 1H), 4.46 – 4.25 (m, 1H), 3.80 (s, 3H).

^{13}C NMR (125 MHz, $CDCl_3$) δ 165.0, 159.6 (d, *J* = 260.4 Hz), 130.0 (d, *J* = 8.1 Hz), 129.4 (d, *J* = 1.0 Hz), 129.3(2C), 114.5(2C), 114.3 (d, *J* = 27.7 Hz), 95.2 (d, *J* = 21.5 Hz), 53.3.

^{19}F NMR (470 MHz, $CDCl_3$) δ -110.25 (m).

Synthesis of ((2,2-difluorocyclopropyl)methyl)benzene (S6)

Compound **S6** was obtained following the general procedure *u*. Purification by silica gel (9:1 hexane/ethyl acetate) gave the pure product as colorless oil (Yield: 70%).

^{1}H NMR (500 MHz, $CDCl_3$) δ 7.30 – 7.08 (m, 5H), 2.78 (dd, *J* = 15.2, 7.9 Hz, 1H), 2.67 (ddd, *J* = 15.2, 7.1, 3.6 Hz, 1H), 1.71 (ddq, *J* = 14.8, 11.2, 7.5 Hz, 1H), 1.47 – 1.31 (m, 1H), 1.00 (dtd, *J* = 12.8, 7.6, 3.5 Hz, 1H).

^{13}C NMR (125 MHz, $CDCl_3$) δ 139.6, 128.6(2C), 128.20(2C), 126.5, 115.6 (t, *J* = 283.6 Hz), 32.8 (d, *J* = 4.1 Hz), 23.3 (t, *J* = 10.7 Hz), 16.4 (t, *J* = 10.8 Hz).

^{19}F NMR (470 MHz, $CDCl_3$) δ -128.27 (dt, *J* = 156.5, 13.3 Hz), -143.04 (ddd, *J* = 156.1, 13.2, 4.1 Hz).

Synthesis of (*E*)-(3-fluorobuta-1,3-dien-1-yl)benzene (P6)

Compound **P6** was obtained following the general procedure *v*. Purification by silica gel (95:5 hexane/ethyl acetate) gave the pure product as a colorless oil (Yield: 81%).

^{1}H NMR (500 MHz, $CDCl_3$) δ 7.39 – 7.14 (m, 5H), 6.83 (d, *J* = 16.1 Hz, 1H), 6.46 (dd, *J* = 24.8, 16.0 Hz, 1H), 4.70 (dd, *J* = 16.1, 2.8 Hz, 1H), 4.49 (dd, *J* = 48.4, 2.9 Hz, 1H).

^{13}C NMR (125 MHz, $CDCl_3$) δ 160.4 (d, *J* = 260.4 Hz), 136.8 (d, *J* = 1.1 Hz), 130.1 (d, *J* = 8.1 Hz), 129.9, 128.8(2C), 127.5(2C), 116.2 (d, *J* = 27.7 Hz), 95.3 (d, *J* = 21.5 Hz).

^{19}F NMR (470 MHz, $CDCl_3$) δ -112.00 (ddd, *J* = 48.3, 24.7, 16.0 Hz).

Synthesis of 1-((2,2-difluorocyclopropyl)methyl)-2-methoxybenzene (S7)

Compound **S7** was obtained following the general procedure *u*. Purification by silica gel (8:2 hexane/ethyl acetate) gave the pure product as an orange oil (Yield: 80%).

^{1}H NMR (600 MHz, $CDCl_3$) δ 7.15 (tt, *J* = 23.5, 7.6 Hz, 2H), 6.92 – 6.75 (m, 2H), 3.82 – 3.65 (m, 3H), 2.83 – 2.60 (m, 2H), 1.90 – 1.71 (m, 1H), 1.31 (dddt, *J* = 16.1, 12.5, 7.9, 4.1 Hz, 1H), 1.08 – 0.88 (m, 1H).

^{13}C NMR (150 MHz, $CDCl_3$) δ 129.61, 128.24, 127.86, 114.9(t, *J* = 290.6 Hz), 110.33, 55.1, 27.51 (t, *J* = 4.2 Hz), 22.46 (td, *J* = 10.0, 9.1, 3.9 Hz), 16.22 (t, *J* = 10.7 Hz).

^{19}F NMR (565 MHz, $CDCl_3$) δ -127.78 (ddq, *J* = 155.7, 42.3, 13.7 Hz), -143.71 (dq, *J* = 155.2, 13.9 Hz).

Synthesis of (*E*)-1-(3-fluorobuta-1,3-dien-1-yl)-2-methoxybenzene (P7)

Compound **P7** was obtained following the general procedure *v*. Purification by silica gel (8:2 hexane/ethyl acetate) gave the pure product as an orange oil (Yield: 55%).

^{1}H NMR (500 MHz, $CDCl_3$) δ 7.57 (ddd, *J* = 7.7, 1.6, 0.7 Hz, 1H), 7.23 – 7.13 (m, 2H), 6.90 – 6.73 (m, 3H), 4.41 – 4.29 (m, 2H),), 3.60 (s, 3H).

^{13}C NMR (125 MHz, $CDCl_3$) δ 163.8 (d, *J* = 260.4 Hz), 156.5, 131.3, 127.8, 127.1, 122.9 (d, *J* = 7.9 Hz), 120.9, 115.7 (d, *J* = 27.7 Hz), 113.5, 95.60 (d, *J* = 21.2 Hz), 55.50.

^{19}F NMR (470 MHz, $CDCl_3$) δ -113.00 (ddd, *J* = 47.9, 25.0, 15.8 Hz).

Synthesis of 5-((2,2-difluorocyclopropyl)methyl)benzo[*d*][1,3]dioxole (S8)

Compound **S8** was obtained following the general procedure *u*. Purification by silica gel (8:2 hexane/ethyl acetate) gave the pure product as an orange oil (Yield: 80%).

^{1}H NMR (600 MHz, $CDCl_3$) δ 6.61 – 6.57 (m, 2H), 6.53 (dd, *J* = 7.9, 1.7 Hz, 1H), 5.74 (s, 2H), 2.58 (dd, *J* = 15.1, 8.0 Hz, 1H), 2.50 (ddd, *J* = 15.1, 7.0, 3.5 Hz, 1H), 1.63 – 1.50 (m, 1H), 1.29 (dddd, *J* = 12.5, 11.4, 7.6, 4.1 Hz, 1H), 0.90 (dtd, *J* = 13.0, 7.6, 3.5 Hz, 1H).

^{13}C NMR (150 MHz, $CDCl_3$) δ 147.9, 146.2, 133.5 (d, *J* = 2.0 Hz), 121.0, 113.8 (t, *J* = 207.0 Hz), 108.7, 108.3, 100.9, 32.6 (d, *J* = 4.3 Hz), 23.6 (t, *J* = 10.6 Hz), 16.2 (t, *J* = 10.8 Hz).

^{19}F NMR (565 MHz, $CDCl_3$) δ -128.02 (dt, *J* = 156.4, 13.4 Hz), -142.97 (ddd, *J* = 156.3, 13.3, 4.1 Hz).

Synthesis of (*E*)-5-(3-fluorobuta-1,3-dien-1-yl)benzo[*d*][1,3]dioxole (P8)

Compound **P8** was obtained following the general procedure *v*. Purification by silica gel (8:2 hexane/ethyl acetate) gave the pure product as an orange oil (Yield: 77%).

^{1}H NMR (500 MHz, $CDCl_3$) δ 7.06 – 6.87 (m, 4H), 6.77 (d, *J* = 8.3 Hz, 1H), 6.02 (s, 2H), 4.41 – 4.31 (m, 2H).

^{13}C NMR (125 MHz, $CDCl_3$) δ 159.39 (d, *J* = 260.4 Hz), 148.2 (d, *J* = 28.6 Hz), 130.4, 130.3, 129.95, 122.9, 114.0 (d, *J* = 27.7 Hz), 108.5, 106.8, 101.1, 95.3 (d, *J* = 21.5 Hz).

^{19}F NMR (470 MHz, $CDCl_3$) δ -112.09 (m)

Synthesis of tert-butyl 6,6-difluoro-3-azabicyclo[3.1.0]hexane-3-carboxylate (S9)

Compound **S9** was obtained following the general procedure *u*. Purification by silica gel (8:2 hexane/ethyl acetate) gave the pure product as an orange oil (Yield: 63%).

^{1}H NMR (500 MHz, C_6D_6) δ 3.73 (d, *J* = 11.5 Hz, 1H), 3.45 (d, *J* = 11.2 Hz, 1H), 3.12 (ddd, *J* = 11.5, 5.5, 3.7 Hz, 1H), 2.99 – 2.90 (m, 1H), 1.40 (s, 9H).

^{13}C NMR (125 MHz, C_6D_6) δ 153.1, 113.6 (dd, *J* = 296.0, 277.5 Hz), 78.9 (2C), 45.0 (2C)(d, *J* = 40.8 Hz), 28.1 (3C), 25.9 (t, *J* = 11.7 Hz), 25.2 (t, *J* = 12.1 Hz).

^{19}F NMR (470 MHz, C_6D_6) δ -129.65 (d, *J* = 161.6, 12.6 Hz), -156.39 (d, *J* = 161.4 Hz).

Synthesis of tert-butyl 4-oxopyridine-1(4*H*)-carboxylate (P9)

Compound **P9** was obtained following the general procedure *u*. Purification by silica gel (7:3 hexane/ethyl acetate) gave the pure product as an orange oil (Yield: 77%).

^{1}H NMR (600 MHz, DMSO-d_6) δ 8.15(d, *J* = 8.1 Hz, 2H), 6.17 (d, *J* = 8.1 Hz, 2H),1.57 (s, 9H).

^{13}C NMR (150 MHz, DMSO-d_6) δ 179.7, 147.9, 135.7(2C), 117.9(2C), 87.1, 27.9(3C).

Synthesis of tert-butyl 2-oxopyrrolidine-1-carboxylate (S10A)

Compound **S10A** was obtained following the general procedure *x* as a white powder (Yield: 97%).

^{1}H NMR (500 MHz, $CDCl_3$) δ 4.22 – 4.17 (m, 2H), 2.50 – 2.44 (m, 2H), 1.89 – 1.82 (m, 2H), 1.49(s, 3H).

^{13}C NMR (125 MHz, $CDCl_3$) δ 174.3, 150.0, 82.3, 46.5, 32.8, 27.9(3C), 17.3.

Synthesis of tert-butyl 2-hydroxypyrrolidine-1-carboxylate (S10B)

Compound **S10B** was obtained following the general procedure *z*. Purification by silica gel (8:2 hexane/ethyl acetate) gave the pure product as a colorless oil (Yield: 63%).

^{1}H NMR (500 MHz, $CDCl_3$) δ 5.45 – 5.17 (m, 1H), 3.50 – 3.33 (m, 1H), 3.28 – 3.02 (m, 1H), 2.01 – 1.57 (m, 4H), 1.40 (s, 9H).

^{13}C NMR (125 MHz, $CDCl_3$) δ 155.1, 82.0, 55.4, 45.9, 32.8, 28.5(3C), 22.8.

Synthesis of tert-butyl 2,3-dihydro-1*H*-pyrrole-1-carboxylate (S10C)

Compound **S10C** was obtained following the general procedure *a2*. Purification by silica gel (9:1 hexane/ethyl acetate) gave the pure product as a colorless oil (Yield: 68%).

^{1}H NMR (500 MHz, C_6D_6) δ 6.63 (d, *J* = 169.7 Hz, 1H), 4.62 (d, *J* = 12.0 Hz, 1H), 3.57 (t, *J* = 9.3 Hz, 1H), 3.33 (t, *J* = 9.3 Hz, 1H), 2.10 (dt, *J* = 38.3, 9.3 Hz, 2H), 1.42 (s, 11H).

^{13}C NMR (125 MHz, C_6D_6) δ 151.1, 130.0, 106.6, 79.1, 44.9, 29.5, 28.1(3C).

Synthesis of tert-butyl 6,6-difluoro-2-azabicyclo[3.1.0]hexane-2-carboxylate (S10)

Compound **S10** was obtained following the general procedure *u*. Purification by silica gel (8:2 hexane/ethyl acetate) gave the pure product as an orange oil (Yield: 51%).

^{1}H NMR (500 MHz, $CDCl_3$) δ 3.67 – 3.56 (m, 2H), 3.30 – 3.05 (m, 1H), 2.12 (qt, *J* = 11.2, 6.2 Hz, 3H), 1.41 (s, 9H).

^{13}C NMR (125 MHz, $CDCl_3$) δ 154.7, 111.1 (t, *J* = 292.1 Hz), 80.4, 46.7 (d, *J* = 61.8 Hz), 42.2 , 28.2(3C), 27.1, 23.0 (d, *J* = 100.5 Hz).

^{19}F NMR (470 MHz, $CDCl_3$) δ -128.33 (dd, *J* = 161.7, 14.3 Hz), -153.59 (dd, *J* = 225.7, 161.7 Hz).

Synthesis of tert-butyl 5-oxo-5,6-dihydropyridine-1(2*H*)-carboxylate (P10)

Compound **P10** was obtained following the general procedure *v*. Purification by silica gel (7:3 hexane/ethyl acetate) gave the pure product as an orange oil (Yield: 74%).

^{1}H NMR (500 MHz, $CDCl_3$) δ 6.50 (dt, *J* = 8.4, 3.7 Hz, 1H), 6.06 (dt, *J* = 8.4, 1.1 Hz, 1H), 4.60 (s, 2H), 4.34 (dd, *J* = 3.7, 1.1 Hz, 2H), 1.46 (s, 9H).

^{13}C NMR (125 MHz, $CDCl_3$) δ 180.9, 154.6, 139.1, 130.2, 79.6, 50.8, 46.7, 28.3(3C).

Synthesis of 1-tosylpyrrolidin-2-one (S11A)

Compound **S11A** was obtained following the general procedure *y* as a white powder (Yield:83%).

^{1}H NMR (500 MHz, $CDCl_3$) δ 7.86 (d, *J* = 6.1 Hz, 1H), 7.29 (d, *J* = 6.1 Hz, 1H), 3.85 (dd, *J* = 8.2, 5.6 Hz, 2H), 2.42 – 2.31 (m, 5H), 2.00 (m, 2H).

^{13}C NMR (125 MHz, $CDCl_3$) δ 173.4, 145.1, 135.1, 129.6(2C), 127.9(2C), 47.27, 32.2, 18.1. (AcOEt: 171.2, 60.3, 14.5),

Synthesis of 1-tosylpyrrolidin-2-ol (S11B) (mixture of enantiomers)

Compound **S11B** was obtained following the general procedure *z*. Purification by silica gel (1:1 hexane/ethyl acetate) gave the pure product as a with powder (Yield:85%).

^{1}H NMR (500 MHz, $CDCl_3$) δ 7.74 (d, *J* = 8.0 Hz, 2H), 7.67 (d, *J* = 8.0 Hz, 2H), 7.25 (d, *J* = 7.9 Hz, 4H), 5.70 (d, *J* = 5.4 Hz, 1H), 5.36 (d, *J* = 5.2 Hz, 1H),3.49 (td, *J* = 9.0, 8.4, 2.7 Hz, 1H), 3.41 (td, *J* = 8.3, 7.9, 4.6 Hz, 1H), 3.11 – 2.89 (m, 2H), 2.36 (s,, 6H), 2.08 – 1.81 (m, 4H), 1.75 – 1.59 (m, 2H), 1.38 (qdd, *J* = 12.7, 7.3, 5.1 Hz, 2H).

^{13}C NMR (125 MHz, $CDCl_3$) δ 143.61, 135.55, 129.78(2C), 127.17(2C), 83.91, 47.52, 34.00, 22.96, 21.49.

Synthesis of 1-tosyl-2,3-dihydro-1*H*-pyrrole (S11C)

Compound **S11C** was obtained following the general procedure *a2*. Purification by silica gel (95:5 hexane/ethyl acetate) gave the pure product as a colorless oil (Yield: 89%).

^{1}H NMR (500 MHz, C_6D_6) δ 7.64 (d, *J* = 7.9 Hz, 2H), 6.76 (d, *J* = 7.9 Hz, 2H), 6.35 (dt, *J* = 4.2, 2.2 Hz, 1H), 4.56 (dt, *J* = 4.6, 2.6 Hz, 1H), 3.20 (t, *J* = 9.1 Hz, 2H), 1.85 (s, 3H), 1.79 (dt, *J* = 9.0, 2.6 Hz, 1H).

^{13}C NMR (126 MHz, C_6D_6) δ 143.2, 134.1, 131.3, 129.6(2C), 128.1(2C), 110.6, 47.3, 29.5, 21.0.

Synthesis of 6,6-difluoro-2-tosyl-2-azabicyclo[3.1.0]hexane (S11)

Compound **S11** was obtained following the general procedure *u*. Purification by silica gel (9:1 hexane/ethyl acetate) gave the pure product as an orange oil (Yield: 60%).

^{1}H NMR (500 MHz, C_6D_6) δ 8.07 – 7.99 (d, *J* = 7.9 Hz, 2H), 6.83 (d, *J* = 7.9 Hz, 2H), 6.30 (d, *J* = 5.2 Hz, 1H), 3.48 – 3.39 (m, 1H), 2.85 (td, *J* = 9.7, 6.8 Hz, 1H), 1.88 (s, 3H), 1.81 (dd, *J* = 11.5, 6.6 Hz, 1H), 1.12 (m, 2H)

^{13}C NMR (125 MHz, C_6D_6) δ 143.1, 136.5, 129.8(2C), 127.9 (2C), 89.3, 48.3, 33.9, 23.2, 21.1.

^{19}F NMR (470 MHz, $CDCl_3$) δ -129.03 (dd, *J* = 160.8, 14.3 Hz), -153.09 (dd, *J* = 225.7, 160.8 Hz).

Synthesis of 5-fluoro-1-tosyl-1,2-dihydropyridine (P11)

Compound **P11** was obtained following the general procedure *v*. Purification by silica gel (95:5 hexane/ethyl acetate) gave the pure product as an orange oil (Yield: 59%).

^{1}H NMR (500 MHz, C_6D_6) δ 7.45 (dd, *J* = 5.6, 3.3 Hz, 1H), 7.36 (d, *J* = 8.3 Hz, 2H), 6.73 (ddd, *J* = 5.9, 3.4, 2.4 Hz, 1H), 6.33 (d, *J* = 8.1 Hz, 2H), 5.80 (t, *J* = 2.4 Hz, 1H), 4.05 – 3.94 (m, 2H), 1.51(s, 3H).

^{19}F NMR (470 MHz, None) δ -132.94 (m).

Synthesis of benzyl 6,6-difluoro-2-azabicyclo[3.1.0]hexane-2-carboxylate (S12)

Compound **S12** was obtained following the general procedure *u*. Purification by silica gel (8:2 hexane/ethyl acetate) gave the pure product as an orange oil (Yield: 58%)

^{1}H NMR (500 MHz, C_6D_6) δ 7.22 (dd, *J* = 20.4, 7.5 Hz, 2H), 7.12 – 6.99 (m, 3H), 5.15 (dd, *J* = 25.3, 12.4 Hz, 1H), 4.96 (t, *J* = 12.2 Hz, 1H), 3.82 – 3.32 (m, 2H), 3.27 – 2.84 (m, 2H), 1.40 (t, *J* = 11.4 Hz, 1H), 1.22 (d, *J* = 11.1 Hz, 1H).

^{13}C NMR (125 MHz, C_6D_6) δ 154.7, 136.9, 128.3(2C), 127.7(2C), 110 (t, *J*=296.2 Hz), 66.99, 47.56, 41.55 – 41.24 (m), 27.02 (t, *J* = 11.1 Hz), 21.85.

^{19}F NMR (470 MHz, C_6D_6) δ -128.2 (ddd, *J* = 161.8, 31.0, 15.1 Hz), -153.6 (dd, *J* = 161.1, 123.8 Hz).

Synthesis of benzyl 5-fluoropyridine-1(2*H*)-carboxylate (P12)

Compound **P12** was obtained following the general procedure *v*. Purification by silica gel (95:5 hexane/ethyl acetate) gave the pure product as an orange oil (Yield: 58%).

Synthesis of tert-butyl 1,1-difluoro-6-azaspiro[2.5]octane-6-carboxylate (S13)

Compound **S13** was obtained following the general procedure *u*. Purification by silica gel (8:2 hexane/ethyl acetate) gave the pure product as an yellow oil (Yield: 60%)

^{1}H NMR (600 MHz, $CDCl_3$) δ 3.51 – 3.40 (m, 2H), 3.30 (ddd, *J* = 13.3, 8.0, 3.7 Hz, 2H), 1.59 – 1.53 (m, 2H), 1.51 – 1.43 (m, 2H), 1.40 (s, 9H), 1.03 (t, *J* = 8.3 Hz, 2H).

^{13}C NMR (150 MHz, $CDCl_3$) δ 154.7, 114.9 (t, *J* = 288.5 Hz), 79.7, 42.9(2C), 28.7(2C), 28.4(3C), 27.2 (t, *J* = 10.1 Hz), 21.3.

^{19}F NMR (565 MHz, $CDCl_3$) δ -139.53 (d, *J* = 9.1 Hz, 2F).

Synthesis of tert-butyl 4-(1-fluorovinyl)-5,6-dihydropyridine-1(2*H*)-carboxylate (P13)

Compound **P13** was obtained following the general procedure *v*. Purification by silica gel (9:1 hexane/ethyl acetate) gave the pure product as an orange oil (Yield: 81%).

^{1}H NMR (500 MHz, $CDCl_3$) δ 6.57 (dt, *J* = 4.5, 1.1 Hz, 1H), 4.42 (d, *J* = 2.9 Hz, 1H), 4.36 – 4.27 (m, 2H), 3.86 – 3.75 (m, 3H), 3.70 (dt, *J* = 3.8, 1.0 Hz, 3H), 2.74 (dt, *J* = 4.3, 1.0 Hz, 2H), 1.46 (s, 9H).

^{13}C NMR (125 MHz, $CDCl_3$) δ 163.9 (d, *J* = 248.0 Hz), 157.9, 129.2(d, *J* = 17.2 Hz), 123.9, 92.1 (d, *J* = 20.3 Hz), 79.4, 44.5, 43.7, 28.4, 26.9(3C).

^{19}F NMR (470 MHz) δ -137.9 (m).

Synthesis of 1-tosylpiperidin-2-one (S14A)

Compound **S14A** was obtained following the general procedure *y* as a white powder (Yield:85%).

^{1}H NMR (600 MHz, $CDCl_3$) δ 7.83 (d, *J* = 8.1 Hz, 2H), 7.23 (d, *J* = 8.0 Hz, 2H), 3.83 (t, *J* = 6.1 Hz, 2H), 2.34 (m, 5H), 1.83 (p, *J* = 6.1 Hz, 2H), 1.70 (p, *J* = 6.4 Hz, 2H).

^{13}C NMR (150 MHz, $CDCl_3$) δ 170.2, 144.7, 136.1, 129.3, 128.7, 46.9, 34.1, 23.3, 21.6, 20.4.

Synthesis of 1**-tosylpiperidin-2-ol (S14B) (mixture of enantiomers)**

Compound **S14B** was obtained following the general procedure *z* (Yield:75%) and used without any purification.

^{1}H NMR (500 MHz, C_6D_6) δ 7.72 (d, *J* = 8.0 Hz,, 2H), 6.77 (d, *J* = 8.0 Hz, 2H), 6.74 (d, *J* = 8.1 Hz, 1H), 5.57 (q, *J* = 3.0 Hz, 1H), 4.65-4.61(m, 2H), 3.53 (dt, *J* = 13.3, 3.4 Hz, 2H), 3.21 – 3.13 (m, 2H), 3.05 – 2.91 (m, 2H), 1.88 (s, 3H).

^{13}C NMR (125 MHz, C_6D_6) δ 142.6, 138.0, 129.3(2C), 128.0(2C), 76.4, 39.9, 31.3, 24.7, 20.7, 17.15.

Synthesis of 1-tosyl-1,2,3,4-tetrahydropyridine (S14C)

Compound **S14C** was obtained following the general procedure *b2*. Purification by silica gel (95:5 hexane/ethyl acetate) gave the pure product as a white powder (Yield: 77%).

^{1}H NMR (500 MHz, C_6D_6) δ 7.64(d, *J* = 8.0 Hz, 2H),), 6.83 (d, *J* = 8.1, 1H), 6.74 (d, *J* = 8.0 Hz, 2H), 4.63 (dt, *J* = 8.1, 3.9 Hz, 2H), 3.15 (m, 2H), 1.85 (s, 3H), 1.37 (ddt, *J* = 6.1, 3.8, 2.1 Hz, 2H), 1.15 (q, *J* = 5.9 Hz, 2H).

^{13}C NMR (125 MHz, C_6D_6) δ 142.7, 135.9, 129.3, 127.1, 125.5, 107.4, 43.6, 20., 20.6, 20.5.

Synthesis of 7,7-difluoro-2-tosyl-2-azabicyclo[4.1.0]heptane (S14)

Compound **S14** was obtained following the general procedure *u*. Purification by silica gel (7:3 hexane/ethyl acetate) gave the pure product as an yellow oil (Yield: 64%).

^{1}H NMR (500 MHz, C_6D_6) δ 7.76 (d, *J* = 8.1 Hz, 2H), 6.81 (d, *J* = 8.0 Hz, 2H), 3.24 (dd, *J* = 11.5, 6.5 Hz, 2H), 2.95 – 2.82 (m, 1H), 2.62 (ddd, *J* = 11.5, 6.9, 4.5 Hz, 1H), 1.87 (s, 3H), 1.13 – 0.93 (m, 2H), 0.86 (td, *J* = 7.6, 3.9 Hz, 2H).

^{13}C NMR (125 MHz, C_6D_6) δ 142.9, 136.3, 129.3, 111.3 (dd, *J* = 294.9, 289.5 Hz), 127.2, 59.7, 32.7 (dd, *J* = 16.0, 9.1 Hz), 21.5, 20.8, 18.9 (t, *J* = 11.7 Hz), 13.2.

^{19}F NMR (470 MHz, C_6D_6) δ -129.32 (ddd, *J* = 162.7, 15.1, 6.6 Hz), -149.37 (d, *J* = 162.7 Hz).

Synthesis of 6-fluoro-1-tosyl-2,3-dihydro-1*H*-azepine (P14)

Compound **P14** was obtained following the general procedure *v*. Purification by silica gel (9:1 hexane/ethyl acetate) gave the pure product as an orange oil (Yield: 68%).

^{1}H NMR (500 MHz, C_6D_6) δ 7.51 (d, *J* = 8.0 Hz, 2H), 7.22 (dd, *J* = 12.7, 2.0 Hz, 1H), 6.63 (d, *J* = 8.0 Hz, 2H), 5.73 (ddd, *J* = 14.5, 12.2, 2.1 Hz, 1H), 5.22 – 5.04 (m, 1H), 3.22 – 3.10 (m, 2H), 1.78 (s, 3H), 1.69 – 1.56 (m, 2H).

^{13}C NMR (125 MHz, C_6D_6) δ 148.5 (d, *J* = 220.6 Hz), 143.2, 136.1, 131.7 (d, *J* = 13.1 Hz), 129.6(2C), 127.1(2C), 121.2 (d, *J* = 39.6 Hz), 114.7 (d, *J* = 55.2 Hz), 45.3, 31.4, 20.7.

^{19}F NMR (470 MHz, None) δ -132.94 (td, *J* = 14.5, 14.1, 4.3 Hz).

Synthesis of 1-tosylpiperidin-4-one (S15A)

Compound **S15A** was obtained following the general procedure *y* as a white powder and used without any purification (Yield:87%).

^{1}H NMR (500 MHz, $CDCl_3$) δ 7.61 (d, *J* = 8.5 Hz, 2H), 6.90 (d, *J* = 8.1 Hz, 2H), 2.86 (q, *J* = 7.2, 6.1 Hz, 4H), 2.05 (s, 3H), 2.00 (t, *J* = 6.1 Hz, 4H).

^{13}C NMR (125 MHz, $CDCl_3$) δ 205.7, 144.2, 133.4, 129.9(2C), 127.6(2C), 45.9, 40.7, 21.6.

Synthesis of 1-tosylpiperidin-4-ol (S15B)

Compound **S15B** was obtained following the general procedure *z* and used without any purification (Yield: 93%).

^{1}H NMR (500 MHz, $CDCl_3$) δ 7.66 (d, *J* = 8.5 Hz, 2H), 7.46 (d, *J* = 8.5 Hz, 2H), 3.74 (m, 1H), 3.47 (ddd, *J* = 12.8, 9.7, 7.5 Hz, 1H), 3.41 – 3.30 (m, 2H), 2.41 (d, *J* = 0.9 Hz, 1H), 1.96 (ddtt, *J* = 19.4, 9.7, 7.3, 4.9 Hz, 2H).

^{13}C NMR (125 MHz, $CDCl_3$) δ 142.1, 138.5, 129.6(2C), 127.9(2C), 66.2, 43.3, 32.8, 21.5.

Synthesis of 1-tosyl-1,2,3,6-tetrahydropyridine (S15C)

Compound **S15C** was obtained following the general procedure *b2* (Yield:93%) and used without any purification.

^{1}H NMR (500 MHz, DMSO-d_6) δ 7.74 (d, *J* = 8.0 Hz, 2H), 7.68 (d, *J* = 8.0 Hz, 2H), 7.51 (d, *J* = 7.8 Hz, 1H), 7.43 (d, *J* = 7.7 Hz, 1H), 3.34 (m, 4H), 2.56 (m, 4H), 2.47 (s, 3H).

^{13}C NMR (125 MHz, DMSO-d_6) δ 142.1, 140.4, 129.5(2C), 128.1(2C), 126.9, 124.4, 48.0, 44.7, 25.2, 21.5.

Synthesis of 7,7-difluoro-3-tosyl-3-azabicyclo[4.1.0]heptane (S15)

Compound **S15** was obtained following the general procedure *u*. Purification by silica gel (7:3 hexane/ethyl acetate) gave the pure product as an yellow oil (Yield: 54%).

^{1}H NMR (500 MHz, $CDCl_3$) δ 7.70 (d, *J* = 8.0 Hz, 2H), 7.45 (d, *J* = 8.0 Hz, 2H), 3.46 – 3.38 (m, 2H), 3.20 (ddt, *J* = 11.1, 5.7, 2.8 Hz, 1H), 3.11 (ddt, *J* = 11.2, 5.6, 2.8 Hz, 1H), 2.53 – 2.44 (m, 1H), 2.38 (s, 3H), 2.27 (tq, *J* = 7.7, 5.6 Hz, 1H), 1.89-1.81 (m, 1H), 1.65-1.56 (m, 1H).

^{13}C NMR (125 MHz, $CDCl_3$) δ 142.1, 134.6, 129.5, 127.3, 105.6 (t, *J* = 290.9 Hz), 45.7, 40.6, 21.8, 20.8 (t, *J* = 16.8 Hz), 18.8 (t, *J* = 12.4 Hz).

^{19}F NMR (470 MHz, CDCl3) δ -129.32 (d, *J* = 162.4 Hz), -149.37 (d, *J* = 162.5 Hz).

Synthesis of 5-fluoro-1-tosyl-2,3-dihydro-1*H*-azepine (P15)

Compound **P15** was obtained following the general procedure *v*. Purification by silica gel (9:1 hexane/ethyl acetate) gave the pure product as an orange oil (Yield: 62%).

^{1}H NMR (500 MHz, $CDCl_3$) δ 7.27 – 7.13 (m, 2H), 7.11 – 6.99 (m, 2H), 6.42 (dd, *J* = 9.3, 4.7 Hz, 1H), 5.28 – 5.14 (m, 2H), 3.83 (t, *J* = 5.8 Hz, 2H), 2.34 (s, 3H), 1.48-1.43 (m, *J* = 5.8, 4.6, 1.1 Hz, 2H).

^{13}C NMR (125 MHz, $CDCl_3$) δ 155.7 (d, *J* = 243.7 Hz), 142.5, 138.3 (d, *J* = 11.7 Hz), 131.5, 130.2 (2C), 1117.4(2C), 96.8 (d, *J* = 20.5 Hz), 93.1 (d, *J* = 37.7 Hz), 47.4 (d, *J* = 1.2 Hz), 27.0, 20.7.

^{19}F NMR (470 MHz, $CDCl_3$) δ -133.04 (td, *J* = 14.2, 14.0, 4.3 Hz).

Synthesis of 7,7-difluorobicyclo[4.1.0]heptan-2-ol (S17)

Compound **S17** was obtained following the general procedure *u* and used without any purification (Yield: 88%).

^{1}H NMR (500 MHz, C_6D_6) δ 3.99 – 3.86 (m, 1H), 2.24 (m, *J* = 6.3 Hz, 1H), 2.11 – 2.02 (m, 1H), 1.75 – 1.45 (m, 5H), 1.35 – 1.27 (m, 1H).

^{13}C NMR (125 MHz, C_6D_6) δ 102.78 (t, *J* = 293.1 Hz), 69.18 (t, *J* = 1.5 Hz), 31.92 (t, *J* = 9.5 Hz), 23.27 (t, *J* = 11.8 Hz), 21.28, 20.33 (t, *J* = 8.3 Hz), 19.17 (t, *J* = 11.9 Hz).

^{19}F NMR (470 MHz, C_6D_6) δ -127.88 (ddt, *J* = 167.5, 17.3, 8.1 Hz), -154.05 (d, *J* = 167.0 Hz).

Synthesis of 3-fluorocyclohepta-2,4-dienol (P17)

Compound **P17** was obtained following the general procedure *v*. Purification by silica gel (8:2 hexane/ethyl acetate) gave the pure product as an orange oil (Yield: 75%).

^{1}H NMR (500 MHz, C_6D_6) δ 5.69 (tt, *J* = 12.9, 2.4 Hz, 1H), 5.61 (ddt, *J* = 11.6, 7.5, 4.4 Hz, 1H), 5.53 – 5.45 (m, 1H), 3.99 – 3.87 (m, 1H), 1.99 (ddt, *J* = 18.2, 11.9, 2.4 Hz, 1H), 1.78 – 1.63 (m, 2H), 1.15 (ddt, *J* = 13.6, 11.7, 1.9 Hz, 1H).

^{13}C NMR (125 MHz, C_6D_6) δ 157.89, 138.00 (d, *J* = 15.7 Hz), 121.74 (d, *J* = 43.0 Hz), 112.20 (d, *J* = 43.5 Hz), 64.39 (d, *J* = 14.3 Hz), 32.20, 23.52.

^{19}F NMR (470 MHz, C_6D_6) δ -99.53 (ddt, *J* = 23.0, 12.7, 5.4 Hz).

Synthesis of 7,7-difluoro-2-oxabicyclo[4.1.0]heptane (S18)

Compound **S18** was obtained following the general procedure *u*. Purification by silica gel (8:2 hexane/ethyl acetate) gave the pure product as an orange oil (Yield: 60%).

^{1}H NMR (500 MHz, C_6D_6) δ 3.39 (dtd, *J* = 30.6, 8.1, 7.3, 3.1 Hz, 2H), 2.73 (tt, *J* = 11.2, 2.1 Hz, 1H), 1.47 – 1.39 (m, 1H), 1.31 (dtdd, *J* = 14.8, 11.7, 6.5, 3.4 Hz, 1H), 1.07 (dtq, *J* = 17.3, 7.4, 2.9 Hz, 1H), 0.94 (dtd, *J* = 17.0, 8.7, 4.7 Hz, 1H), 0.79 (ddt, *J* = 13.3, 7.0, 2.8 Hz, 1H).

^{13}C NMR (125 MHz, C_6D_6) δ 116.81 – 107.98 (m), 63.31 (d, *J* = 3.2 Hz), 52.36 (dd, *J* = 17.0, 9.7 Hz), 21.09 (d, *J* = 2.4 Hz), 18.12 (d, *J* = 11.5 Hz), 12.91 (d, *J* = 1.9 Hz).

^{19}F NMR (470 MHz, C_6D_6) δ -129.87 (ddt, *J* = 167.5, 17.3, 8.1 Hz), -155.05 (d, *J* = 167.0 Hz).

Synthesis of 6,6-difluoro-3-oxabicyclo[3.1.0]hexane (S19)

Compound **S19** was obtained following the general procedure *u* and used without any purification (Yield: 50%).

^{1}H NMR (600 MHz, C_6D_6) δ 3.94 (dd, *J* = 9.0, 1.5 Hz, 2H), 3.68 (tt, *J* = 5.0, 2.2 Hz, 2H), 1.55 (dq, *J* = 6.4, 3.5, 2.9 Hz, 2H).

^{13}C NMR (150 MHz, C_6D_6) δ 113.28 (dd, *J* = 299.1, 274.2 Hz), 67.11(2C), 27.84 (dd, *J* = 13.0, 10.3 Hz) (2C).

^{19}F NMR (565 MHz, C_6D_6) δ -127.01 (dt, *J* = 161.9, 12.8 Hz).), -154.09 (d, *J* = 160.8 Hz).

Synthesis of 4-fluoro-2*H*-pyran (P19)

Compound **P19** was obtained following the general procedure *v* or w (Maximum yield:36%). Purification by silica gel (8:2 hexane/ethyl acetate) gave the pure product as an orange oil.

^{1}H NMR (600 MHz, $CDCl_3$) δ 7.64 (dd, *J* = 5.7, 1H), 7.49 – 7.40 (m, 1H), 6.70 (dd, *J* = 4.9, 1.4 Hz, 2H), 4.08 – 3.95 (m, 2H).

^{19}F NMR (565 MHz, $CDCl_3$) δ -72.72(s).

Synthesis of di-tert-butyl 5-fluoro-3-phenylpyridazine-1,2(3*H*,6*H*)-dicarboxylate (P20)

Compound **P20** was obtained following the general procedure *e2* and purify by silica gel using a mixture 95/5 hexane/ethyl acetate (Maximum yield: 93%).

^{1}H NMR (600 MHz, C_6D_6) δ 7.19 – 7.04 (m, 2H), 6.90 – 6.79 (m, 3H), 5.78 (s, 1H), 4.88 (d, *J* = 15.9 Hz, 1H), 4.65 – 4.48 (m, 1H), 3.50 (d, *J* = 16.9 Hz, 1H), 1.21 (s, 9H), 0.97 (d, *J* = 65.6 Hz, 9H).

^{13}C NMR (150 MHz, C_6D_6) δ 156.3 (d, *J* = 260.5 MHz), 153.8, 153.2, 138.6, 128.7, 128.2, 127.5, 102.3(d, *J* =16.8 MHz), 79.9 (2C), 53.9, 41.7 (d, *J* = 40.8MHz), 27.9(3C), 27.4(3C).

^{19}F NMR (470 MHz, None) δ -112.23 (d, *J* = 15.5 Hz).

Synthesis of (11*bS*)-4-hydroxydinaphtho[2,1-*d*:1',2'-*f*][1,3,2]dioxaphosphepine 4-oxide ((*S*)-CT2):

Compound **(*S*)-CT2** was obtained following the general procedure *d2* and purified by silica gel using a mixture 7/3 hexane/ethyl acetate (Yield:74%).

^{1}H NMR (500 MHz, C_6D_6) δ 8.28 – 8.24 (m, 2H), 7.45 – 7.34 (m, 4H), 7.16 (d, *J* = 8.6 Hz, 2H), 6.73 – 6.67 (m, 2H), 6.56 – 6.48 (m, 2H).

^{13}C NMR (125 MHz, DMSO) δ 143.0(2C), 132.2(2C), 131.3(2C), 131.1(2C), 129.0(2C), 127.5(2C), 127.4(2C), 127.1(2C), 126.5(2C), 125.6(2C), 122.0(2C), 121.7(2C).

^{31}P NMR (202 MHz, C_6D_6) δ 4.13 (s).

Synthesis of (11*bS*)-N,N-dimethyldinaphtho[2,1-*d*:1',2'-*f*][1,3,2]dioxaphosphepin-4-amine ((*S*)-CT3):

Compound **(*S*)-CT3** was obtained following the general procedure *e2* and purified by silica gel using a mixture 8/2 hexane/ethyl acetate (Yield:86%).

^{1}H NMR (600 MHz, $CDCl_3$) δ 7.91 (dd, *J* = 9.0, 0.8 Hz, 2H), 7.82 (d, *J* = 9.0, 2H), 7.34 – 7.28 (m, 4H), 7.26 – 7.21 (m, 2H), 7.10 – 7.07 (m, 2H), 2.48(s,3H), 2.47(s, 3H).

^{13}C NMR (150 MHz, $CDCl_3$) δ 152.6(2C), 133.3(2C), 131.3(2C), 128.4(2C), 127.3(2C), 126.1(2C), 124.2(2C), 125.9(2C), 124.2(2C), 124.0(2C), 123.9(2C), 117.4(2C), 110.8(2C), 36.0, 35.8.

^{31}P NMR (243 MHz, $CDCl_3$) δ 14.17.

Synthesis of (11*bS*)-N,N-diethyldinaphtho[2,1-*d*:1',2'-*f*][1,3,2]dioxaphosphepin-4-amine ((*S*)-CT4)

Compound **(*S*)-CT4** was obtained following the general procedure *f2* and purified by silica gel using a mixture 8/2 hexane/ethyl acetate (Yield:80%).

^{1}H NMR (500 MHz, $CDCl_3$) δ 8.06 – 8.02 (m, 2H), 7.85 (d, *J* = 7.9 Hz, 2H), 7.40 – 7.32 (m, 4H), 7.33 – 7.26 (m, 4H), 3.28 (m, 4H), 1.23 (t, *J* = 4.3, 1.1 Hz, 3H).

^{13}C NMR (150 MHz, $CDCl_3$) δ 153.4(2C), 132.2(2C), 131.0(2C), 128.3(2C), 127.7(2C), 126.4(2C), 125.4(2C), 125.9(2C), 124.2(2C), 123.7(2C), 121.1(2C) 117.4(2C), 110.8(2C), 39.6(2C), 15.4(2C).

^{31}P NMR (202 MHz, $CDCl_3$) δ 15.90.

Synthesis of (S)-CT6

Compound **(*S*)-CT6** was obtained from (*S*)-BINOL following the general procedure *g2* and purified by pentane crystallization (Yield:75%).

^{1}H NMR (500 MHz, $CDCl_3$) δ 7.91 (d, *J* = 9.0 Hz, 1H), 7.83 (d, *J* = 8.0 Hz, 1H), 7.34 – 7.28 (m, 2H), 7.24 (ddd, *J* = 8.2, 6.8, 1.4 Hz, 1H), 7.08 (d, *J* = 8.0, 1H).

^{13}C NMR (125 MHz, $CDCl_3$) δ 152.8(2C), 133.3(2C), 133.2(2C), 131.5(2C), 129.5(2C), 128.5(2C), 128.4(2C), 127.5(2C), 124.2(2C), 124.06(2C), 117.77(2C), 110.81(2C).

Synthesis of (*S*)-CT12

Compound **(*S*)-CT12** was obtained following the general procedure *h2* and purified by silica gel using a mixture 9/1 hexane/ethyl acetate (Yield:66%).

^{1}H NMR (500 MHz, C_6D_6) δ 7.63 (d, *J* = 8.1 Hz, 2H), 7.57 (d, *J* = 8.5 Hz, 2H), 7.29 – 7.26 (m, 4H), 7.18(s, 2H), 7.13 – 7.10 (m, 2H), 6.99 (ddd, *J* = 8.5, 6.3, 1.3 Hz, 2H), 4.63 (d, *J* = 5.9 Hz, 2H), 4.44 (d, *J* = 5.8 Hz, 2H), 3.15 (h, *J* = 6.8 Hz, 4H), 2.95 – 2.84 (m, 2H), 2.57 (m, 4H), 1.48 (d, *J* = 6.7 Hz, 6H), 1.31 (q, *J* = 6.9, 6.1 Hz, 24H), 1.14 (d, *J* = 6.8 Hz, 6H), 0.50 (t, *J* = 7.0 Hz, 6H).

^{13}C NMR (125 MHz, C_6D_6) δ 152.9(2C), 148.5(2C), 147.9(2C), 147.1(2C), 134.4(2C), 133.9(2C), 131.2(2C), 130.7(2C), 127.1(2C), 126.5(2C), 126.2(2C), 124.9(2C), 120.4(2C), 120.5(2C), 96.7(2C), 96.6(2C), 63.8(2C), 63.7(2C), 34.5(2C), 31.1(2C), 30.8(2C), 25.8(2C), 25.2(2C), 24.1(2C), 24.0(2C), 23.2, (2C) 23.4(2C), 22.7(2C), 14.3(2C), 14.2(2C).

Synthesis of (*S*)-CT13

Compound **(*S*)-CT13** was obtained from compound **(*S*)-CT12** following the general procedure *i2* and purified by silica gel using a mixture 8/2 hexane/ethyl acetate (Yield:90%).

^{1}H NMR (500 MHz, C_6D_6) δ 7.74 (s, 2H), 7.70 (dd, *J* = 7.5, 1.8 Hz, 2H), 7.54 (dd, *J* = 7.9, 1.6 Hz, 2H), 7.29 (d, *J* = 2.0 Hz, 4H), 7.19 – 7.12 (m, 4H), 3.20 – 3.11 (m, 2H), 2.90 (dp, *J* = 15.8, 6.9 Hz, 4H), 1.29 (ddd, *J* = 12.6, 11.5, 6.9 Hz, 24H), 1.18 (dd, *J* = 9.8, 6.8 Hz, 12H).

^{13}C NMR (125 MHz, C_6D_6) δ 150.1(2C), 148.4(2C), 147.3(2C), 147.1(2C), 133.1(2C), 130.3(2C), 129.9(2C), 128.6(2C), 128.5(2C), 127.5(2C), 127.1(2C), 126.7(2C), 125.9(2C), 123.9(2C), 123.1(2C), 120.3(2C), 120.2(2C), 112.8(2C), 33.66(2C), 30.25(2C), 30.13(2C), 23.3(2C), 23.1(2C), 23.0(2C), 22.9(2C), 21.8(2C), 13.1 (2C).

Synthesis of (*S*)-CT7

Compound **(*S*)-CT7** was obtained from compound **(*S*)-CT13** following the general procedure *g2* and purified by pentane crystallization (Yield: 76%).

^{1}H NMR (500 MHz, $CDCl_3$) δ 7.82 (d, *J* = 8.1 Hz, 2H), 7.72 (s, 2H), 7.34 – 7.30 (m, 2H), 7.29 – 7.23 (m, 4H), 7.11 – 7.04 (m, 4H), 2.90 (q, *J* = 6.9 Hz, 2H), 2.80 (p, *J* = 6.9 Hz, 2H), 2.69 – 2.58 (m, 2H), 1.26 (d, *J* = 6.9 Hz, 12H), 1.15 (d, *J* = 6.8 Hz, 6H), 1.05 (dd, *J* = 11.8, 6.8 Hz, 12H), 0.98 (d, *J* = 6.8 Hz, 6H).

^{13}C NMR (1265 MHz, $CDCl_3$) δ 149.6(2C), 148.1(2C), 146.7(2C), 146.7(2C), 132.4(2C), 129.7(2C), 129.6(2C), 129.3(2C), 128.1(2C), 128.0(2C), 127.2(2C), 125.6(2C), 123.5(2C), 122.7(2C), 120.2(2C), 120.1(2C), 112.1(2C), 112.0(2C), 33.3(2C), 29.8(2C), 29.7(2C), 23.3(2C), 23.2(2C), 23.0(2C), 22.9(2C), 22.8(2C), 22.7(2C).

Synthesis of ((4*S*,5*S*)-2,2-dimethyl-1,3-dioxolane-4,5-diyl)bis(bis(2,4,6-triisopropylphenyl)methanol) ((*S*,*S*)-CT14)

Compound **(*S*,*S*)-CT14** was obtained following the general procedure *j2* and purified by silica gel using a mixture 1/1 hexane/ethyl acetate (Yield: 45%).

^{1}H NMR (600 MHz, $CDCl_3$) δ 7.02 (s, 8H), 5.71 (s, 2H), 3.91 (s, 1H), 3.79 (s, 6H), 3.77(s, 1H), 2.91 (p, *J* = 6.9 Hz, 4H), 2.63 (p, *J* = 6.7 Hz, 8H), 1.26 (d, *J* = 6.9, 24H), 1.18 (m, 48H).
^{13}C NMR (150 MHz, $CDCl_3$) δ NMR 165.2(4C), 150.57(4C), 145.5(4C), 132.3(4C), 121.1(8C), 118.1, 97.5(2C), 51.6(2C), 34.5(4C), 34.4(8C), 31.7 (2C), 31.3(8C), 23.7(16C).

Synthesis of (*S*,*S*)-CT8

Compound **(*S*,*S*)-CT8** was obtained from compound **(*S*,*S*)-CT14** following the general procedure *j2* and purified by pentane crystallization (Yield: 50%).

^{1}H NMR (500 MHz, C_6D_6) δ 7.21 (d, *J* = 2.5 Hz, 4H), 7.07 (d, *J* = 2.6 Hz, 4H), 5.96 – 5.85 (s, 2H), 3.98 (s, 3H), 3.32 (s, 3H), 2.87 (p, *J* = 6.7 Hz, 4H), 2.64 (p, *J* = 6.7 Hz, 8H), 1.34 – 1.03 (m, 72H),
^{13}C NMR (150 MHz, $CDCl_3$) δ NMR 165.2(4C), 150.57(4C), 145.5(4C), 132.3(4C), 121.1(8C), 87.5(2C), 83.5(2C), 51.6(2C), 34.5(4C), 34.4(8C), 31.7 (2C), 31.3(8C), 23.7(16C).

List of abbreviations

5-H(p)ETE	Arachidonic acid 5-hydroperoxide
5-LO	5-Lipoxygenase
ADME	Absorption, distribution, metabolism, excretion
AML	Acute myeloid leukemia
AR	Androgen receptor
B4GALT1	Beta-1,4-galactosyltransferase 1
BAZ2B	Bromodomain adjacent to zinc finger domain 2B [(human)]
BET	Bromodomain and extraterminal proteins
BINOL-PHOS	1,1'-Bi-2-naphthol phosphoric acid
BRD2	Bromodomain-containing protein 2
BRD2-BD1	Bromodomain-containing protein 2-domain 1
BRD2-BD2	Bromodomain-containing protein 2-domain 2
BRD3	Bromodomain-containing protein 3
BRD3-BD1	Bromodomain-containing protein 3-domain 1
BRD3-BD2	Bromodomain-containing protein 3-domain 2
BRD4	Bromodomain-containing protein 4
BRD4-BD1	Bromodomain-containing protein 4-domain 1
BRD4-BD2	Bromodomain-containing protein 4-domain 2
BRD7	Bromodomain-containing protein 7
BRD9	Bromodomain-containing protein 9
BRDs	Bromodomain
BRDT-BD1	Bromodomain testis-domain 1
COXs	Cyclooxygenase-1/2
cPGES	5-lipoxygenase activating protein
CREBBP	Proteina legante CREB
CYPs	Cytochromes P450 **enzymes**
DA	Diels-alder reactions
DavePhos	2-Dicyclohexylphosphino-2′-(N,N-dimethylamino)biphenyl ligand
DHETs	Dihydroxyeicosatrienoic acids
DIPEA	N,N-Diisopropylethylamine
DMF	Dimethylformamide
DMSO	Dimethyl sulfoxide
EDC·HCl	1-ethyl-3- (3-dimethylaminopropyl) Carbodiimide Hydrochloride
ee	Enantiomeric excess
EETs	Epoxyeicosatrienoic acids
EH1	Epoxide hydrolase 1
EH3	Epoxide hydrolase 3
EH4	Epoxide hydrolase 4
ESI	Electrospray ionization
ESMS	Electrospray mass spectrometry
ESR1	Estrogen receptor
FLAP	5-lipoxygenase activating protein
FRET	Fluorescence resonance energy transfer
GSH	Glutathione
HAT	Histone acetyltransferases
HDACs	Histone deacetylases
HOBt	Hydroxybenzotriazole

HOMO	Highest Occupied Molecular Orbital
HPLC	High performance liquid chromatography
HTS	High Throughput Screening
HTVS)	High-Throughput Virtual Screening scoring and sampling
IBA	Interaction-based approach
IL-1β	Interleukin-1β
IVS	Inverse Virtual Screening
LDA	Lithium diisopropyl amide
LPS	Lipopolysaccharide
LT	Leukotriene
LTA4	Leukotriene A4
LTB4	Leukotriene B4
LTC4S	Leukotriene C4 synthase
LUMO	Lowest Unoccupied Molecular Orbital
MAPEG	Membrane-associated proteins in eicosanoid and glutathione metabolism
mEH	Microsomal Hydrolase activity
MGST1	Microsomal glutathione S-transferase 1
MGST2	Microsomal glutathione S-transferase 2
MGST3	Microsomal glutathione S-transferase 3
mPGES-1	Microsomal prostaglandin E2 synthase-1
mPGES-2	Microsomal prostaglandin E2 synthase-2
MW	Microwave
NRB	Nuclear receptor binding peptide
NSAIDs	Nonsteroidal anti-inflammatory drugs
PAINS	Pan-Assay Interference Compounds
PAMPA	Parallel artificial membrane permeability assa
PGD2	Prostaglandin D2
PGE2	Prostaglandin E2
PGF2α	Prostaglandin F2α
PGG2	Prostaglandin G2
PGH2	Prostaglandin H2
PGI2	Prostaglandin I2
PGs	Prostaglandins
PTSA	Para-toluenesulfonic acid
(*S*)-TRIP	(11bS)-4-idrossi-2,6-bis[2,4,6-tris(1-metiletil)fenil]dinafto[2,1-d:1μ ,2μ-f]-1,3,2-diossafosfepina 4-ossido, (S)-3,3μ-Bis(2,4,6-triisopropilfenil)-1,1μ-bi-2-naftolo Monofosfato ciclico
SBPA	Structure-based three-dimensional pharmacophore approach
sEH	Soluble epoxide
sEH-H	Soluble epoxide Hydrolase activity
sEH-P	Soluble epoxide phosphatase activity
SM	Starting material
SP	Standard precision
SUMO	Small Ubiquitin-like Modifier
SWI/SNF	mammalian switch/sucrose non-fermentable
TBHP	Tert-Butyl hydroperoxide
TFA	Trifluoroacetic acid
THF	Tetrahydrofuran
TLC	Thin layer chromatography

TMS-CF3	Trifluoromethyltrimethylsilane
TNF-α	Tumor necrosis factor α
XP	Extra precision

References

1. Rajanarendar, E.; Venkateshwarlu, P.; Krishna, S. R.; Reddy, K. G.; Thirupathaiah, K., One-Pot Three Component Domino Reaction for the Synthesis of Novel Isoxazolo [2, 3-*c*][1, 3, 5] Thiadiazepin-2-Ones Catalyzed by PTSA. Green Chemistry Approach. *Green and Sustainable Chemistry* **2015**, *5* (03), 107-114.
2. Springfield, S. A.; Marcantonio, K.; Ceglia, S.; Albaneze-Walker, J.; Dormer, P. G.; Nelson, T. D.; Murry, J. A., A convenient one-pot synthesis of 1, 8-naphthyridones. *The Journal of Organic Chemistry* **2003**, *68* (11), 4598-4599.
3. Gao, X.; Pan, Y.-m.; Lin, M.; Chen, L.; Zhan, Z.-p., Facile one-pot synthesis of three different substituted thiazoles from propargylic alcohols. *Organic & Biomolecular Chemistry* **2010**, *8* (14), 3259-3266.
4. Bhandari, M.; Raj, S., Practical approach to green chemistry. *International Journal of Pharmacy and Pharmaceutical Science* **2017**, *9(1)*, 10-26.
5. Grewal, A. S.; Kumar, K.; Redhu, S.; Bhardwaj, S., Microwave assisted synthesis: a green chemistry approach. *International Research Journal of Pharmaceutical and Applied Sciences* **2013**, *3* (5), 278-285.
6. Chen, Q. W.; Zhu, X.; Li, Y.; Meng, Z., Epigenetic regulation and cancer. *Oncology Reports* **2014**, *31* (2), 523-532.
7. Baylin, S. B.; Jones, P. A., A decade of exploring the cancer epigenome—biological and translational implications. *Nature Reviews Cancer* **2011**, *11* (10), 726-734.
8. Kouzarides, T., Chromatin modifications and their function. *Cell* **2007**, *128* (4), 693-705.
9. Dawson, M. A.; Kouzarides, T., Cancer epigenetics: from mechanism to therapy. *Cell* **2012**, *150* (1), 12-27.
10. Minucci, S.; Pelicci, P. G., Histone deacetylase inhibitors and the promise of epigenetic (and more) treatments for cancer. *Nature Reviews Cancer* **2006**, *6* (1), 38-51.
11. Bannister, A. J.; Kouzarides, T., Regulation of chromatin by histone modifications. *Cell Research* **2011**, *21* (3), 381-395.
12. Adolph, K. W.; Song, M.-K. H., Variations in ADP-ribosylation of nuclear scaffold proteins during the HeLa cell cycle. *Biochemical and Biophysical Research Communications* **1985**, *126* (2), 840-847.
13. Hassa, P. O.; Haenni, S. S.; Elser, M.; Hottiger, M. O., Nuclear ADP-ribosylation reactions in mammalian cells: where are we today and where are we going? *Microbiology and Molecular Biology Reviews* **2006**, *70* (3), 789-829.
14. Zhang, L.; Zhang, J.; Jiang, Q.; Zhang, L.; Song, W., Zinc binding groups for histone deacetylase inhibitors. *Journal of Enzyme Inhibition and Medicinal Chemistry* **2018**, *33* (1), 714-721.
15. Seto, E.; Yoshida, M., Erasers of histone acetylation: the histone deacetylase enzymes. *Cold Spring Harbor Perspectives in Biology* **2014**, *6* (4), 713-731.
16. Biswas, S.; Rao, C. M., Epigenetic tools (The Writers, The Readers and The Erasers) and their implications in cancer therapy. *European Journal of Pharmacology* **2018**, *837(1)*, 8-24.
17. Filippakopoulos, P.; Picaud, S.; Mangos, M.; Keates, T.; Lambert, J.-P.; Barsyte-Lovejoy, D.; Felletar, I.; Volkmer, R.; Müller, S.; Pawson, T., Histone recognition and large-scale structural analysis of the human bromodomain family. *Cell* **2012**, *149* (1), 214-231.
18. Taniguchi, Y., The bromodomain and extra-terminal domain (BET) family: functional anatomy of BET paralogous proteins. *International Journal of Molecular Sciences* **2016**, *17* (11), 1849-1873.
19. Yu, X.; Li, Z.; Shen, J., BRD7: a novel tumor suppressor gene in different cancers. *American Journal of Translational Research* **2016**, *8* (2), 742-748.
20. Flynn, E. M.; Huang, O. W.; Poy, F.; Oppikofer, M.; Bellon, S. F.; Tang, Y.; Cochran, A. G., A subset of human bromodomains recognizes butyryllysine and crotonyllysine histone peptide modifications. *Structure* **2015**, *23* (10), 1801-1814.
21. Euskirchen, G. M.; Auerbach, R. K.; Davidov, E.; Gianoulis, T. A.; Zhong, G.; Rozowsky, J.; Bhardwaj, N.; Gerstein, M. B.; Snyder, M., Diverse roles and interactions of the SWI/SNF chromatin remodeling complex revealed using global approaches. *PLoS Genetics* **2011**, *7* (3), 2008-2028.

22. Yap, K. L.; Zhou, M.-M., Structure and mechanisms of lysine methylation recognition by the chromodomain in gene transcription. *Biochemistry* **2011**, *50* (12), 1966-1980.
23. Hui, M.; Jian, Z.; Peiyuan, Z.; Zhenwei, W.; Huibin, Z., Research progress of selective small molecule bromodomain-containing protein 9 inhibitors. *Future Medicinal chemistry* **2018**, *10* (8), 895-906.
24. Clark, P. G.; Vieira, L. C.; Tallant, C.; Fedorov, O.; Singleton, D. C.; Rogers, C. M.; Monteiro, O. P.; Bennett, J. M.; Baronio, R.; Müller, S., LP99: discovery and synthesis of the first selective BRD7/9 bromodomain inhibitor. *Angewandte Chemie* **2015**, *127* (21), 6315-6319.
25. Theodoulou, N. H.; Bamborough, P.; Bannister, A. J.; Becher, I.; Bit, R. A.; Che, K. H.; Chung, C.-w.; Dittmann, A.; Drewes, G.; Drewry, D. H., Discovery of I-BRD9, a selective cell active chemical probe for bromodomain containing protein 9 inhibition. *Journal of Medicinal Chemistry* **2016,** *59* (4), 1425-1439.
26. Funk, C. D., Prostaglandins and leukotrienes: advances in eicosanoid biology. *Science* **2001**, *294* (5548), 1871-1875.
27. Dennis, E. A.; Norris, P. C., Eicosanoid storm in infection and inflammation. *Nature Reviews Immunology* **2015**, *15* (8), 511-523.
28. Wallace, J. L., Prostaglandian biology in inflammatory bowel disease. *Gastroenterology Clinics* **2001**, *30* (4), 971-980.
29. Levy, B. D.; Clish, C. B.; Schmidt, B.; Gronert, K.; Serhan, C. N., Lipid mediator class switching during acute inflammation: signals in resolution. *Nature Immunology* **2001**, *2* (7), 612-619.
30. Tang, X.; Edwards, E. M.; Holmes, B. B.; Falck, J. R.; Campbell, W. B., Role of phospholipase C and diacylglyceride lipase pathway in arachidonic acid release and acetylcholine-induced vascular relaxation in rabbit aorta. *American Journal of Physiology-Heart and Circulatory Physiology* **2006**, *290* (1), 37-45.
31. Bell, R.; Kennerly, D. A.; Stanford, N.; Majerus, P. W., Diglyceride lipase: a pathway for arachidonate release from human platelets. *Proceedings of the National Academy of Sciences* **1979**, *76* (7), 3238-3241.
32. Park, J. Y.; Pillinger, M. H.; Abramson, S. B., Prostaglandin E_2 synthesis and secretion: the role of PGE_2 synthases. *Clinical immunology* **2006**, *119* (3), 229-240.
33. Tanioka, T.; Nakatani, Y.; Semmyo, N.; Murakami, M.; Kudo, I., Molecular identification of cytosolic prostaglandin E_2 synthase that is functionally coupled with cyclooxygenase-1 in immediate prostaglandin E_2 biosynthesis. *Journal of Biological Chemistry* **2000**, *275* (42), 32775-32782.
34. Koeberle, A.; Werz, O., Perspective of microsomal prostaglandin E2 synthase-1 as drug target in inflammation-related disorders. *Biochemical Pharmacology* **2015**, *98* (1), 1-15.
35. Tanikawa, N.; Ohmiya, Y.; Ohkubo, H.; Hashimoto, K.; Kangawa, K.; Kojima, M.; Ito, S.; Watanabe, K., Identification and characterization of a novel type of membrane-associated prostaglandin E synthase. *Biochemical and Biophysical Research Communications* **2002**, *291* (4), 884-889.
36. Luz, J. G.; Antonysamy, S.; Kuklish, S. L.; Condon, B.; Lee, M. R.; Allison, D.; Yu, X.-P.; Chandrasekhar, S.; Backer, R.; Zhang, A., Crystal structures of mPGES-1 inhibitor complexes form a basis for the rational design of potent analgesic and anti-inflammatory therapeutics. *Journal of Medicinal Chemistry* **2015**, *58* (11), 4727-4737.
37. Bergqvist, F.; Morgenstern, R.; Jakobsson, P.J., A review on mPGES-1 inhibitors: From preclinical studies to clinical applications. *Prostaglandins & Other Lipid Mediators* **2020**, *147*(1), 1-11.
38. Koeberle, A.; Werz, O., Natural products as inhibitors of prostaglandin E_2 and pro-inflammatory 5-lipoxygenase-derived lipid mediator biosynthesis. *Biotechnology Advances* **2018**, *36* (6), 1709-1723.
39. Yang, J.; Bratt, J.; Franzi, L.; Liu, J.-Y.; Zhang, G.; Zeki, A. A.; Vogel, C. F.; Williams, K.; Dong, H.; Lin, Y., Soluble epoxide hydrolase inhibitor attenuates inflammation and airway hyperresponsiveness in mice. *American Journal of Respiratory Cell and Molecular Biology* **2015**, *52* (1), 46-55.
40. McReynolds, C. B.; Hwang, S. H.; Yang, J.; Wan, D.; Wagner, K.; Morisseau, C.; Li, D.; Schmidt, W. K.; Hammock, B. D., Pharmaceutical effects of inhibiting the soluble epoxide hydrolase in canine osteoarthritis. *Frontiers in Pharmacology* **2019**, *10(1)*, 533-545.
41. Qu, Q.; Xuan, W.; Fan, G. H., Roles of resolvins in the resolution of acute inflammation. *Cell Biology International* **2015**, *39* (1), 3-22.
42. Morisseau, C., Role of epoxide hydrolases in lipid metabolism. *Biochimie* **2013**, *95* (1), 91-95.

43. Bettaieb, A.; Koike, S.; Chahed, S.; Zhao, Y.; Bachaalany, S.; Hashoush, N.; Graham, J.; Fatima, H.; Havel, P. J.; Gruzdev, A., Podocyte-specific soluble epoxide hydrolase deficiency in mice attenuates acute kidney injury. *Wiley Online Library* **2017**; 284(1), 1970-1986.
44. Stichtenoth, D. O.; Thorén, S.; Bian, H.; Peters-Golden, M.; Jakobsson, P.-J.; Crofford, L. J., Microsomal prostaglandin E synthase is regulated by proinflammatory cytokines and glucocorticoids in primary rheumatoid synovial cells. *The Journal of Immunology* **2001**, *167* (1), 469-474.
45. Jakobsson, P.-J.; Thorén, S.; Morgenstern, R.; Samuelsson, B., Identification of human prostaglandin E synthase: a microsomal, glutathione-dependent, inducible enzyme, constituting a potential novel drug target. *Proceedings of the National Academy of Sciences* **1999**, *96* (13), 7220-7225.
46. Jakobsson, P.-J.; Morgenstern, R.; Mancini, J.; Ford-Hutchinson, A.; Persson, B., Common structural features of MAPEG—a widespread superfamily of membrane associated proteins with highly divergent functions in eicosanoid and glutathione metabolism. *Protein Science* **1999**, *8* (3), 689-692.
47. Jakobsson, P.-J.; Mancini, J. A.; Ford-Hutchinson, A. W., Identification and characterization of a novel human microsomal glutathione S-transferase with leukotriene C4 synthase activity and significant sequence identity to 5-lipoxygenase-activating protein and leukotriene C4 synthase. *Journal of Biological Chemistry* **1996**, *271* (36), 22203-22210.
48. Jegerschöld, C.; Pawelzik, S.-C.; Purhonen, P.; Bhakat, P.; Gheorghe, K. R.; Gyobu, N.; Mitsuoka, K.; Morgenstern, R.; Jakobsson, P.-J.; Hebert, H., Structural basis for induced formation of the inflammatory mediator prostaglandin E_2. *Proceedings of the National Academy of Sciences* **2008**, *105* (32), 11110-11115.
49. Sjögren, T.; Nord, J.; Ek, M.; Johansson, P.; Liu, G.; Geschwindner, S., Crystal structure of microsomal prostaglandin E2 synthase provides insight into diversity in the MAPEG superfamily. *Proceedings of the National Academy of Sciences* **2013**, *110* (10), 3806-3811.
50. Brock, J. S.; Hamberg, M.; Balagunaseelan, N.; Goodman, M.; Morgenstern, R.; Strandback, E.; Samuelsson, B.; Rinaldo-Matthis, A.; Haeggström, J. Z., A dynamic Asp–Arg interaction is essential for catalysis in microsomal prostaglandin E_2 synthase. *Proceedings of the National Academy of Sciences* **2016**, *113* (4), 972-977.
51. Koeberle, A.; Northoff, H.; Werz, O., Curcumin blocks prostaglandin E2 biosynthesis through direct inhibition of the microsomal prostaglandin E_2 synthase-1. *Molecular Cancer Therapeutics* **2009**, *8* (8), 2348-2355.
52. Koeberle, A.; Bauer, J.; Verhoff, M.; Hoffmann, M.; Northoff, H.; Werz, O., Green tea epigallocatechin-3-gallate inhibits microsomal prostaglandin E_2 synthase-1. *Biochemical and Biophysical Research Communications* **2009**, *388* (2), 350-354.
53. Koeberle, A.; Northoff, H.; Werz, O., Identification of 5-lipoxygenase and microsomal prostaglandin E_2 synthase-1 as functional targets of the anti-inflammatory and anti-carcinogenic garcinol. *Biochemical Pharmacology* **2009**, *77* (9), 1513-1521.
54. Koeberle, A.; Rossi, A.; Bauer, J.; Dehm, F.; Verotta, L.; Northoff, H.; Sautebin, L.; Werz, O., Hyperforin, an anti-inflammatory constituent from St. John's wort, inhibits microsomal prostaglandin E_2 Synthase-1 and Suppresses Prostaglandin E_2 Formation *in vivo*. *Frontiers in Pharmacology **2011**, 2(7), 1-10.*
55. Bauer, J.; Kuehnl, S.; Rollinger, J. M.; Scherer, O.; Northoff, H.; Stuppner, H.; Werz, O.; Koeberle, A., Carnosol and carnosic acids from Salvia officinalis inhibit microsomal prostaglandin E2 synthase-1. *Journal of Pharmacology and Experimental Therapeutics* **2012**, *342* (1), 169-176.
56. Schaible, A. M.; Traber, H.; Temml, V.; Noha, S. M.; Filosa, R.; Peduto, A.; Weinigel, C.; Barz, D.; Schuster, D.; Werz, O., Potent inhibition of human 5-lipoxygenase and microsomal prostaglandin E2 synthase-1 by the anti-carcinogenic and anti-inflammatory agent embelin. *Biochemical Pharmacology* **2013**, *86* (4), 476-486.
57. Shiro, T.; Takahashi, H.; Kakiguchi, K.; Inoue, Y.; Masuda, K.; Nagata, H.; Tobe, M., Synthesis and SAR study of imidazoquinolines as a novel structural class of microsomal prostaglandin E_2 synthase-1 inhibitors. *Bioorganic & Medicinal Chemistry Letters* **2012**, *22* (1), 285-288.
58. Riendeau, D.; Aspiotis, R.; Ethier, D.; Gareau, Y.; Grimm, E. L.; Guay, J.; Guiral, S.; Juteau, H.; Mancini, J. A.; Méthot, N., Inhibitors of the inducible microsomal prostaglandin E_2 synthase (mPGES-1) derived from MK-886. *Bioorganic & Medicinal Chemistry Letters* **2005**, *15* (14), 3352-3355.

59. Wu, T. Y.; Juteau, H.; Ducharme, Y.; Friesen, R. W.; Guiral, S.; Dufresne, L.; Poirier, H.; Salem, M.; Riendeau, D.; Mancini, J., Biarylimidazoles as inhibitors of microsomal prostaglandin E_2 synthase-1. *Bioorganic & Medicinal Chemistry Letters* **2010**, *20* (23), 6978-6982.
60. Giroux, A.; Boulet, L.; Brideau, C.; Chau, A.; Claveau, D.; Côté, B.; Ethier, D.; Frenette, R.; Gagnon, M.; Guay, J., Discovery of disubstituted phenanthrene imidazoles as potent, selective and orally active mPGES-1 inhibitors. *Bioorganic & Medicinal Chemistry letters* **2009**, *19* (20), 5837-5841.
61. Singh Bahia, M.; Silakari, O., Exploring the biological potential of urea derivatives against mPGES-1: a combination of quantum mechanics, pharmacophore modelling and QSAR analyses. *Medicinal Chemistry* **2013**, *9* (1), 138-151.
62. Arhancet, G. B.; Walker, D. P.; Metz, S.; Fobian, Y. M.; Heasley, S. E.; Carter, J. S.; Springer, J. R.; Jones, D. E.; Hayes, M. J.; Shaffer, A. F., Discovery and SAR of PF-4693627, a potent, selective and orally bioavailable mPGES-1 inhibitor for the potential treatment of inflammation. *Bioorganic & Medicinal Chemistry Letters* **2013**, *23* (4), 1114-1119.
63. Walker, D. P.; Arhancet, G. B.; Lu, H.-F.; Heasley, S. E.; Metz, S.; Kablaoui, N. M.; Franco, F. M.; Hanau, C. E.; Scholten, J. A.; Springer, J. R., Synthesis and biological evaluation of substituted benzoxazoles as inhibitors of mPGES-1: use of a conformation-based hypothesis to facilitate compound design. *Bioorganic & Medicinal Chemistry Letters* **2013**, *23* (4), 1120-1126.
64. Banerjee, A.; Pawar, M. Y.; Patil, S.; Yadav, P. S.; Kadam, P. A.; Kattige, V. G.; Deshpande, D. S.; Pednekar, P. V.; Pisat, M. K.; Gharat, L. A., Development of 2-aryl substituted quinazolin-4 (3H)-one, pyrido [4, 3-d] pyrimidin-4 (3H)-one and pyrido [2, 3-d] pyrimidin-4 (3H)-one derivatives as microsomal prostaglandin E_2 synthase-1 inhibitors. *Bioorganic & Medicinal Chemistry Letters* **2014**, *24* (20), 4838-4844.
65. Jin, Y.; Smith, C.; Hu, L.; Campanale, K.; Stoltz, R.; Huffman Jr, L.; McNearney, T.; Yang, X.; Ackermann, B.; Dean, R., Pharmacodynamic comparison of LY3023703, a novel microsomal prostaglandin e synthase 1 inhibitor, with celecoxib. *Clinical Pharmacology & Therapeutics* **2016**, *99* (3), 274-284.
66. Decker, M.; Arand, M.; Cronin, A., Mammalian epoxide hydrolases in xenobiotic metabolism and signalling. *Archives of Toxicology* **2009**, *83* (4), 297-318.
67. Marowsky, A.; Burgener, J.; Falck, J.; Fritschy, J.-M.; Arand, M., Distribution of soluble and microsomal epoxide hydrolase in the mouse brain and its contribution to cerebral epoxyeicosatrienoic acid metabolism. *Neuroscience* **2009**, *163* (2), 646-661.
68. Fulton, D.; Falck, J.; McGiff, J.; Carroll, M.; Quilley, J., A method for the determination of 5, 6-EET using the lactone as an intermediate in the formation of the diol. *Journal of Lipid Research* **1998**, *39* (8), 1713-1721.
69. Kramer, J.; Proschak, E., Phosphatase activity of soluble epoxide hydrolase. *Prostaglandins & Other Lipid Mediators* **2017,** *133(1)*, 88-92.
70. Morisseau, C.; Hammock, B. D., Gerry Brooks and epoxide hydrolases: four decades to a pharmaceutical. Pest Management Science: Formerly Pesticide Science 2008, 64 (6), 594-609.
71. Cronin, A.; Mowbray, S.; Dürk, H.; Homburg, S.; Fleming, I.; Fisslthaler, B.; Oesch, F.; Arand, M., The N-terminal domain of mammalian soluble epoxide hydrolase is a phosphatase. *Proceeding of the Natural Academy of Science USA* **2003**, 100 (4), 1552-1557.
72. Schiøtt, B.; Bruice, T. C., Reaction mechanism of soluble epoxide hydrolase: insights from molecular dynamics simulations. *Journal of the American Chemical Society* **2002**, *124* (49), 14558-14570.
73. Hopmann, K. H.; Himo, F., Theoretical study of the full reaction mechanism of human soluble epoxide hydrolase. *Chemistry–A European Journal* **2006,** *12* (26), 6898-6909.
74. Evans, J. F.; Ferguson, A. D.; Mosley, R. T.; Hutchinson, J. H., What's all the FLAP about?: 5-lipoxygenase-activating protein inhibitors for inflammatory diseases. *Trends in Pharmacological Sciences* **2008**, *29* (2), 72-78.
75. Morisseau, C.; Goodrow, M. H.; Newman, J. W.; Wheelock, C. E.; Dowdy, D. L.; Hammock, B. D., Structural refinement of inhibitors of urea-based soluble epoxide hydrolases. *Biochemical Pharmacology* **2002**, *63* (9), 1599-1608.
76. Argiriadi, M. A.; Morisseau, C.; Goodrow, M. H.; Dowdy, D. L.; Hammock, B. D.; Christianson, D. W., Binding of alkylurea inhibitors to epoxide hydrolase implicates active site tyrosines in substrate activation. *Journal of Biological Chemistry* **2000**, *275* (20), 15265-15270.

77. Kim, I. H.; Heirtzler, F. R.; Morisseau, C.; Nishi, K.; Tsai, H.-J.; Hammock, B. D., Optimization of amide-based inhibitors of soluble epoxide hydrolase with improved water solubility. *Journal of Medicinal Chemistry* **2005**, *48* (10), 3621-3629.
78. Shen, H. C.; Hammock, B. D., Discovery of inhibitors of soluble epoxide hydrolase: a target with multiple potential therapeutic indications. *Journal of Medicinal Chemistry* **2012**, *55* (5), 1789-1808.
79. Mandal, D. K., *Pericyclic Chemistry*. **2018**.
80. Hoffmann, R.; Woodward, R. B., Conservation of orbital symmetry. *Accounts of Chemical Research* **1968**, *1* (1), 17-22.
81. Diels, O. A., K. , Synthesen in der hydroaromatischen Reihe. *Justus Liebigs Annual der Chemie* **1928**, *460(1)*, 98-112.
82. Gajewski, J. J.; Peterson, K. B.; Kagel, J. R.; Huang, Y. J., Transition-state structure variation in the Diels-Alder reaction from secondary deuterium kinetic isotope effects. The reaction of nearly symmetrical dienes and dienophiles is nearly synchronous. *Journal of the American Chemical Society* **1989**, *111* (25), 9078-9081.
83. Houk, K.; Lin, Y. T.; Brown, F. K., Evidence for the concerted mechanism of the Diels-Alder reaction of butadiene with ethylene. *Journal of the American Chemical Society* **1986**, *108* (3), 554-556.
84. Goldstein, E.; Beno, B.; Houk, K., Density functional theory prediction of the relative energies and isotope effects for the concerted and stepwise mechanisms of the Diels− Alder reaction of butadiene and ethylene. *Journal of the American Chemical Society* **1996**, *118* (25), 6036-6043.
85. Otto, S.; Bertoncin, F.; Engberts, J. B., Lewis acid catalysis of a Diels− Alder reaction in water. *Journal of the American Chemical Society* **1996**, *118* (33), 7702-7707.
86. Evers, J. T. M.; Mackor, A., Photocatalysis (II) photochemical cycloadditions of cyclohexenes and cycloheptene with conjugated dienes catalysed by copper (I) trifluoromethane sulphonate. *Tetrahedron Letters* **1978**, *19* (26), 2317-2320.
87. Otto, S.; Blokzijl, W.; Engberts, J. B., Diels-Alder reactions in water. effects of hydrophobicity and hydrogen bonding. *The Journal of Organic Chemistry* **1994**, *59* (18), 5372-5376.
88. Lubineau, A.; Augé, J.; Queneau, Y., Water-promoted organic reactions. *Synthesis* **1994**, *1994* (08), 741-760.
89. Evans, D. A.; Woerpel, K. A.; Hinman, M. M.; Faul, M. M., Bis (oxazolines) as chiral ligands in metal-catalyzed asymmetric reactions. Catalytic, asymmetric cyclopropanation of olefins. *Journal of the American Chemical Society* **1991**, *113* (2), 726-728.
90. Corey, E.; Imai, N.; Zhang, H. Y., Designed catalyst for enantioselective Diels-Alder addition from a C2-symmetric chiral bis (oxazoline)-iron (III) complex. *Journal of the American Chemical Society* **1991**, *113* (2), 728-729.
91. Northrup, A. B.; MacMillan, D. W., The first general enantioselective catalytic diels− alder reaction with simple α, β-unsaturated ketones. *Journal of the American Chemical Society* **2002**, *124* (11), 2458-2460.
92. Ghosh, S.; Das, S.; De, C. K.; Yepes, D.; Neese, F.; Bistoni, G.; Leutzsch, M.; List, B., Strong and Confined Acids Control Five Stereogenic Centers in Catalytic Asymmetric Diels–Alder Reactions of Cyclohexadienones with Cyclopentadiene. *Angewandte Chemie International Edition* **2020**, *59* (30), 12347-12351.
93. Pierri, M.; Gazzillo, E.; Chini, M. G.; Ferraro, M. G.; Piccolo, M.; Maione, F.; Irace, C.; Bifulco, G.; Bruno, I.; Terracciano, S.; Lauro, G., Introducing structure-based three-dimensional pharmacophore models for accelerating the discovery of selective BRD9 binders. *Bioorganic Chemistry* **2022**, *118(2022)*, 105480-105556.
94. Ogawa, K.; Matsushita, Y.-i., Synthesis and Antiarrhythmic Activity of 2, 5-Disubstituted 2, 3-Dihydro-1, 2, 5-benzothiadiazepin-4 (5*H*)-one 1, 1-Dioxides. *Chemical and Pharmaceutical Bulletin* **1992**, *40* (9), 2442-2447.
95. Zhu, J.; Mo, J.; Lin, H.-z.; Chen, Y.; Sun, H.-P., The recent progress of isoxazole in medicinal chemistry. *Bioorganic & Medicinal Chemistry* **2018**, *26* (12), 3065-3075.
96. Combiglide. *LLC, Schrödinger New York, NY* **2015**.
97. LigPrep, LLC. *Schrödinger New York, NY*, **2015**.
98. QikProp. *Schrödinger New York, NY, 2015*. **2015**.
99. Lipinski, C. A., Lead-and drug-like compounds: the rule-of-five revolution. *Drug Discovery Today: Technologies* **2004**, *1* (4), 337-341.

100. Philpott, M.; Yang, J.; Tumber, T.; Fedorov, O.; Uttarkar, S.; Filippakopoulos, P.; Picaud, S.; Keates, T.; Felletar, I.; Ciulli, A., Bromodomain-peptide displacement assays for interactome mapping and inhibitor discovery. *Molecular BioSystems* **2011**, *7* (10), 2899-2908.
101. Chini, M. G.; Lauro, G.; Bifulco, G., Addressing the target identification and accelerating the repositioning of anti-inflammatory/anti-cancer organic compounds by computational approaches. *European Journal of Organic Chemistry* **2021**, *2021* (21), 2966-2981.
102. Lauro, G.; Masullo, M.; Piacente, S.; Riccio, R.; Bifulco, G., Inverse virtual screening allows the discovery of the biological activity of natural compounds. *Bioorganic & Medicinal Chemistry* **2012**, *20* (11), 3596-3602.
103. Martin, L. J.; Koegl, M.; Bader, G.; Cockcroft, X.-L.; Fedorov, O.; Fiegen, D.; Gerstberger, T.; Hofmann, M. H.; Hohmann, A. F.; Kessler, D., Structure-based design of an in vivo active selective BRD9 inhibitor. *Journal of Medicinal Chemistry* **2016**, *59* (10), 4462-4475.
104. Ojha, M.; Yadav, D.; Kumar, A.; Dasgupta, S.; Yadav, R., 1,8-Naphthyridine Derivatives: A Privileged Scaffold for Versatile Biological Activities. *Mini Reviews in Medicinal Chemistry* **2021**, *21* (5), 586-601.
105. Schrödinger, New York, NY, Maestro, version 10.2. **2015**.
106. Malbec, F.; Milcent, R.; Vicart, P.; Bure, A. M., Synthesis of new derivatives of 4-amino-2, 4-dihydro-1, 2, 4-triazol-3-one as potential antibacterial agents. *Journal of Heterocyclic Chemistry* **1984**, *21* (6), 1769-1774.
107. Demirbas, N.; Demirbas, A.; Karaoglu, S. A.; Celik, E., Synthesis and antimicrobial activities of some new [1, 2, 4] triazolo [3, 4-*b*][1, 3, 4] thiadiazoles and [1, 2, 4] triazolo [3, 4-*b*][1, 3, 4] thiadiazines. *Molecules* **2005**, 15(4), 2427–2438.
108. Crawford, T. D.; Tsui, V.; Flynn, E. M.; Wang, S.; Taylor, A. M.; Côté, A.; Audia, J. E.; Beresini, M. H.; Burdick, D. J.; Cummings, R., Diving into the water: inducible binding conformations for BRD4, TAF1 (2), BRD9, and CECR2 bromodomains. *Journal of Medicinal Chemistry* **2016**, *59* (11), 5391-5402.
109. Daina, A.; Michielin, O.; Zoete, V., SwissADME: a free web tool to evaluate pharmacokinetics, drug-likeness and medicinal chemistry friendliness of small molecules. *Scientific reports* **2017**, *7* (1), 1-13.
110. Zoppi, V.; Hughes, S. J.; Maniaci, C.; Testa, A.; Gmaschitz, T.; Wieshofer, C.; Koegl, M.; Riching, K. M.; Daniels, D. L.; Spallarossa, A.; Ciulli, A., Iterative Design and Optimization of Initially Inactive Proteolysis Targeting Chimeras (PROTACs) Identify VZ185 as a Potent, Fast, and Selective von Hippel-Lindau (VHL) Based Dual Degrader Probe of BRD9 and BRD7. *Journal of Medicinal Chemistry* **2019**, *62* (2), 699-726.
111. Troup, R. I.; Fallan, C.; Baud, M. G., Current strategies for the design of PROTAC linkers: a critical review. *Exploration of Targeted Anti-tumor Therapy* **2020,** *1(1)*, 273-312.
112. Honn, K. V.; Marnett, L. J.; Nigam, S.; Jones, R. L.; Wong, P. Y., *Eicosanoids and Other Bioactive Lipids in Cancer, Inflammation, and Radiation Injury 3*. Springer Science & Business Media **2013**.
113. Lauro, G.; Terracciano, S.; Cantone, V.; Ruggiero, D.; Fischer, K.; Pace, S.; Werz, O.; Bruno, I.; Bifulco, G., A Combinatorial Virtual Screening Approach Driving the Synthesis of 2, 4-Thiazolidinedione-Based Molecules as New Dual mPGES-1/5-LO Inhibitors. *ChemMedChem* **2020**, *15* (6), 481-489.
114. Hieke, M.; Greiner, C.; Thieme, T. M.; Schubert-Zsilavecz, M.; Werz, O.; Zettl, H., A novel class of dual mPGES-1/5-LO inhibitors based on the α-naphthyl pirinixic acid scaffold. *Bioorganic & Medicinal Chemistry Letters* **2011,** *21* (5), 1329-1333.
115. Kini, D.; Ghate, M., Synthesis and Oral Hypoglycemic Activity of 3-[5'-Methyl-2'-aryl-3'-(thiazol-2″-yl amino) thiazolidin-4'-one] coumarin Derivatives. *European Journal of Chemistry* **2011**, *8* (1), 386-390.
116. Kanagarajan, V.; Thanusu, J.; Gopalakrishnan, M., Three component one-pot synthesis of novel pyrimidino thiazolidin-4-ones catalyzed by activated fly ash. *Green Chemistry Letters and Reviews* **2009**, *2* (3), 161-167.
117. Ruijter, E.; Scheffelaar, R.; Orru, R. V., Multicomponent reaction design in the quest for molecular complexity and diversity. *Angewandte Chemie International Edition* **2011**, *50* (28), 6234-6246.

118. Bolognese, A.; Correale, G.; Manfra, M.; Lavecchia, A.; Novellino, E.; Barone, V., Thiazolidin-4-one formation. Mechanistic and synthetic aspects of the reaction of imines and mercaptoacetic acid under microwave and conventional heating. *Organic & Biomolecular Chemistry* **2004**, *2* (19), 2809-2813.
119. Koeberle, A.; Siemoneit, U.; Bühring, U.; Northoff, H.; Laufer, S.; Albrecht, W.; Werz, O., Licofelone suppresses prostaglandin E2 formation by interference with the inducible microsomal prostaglandin E2 synthase-1. *Journal of Pharmacology and Experimental Therapeutics* **2008**, *326* (3), 975-982.
120. Argiriadi, M. A.; Morisseau, C.; Hammock, B. D.; Christianson, D. W., Detoxification of environmental mutagens and carcinogens: structure, mechanism, and evolution of liver epoxide hydrolase. *Proceedings of the National Academy of Sciences* **1999**, *96* (19), 10637-10642.
121. Shen, H. C., Soluble epoxide hydrolase inhibitors: a patent review. *Expert Opinion on Therapeutic Patents* **2010**, *20* (7), 941-956.
122. Temml, V.; Garscha, U.; Romp, E.; Schubert, G.; Gerstmeier, J.; Kutil, Z.; Matuszczak, B.; Waltenberger, B.; Stuppner, H.; Werz, O., Discovery of the first dual inhibitor of the 5-lipoxygenase-activating protein and soluble epoxide hydrolase using pharmacophore-based virtual screening. *Scientific Reports* **2017,** *7* (1), 1-8.
123. Lauro, G.; Manfra, M.; Pedatella, S.; Fischer, K.; Cantone, V.; Terracciano, S.; Bertamino, A.; Ostacolo, C.; Gomez-Monterrey, I.; De Nisco, M., Identification of novel microsomal prostaglandin E_2 synthase-1 (mPGES-1) lead inhibitors from Fragment Virtual Screening. *European Journal of Medicinal Chemistry* **2017**, *125(1)*, 278-287.
124. Chini, M. G.; Giordano, A.; Potenza, M.; Terracciano, S.; Fischer, K.; Vaccaro, M. C.; Colarusso, E.; Bruno, I.; Riccio, R.; Koeberle, A.; Werz, O.; Bifulco, G.,Targeting mPGES-1 by a combinatorial approach: identification of the aminobenzothiazole scaffold to suppress PGE_2 levels. *ACS Medicinal Chemistry Letters* **2020**, *11* (5), 783-789.
125. Vu, L. P.; Gütschow, M., Synthesis and Biological Activities of 4 H-3, 1-Benzothiazin-4-Ones. *Chemistry of Heterocyclic Compounds* **2020,** *56* (6), 708-714.
126. Chen, D.; Bao, W., An Efficient Domino Synthesis of Quinoxalin-2-(1*H*)-ones via an SNAr/Coupling/Demesylation Reaction Catalyzed by Copper (I) as Key Step. *Advanced Synthesis & Catalysis* **2010**, *352* (6), 955-960.
127. Raghunadh, A.; Tadiparthi, K.; Meruva, S. B.; Murthy, V. N.; Rao, L. V.; Kumar, U. S., Synthesis of Quinoxalin-2-(1*H*)-ones and Hexahydroquinoxalin-2 (1H)-ones via Oxidative Amidation–Heterocycloannulation. *SynOpen* **2020**, *4* (03), 55-61.
128. Jdaa, R.; Benali, B.; El Assyry, A.; Lakhrissi, B., Solvatochromic effect on photophysical properties of Quinoxalin-2 (1*H*)-one and 3-Benzylquinoxalin-2 (1*H*)-one. *Optical and Quantum Electronics* **2017**, *49* (2), 79.
129. Wolf, C.; Liu, S.; Mei, X.; August, A. T.; Casimir, M. D., Regioselective copper-catalyzed amination of bromobenzoic acids using aliphatic and aromatic amines. *The Journal of Organic Chemistry* **2006**, *71* (8), 3270-3273.
130. Sharma, G.; Begum, A.; Rakesh; Krishna, P. R., Zirconium (IV) Chloride Mediated Cyclodehydration of 1, 2-Diacylhydrazines: A Convenient Synthesis of 2, 5-Diaryl 1,3,4-Oxadiazoles. *Synthetic Communications* **2004**, *34* (13), 2387-2391.
131. . Castillo, J. C.; Orrego-Hernández, J.; Portilla, J., Cs2CO3-Promoted Direct N-Alkylation: Highly Chemoselective Synthesis of N-Alkylated Benzylamines and Anilines. *European Journal of Organic Chemistry* **2016**, *2016* (22), 3824-3835.
132. Bromidge, S. M.; Arban, R.; Bertani, B.; Bison, S.; Borriello, M.; Cavanni, P.; Dal Forno, G.; Di-Fabio, R.; Donati, D.; Fontana, S., Design and Synthesis of Novel Tricyclic Benzoxazines as Potent 5-HT1A/B/D Receptor Antagonists Leading to the Discovery of 6-{2-[4-(2-methyl-5-quinolinyl)-1-piperazinyl] ethyl}-4 H-imidazo [5, 1-c][1, 4] benzoxazine-3-carboxamide (GSK588045). *Journal of Medicinal Chemistry* **2010**, *53* (15), 5827-5843.
133. Kim, H. S.; Kim, S. K.; Kang, K. W., Differential effects of sEH inhibitors on the proliferation and migration of vascular smooth muscle cells. *International Journal of Molecular Sciences* **2017,** *18* (12), 2683-2689.
134. Kobayashi, Y.; Morikawa, T.; Yoshizawa, A.; Taguchi, T., A stereospecific synthesis of conjugated fluorodienes by a ring-opening reaction of gem-difluorocyclopropane derivatives. *Tetrahedron Letters* **1981**, *22* (52), 5297-5300.

135. Schlosser, M.; Spahic, B.; Tarchini, C.; Le Van, C., Insertion of a carbon atom into olefinic double bonds: synthesis of fluorodienes and fluoroalkenes. *Angewandte Chemie, International Edition* **1975**, *14* (1), 365-366.
136. Kobayashi, Y.; Taguchi, T.; Morikawa, T.; Takase, T.; Takanashi, H., Ring opening reaction of gem-difluorocyclopropyl ketones with nucleophiles. *Tetrahedron Letters* **1980**, *21* (11), 1047-1050.
137. Eddarir, S.; Mestdagh, H.; Rolando, C., Synthesis of fluorinated enynes and dienes via 1-bromo 2-fluoro alkenes. *Tetrahedron letters* **1991**, *32* (1), 69-72.
138. Ahmed, E.-A. M.; Suliman, A. M.; Gong, T.-J.; Fu, Y., Palladium-catalyzed stereoselective defluorination Arylation/Alkenylation/Alkylation of gem-difluorinated cyclopropanes. *Organic letters* **2019**, *21* (14), 5645-5649.
139. Jiang, Z. T.; Huang, J.; Zeng, Y.; Hu, F.; Xia, Y., Rhodium Catalyzed Regioselective C− H Allylation of Simple Arenes via C− C Bond Activation of Gem-difluorinated Cyclopropanes. *Angewandte Chemie* **2021**, *133* (19), 10720-10725.
140. Prakash, G. S.; Krishnamurti, R.; Olah, G. A., Fluoride-Induced Trifluoromethylation of Carbonyl Compounds with Trifluoromethyltrimethylsilane (TMS-CF 3): A Trifluoromethide Equivalent. *Journal of the American Chemical Society* **1989**, 111(1), 393–395.
141. Hayashi, T.; Usuki, Y.; Wakamatsu, Y.; Iio, H., Synthesis of (E)-1-Benzyloxy-3-fluoro-1, 3-butadiene: A Novel Fluorinated Diene for Diels-Alder Reactions. *Synlett* **2010**, *2010* (19), 2843-2846.
142. Essers, M.; Ernet, T.; Haufe, G., Enantioselective Diels–Alder reactions of α-fluorinated α, β-unsaturated carbonyl compounds: Part 5. Chemical consequences of fluorine substitution. *Journal of Fluorine Chemistry* **2003**, *121* (2), 163-170.
143. Jorgensen, W. L.; Maxwell, D. S.; Tirado-Rives, J., Development and testing of the OPLS all-atom force field on conformational energetics and properties of organic liquids. *Journal of the American Chemical Society* **1996**, *118* (45), 11225-11236.
144. Benet, L. Z.; Hosey, C. M.; Ursu, O.; Oprea, T. I., BDDCS, the rule of 5 and drugability. *Advanced Drug Delivery Reviews* **2016**, *101*, 89-98.
145. Friesner, R. A.; Banks, J. L.; Murphy, R. B.; Halgren, T. A.; Klicic, J. J.; Mainz, D. T.; Repasky, M. P.; Knoll, E. H.; Shelley, M.; Perry, J. K., Glide: a new approach for rapid, accurate docking and scoring. 1. Method and assessment of docking accuracy. *Journal of Medicinal Chemistry* **2004**, *47* (7), 1739-1749.
146. Maestro, LLC. *Schrödinger New York, NY, 2015*. **2015**.
147. Li, D.; Howe, N.; Dukkipati, A.; Shah, S. T.; Bax, B. D.; Edge, C.; Bridges, A.; Hardwicke, P.; Singh, O. M.; Giblin, G., Crystallizing membrane proteins in the lipidic mesophase. Experience with human prostaglandin E_2 synthase 1 and an evolving strategy. *Crystal Growth & Design* **2014**, *14* (4), 2034-2047.
148. Sherman, W.; Day, T.; Jacobson, M. P.; Friesner, R. A.; Farid, R., Novel procedure for modeling ligand/receptor induced fit effects. *Journal of Medicinal* Chemistry **2006**, *49* (2), 534-553.
149. Glover, B.; Harvey, K. A.; Liu, B.; Sharp, M. J.; Tymoschenko, M. F., Regioselective palladium-catalyzed arylation of 3-carboalkoxy furan and thiophene. *Organic Letters **2003**, 5* (3), 301-304.
150. Méndez-Rojas, C.; Quiroz, G.; Faúndez, M.; Gallardo-Garrido, C.; Pessoa-Mahana, C. D.; Chung, H.; Gallardo-Toledo, E.; Saitz-Barría, C.; Araya-Maturana, R.; Kogan, M. J., Synthesis and biological evaluation of potential acetylcholinesterase inhibitors based on a benzoxazine core. *Archiv der Pharmazie* **2018,** *351* (5), 1-17.
151. Xu, T.; Cuyamendous, C.; Brown, S. L.; Andreassend, S. K.; Cumming, H.; Evans, G. B.; Teesdale-Spittle, P. H.; Harvey, J. E., Gold (I)-catalyzed, one-pot, oxidative formation of 2, 4-disubstituted thiazoles: Application to the synthesis of a pateamine related macrodiolide. *Tetrahedron* **2021**, *88*(1), 1-12.

Acknowledgements

Chi mi conosce sa bene che non esterno facilmente i miei sentimenti, ma vorrei esprimere la mia riconoscenza a tutti coloro che hanno percorso questo cammino assieme a me.

Primo fra tutti, voglio ringraziare il mio Tutor, il Prof. Giuseppe Bifulco, che mi ha accolta fin da subito nel Suo laboratorio. Ho sempre apprezzato il Suo lasciar liberi, nel lavoro come nelle scelte. Lo ringrazio per essere stato l'unico ad appoggiarmi quando, nonostante la COVID, volessi andare oltre oceano, e per avermi costantemente incitato a studiare invece di "fare la praticona"!

Un sincero ringraziamento va soprattutto ai suoi collaboratori che mi hanno seguito in questi tre anni. Ringrazio Susy per avermi supportato nella parte sintetica, per avermi formata ed esserci stata ogni giorno.

Ringrazio Maria Giovanna, per i consigli, le dritte e i nostri discorsi. Con lei so sempre chi chiamare quando ho bisogno di un consiglio!

Ringrazio Gianluigi per avermi costantemente stimolata e aiutata durante questo percorso.

Un doveroso ringraziamento va anche alla Prof.ssa Stefania Terracciano, per essere stata per me un punto di riferimento nel corso di questi anni, e alla Prof.ssa Maria Chiara Monti per l'aiuto con il "tenebroso" AlphaScreen.

E ora, passiamo a chi mi è stato ogni giorno vicino in questi anni. Ringrazio Marianna per essere stata prima il mio capo, poi amica e, infine, collega. Grazie per tutti i pianti, le telefonate e gli sfoghi che ti sei dovuta subire; si sente la tua mancanza in laboratorio. Ringrazio la mia amica Pierri per le risate, i consigli e l'affetto mostratomi, perché si sa che ormai ci capiamo con un solo sguardo!

Ringrazio Dafne per essermi stata vicina, soprattutto nei vari alti e bassi dell'ultimo periodo. Parlare con lei mi mette sempre serenità. Ringrazio Simona ed Erica, per i caffè e le chiacchere

ma, soprattutto, per l'importante aiuto con il PC! Infine, Arianna, che anche se da poco entrata nel nostro gruppo porta sempre tanta gioia.

Un grazie speciale va ai tanti tesisti che sono passati per il Lab 10, ognuno con la propria storia, ognuno con le proprie qualità. Tutti mi hanno lasciato un ricordo che porterò sempre nel cuore.

Un doveroso grazie va al Prof. Toste e al suo team. In particolare, ai miei compagni di merenda Chin Ho e Vlad per essere stati i primi ad accogliermi quando ero sola e spaesata, per avere avuto sempre una risposta ai miei dubbi chimici, per la grande disponibilità. Ringrazio le mie best tedesche Alessa ed Elena, per le nostre risate e per aver reso più spensierato il mio periodo a Berkeley.

Un grazie speciale va a Chiara: non c'è bisogno di tante parole per esprimere la mia gratitudine, ma è semplicemente l'amica che mi ascolta da una vita.

In ultimo, il ringraziamento forse più grande va a Daniele, per tutto l'aiuto che mi ha dato nel periodo più difficile di questi tre anni, quando ero a Berkeley. Grazie per le revisioni d'inglese, per aver ascoltato presentazioni e presentazioni sul "tytanium catalyst"; grazie per essere stato la mia spalla quando ero fragile ed il pagliaccio quando ero serena.

Vorrei infine ringraziare la mia famiglia e i miei amici per essere stati costantemente al mio fianco. So che non è semplice capire per chi non appartiene a questo mondo ma ognuno, a modo suo, mi ha sostenuta e aiutata.

E, infine, un grazie va anche a me perché in fondo, in fondo, è anche un po' merito mio!